ЖУРНАЛ
ПРИКЛАДНОЙ ХИМИИ

JOURNAL OF
APPLIED CHEMISTRY
OF THE USSR

(ZHURNAL PRIKLADNOI KHIMY)

IN ENGLISH TRANSLATION

VOL. 30 NO. 6

CONSULTANTS BUREAU, INC.

227 WEST 17TH STREET, NEW YORK 11, N. Y.

an agency for the interpretation of international knowledge

JOURNAL OF APPLIED CHEMISTRY OF THE USSR

(ZHURNAL PRIKLADNOI KHIMII)

Volume 30, No. 6

June, 1957

(A Publication of the Academy of Sciences of the U.S.S.R)

IN ENGLISH TRANSLATION

Copyright, 1958

CONSULTANTS BUREAU, INC.

227 West 17th Street

New York 11, N. Y.

Printed in the United States

	Domestic	Foreign
Annual Subscription	$60.00	$65.00
Annual Subscription for libraries of non-profit academic institutions	20.00	25.00
Single Issue	7.50	

Note: The sale of photostatic copies of any portion of this copyright translation is expressly prohibited by the copyright owners.

SIGNIFICANCE OF ABBREVIATIONS MOST FREQUENTLY ENCOUNTERED IN SOVIET PERIODICALS

FIAN	Phys. Inst. Acad. Sci. USSR.
GDI	Water Power Inst.
GITI	State Sci.-Tech. Press
GITTL	State Tech. and Theor. Lit. Press
GONTI	State United Sci.-Tech. Press
Gosenergoizdat	State Power Press
Goskhimizdat	State Chem. Press
GOST	All-Union State Standard
GTTI	State Tech. and Theor. Lit. Press
IL	Foreign Lit. Press
ISN (Izd. Sov. Nauk)	Soviet Science Press
Izd. AN SSSR	Acad. Sci. USSR Press
Izd. MGU	Moscow State Univ. Press
LEIIZhT	Leningrad Power Inst. of Railroad Engineering
LET	Leningrad Elec. Engr. School
LETI	Leningrad Electrotechnical Inst.
LETIIZhT	Leningrad Electrical Engineering Research Inst. of Railroad Engr.
Mashgiz	State Sci.-Tech. Press for Machine Construction Lit.
MEP	Ministry of Electrical Industry
MES	Ministry of Electrical Power Plants
MESEP	Ministry of Electrical Power Plants and the Electrical Industry
MGU	Moscow State Univ.
MKhTI	Moscow Inst. Chem. Tech.
MOPI	Moscow Regional Pedagogical Inst.
MSP	Ministry of Industrial Construction
NII ZVUKSZAPIOI	Scientific Research Inst. of Sound Recording
NIKFI	Sci. Inst. of Modern Motion Picture Photography
ONTI	United Sci.-Tech. Press
OTI	Division of Technical Information
OTN	Div. Tech. Sci.
Stroiizdat	Construction Press
TOE	Association of Power Engineers
TsKTI	Central Research Inst. for Boilers and Turbines
TsNIEL	Central Scientific Research Elec. Engr. Lab.
TsNIEL-MES	Central Scientific Research Elec. Engr. Lab.—Ministry of Electric Power Plants
TsVTI	Central Office of Economic Information
UF	Ural Branch
VIESKh	All-Union Inst. of Rural Elec. Power Stations
VNIIM	All-Union Scientific Research Inst. of Meteorology
VNIIZhDT	All-Union Scientific Research Inst. of Railroad Engineering
VTI	All-Union Thermotech. Inst.
VZEI	All-Union Power Correspondence Inst.

Note: Abbreviations not on this list and not explained in the translation have been transliterated, no further information about their significance being available to us. – Publisher.

STUDY OF THE REACTIONS OF SULFUR DIOXIDE WITH METAL OXIDES IN PRESENCE OF CARBON

V. V. Pechkovsky

The A. M. Gorky State University, Molotov

Reactions of sulfur dioxide with metal oxides in presence of solid or gaseous reducing agents are widely used in various industrial operations [1-4].

In nonferrous metallurgy, reactions between sulfur dioxide and metal oxides in presence of reducing agents play an important part in the smelting of copper and nickel ores [2, 5], in ferrous metallurgy this process is the basis of desulfurization of iron in blast furnace smelting [1, 6], while in inorganic technology the process often determines the composition of the products formed by reduction roasting of sulfates [3, 7, 8].

In view of the importance of this process and of the fact that it has been studied relatively little, the present investigation was devoted to the study of the reactions of sulfur dioxide with various metal oxides in presence of solid carbon.

When sulfur dioxide reacts with metal oxides in presence of carbon, the solid products may, in general, consist of sulfites, sulfides, and sulfates. These compounds may be formed in several different ways. Sulfites are formed when sulfur dioxide reacts with metal oxides according to the equation

$$MeO + SO_2 \rightleftharpoons MeSO_3. \quad (1)$$

However, as Foerster and Kubel [9] report, the sulfites of most metals are unstable compounds, and decompose at relatively low temperatures according to the equation

$$4MeSO_3 = MeS + 3MeSO_4. \quad (2)$$

Moreover, sulfites formed according to Equation (1) may under certain conditions be oxidized according to the equation

$$MeSO_3 + {}^1/_2O_2 = MeSO_4. \quad (3)$$

However, it must be stated that when sulfur dioxide interacts with metal oxides in presence of carbon, the formation of sulfites, sulfides, and sulfates according to Equations (1) - (3) is possible, for most oxides, only at relatively low temperatures, when the reduction of sulfur dioxide occurs at a relatively low rate. Sulfides may therefore be formed by another route. This route of sulfide formation in the interaction of sulfur dioxide with metal oxides in presence of carbon can be represented by the following overall equations:

$$2MeO + 2SO_2 + 3C = 2MeS + 3CO_2, \quad (4)$$

$$MeO + SO_2 + 3C = MeS + 3CO. \quad (5)$$

Leaving an all-round examination of the complex mechanism of this process on one side for the moment, let us consider its individual stages. The most important of these stages are: reduction of sulfur dioxide to elementary sulfur, reduction of the metallic oxide, reaction of elemental sulfur with the oxide undergoing reduction to give a sulfide. The complex combination of the reactions taking place in the reduction of sulfur dioxide with carbon can be represented by the following principal equations:

$$SO_2 + C \rightleftharpoons CO_2 + 1/_2S_2, \quad (6)$$

$$CO_2 + C \rightleftharpoons 2CO, \quad (7)$$

$$C + S_2 \rightleftharpoons CS_2, \quad (8)$$

$$CO + 1/2S_2 \rightleftharpoons COS. \quad (9)$$

To determine the degree of reduction of sulfur dioxide by carbon, we carried out a thermodynamic analysis of this system. The equilibrium composition of the gas phase, consisting of S_2, CO_2, CO, CS_2, COS, and SO_2, was calculated for different temperatures and SO_2 concentrations in the original gas. The calculations were made for a total pressure of 1 atmosphere.

Table 1 contains our calculated equilibrium concentrations of elemental sulfur in the gas phase for reduction of 100% SO_2 with carbon, and also for reduction of gaseous mixtures containing 80, 60, and 40% SO_2 (the rest being air).

TABLE 1

Equilibrium Concentrations of Sulfur in the Gas Phase in the Reduction of Sulfur Dioxide with Carbon

Concentration of SO_2 in the original mixture (%)	Log p_{S_2} at temperatures (°C)				
	600	700	800	1000	1200
100	—2.301	—2.155	—1.966	—1.742	—1.633
80	—2.398	—2.260	—2.046	—1.795	—1.699
60	—2.523	—2.366	—2.125	—1.886	—1.757
40	—2.700	—2.523	—2.236	—1.990	—1.879

Lepsoe [10] studied the rate of reduction of sulfur dioxide with carbon. He found that reduction of sulfur dioxide by wood charcoal already occurs at 500°, and at 800° the reaction proceeds at a high rate. He also found that the rate of reduction of sulfur dioxide greatly depends on the reactivity of the solid reducing agent. For example, the rate of reduction of SO_2 by coke made from coal was 4 times lower than by wood charcoal under the same conditions. Lepsoe [10] states that the reduction of sulfur dioxide by charcoal is a heterogeneous catalytic reaction in which the carbon surface acts as the catalyst.

We now consider the next stage of the process – reduction of metal oxides. The most widely held view on the reduction of metal oxides with solid carbon is that the reaction occurs according to the scheme [1]:

$$MeO + CO \rightleftharpoons Me + CO_2, \quad (10)$$

$$C + CO_2 \rightleftharpoons 2CO. \quad (11)$$

If MeO and Me are present in condensed phases and do not form solid or liquid solutions, the equilibrium constant for Reaction (10) can be represented as:

$$K = \frac{p_{CO_2}}{p_{CO}}$$

The extent and sequence of the reduction of certain metal oxides with carbon monoxide can be found from the values of the equilibrium CO/CO_2 ratios at 800°, given in Table 2.

TABLE 2

Logarithms of Equilibrium CO/CO_2 Ratios in the Reduction of Various Metal Oxides with Carbon Monoxide (t = 800°)

Metal oxide	Cu_2O	CoO	FeO	ZnO	MnO
$\log \frac{p_{CO}}{p_{CO_2}}$	—5.0	—2.5	+0.2	+1.1	+6.0

The problem of determing the equilibrium gas phase composition, the sequence, and to some extent the rates of reduction of the metal oxides is considerably easier if the dissociation pressures of the oxides are known. As is known, the dissociation pressure of an oxide is a quantity equivalent to the standard free energy change of the system, and in a number of cases it can therefore be found from the equation:

$$\Delta F^\circ = -2.3\ RT \log p_{O_2}.$$

The common logarithms of the dissociation pressures of some metal oxides are given in Fig. 1 [11, 12]. The

logarithms of the equilibrium oxygen pressures in the dissociation of carbon dioxide and carbon monoxide, calculated for a total pressure of one atmosphere, are plotted on the same diagram.

The data in Fig. 1 can be used to divide all metal oxides into 3 arbitrary groups.

The first group consists of oxides of metals the lower oxides of which have higher dissociation pressures than the equilibrium oxygen pressure in the dissociation of carbon dioxide. The data in Fig. 1 show that this group includes cuprous oxide, cobaltous oxide, etc. The lower oxides of the metals of this group are relatively easily reduced with carbon monoxide and, as the data in Table 2 and Fig. 1 indicate, the gaseous reduction products consist mainly of carbon dioxide.

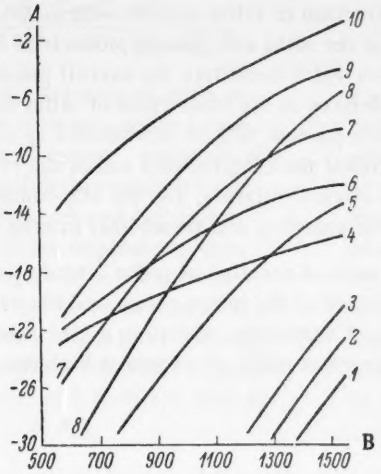

Fig. 1. Variation of dissociation pressures of oxides with the temperature.
A) Common logarithm of the dissociation pressure of the oxide (log p_{O_2}), B) temperature (°C).
Oxides: 1) CaO, 2) MgO, 3) Al_2O_3, 4) CO, 5) MnO, 6) CO_2, 7) FeO, 8) ZnO, 9) CoO, 10) Cu_2O.

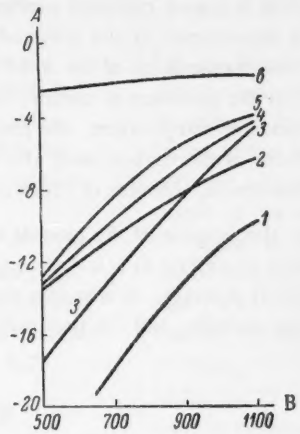

Fig. 2. Variation of dissociation pressures of sulfides with the temperature.
A) Common logarithm of the dissociation pressure of the sulfide (log p_{S_2}), B) temperature (°C).
Sulfides: 1) MnS, 2) Cu_2S, 3) ZnS, 4) FeS, 5) Ni_3S_2, 6) logarithm of the equilibrium sulfur concentration in the gas phase in the reduction of 100% SO_2 with carbon.

The second group consists of oxides of metals the lower oxides of which have higher dissociation pressures than the equilibrium oxygen pressure in the dissociation of carbon monoxide. The data in Fig. 1 show that ferrous, manganous, and zinc oxides can be included in this group. The lower oxides of the metals in this group can be reduced with carbon monoxide in presence of carbon only with great difficulty and only at high temperatures. The data in Table 2 and Fig. 1 indicate that the equilibrium gas phase in the reduction of metal oxides of this group will consist mainly of carbon monoxide.

The third group consists of oxides of metals the lower oxides of which have lower dissociation pressures than the equilibrium oxygen pressure in the dissociation of carbon monoxide. The data in Fig. 1 indicate that the oxides of aluminum, magnesium, and calcium are examples of this group. The lower oxides of the metals of this group are not reduced in the 600-1000° temperature range even in presence of solid carbon [1, 2].

The final stage of the process in question is conversion of the oxide to sulfide by means of elemental sulfur. This stage can be schematically represented by the equation

$$Me + 1/2S_2 \rightleftharpoons MeS. \qquad (12)$$

Sulfide formation according to Equation (12) is thermodynamically possible if the pressure of elemental sulfur in the gas phase is higher than the equilibrium dissociation pressure of the sulfide.

Values of the logarithms of the dissociation pressures of various sulfides, taken from literature sources [2, 11, 12], are given in Fig. 2. The logarithms of the equilibrium sulfur pressure in the reduction of 100% sulfur dioxide with carbon are also plotted on the same diagram.

The relative positions of the curves in Fig. 2 show that 100% sulfur dioxide in presence of carbon in the 500-1200° range can be used to obtain sulfides of iron, nickel, copper, and zinc, apart from other metals the sulfides of which have lower dissociation pressures.

In concluding this discussion of some aspects of the process, we must point out that the elemental sulfur formed in the reduction of sulfur dioxide can be adsorbed by solid carbon even at high temperatures. This interesting fact has been reported by Juza and Blanke [13], and by Huff and Holz [14].

All the foregoing leads to the general conclusion that the interaction of sulfur dioxide with metal oxides in presence of carbon is a very complex process. The composition of the solid and gaseous products of this interaction will be determined by the rate and extent of the reactions which constitute the overall process. In the general case, the composition of the solid and gaseous products formed in the interaction of sulfur dioxide with metal oxides in the presence of carbon, and the rate of the whole process, will be determined by numerous factors which include the temperature, the physicochemical properties of the metal oxides and of the compounds formed, the reactivity of the carbon used, the carbon content in the original mixture, and the SO_2 concentration in the original gas mixture. Studies of these relationships are of great practical and theoretical interest.

Accordingly, the purpose of the present work was to study the rates of reaction of sulfur dioxide with metal oxides in presence of carbon in relation to the temperature, the nature of the metal oxide, and the carbon content in the original mixture. It was also desired to study the rate of conversion of various metal oxides to the sulfates by sulfur dioxide, and the possibility of adsorption of elemental sulfur on carbon at high temperatures.

EXPERIMENTAL

Dry CuO, Co_2O_3, Fe_2O_3, ZnO, Mn_2O_3, Al_2O_3, MgO (analytical reagent grade) and Kahlbaum's blood charcoal free from volatile matter and sulfur, were used for the experiments. For studies of the reaction rates, the pure metal oxides, charcoal, and mixtures of metal oxides and charcoal, were heated in a laboratory tube furnace in a stream of dry 100% sulfur dioxide in the 300-800° range. The furnace temperature was measured by means of a thermocouple and galvanometer, and regulated by means of an autotransformer, type LATR-1. The gas rate in the system was 3.0 liters/hour in all experiments, and the duration was 15 minutes.

To study the effect of the contents of reducing agent on the rate of the process, mixtures of metal oxides with carbon, containing from 0.5 to 8.0 moles of carbon per mole of oxide, were heated. The reaction of sulfur dioxide with zinc oxide in presence of carbon was studied for mixtures with carbon contents (M*) of 0.5, 1.0, 2.0, 3.0, and 4.0, equivalent to carbon contents of 6.9, 12.9, 22.7, 30.6 and 37.1% by weight in the original mixture. The weight of metal oxide was 0.5 g in each case. The solid reaction products were analyzed.

It was found that the Eschka method [15] gives the most accurate results in determinations of sulfur in samples containing carbon. Therefore, the total sulfur in samples containing carbon was determined by this method. The results obtained for the interaction of sulfur dioxide with metal oxides in presence of carbon were calculated as percentages of sulfide sulfur. Samples obtained in the treatment of metal oxides with sulfur dioxide were analyzed for sulfate sulfur. For this, the reaction products were leached out with 2% stannous chloride and sulfate was determined gravimetrically. The results were calculated as percentages of sulfate formed.

The principal results of the experiments and the thermodynamic calculations are given in Tables 1-5 and Figs. 1-5.

The data in Table 3 show that the sulfur content of the carbon after treatment with 100% sulfur dioxide increases with the temperature. It was found in special experiments that the adsorbed sulfur is firmly bound by

* Here and subsequently M is the content of carbon in the original mixture in moles of carbon per mole of metal oxide.

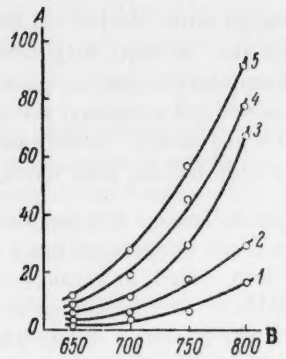

Fig. 3. Reaction of sulfur dioxide with zinc oxide in presence of carbon. Variation of the sulfidation rate with the temperature and carbon content of the original mixture. A) Degree of sulfidation of ZnO (%), B) temperature (°C). Carbon content M of the original mixture (in moles C/mole oxide): 1) 0.5, 2) 1.0, 3) 2.0, 4) 3.0, 5) 4.0.

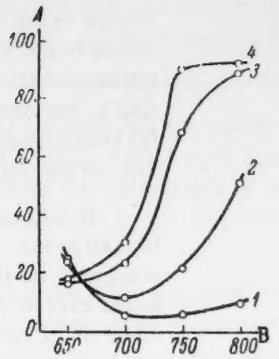

Fig. 4. Reaction of sulfur dioxide with manganese oxide in presence of carbon. Variation of the sulfidation rate with the temperature and carbon content of the original mixture. A) Degree of sulfidation of Mn_2O_3 (%), B) temperature (°C). Carbon content M of the original mixture (in moles C/mole oxide): 1) 1.0, 2) 3.0, 3) 6.0, 4) 8.0.

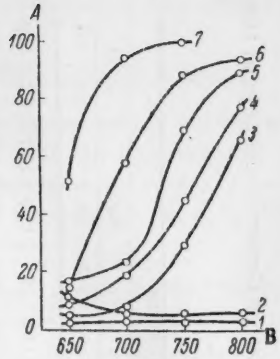

Fig. 5. Reactions of sulfur dioxide with metal oxides in presence of carbon. Variation of the sulfidation rate with the temperature and the nature of the oxide. A) Degree of sulfidation of the oxides (%), B) temperature (°C). Oxides: 1) Al_2O_3, 2) MgO, 3) Fe_2O_3, 4) ZnO, 5) Mn_2O_3, 6) Co_2O_3, 7) CuO. Carbon contents of the original mixtures, 30%.

the carbon. This sulfur could not be extracted from the carbon even by treatment with carbon disulfide or toluene for three days.

These facts show that not simple but activated adsorption of sulfur by solid carbon occurs in this case.

Data on the rate of sulfate formation by the action of 100% sulfur dioxide on various metal oxides are given in Table 4.

TABLE 3

Effect of Temperature on the Degree of Sorption of Elemental Sulfur by Carbon

Temperature (°C)	600	650	700	750	800
Sulfur content in carbon after experiment (%)	2.2	4.3	5.8	6.3	6.5

TABLE 4

Reactions of Sulfur Dioxide with Various Metal Oxides. Effect of Temperature on the Rate of Sulfate Formation

Metal oxide	Conversion of oxide to sulfate (%) at temperatures (°C)				
	300	400	500	600	700
Mn_2O_3	15.0	28.6	47.2	50.0	22.5
Co_2O_3	7.1	11.3	23.6	21.8	7.4
Fe_2O_3	4.4	9.3	4.2	0.0	0.0
MgO	1.8	2.6	3.5	4.1	4.4

TABLE 5

Reactions of Sulfur Dioxide with Various Metal Oxides in Presence of Carbon. Effects of Temperature and of Carbon Content in the Original Mixture on the Rate of Sulfidation of the Oxides

Temperature (°C)	Degree of sulfidation of oxide (in %) with carbon content M in the original mixture																							
	Mn_2O_3				ZnO				Fe_2O_3				CuO				Co_2O_3				MgO			Al_2O_3
	1.0	3.0	6.0	8.0	0.5	1.0	2.0	3.0	4.0	2.0	6.0	8.0	0.5	1.0	2.0	3.0	1.0	3.0	6.0	1.0	2.0	3.0	1.0	3.0
650	24.9	23.8	16.9	17.9	1.4	3.4	5.9	8.9	12.2	1.6	4.9	6.7	22.7	22.7	41.0	52.0	25.6	7.7	14.3	5.7	11.0	14.7	1.1	2.0
700	5.7	11.6	23.6	31.0	3.7	5.7	11.6	19.0	27.4	2.6	7.3	12.8	20.2	54.0	74.5	94.5	15.4	47.4	57.6	5.0	5.9	8.2	1.4	2.5
750	6.3	22.2	69.0	91.0	6.5	18.0	29.9	45.6	56.7	4.4	29.3	44.5	26.7	77.5	93.0	100.0	15.7	65.0	88.2	4.0	5.5	8.0	1.0	2.5
800	10.9	51.8	89.8	93.0	16.3	29.3	67.5	77.5	91.8	9.0	65.7	99.7	23.0	83.0	99.0	—	22.6	73.0	93.8	4.5	5.9	7.5	1.0	2.6

The oxides ZnO, MgO, Fe_2O_3, Co_2O_3 and Mn_2O_3 were chosen for the experiments. It was found by preliminary qualitative analyses that the final solid products formed in the reactions between sulfur dioxide and the oxides in the 300-700° range are: for MgO, magnesium sulfate and traces of magnesium sulfite; for Fe_2O_3 and Co_2O_3, the corresponding sulfates and elemental sulfur; for Mn_2O_3, manganese sulfate and sulfide. In the case of ZnO no compounds of sulfur with the zinc were found.

It follows from the data in Table 4 that the sulfate formation rate as a function of the temperature has a maximum for the oxides of iron, cobalt, and manganese. In the case of magnesium oxide no such maximum is found in the 300-700° range, as magnesium sulfate decomposes at a lower rate than the sulfates of iron [7], cobalt, and manganese [8]. The results of these experiments show that when 100% sulfur dioxide reacts with metal oxides, sulfates are formed according to Equations (1) and (3); the sulfites are oxidized by sulfur dioxide, and, for oxides of iron, cobalt, and manganese, also by the oxygen which may be formed according to the equation

$$Me_2O_3 \rightleftharpoons 2MeO + {}^1/_2O_2. \qquad (13)$$

The cause of the maximum on the sulfate formation rate – temperature curve is that at low temperatures the rate of sulfite oxidation, i.e., of Reaction (3), is low, while at high temperatures the rate of sulfite formation, i.e., of Reaction (1), is low.

Data on the reactions of 100% sulfur dioxide with various metal oxides in presence of carbon are given in Table 5 and Figs. 3-5.

It was established by preliminary qualitative analyses that, in 650-800° temperature range, the final solid products of these reactions are: for Al_2O_3, elemental sulfur only; for MgO, elemental sulfur and magnesium sulfate and sulfide; for ZnO and Fe_2O_3, elemental sulfur and the corresponding sulfides; for Co_2O_3, Mn_2O_3, and CuO, elemental sulfur, the corresponding sulfides and sulfates at low temperatures, and only the sulfides at high temperatures. The data in Table 5 and Figs. 3-5 indicate that the sulfidation rate in general rises with increasing temperature and carbon content of the original mixture. The increase of the sulfidation rate with increasing temperature and carbon content in the original mixture is due to the increased rates of Reactions (6), (10)-(12) in these conditions. It is true that in the low-temperature region the relationship between the sulfidation rate and temperature is somewhat different for the oxides of cobalt, manganese, and magnesium. However, the decrease of the total sulfur content in the reaction products with increase of temperature for these oxides is due to the fact that, as follows from the data in Table 3, these oxides are converted fairly rapidly into sulfates by Reactions (1) and (3). As the temperature rises, the rate of sulfate formation by Reactions (1)

and (3) diminishes; the reasons for this were discussed earlier. It is also interesting to note that, as is shown by the data in Table 5 and Fig. 3, sulfidation of zinc oxide proceeds at an appreciable rate even at 650-700°, i.e., at a temperature at which the reduction of zinc oxide by carbon proceeds at a low rate. Hence we may conclude that the presence of sulfur in the gas phase increases the rate of reduction of zinc oxide, while presence of carbon in the mixture weakens the bonds between zinc and oxygen. Favorable conditions are thus created for exchange between elemental sulfur in the gas phase and the oxygen in zinc oxide.

It follows from the data in Table 5 and Fig. 5 that different oxides have different sulfidation rates.

For equal carbon contents in the original mixtures, all the oxides studied can be arranged in the following sequence of degree of sulfidation: Al_2O_3, MgO, Fe_2O_3, ZnO, Mn_2O_3, Co_2O_3, CuO. This very important fact has a perfectly definite explanation. It shows that the rate of reaction of sulfur dioxide with metal oxides in presence of carbon, in the kinetic region, is limited either by the rate of reduction of the metal oxide, or by the rate of sulfide formation.

If we return to the arbitrary division of all the lower oxides of metals into three groups, we find from Table 5 and Fig. 5 that within each of these groups the rate of reaction of sulfur dioxide with metal oxides in presence of carbon is limited by the rate of sulfide formation. In the kinetic region, the rate of sulfide formation under equal conditions will be proportional to the difference between the partial pressure of elemental sulfur in the gas phase and the dissociation pressure of the lower sulfide formed. This conclusion can be confirmed by analysis of the data in Figs. 1, 2, and 5. It is true that Fig. 2 does not contain data on the dissociation pressures of the sulfides of cobalt, magnesium, and aluminum, since such data are not available at present. However, as Volsky [11] showed, in a number of cases there is a more or less pronounced relationship between the dissociation pressure of a sulfide and its heat formation from the elements.

The heats of formation of sulfides per mole of gaseous sulfur have the following values (in kcal/mole) [11]: CaS 252.4, MgS 198.0, MnS 127.4, Al_2S_3 123.6, ZnS 120.6, CoS 71.0, NiS 70.0.

These values suggest that magnesium sulfide should have a low dissociation pressure, while the dissociation pressures of nickel and cobalt sulfides probably differ for each other only slightly.

If we now turn to Figs. 1, 2, and 5, we find that, corresponding to the dissociation pressures of the sulfides formed, the metal oxides form the following sequence according to degree of sulfidation: in the first group of oxides, Co_2O_3, CuO (lower oxides CoO and Cu_2O); in the second group, Fe_2O_3, ZnO, Mn_2O_3 (lower oxides FeO, MnO); and in the third group, Al_2O_3 and MgO.

The results of investigations of the reactions of sulfur dioxide with metal oxides in presence of carbon are not only of theoretical but also of practical interest. The conclusions drawn from the results of this study can be used for prediction of some aspects of the behavior of various oxides in smelting.

The relationships which have been found can be used to predict the composition of the solid products of sulfate reduction, and to explain many features of this process, which is important in inorganic technology. For example, it can be stated in advance that in the reduction of cobalt sulfate, sulfide formation will be considerable, and in the reduction of magnesium sulfate it will be slight.

Some aspects of the complex process of sulfidation of metal oxides with sulfur dioxide in presence of carbon have not yet been studied, and research in this very interesting direction will be continued.

LITERATURE CITED

[1] M. A. Pavlov, Metallurgy of Cast Iron, II (Metallurgy Press, 1949).*

[2] V. I. Smirnov, Metallurgy of Copper and Nickel (Metallurgy Press, 1950).*

[3] M. E. Pozin, Technology of Mineral Salts (Goskhimizdat, 1949).*

[4] A. V. Avdeeva, Gaseous Sulfur (Goskhimizdat, 1950).*

[5] V. A. Vanyukov, A. V. Vanyukov, and A. N. Kudrin, Nonferrous Metals 3, 17 (1954).

[6] V. G. Voskoboinikov, Steel, 7, 583 (1955).

[7] M. E. Pozin and A. M. Ginstling, J. Appl. Chem. 24, 134 (1951).**

* In Russian.

** Original Russian pagination. See C. B. Translation.

[8] V. V. Pechkovsky, J. Appl. Chem. 28, 237 (1955).*

[9] F. Foerster, K. Kubel, Z. anorg. Ch., 139, 261 (1924).

[10] R. Lepsoe, Ind. Eng. Ch. 30, 92 (1938); 32, 7 (1940).

[11] A. N. Volsky, Fundamentals of Metallurgical Smelting Theory (Metallurgy Press, 1943).* *

[12] O. A. Esin and P. V. Geld, Physical Chemistry of Pyrometallurgical Processes, I (Metallurgy Press, 1950).* *

[13] R. Juza, W. Blanke, Z. anorg. Ch., 210, 82 (1933).

[14] W. Huff, J. Holz, Ind. Eng. Ch., 22, 639 (1930).

[15] E. V. Alekseevsky, R. K. Golts, and A. P. Musakin, Quantitative Analysis (Goskhimizdat, 1953).* *

Received November 21, 1955

* Original Russian pagination. See C. B. translation.

* * In Russian.

DETERMINATION OF THE SOLUBILITY OF CARBON DIOXIDE IN AQUEOUS SOLUTIONS OF SULFURIC ACID BY THE ISOTOPIC DILUTION METHOD

M. K. Shchennikova, G. G. Devyatykh, and I. A. Korshunov

The Gorky State University

The isotopic dilution method can be used for determinations of the solubilities of sparingly soluble gases in liquids.

We used this method for determination of the solubility of carbon dioxide in aqueous sulfuric acid solutions. This is a matter of practical importance, as it is related to the conditions necessary for the most complete recovery of carbon dioxide from solutions by means of sulfuric acid.

The solubility of carbon dioxide in aqueous sulfuric acid solutions has been determined by several workers by the usual methods, and at room temperatures only. Thus, Secenow (Sechenov) [1] carried out determinations at 17°, Geffeken [2], at 15 and 25° (in dilute sulfuric acid solutions up to 4 N), Markham and Cobe [3], at 25°, and Christoff [4], at 17 and 20°.

With the use of the isotopic dilution method we were able to carry out the determinations at higher temperatures (up to 70-75°), at which the solubility of carbon dioxide is low and its determination by the usual methods is very difficult.

EXPERIMENTAL

Reagents. Chemically pure sulfuric acid was used; solutions of the required concentrations were prepared in redistilled water. The purity of the solutions was verified polarographically. The visual polarograph made by the Gorky Chemical Research Institute at the Gorky State University was used, at a shunt ratio of 1/25, the polarograms being taken after hydrogen had been blown through the solutions for 40 minutes. The sensitivity of the mirror galvanometer was $0.7 \cdot 10^{-9}$ amp. $\frac{mm}{m}$. The carbon tracer was the radioactive carbon isotope of mass number 14.

Method. The apparatus used for the solubility determinations is shown in Fig. 1. The principal components of the unit were: the column C, in which the previously degasified solution was saturated with radioactive carbon dioxide; a flask D, into which samples of the saturated solutions were taken and in which the active carbon dioxide in the samples was diluted with inactive carbon dioxide; and an internally filled counter T, used for determinations of the radioactivity of the original gas and of the gas in the sample after dilution. All the apparatus was made from molybdenum glass. The part of the apparatus shown in the upper region on the diagram was used for saturating the solution in the column C with active carbon dioxide. This was made by decomposition of a mixture of $NaHCO_3$ and $BaC^{14}O_3$ by means of 60% sulfuric acid in the vessel *a*.

The temperature of the column was kept constant by circulation of water from an ultrathermostat through its jacket. The lower part of the column, with a side tube for the gas feed, was kept at constant temperature by means of an electric heater. The temperature in the column was recorded by means of an internal thermometer. The bulbs A, from 0.4 to 1 liter in capacity, were used for storage of the active carbon dioxide. The mercury pump P was used to maintain constant pressure of carbon dioxide while the gas was bubbled through the solution, and also for pumping the gas from one vessel into another. The solution saturation time was usually between 1.5 and 3 hours, depending on the viscosity of the solution. Various stopcocks are indicated by the

numbers 1-32. Mercury manometers M were used to record the pressure in the system. Air and water vapor were removed from the carbon dioxide by freezing it by means of liquid oxygen in the traps T, followed by evacuation of the air by means of an oil pump. These traps, and the flasks b and D, were connected to the system by ground-glass joints.

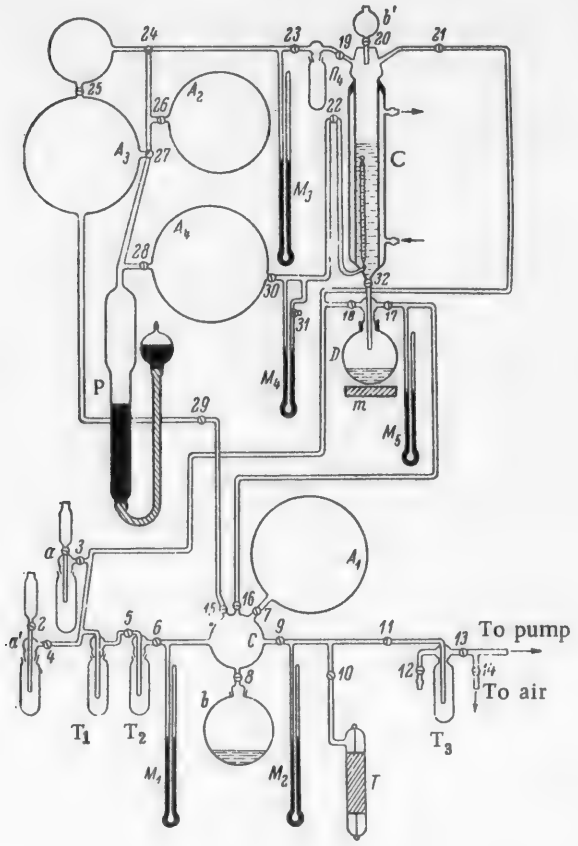

Fig. 1. Apparatus for determination of the solubility of carbon dioxide by the isotopic dilution method.
Explanation in text.

The part of the apparatus shown in the lower portion of the diagram was the internally filled counter system. The internally filled counter was a gamma-ray tube with a copper cathode and a tungsten anode. The counter tube was contained in a lead case and connected to a type B counter unit. The position of the "plateau" of the counter tube was checked at intervals. It remained practically unchanged after repeated filling of the counter with the solution.

The absorption coefficient α (the volume of gas in ml, reduced to standard conditions, absorbed by 1 ml of the solvent at the temperature of the experiment, at a partial gas pressure of 760 mm Hg) was calculated by means of the equation:

$$\alpha = \frac{V_{CO_2} \cdot A_1 \cdot d \cdot 760}{a\,(A_0 - A_1)\,(P - p)} \,. \qquad (1)$$

Here V_{CO_2} is the volume of carbon dioxide (in ml), reduced to standard conditions, taken for dilution of the sample; A_1 is the activity of the gas (in pulses per minute) in the liquid sample after dilution; A_0 is the initial activity of the gas used for saturation of the solution in the column; a is the weight of the solution sample (in g); d is the density of the solvent (in g/cc) at the temperature of the experiment; P is the pressure of the gas during saturation (in mm Hg) as shown by the manometer M_3; p is the vapor pressure of the solution in the experimental conditions. To test the accuracy and reproducibility of the experiments, the solubility of carbon dioxide in distilled water was determined; this value is relatively high and has been determined by a number of workers [5] by means of the usual methods.

The results of our determinations are given in Table 1.

It is seen that our values for the absorption coefficient α are in fairly good agreement with the literature data, while deviations between the results of parallel experiments do not exceed 7%.

TABLE 1

Solubility of Carbon Dioxide in Distilled Water

Temperature (°C)	Solubility α (ml/ml)		Temperature (°C)	Solubility α (ml/ml)	
	our data	literature data		our data	literature data
20	0.88		50	0.441	0.436
20	0.90		60	0.336	
20	0.88		60	0.341	
20	0.91		60	0.333	
			60	0.329	
mean	0.89	0.878	60	0.324	
			60	0.313	
28	0.72		60	0.349	
40	0.55		60	0.356	
40	0.54		60	0.330	
mean	0.545	0.530	mean	0.335	0.359
			75	0.235	

The results of solubility determinations, carried out by this method, for carbon dioxide in aqueous sulfuric acid solutions are given in Table 2. Here N_s is the solubility of carbon dioxide expressed in mole fractions.

DISCUSSION OF RESULTS

Effect of temperature on the solubility of carbon dioxide in aqueous sulfuric acid solution. The temperature coefficient of the solubility of carbon dioxide is negative for all the solutions studied. A typical solubility – temperature graph for carbon dioxide is shown in Fig. 2.

As is known, if a solution of a gas in a liquid obeys the ideal solution laws, a graph plotted in log $N_s - \frac{1}{T}$, coordinates can be used to calculate the differential heat of solution of the gas.

In Fig. 3 log N_s is plotted against 1/T from the data in Table 2. The differential heats of solution are given in Table 3.

It is seen from Table 3 that the heat of solution of carbon dioxide decreases with increasing sulfuric acid concentration. This can evidently be attributed to a lower degree of chemical interaction of carbon dioxide in sulfuric acid solutions as compared with solutions of carbon dioxide in water. This is in good agreement with the higher values for the heats of solution of gases which react chemically with the solvents [6, 7]. These data can evidently be used for determination of the ratio between the chemically bound and the physically dissolved carbon dioxide.

Effect of sulfuric acid concentration on the solubility of carbon dioxide. Fig. 4 shows the solubility of carbon dioxide as a function of the sulfuric acid concentration, based on the data in Tables 1 and 2.

TABLE 2

Solubility of Carbon Dioxide in Aqueous Sulfuric Acid Solutions

H_2SO_4 concentration (in wt. %)	Temperature (°C)	Solubility α (in ml / ml)	$N_s \cdot 10^4$	H_2SO_4 concentration (in wt. %)	Temperature (°C)	Solubility α (in ml / ml)	$N_s \cdot 10^4$
9.25	19	0.82	6.78	61.6	15	0.85	9.12
	19	0.85	7.00		15	0.87	9.27
	25	0.72	5.94		15	0.82	8.78
	27	0.67	5.57		17	0.76	8.20
	38	0.525	4.36		17	0.75	8.08
	38	0.531	4.41		18	0.76	8.17
	45	0.438	3.65		18	0.74	7.91
	50	0.415	3.47		18	0.73	7.86
	50	0.412	3.44		18	0.73	7.87
	56	0.355	2.98		21	0.69	7.38
	56	0.345	2.89		25	0.70	7.58
	60	0.337	2.83		25	0.68	7.34
	60	0.329	2.76		25	0.68	7.37
30.5	18.5	0.71	6.22		25	0.70	7.53
	19	0.69	6.10		25	0.72	7.75
	26	0.56	4.95		25	0.64	6.88
	26	0.55	4.88		25	0.63	6.80
	41	0.423	3.77		25	0.64	6.90
	52	0.329	2.96		25	0.63	6.74
	64	0.258	2.33		25	0.63	6.82
	77	0.219	1.99		25	0.63	6.79
36.9	19.5	0.68	6.20		25	0.64	6.90
	19.5	0.71	6.49		25	0.68	7.30
	24	0.65	5.88		26	0.62	6.72
	33	0.497	4.54		31	0.57	6.20
42	20	0.72	6.70		37	0.54	5.82
	20	0.70	6.52		51.5	0.409	4.47
	24.5	0.62	5.83		61	0.333	3.66
	26	0.60	5.60		75	0.243	2.70
	30	0.58	5.41	77.6	21	0.62	8.09
	30	0.57	5.34		25	0.62	8.11
	31	0.57	5.39		26	0.62	8.05
	40	0.47	4.43		42	0.488	6.43
	40	0.464	4.38		46	0.473	6.23
	40	0.470	4.43	78.8	32	0.497	6.58
	44	0.436	4.13		40	0.473	6.34
	50	0.374	3.55		50	0.444	5.98
	54	0.350	3.33		60	0.352	4.78
	70	0.248	2.38	84.48	20	0.63	9.33
	76	0.216	2.08				

TABLE 3

Differential Heats of Solution L of Carbon Dioxide

Solvent	Temperature range (°C)	L cal/ mole (± 10%)
Distilled water	20 —60	5000
9.25% H_2SO_4	19 —60	4400
30.5% H_2SO_4	18.5—77	4300
42% H_2SO_4	20 —76	4150
61.6% H_2SO_4	15 —75	3700
77.6% H_2SO_4	25 —46	2300

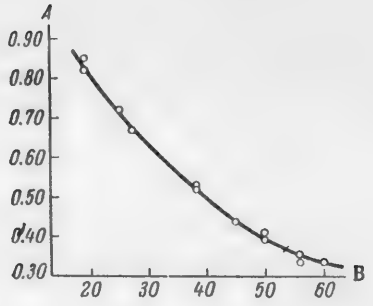

Fig. 2. Effect of temperature on the solubility of carbon dioxide in 9.25% sulfuric acid.
A) Absorption coefficient α, B) temperature (°C).

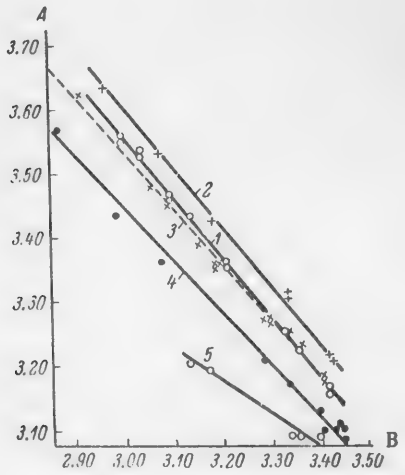

Fig. 3. Log N_S as a function of 1/T.
A) log N_S, B) $\frac{1}{T} \cdot 10^3$.
Concentrations of H_2SO_4 (in %): 1) 9.25, 2) 30.5, 3) 42, 4) 61.6, 5) 77.6.

It is seen that the solubility curve passes through two minima, at acid concentrations of 30 and 85% by weight. This is in agreement with data for room temperatures [1, 4]. We did not determine the solubility of carbon dioxide at acid concentrations above 85%, and the value for concentrated sulfuric acid was taken from the literature [1].

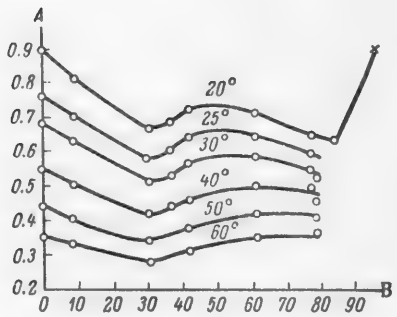

Fig. 4. Variation of the solubility of carbon dioxide with sulfuric acid concentration at various temperatures.
A) Absorption coefficient α, B) H_2SO_4 concentration (in % by weight).

It is clear from Fig. 4 that as the temperature increases the "depth" of these minima diminishes, and the curves become flatter. The decreasing solubility of carbon dioxide with increase of sulfuric acid concentration in dilute solutions (up to ~ 30%) may be attributed to the fact that in this concentration range sulfuric acid is a typical electrolyte (the conductivity maximum of sulfuric acid is at about 30% [8]) and therefore, in accordance with Sechenov's equation [9], the solubility of the gas should vary steadily with increasing electrolyte concentration.

The presence of a maximum on the solubility – sulfuric acid concentration curve at a concentration of the order of 55%, and of a minimum at a concentration of ~85% may be attributed to the existence of sulfuric acid hydrates in the solution ($H_2SO_4 \cdot 4H_2O$, in the first case, and $H_2SO_4 \cdot H_2O$ in the second) which absorb the gas to different extents. The existence of sulfuric acid hydrates was first reported by Mendeleev [10]. Kurnakov [11] studied the phase diagram for the system sulfuric anhydride – water and concluded that the following hydrates exist in solution: $H_2SO_4 \cdot SO_3$, H_2SO_4, $H_2SO_4 \cdot H_2O$, $H_2SO_4 \cdot 2H_2O$, $H_2SO_4 \cdot 4H_2O$, $H_2SO_4 \cdot nH_2O$ (n = 6.8). The existence of hydrates at sulfuric acid concentrations of ~ 55 and 85% is confirmed by Fig. 5, which shows the phase diagram for the system sulfuric acid – water, viscosity isotherms for this system at 35 and 50° (from Kurnakov's

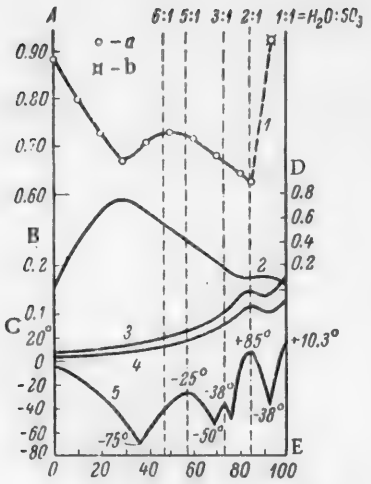

Fig. 5. Comparison of various properties for the system sulfuric acid – water. A) Solubility of CO_2 (α), B) viscosity coefficient, C) temperature (°C), D) conductivity κ (in $ohm^{-1} \cdot cm^{-1}$), E) H_2SO_4 concentration (%). Curves: 1) Solubility of carbon dioxide at 20°; a) our data, b) Secenow's data [1]; 2) conductivity at 18° [8]; 3 and 4) viscosity coefficient η at 35 and 50° respectively [11]; 5) phase diagram, from Kurnakov's data [11].

data [11]), the electrical conductivity isotherm at 18°. [8], and the solubility isotherm for carbon dioxide at 20° from our data (except for the value of α in 96.5% sulfuric acid, taken from the literature [1]).

Varlamov [12] also demonstrated the existence of special points on the viscosity – composition curve corresponding to sulfuric acid concentrations of 55 and 85%. It is seen in Fig. 4 that the solubility curves become flatter with increase of temperature; this can be attributed to dissociation of the hydrates into the components.

SUMMARY

1. The solubilities of carbon dioxide in aqueous sulfuric acid solutions have been determined over the 18-75° range by the isotopic dilution method, with radioactive carbon C^{14} as tracer.

2. The temperature – solubility relationship was used to calculate the differential heats of solution of carbon dioxide.

3. It is shown that the solubility curve of carbon dioxide in aqueous sulfuric acid solutions has "special points" associated with the existence of hydrates.

LITERATURE CITED

[1] I. Secenow, Bull. l' Acad. sc. st. Petersb., 22, 102 (1877).

[2] G. Geffcken, Z. phys. Ch., 49, 257 (1904).

[3] A. E. Markham a. K. A. Cobe, J. Am. Chem. Soc., 63, 512 (1941).

[4] A. Christoff, Z. phys. Ch., 53, 321 (1906); 55, 622 (1906); 79, 456 (1912).

[5] A. Seidell, Solubilities of Inorganic and Metal Organic Compounds, I, 221 (1940).

[6] Technical Encyclopedia, Physical, Chemical, and Technological Data, VII (Moscow, 1931) pp. 375, 378.*

[7] M. A. Lyudkovskaya and A. G. Leibush, J. Appl. Chem. 22, 558 (1949).

[8] Chemist's Reference Book III (State Chem. Press, Moscow – Leningrad 1952) p. 443.*

[9] I. M. Sechenov, J. Russ. Phys. -Chem. Soc. 18, section 1, 63 (1886).

[10] D. I. Mendeleev, Works, IV (ONTI, Chem. Theoret. Press, Leningrad, 1937) pp. 159, 405.*

[11] N. S. Kurnakov, Introduction to Physicochemical Analysis (Izd. AN SSSR, Moscow – Leningrad, 1940).*

[12] M. L. Varlamov, J. Appl. Chem. 25, 553 (1952).**

Received December 10, 1955

* In Russian.

** Original Russian pagination. See C. B. translation.

SECONDARY PROCESSES ON AMPHOTERIC ION EXCHANGE RESINS AND THE POSSIBILITY OF THEIR PRACTICAL UTILIZATION

A. B. Davankov, V. M. Laufer, and L. A. Shits

Synthetic resins obtained by polycondensation and polymerization reactions are widely used in various branches of the national economy.

A comparatively new field of application for synthetic resins is sorption technology. However, in this field also considerable progress has been made in a short time. Evidence for this is the extensive patent and periodical literature on the theory and practice of ion exchange. The great majority of the investigations have dealt with studies of the properties and applications of ion exchange resins, determinations of the laws governing ion exchange processes, etc. [1].

However, the secondary processes accompanying ion exchange have not received due attention in the literature, although in some instances they are of great importance and have a significant influence on the final results of the investigations. Moreover, secondary processes occurring in parallel with ion exchange or subsequent to it are of independent importance and can sometimes be utilized for practical purposes, such as extraction and accumulation of adsorbed substances on the resins in amounts greater than the total exchange capacities of the resins.

Secondary processes accompanying ion exchange include molecular adsorption, oxidation – reduction reactions, coagulation ofvarious types of dispersions (latexes, metallic suspensions, etc.) by the resins, etc.

This last property of ion exchange resins was used in one of our earlier investigations both for quantitative determinations of precious metals in aqueous dispersions, and for recovery of precious metals (gold and silver) from production wastes [2]. In these processes the multivalent ions of the resin adsorbents had a much greater coagulating effect than the usual electrolytes such as $Al_2(SO_4)_3$, $FeCl_3$ etc.; this, however, is in full agreement with the Shulze – Hardy rule.

The results suggest that ion exchange resins will soon come into practical use as a new and highly effective means of coagulation.

In the present paper we consider the practical utilization of reduction – oxidation processes on ion exchange resins; amphoteric resins, the properties of which have been studied little so far, were investigated in relation to their reducing activity. This group of adsorbents, which include both acid and basic groups in their composition, are of definite interest from our point of view: such resins can be used both as cation and as anion exchangers [3]. Amphoteric ion exchange resins have special advantages for the extraction of amphoteric elements and also of elements capable of forming complexes.

Among the large group of ion exchange resins, the greatest reducing power, according to Losev and Tevlina [4], is found in resins made by condensation of phenol and its derivatives with formaldehyde. This property is found to a smaller extent in resins obtained by sulfonation of styrene – divinylbenzene copolymers.

Reduction processes on ion exchange resins were observed by Prokhorov and Yankovsky [5] in the extraction of silver ions from aqueous solutions by means of Wofatit P.

A similar effect in relation to silver ions was also observed by Lurye and Peremyslova [6] in tests on Wofatit P. They found that in this case the silver is reduced by the resin itself, which undergoes a chemical change and ultimately loses its ion exchange properties.

In contrast to cation exchange resins, anion exchangers, according to the same authors, are typical catalysts and do not change their capacity in course of time. In their presence adsorbed anions containing silver, such as $[Ag(S_2O_3)_2]'''$, decompose according to the equation

$$2[Ag(S_2O_3)_2]''' \rightleftharpoons Ag_2S_2O_3 + 3S_2O_3''$$

$$Ag_2S_2O_3 + H_2O \rightarrow Ag_2S + H_2SO_4.$$

The silver sulfide formed remains on the adsorbent and the adsorption capacity of the resin for the complex silver anion returns to the original level. Thus, after a certain "rest" period the resin again becomes capable of exchanging the SO_4' ions present in it for $[Ag(S_2O_3)_2]'''$ ions.

In 28 cycles of silver-ion sorption (with regeneration of the resin after each cycle with caustic soda solution, and "charging" of the resin with SO_4' ions), these authors [6] succeeded in accumulating 61% of silver, calculated on the resin weight, on the anion exchanger.

In addition to reduction of silver, the reduction of mercury and other metals from their salts has been reported in the literature.

All this shows that the secondary processes accompanying ion exchange, and also processes inducted artificially on ion exchange resins, might be very effectively used for practical purposes, such as the extraction of precious metals (gold, platinum, silver, etc.) from industrial wastes.

The aim of the present investigation was to confirm that amphoteric ion exchange resins have reducing properties and to use both natural and artificial reduction for accumulation of considerable amounts of metallic silver on ion exchange resins during the sorption process. Artificial reduction, induced on ion exchange resins with the aid of available reducing agents, may have advantages over spontaneous reduction by the catalytic action or oxidizability of the resins, both with regard to a considerable saving of time, and with regard to reproducibility of the results.

In addition to reduction processes, we also studied the possibility of simultaneous or consecutive sorption of cations and anions on the same adsorbent, and compared the capacities of amphoteric resins with the ion exchange capacities of known anion and cation exchangers.

The material used was "VST" amphoteric resin synthesized by us; this differed from the previously described "VS" resin by a higher sulfur content (10.25% on the weight of the resin), of which not more than one third belongs to active SO_3H groups. The remaining sulfur in the resin is not active, as it forms part of the resin "skeleton" and has no significant influence on the ion exchange process.

A second characteristic of "VST" amphoteric resin is the higher nitrogen content, and hence greater basicity, than that of "VS" resin.

The technical characteristics of "VST" resin are: white color, bulk density of the air-dry resin (with 0.5-1.0 mm grains) 0.46, moisture content of the air-dry resin 15%, true specific gravity 1.135, volume increase on swelling in water 12%.

The static exchange capacities (in meq/g) for ions of 0.1 N solutions of acids and salts are: Cl' 3.3; SO_4' 3.8, CH_3COO' 0.95, K^+ 1.0; Ag^+ 1.02.

The extraction of silver ions was carried out under dynamic conditions. 5 g of the air-dry resin was placed in a glass tube of 50 mm^2 cross-section. Through a 30 cm layer of this resin 5% NaOH solution was passed in order to convert the acid groups of the resin into the Na form; this was followed (after excess alkali had been washed out with distilled water) by silver nitrate solution with a concentration of 0.0695 g-equiv/liter in the first 8 cycles, and 0.0750 g-equiv/liter in all subsequent cycles; the percolation rate of the solution through the resin was 2 ml/minute. "Breakthrough" of Ag^+ ions was tested for by means of NaCl solution. After "breakthrough" occurred in the first two sorption cycles, the resin was washed with water until all traces of $AgNO_3$ had been removed from the resin, and the flow of solution through the resin was resumed. In all the subsequent cycles the adsorbent was not washed with water. Together with the sorption of silver ions, especially after the resin had been left at rest for some time, the reduction of silver ions to the metal was observed on the resin, as indicated by blackening of the resin and recovery of its capacity for further absorption of silver ions from solution.

When silver ions appeared in the filtrate, the flow of the silver nitrate solution was stopped, and 25 ml of hydroquinone solution, containing 0.5 ml of 25% ammonia solution, was passed through the resin. The silver cations extracted by the resin were then reduced to the metal by the hydroquinone.

At the end of the experiment the resin grains became coated with silver, crystals of which were visible to the naked eye. The reduction of silver ions to the metal occurred according to the scheme:

$$2HOR - SO_3Ag + C_6H_4(OH)_2 + 2NH_4OH \rightarrow$$

$$2HOR - SO_3NH_4 + C_6H_4O_2 + 2Ag^{\circ} + 2H_2O.$$

In the subsequent adsorption cycles the NH^4 (or H^+) ions were again replaced by Ag^+ ions, and this was repeated until, as the result of 22 consecutive sorption cycles and the same number of reductions, 4.57 g of metallic silver accumulated on the resin, corresponding to 107% on the dry resin weight, or 9.96 meq/g. The sorption capacity of the resin was not fully exhausted, as is shown by the data in the Table, although the relative capacity of the resin fell gradually in successive cycles.

Extraction of Silver Ions from $AgNO_3$ Solution by "VST" Amphoteric Resin

Concentration of $AgNO_3$ solution (meq/liter)	Number of ml of $AgNO_3$ solution passed before breakthrough of Ag^+ ions	Amount of Ag adsorbed		
		g	% on the weight of dry resin	meq/g
0.0695	60	0.4493	10.57	0.98
	20	0.1498	3.52	0.33
	45	0.3371	7.93	0.73
	40	0.2996	7.05	0.65
	31	0.2321	5.47	0.51
	32	0.2397	5.64	0.52
	32	0.2397	5.64	0.52
	30	0.2246	5.28	0.49
0.0750	27	0.2180	5.13	0.48
	28	0.2261	5.33	0.49
	23	0.1857	4.37	0.40
	23	0.1857	4.37	0.40
	27	0.2180	5.13	0.48
	26	0.2100	4.94	0.46
	24	0.1939	4.56	0.42
	17	0.1373	3.23	0.30
	15	0.1211	2.85	0.26
	17	0.1375	3.23	0.30
	15	0.1211	2.85	0.26
	20	0.1615	3.80	0.36
	18	0.1453	3.42	0.32
	17	0.1373	3.23	0.30
Total	587	4.5704	107.54	9.96

It is difficult to say whether the decrease of the exchange capacity of the resin was the result of chemical changes in its composition, as was the case in Lurye and Peremyslova's experiments with a cation exchange resin, or whether it was the result of filling of the surface and the internal pores of the amphoteric resin with crystals of metallic silver, so that the functional groups in the resin became less accessible to the silver ions present in solution. This question can only be answered after removal of the silver from the surface of the resin and repeated tests of the ion exchange capacity of the regenerated resin.

In the present investigation silver was isolated from the resin by combustion of the latter; the amounts of silver obtained in this way were in good agreement with calculated data (i.e., amounts of silver present in the solution before it entered the adsorption column).

An x-ray photograph showed that most of the silver was present in the upper layers of the adsorbent, while the silver content of the lower layers was considerably less.

In this way the conditions were found for accumulation of considerable amounts of silver on the absorbent by alternate utilization of cation exchange and secondary processes (reduction) on an ion exchange resin.

A similar attempt was then made in the extraction of complex $Ag(CN)_2^-$ anions from $[KAg(CN)_2]$. However, this attempt was not successful because the basic groups of the amphoteric resin dissociate only very slightly in neutral and alkaline solutions; when the $[KAg(CN)_2]$ solution was acidified, AgCN was precipitated.

To avoid this difficulty and to demonstrate the possibility of simultaneous or consecutive sorption of cations and anions on amphoteric ion exchange resins, we used a solution of potassium cyanoaurate; acidification of this salt (in contrast to the analogous silver salt) yields the fairly stable cyanoauric acid $[HAu(CN)_2]$, the complex anion of which, $Au(CN)_2^-$, was satisfactorily exchanged with the corresponding anions of the amphoteric resin (OH^-, Cl^-, NO_3^-, etc.). No insoluble precipitate of gold cyanide was formed in this case.

The extraction of $Au(CN)_2^-$ anions was carried out under the same conditions as for silver cations, the only difference being that the pH of the original solution was 3.5, and the gold concentration was 20 mg (as metallic gold) per liter; the amphoteric resin was used in the chloride form; the solution was percolated through the adsorption column with the resin at an average rate of 2-3 ml/minute.

Breakthrough of gold anions was detected after 22.625 liters of solution had passed through the adsorbent; from this, 5 g of the air-dry resin extracted 425.5 mg of gold, which was 10.01% on the weight of the absolutely dry resin, or 0.92 meq/liter.

The flow of potassium cyanoaurate solution was then stopped, and the resin was washed first with 100 ml of 5% ammonia solution, and then with distilled water.

The reason for using ammonia to wash the adsorbent was to replace the hydrogen ions in the acid groups of the resin by NH_4^+ ions (according to the scheme $HOR \cdot SO_3H + NH_4OH \rightarrow HOR - SO_3NH_4 + H_2O$) which are more readily exchanged than are hydrogen ions, in particular for silver cations Ag^+, as it was intended to use the resin for adsorption of the latter without previous removal of the adsorbed gold cations.

However, the attempt to bring about consecutive sorption and accumulation of considerable amounts of gold anions and silver cations on the amphoteric resin proved unsuccessful, as the ammonia solution displaced 95% of the initial gold content from the resin. This high degree of regeneration of the resin by weak ammonia solution proved somewhat unexpected, although very interesting from the practical standpoint, despite the fact that it prevented us from taking the experiment to its logical conclusion.

A fresh portion of air-dry "VST" amphoteric resin, 5 g in weight, was taken, and 666 ml of 0.01 N $AgNO_3$ solution (K = 1.26) was passed at a rate of 6 ml/minute through a 25 cm layer of this resin in a glass tube 7.5 mm in diameter. The resin was taken in the hydroxyl form, and the silver nitrate solution was passed in four stages, with intervals of several hours (3-16) to 3 days.

After "rest" the resin regained its capacity for ion exchange, and it was thus possible to accumulate 634 mg of silver, calculated as the metal, on it. (The amount of silver adsorbed by the resin was found from the difference of the silver contents of the solution before and after percolation through the resin.)

The resin was then washed with 5% hydrochloric acid solution to convert the basic groups into the chloride form (HO_3SRNH_3Cl), and then 19 liters (until "breakthrough" of gold ions) of potassium cyanoaurate solution containing 20 mg of gold per liter, acidified to pH 3.5 was passed through it. After combustion of the resin and cupellation of the ash, an alloy of gold and silver weighting 0.9724 g was obtained; 0.380 g of this was gold, and 0.5924 g silver.

It was thus demonstrated that consecutive extraction of silver cations and gold anions from aqueous solutions by means of the same adsorbent, namely "VST" ion exchange resin, is possible. Therefore, amphoteric ion exchange resins may have certain advantages in this respect over the usual cation and anion exchangers, especially if, in addition to ion exchange processes, secondary processes (reduction, coagulation, precipitation, etc.) are used for accumulation of valuable substances on them.

SUMMARY

1. The possibility of separate or consecutive extraction of silver cations and gold anions from aqueous solutions by means of a synthetic amphoteric ion exchange resin has been demonstrated.

2. By the use of ion exchange and of secondary reactions on ion exchange resins it is possible to concentrate considerable amounts of adsorbate (over 100% on the weight of the adsorbent) on the resins.

Conditions for regeneration of the resin and extraction of precious metals from it after adsorption have been found.

LITERATURE CITED

[1] Ion Exchange, Collected Papers (IL, Moscow, 1951); *Proc. All-Union Conf. on Chromatography (Izd. AN SSSR, 1952); **V.V.Rachinsky and G. B. Gapon, Chromatography in Biology (Izd. AN SSSR, 1953); ** R. Kunin and R. Myers, Ion Exchange Resins (IL, Moscow, 1953); * F. M. Shemyakin, E. S. Mitselovsky, and D. V. Ramanov, Chromatographic Analysis (Goskhimizdat, 1955). **

[2] A. B. Davankov and V. M. Laufer, Authors' Certif. 37/1821, August 21, 1954.

[3] A. B. Davankov, N. E. Ogneva, and V. M. Laufer, J. Chem. Ind. 11, 18 (1951); A. B. Davankov, G. S. Petrov, N. E. Ogneva, and V. M. Laufer, Authors' Certif. 100,692 (1950).

[4] I. P. Losev and A. S. Tevlina, Abstracts of Papers at the Conference on the Applications of Chromatographic Methods (Izd. AN SSSR). **

[5] F. G. Prokhorov and K. A. Yankovsky, Factory Labs. 6 (1947).

[6] Yu. Yu. Lurye and E. S. Peremyslova, J. Appl. Chem. 27, 11, 1207 (1954). ***

Received October 31, 1955

* Russian translation.

** In Russian.

*** Original Russian pagination. See C. B. translation.

CHEMICAL SELECTIVITY OF PHOSPHATE AND CALCITE IN ORES WITH RECOVERY OF THE REAGENTS

A. S. Chernyak

Beneficiation of skarn rocks and certain sedimentary rocks yields collective concentrates which contain calcite in addition to valuable calcium minerals (scheelite, apatite, phosphate). Separation of these concentrates frequently involves technical difficulties and high losses of valuable minerals with the calcite.

Combinations of calcium minerals which have to be separated are "calcite – scheelite," "calcite – apatite," "calcite – phosphate," and "calcite – scheelite – apatite."

For ores in which these minerals are finely disseminated, mechanical separation is impossible at the degrees of subdivision possible in practice. Together with the known instances of successful separation of calcium minerals by flotation and other mechanical beneficiation methods, examples may be cited when these methods have been unsuccessful. For example, at the Getchell Mine in the U.S.A., where scheelite ores from six different sources are treated [1], and in the beneficiation of certain phosphorite rocks [2], the problem was solved only by chemical beneficiation of the combined concentrates, by leaching out the calcite with hydrochloric acid or ammonium chloride solutions.

Selective separation of calcite from such ores is necessary, as in many cases acid processes for the winning of valuable minerals are used.

The development of acceptable methods for separation of calcite is especially important in relation to the utilization of low grade sedimentary rocks containing large reserves of valuable components.

The foregoing considerations prompted the present work on the chemical separation of calcium minerals in ores.

Two methods of chemical separation were of greatest practical interest in this connection: 1) selective dissolution of calcite or apatite, whereby it is possible to obtain flotation concentrates of good quality, to separate calcite, apatite, and scheelite, and to decrease the consumption of acid in the subsequent treatment; 2) binding of the carbonate calcium in the form of compounds which are insoluble during the subsequent leaching of the valuable component, in order to decrease acid consumption.

It was taken into consideration that either method could only be technologically suitable and economically acceptable on the condition that the reagents used for the chemical separation are recovered.

In our opinion, recovery schemes in which components liberated into the gas phase are recovered are of considerable interest.

Alternative methods for solving this problem in relation to low-grade carbonate – phosphate rocks are given below.

These methods and schemes for chemical separation have been designed in relation to conversion of the raw material into precipitated dicalcium phosphate. However, they may be used in other cases with the object of reducing the consumption of acid for decomposition of calcite.

The investigations on the selective leaching of calcite were carried out by the author, with the participation of N. G. Rudenko and V. A. Rudakov in some sections of the work.

The method for binding carbonate calcium, suggested by I. K. Skobeev and V. V. Lodeishchikov in Irgiredmet,* was studied on a larger scale and in an experimental semiworks unit by the author with V. V. Lodeishchikov.

EXPERIMENTAL

Flotation concentrates obtained by beneficiation of a lean carbonate – phosphate rock were used for the investigation. The rock contained 2-4% P_2O_5. From it was isolated a combined carbonate – phosphate flotation concentrate containing 6-13% P_2O_5 and 40-50% of calcite. Flotation separation of this concentrate involved phosphorus losses of the order of 10% and over, but despite this the selective flotation concentrates contained 20-25% of calcite. In addition, this stage yielded a carbonate – phosphate product, similar in composition to the combined flotation concentrate, in 3% yield calculated on the rock, with 8% extraction of phosphorus from it.

Acidulation both of the combined and of the selective flotation concentrates involves very high consumption of sulfuric acid, as decomposition of the calcite requires 400-450 kg of sulfuric acid per ton of flotation concentrate in the first case, and about 200 kg in the second.

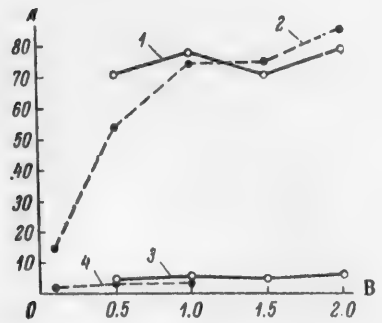

Fig. 1. Selective leaching of calcite with dilute solutions of hydrochloric and nitric acids.
A) Extraction into solution (%), B) concentration of acid (%).
1, 2) Extraction of carbonate calcium into solutions of HCl and HNO_3 respectively, 3, 4) extraction of phosphorus into the same solutions.

Selective leaching of calcite. The experiments commenced with a search for selective solvents for calcite. It is known that this mineral is chemically less stable than apatite or sedimentary phosphate.

Very dilute (0.5-2.0%) solutions of hydrochloric and nitric acids were found to act as selective solvents for the material in question. The use of nitric acid is to some extent economically justifiable, as calcium nitrate can be isolated from the resultant liquors.

The results of selective leaching of calcite and phosphate with dilute solutions of mineral acids are shown graphically in Fig. 1.

The positive result obtained with dilute solutions of strong acids suggested the use of an acid of moderate strength – sulfurous – for this purpose. The decomposition of phosphate rocks with sulfurous acid has already been studied in detail. However, examination of the literature data on this subject [3-5] showed that for satisfactory decomposition of phosphate or apatite it is necessary to use a 4 to 6-fold excess of sulfur dioxide over the theoretical amount, even if 100% sulfur dioxide or saturated aqueous SO_2 is used. In many cases the phosphorous remains in the solid phase as dicalcium phosphate. It is known, however, the calcite is easily leached out with dilute solutions of sulfurous acid.

Technical sulfur dioxide, supplied in cylinders by the Chernorechensky Combine, was used for the experiments.

The first experiments were performed with a fairly dense aqueous pulp (with liquid – solid ratios of 2 to 5 to 1), through which sulfur dioxide was passed continuously with stirring, with the H_2SO_3 concentration in the solution maintained at the desired level.

It was later found that the factor determining complete dissolution of the calcite is the total amount of sulfurous acid supplied into the process. It was therefore possible to use another method. A solution of definite

* The Irkutsk State Institute of Rare Metals.

concentration, containing the amount of sulfurous acid necessary for leaching out the calcite, was first prepared. The degree of dilution of the pulp depended on the concentration and the total amount of sulfur dioxide.

The amount of sulfurous acid required, determined experimentally, is in practice close to the stoichiometric amount as given by the equation

$$CaCO_3 + 2H_2SO_3 \rightarrow Ca(HSO_3)_2 + CO_2^{\uparrow} + H_2O. \quad (1)$$

Analysis of the cakes obtained under different conditions of sulfur dioxide leaching showed that usually the calcite was almost entirely decomposed, and that the degree of removal of calcium mainly depends on the degree of conversion of calcium sulfite to bisulfite.

It was found experimentally that sulfurous acid solutions containing about 30-50 g H_2SO_3 per liter dissolve calcite almost completely (to 80-90%) with hardly any extraction of phosphorus. The results of laboratory trials of sulfurous acid leaching carried out on 200 g samples of flotation concentrate, are given in the Table.

Results of Laboratory Experiments on Leaching of Calcite with Sulfurous Acid from Flotation Concentrates with Different Concentrations of Calcite and Phosphate

Contents in the original flotation concentrate (%)		Leaching conditions		Extracted into solution (%)	
Carbonate CaO	P_2O_5	residual concentration of H_2SO_3 (in g/lit.)	liquid-solid ratio	Carbonate CaO	P_2O_5
19.4	12.4	74	2 : 1	59.8	Traces
19.4	12.4	75	2.5 : 1	71.2	
19.4	12.4	76	3 : 1	84.2	2.8
19.4	12.4	65	4 : 1	84.5	3.5
19.4	12.4	38	5 : 1	71.0	0.5
19.4	12.4	51	5 : 1	88.0	1.2
19.4	12.4	62	5 : 1	88.5	3.9
19.4	12.4	65	5 : 1	86.0	3.2
16.9	12.0	50	5 : 1	82.0	Traces
20.0	11.6	50	5 : 1	93.4	
19.4	12.4	38	10 : 1	86.0	7.1
19.4	12.4	50	10 : 1	90.5	6.4
28.3	5.7	51	4 : 1	76.9	1.2
28.3	5.7	57	4 : 1	72.4	2.2
28.3	5.7	59	6 : 1	75.0	7.5
28.3	5.7	73	6 : 1	87.8	4.4
28.3	5.7	56	8 : 1	80.0	14.0
28.3	5.7	24	10 : 1	55.6	8.7
28.3	5.7	41	10 : 1	80.6	13.8
28.3	5.7	100	10 : 1	95.8	15.4
28.8	6.4	40*	17 : 1	42.0	7.0
28.8	6.4	40*	18 : 1	63.0	18.8
28.8	6.4	30*	23 : 1	44.0	10.4

* Initial concentration.

The extraction of phosphorus into the sulfurous acid solution depends to a considerable extent on the dilution of the pulp – the liquid – solid ratio -- and increases at liquid – solid ratios of 8 : 1 and over. This was especially prominent in experiments carried out by the second alternative method with liquid – solid ratios between 17 and 23 to 1. With thicker pulps the extraction of phosphorus into solution does not exceed 1-5%.

Study of the chemical properties and characteristics of the calcium salts of sulfurous and phosphoric acids provided the solution to another important problem – recovery of the sulfurous acid, as without recovery chemical separation would merely result in replacement of part of the sulfuric acid by sulfurous.

The calcium bisulfite formed according to Equation (1) is a readily soluble salt, but it can only exist in solution in presence of excess SO_2. When the latter is removed from solution, the normal salt $CaSO_3 \cdot 2H_2O$ is quantitatively precipitated:

$$Ca(HSO_3)_2 + H_2O \rightarrow CaSO_3 \cdot 2H_2O + SO_2\uparrow. \quad (2)$$

Decomposition of the acid salt in solution is therefore accompanied by liberation into the gas phase of half the total SO_2 used for leaching out the calcite.

Moreover, it was found that the SO_2 combined in normal calcium sulfite can also be recovered. The reduction of calcium sulfite to sulfide, with treatment of the CaS with steam followed by combustion of the hydrogen sulfide, was first studied. The experiments showed that up to 80% of the SO_2 present in $CaSO_3$ can be recovered in this way. The reduction is most complete at 700°. Attempts were made, without success, to bring about thermal dissociation of calcium sulfite. A simpler and acceptable solution to the problem was then found – decomposition of calcium sulfite by phosphoric acid solution.

It was found that SO_2 can be liberated quantitatively from calcium sulfite if the latter is put into phosphoric acid solution. As in the process under consideration phosphoric acid solutions are obtained, used later for precipitation of dicalcium phosphate, this method must be regarded as the most suitable.

This stage of the process can be represented by the equation

$$H_3PO_4 + CaSO_3 \cdot 2H_2O \rightarrow CaHPO_4 \cdot 2H_2O + SO_2\uparrow + H_2O. \quad (3)$$

This course of Reaction (3) and its definite shift to the right were confirmed by x-ray structure analysis of the solid reaction product.

These results led to the development of a recovery process associated with the process for extraction of phosphorus from the raw material to give dicalcium phosphate.

The process is represented schematically in Fig 2.

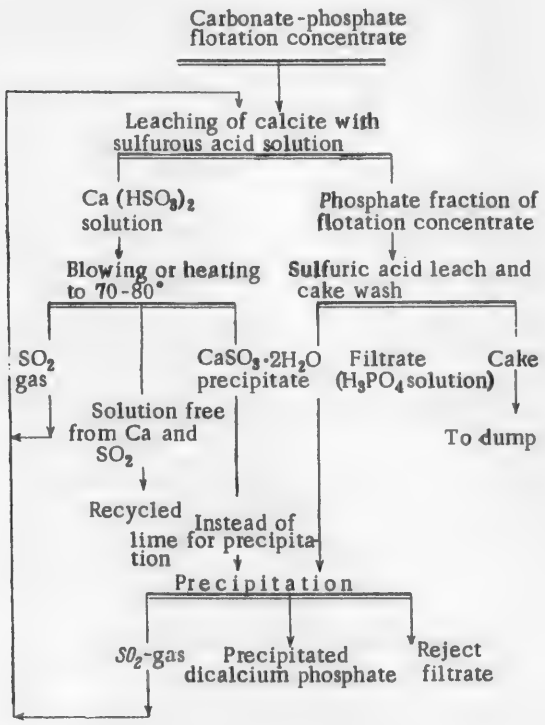

Fig. 2. Flow sheet for selective separation of phosphate and calcite be means of sulfurous acid, and recovery of the latter.

The individual stages of the process were studied in laboratory conditions. In addition, the process for selective leaching of calcite was tested on the semiworks scale with 370 kg of flotation concentrate. The concentrate used for the latter trial contained 51.4% of calcite and only 6.4% P_2O_5, and was technologically very unfavorable.

The concentrates of this composition were obtained from a rock variety with calcium phosphate present mainly in a finely divided state, and only 1/3 of it was in the form of granular crystalline phosphate with grains between 0.001 × 0.006 mm and 0.02 × 0.06 mm.

The experiment was carried out by the second alternative method at a liquid – solid ratio of 19 : 1. The sulfurous acid concentration of the original solution was 38.6 kg/m^3. The leaching was performed at 18° with vigorous stirring of the pulp. The yield of phosphate fraction was 229 kg, or 62%. 74% of the carbonate calcium was removed. 12.8% of the phosphorus was dissolved, but the phosphorus which passed into solution became concentrated in the calcium sulfite precipitate, which was analyzed and found to have the following chemical composition (%): 31.3 CaO, 41.9 sulfur calculated as SO_2; 1.05 FeO, 2.88 Fe_2O_3, 1.02 Al_2O_3, 3.05 P_2O_5 and 0.32 SiO_2.

As this precipitate is used in the precipitation of dicalcium phosphate, there is practically no loss of phosphorus.

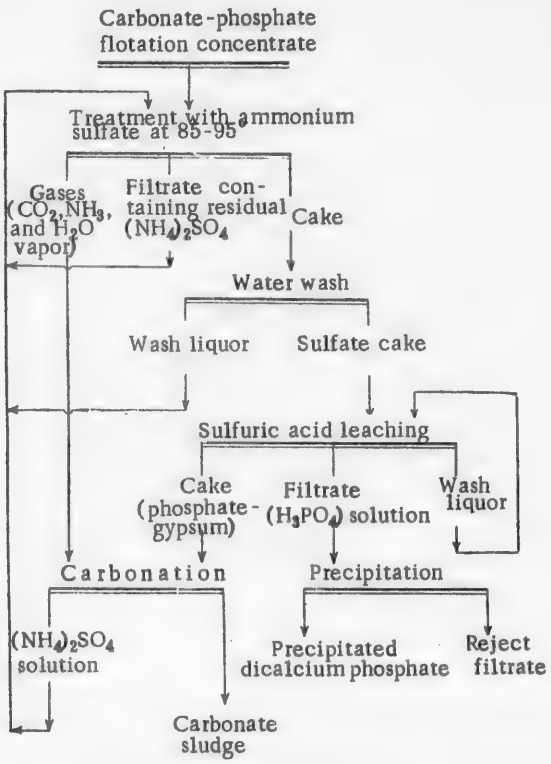

Fig. 3. Flow sheet for selective separation of phosphate and calcite by means of ammonium sulfate, with regeneration of the latter.

Sulfuric acid leaching of the phosphate fraction was also tested on the semiworks scale. The extraction of phosphorus into solution was then 90% as compared with 86% obtained by leaching of the original flotation concentrate under the same conditions. The explanation is that the material used for sulfuric acid leaching had 1.4 times the phosphorus content of the other. The consumption of acid in the treatment decreased by ~400 kg

per ton, i.e., by 60% as compared with the direct treatment of concentrates; the total consumption was 65 kg per ton of the original rock, with a small additional consumption of pyrite for production of sulfur dioxide.

It should be pointed out that the consumption of sulfuric acid for the treatment of the products of selective flotation obtained from the same rock was 90-100 kg/ton.

Binding of carbonate calcium in the form of a compound not decomposed by sulfuric acid. Somewhat later another method was suggested and developed; in this, calcite was combined into a form insoluble in sulfuric acid. The method is based on the reaction between calcite and ammonium sulfate solution at 85-95°, with formation of calcium sulfate and of gases which are subsequently used for regeneration of ammonium sulfate.

The reaction

$$CaCO_3 + (NH_4)_2SO_4 \rightleftharpoons CaSO_4 + 2NH_3 + CO_2 + H_2O \qquad (4)$$

is reversible, and can be made to go to the left under suitable conditions (temperature, gas concentrations). The proposed method for regeneration of ammonium sulfate is based on this. Reaction (4), proceeding in the leftward direction, is used in practice for ammonium sulfate production [6, 7]; a high degree of utilization of ammonia (over 96%) is reached, and concentrated (up to 50%) solutions of ammonium sulfate are obtained. The carbonate sludge formed in the process can be used in the production of cement.

The flow sheet for the treatment of carbonate – phosphate raw material with ammonium sulfate treatment before the sulfuric acid leaching is given in Fig. 3.

As the production of ammonium sulfate from calcium sulfate, ammonia, and carbon dioxide is an industrial process, the main problem to be worked out and tested was the binding of calcite as the result of treatment with ammonium sulfate.

The same raw material as in the preceding process was used. The trials were carried out in the following sequence. Carbonate – phosphate flotation concentrate was added with continuous stirring to ammonium sulfate solution (of about 50% concentration) heated to 40-50°. The pulp was then warmed to the same temperature. Foam and gases (CO_2 and NH_3) were evolved copiously during the process. At the end of the reaction, as indicated by cessation of foaming, the pulp was filtered.

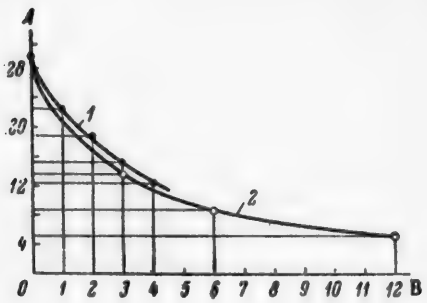

Fig. 4. Rate of binding of carbonate calcium by ammonium sulfate in semiworks trials.
A) Contents of carbonate lime in cake (%),
B) duration of experiment (hours).
1, 2) Results of two experiments differing in duration only.

Laboratory experiments and larger scale laboratory trials with 2.5 kg lots showed that the degree of binding of carbonate lime in the form of calcium sulfate reaches 85-86% in the optimum conditions, and the phosphorus all remains in the sulfate cake.

The results of the laboratory experiments were confirmed by trials in a semiworks unit with 80-120 kg charges of flotation concentrate.

It must be pointed out that when the experiments were performed on a small scale the process was usually complete within 4-6 hours, while the semiworks trials lasted 12-16 hours, probably because the temperature conditions were less stable. The graph (Fig. 4), based on the results of the semiworks scale trials gives an indication of the rate of the process.

The sulfuric acid leaching of phosphorus from the sulfate cakes was studied in detail; an experiment on the semiworks scale was carried out for this purpose. The experiments showed that the consumption of acid for treatment of the sulfate cake was 64% lower than the consumption for the original combined concentrate. The acid consumption per 1 ton of rock was 59 kg, with an additional ammonia consumption of 3-4 kg.

The extraction of phosphorus from the sulfate cake was 93-94%, as compared with 86% in the direct treatment of the concentrate.

The removal of water from the waste cakes was considerably easier and more rapid than from the cakes resulting from direct acid treatment of the flotation concentrate. The moisture content of the cakes was 20-30%, instead of 40% as in the second case. The explanation is that the sulfate cake contained over 50% by weight of calcium sulfate as "filler." Most of the calcium sulfate crystals were 0.03-0.07 mm in size, and one fifth of the whole sulfate consisted of crystals 0.3-0.7 mm in size.

Therefore, ammonium sulfate treatment of carbonate – phosphate flotation concentrate also has a favorable effect on the leaching of phosphorus from acid-treated cakes.

SUMMARY

1. Two methods are described for chemical separation of calcite and phosphate, whereby it is possible to reduce by 60-64% the consumption of acid in the treatment of low-grade carbonate – phosphate rocks and to improve the degree of extraction by better leaching of dissolved phosphates from the cakes. Schemes are proposed for recovery of the sulfur dioxide and ammonium sulfate used in the selective separation of phosphate and calcite.

2. The approach toward reducing the consumption of reagents for treatment of the raw material and developing recovery schemes may be of technological interest not only in relation to nonmetallic mineral sources, but also in relation to the treatment of ores of nonferrous and rare metals.

Selective chemical separation with recovery of the reagents, as a method for beneficiation of raw materials, may be used in the extraction of products suitable for processes of chemical technology or hydrometallurgy if mechanical beneficiation does not yield concentrates of the required degree of purity or gives a low degree of extraction.

LITERATURE CITED

[1] Mining Congr. J., 39, 1 (1953).

[2] L. M. Chernyi, "Beneficiation of Phosphorite Carbonate Rocks," Proc. Conf. on Theory and Practice of Flotation Beneficiation (Izd. AN SSSR, 1952).*

[3] W. Stollenwerk, Conversion of Phosphorite with Sulfurous Acid and its Ammonium Salt (ONTI, State Chem. Tech. Press, 1934).**

[4] A. E. Hughes and F. K. Cameron, Action of Sulfur Dioxide on Phosphates of Calcium (ONTI, State Chem. Tech. Press, 1934).**

[5] Z. P. Rozenknop, Extraction of Sulfur Dioxide from Gases (Goskhimizdat, 1952).**

[6] Col. "Gypsum and Phosphogypsum" Trans. Sci. Res. Inst. Fertilizers and Insectofungicides (1933).

[7] A. M. Dubovitsky and A. I. Shereshevsky, Technology of Mineral Fertilizers (Goskhimizdat, 1947).*

Received November 10, 1955

* In Russian.

** Russian translation.

THERMODYNAMIC ANALYSIS OF THE SYSTEM Ca–C–O

F. S. Maron

The reduction of calcium oxide by carbon is one of the principal reactions in many technological processes, as in the production of calcium carbide, calcium – silicon alloy, and phosphorus, and in certain special thermal metallurgical processes.

Investigations of this problem [1, 2] have shown that the reduction of calcium oxide may yield either calcium carbide or metallic calcium, depending on the reaction conditions.

A thermodynamic analysis of these reactions is given in this paper. The calculations given here show what external conditions (pressure, temperature) result in the formation of calcium carbide or of metallic calcium; these calculations differ from others [3] in this field by the fact that the mutual solubility of CaO and CaC_2 was taken into account.

Phase composition of the system. The most important individual reactions which may occur in the system Ca–C–O are:

$$CaO + 3C \rightleftharpoons CaC_2 + CO_g, \quad (I)$$

$$CaO + C \rightleftharpoons Ca_g + CO_g, \quad (II)$$

$$2CaO + CaC_2 \rightleftharpoons 3Ca_g + 2\,CO_g, \quad (III)$$

$$CaC_2 \rightleftharpoons Ca_g + 2C_s. \quad (IV)$$

Only two of these reactions are independent; the characteristics of the others can be calculated with the aid of the Hess law from the first two.

To determine the equilibrium conditions in all these individual systems it is first necessary to solve the problem of their phase composition. This does not involve any complications for some of the reactants.

Thus, carbon monoxide and calcium constitute a single gas phase in the high-temperature region in electrothermal processes. The presence of carbon dioxide which may be formed by decomposition of CO ($2CO \rightleftharpoons C + CO_2$), may be ignored, both because its equilibrium concentrations would be low at the temperatures in question, and because this process is slow and develops only in the presence of metallic iron.

It can also be stated with a fair degree of certainty that carbon forms an independent phase. The fact that it can dissolve calcium to some extent can hardly give rise to serious error.

The question of the phase composition of calcium oxide and carbide is more complicated. It can be solved by consideration of the phase diagram for the system $CaO–CaC_2$ in order to determine: a) formation of chemical compounds in the system; b) the limits of mutual solubility of CaO and CaC_2 in the solid and liquid states.

The best-known investigations in this field are those of Ruff and Foerster [4], and Flusin and Aall [5]. According to the former two authors, who studied the liquidus line only, by the immersed rod method, CaO and CaC_2 form a simple eutectic system (Fig. 1). The eutectic corresponds to a temperature of 1630° and a CaO content of 70.9% in the condensed phase. From these data the authors conclude that CaO and CaC_2 are mutually soluble in all proportions in the liquid state (the curve does not show an immiscibility hump) and that chemical compounds are not formed in the system.

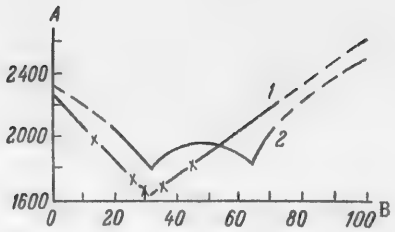

Fig. 1. Phase diagrams for the system $CaO-CaC_2$.
A) Temperature T (°C), B) CaO content (%).
Curves based on data of: 1) Ruff and Foerster, 2) Flusin and Aall.

The results of Flusin and Aall are significantly different. While they reached the same conclusion as Ruff and Foerster concerning the absence of phase separation in the liquid phase, they obtained different results with regard to the nature of the liquidus line and the possibility of formation of chemical compounds (Fig. 1).

First, the liquidus curve, based on data on the surface melting of blocks made from solidified melts [6], indicates the existence of two eutectics, the first of which is close to that found previously by Ruff and Foerster (at 1750° and 68% CaC_2), and the second corresponds to 1800° and 35.6% of calcium carbide. Moreover, Flusin and Aall concluded from the hump-shaped form of the liquidus line that the chemical compound of the formula $CaOCaC_2$, melting at 1980°, exists in the system. Later Aall [6] attempted to confirm its existence by investigations of a number of properties (conductivity, hardness, etc.) of the system $CaO-CaC_2$ in relation to its composition.

Unfortunately, this paper gives no information on the possibility of mutual solution of CaO and CaC_2 in the solid state – the solidus line was not investigated.

This fact, and also the dubious character of the data of Flusin and Aall in relation to the possible formation of calcium oxycarbide (the experimental procedure was unreliable and the lattice of such a compound seems difficult to construct), caused us to undertake, jointly with Geld and Serebrennikov [7], a further study of the system CaC_2-CaO in the solid state. This study was based on the well-known polymorphism of CaC_2, including the reversible transition, at 435°, of the low-temperature modifications of carbide (of complex structure) into a high-temperature modification with cubic syngony.

Technical calcium carbide and synthetic melts of it with different proportions of calcium oxide were used for the investigation.

The results show that a pure calcium carbide phase is retained in solidified melts of calcium oxide and carbide over a very wide range of concentrations; as stated earler, calcium carbide undergoes a phase transition at about 435°. This fact, and also the almost linear decrease of the transition effect with decreasing CaC_2 content in the specimens shows, first, that Flusin and Aall's views concerning the formation of calcium oxycarbide in the system $CaO-CaC_2$, and the consequent absence of a pure carbide phase in the equilibrium system containing over 50% (molar) of CaO, are erroneous.

Moreover, the fact that the transition temperature of the carbide does not vary with the composition of the mixtures studied is reliable evidence that little mutual solution of CaO and CaC_2 can occur in the solid state. Of course, our data give no information on the possible formation of solid solutions with a low concentration of one of the components. However, comparison of our data with the results of the x-ray structure investigations carried out by Stackelberg [8], Franck [9], and Bredig [10] indicates that even limited mutual solubility (above 0.5%) of CaO and CaC_2 may be discounted.

Indeed, despite the fact that these authors used samples containing different amounts of calcium oxide (from 5 to 0.5%), they obtained very similar values for the lattice parameter of the tetragonal modification of calcium carbide.

In our opinion, the following answers can be given on the basis of the foregoing to the questions put forward earlier:

a) chemical compounds are not formed in the system calcium oxide – calcium carbide;

b) the mutual solubility of calcium oxide and carbide in the solid state is low, and may be neglected for practical purposes;

c) phase separation does not occur in the system in the liquid state;

d) Flusin and Aall's data on the form of the liquidus curve are doubtful; preference must be given to the results obtained by Ruff and Foerster.

Thermodynamic Analysis of the Reduction of Calcium Oxide by Carbon (Reactions I and II)

The reduction of calcium oxide by carbon to give calcium carbide occurs according to the equation

$$CaO_{cond} + 3C_s = CaC_{2cond} + CO_g. \qquad (I)$$

The system may have a different number of degrees of freedom, depending on whether the calcium compounds are present in the solid or the liquid state.

When calcium oxide and carbide constitute independent solid phases, i.e., at temperatures below the liquidus line, the three-component, four-phase system

$$CaO_s + 3C_s = CaC_{2s} + CO_g \qquad (I')$$

will have one degree of freedom. This means that of the two parameters which determine its equilibrium (T and $p_{CO} = P$), only one is independent, while the other is a function of it, i.e., $p_{CO} = F(T)$. This function may be represented by means of the expression for the equilibrium constant

$$K'_1 = \frac{a_{CaC_2} f_{CO}}{a_{CaO} \cdot a_C^3} = F'(T).$$

Assuming, with sufficient accuracy for our purposes, that the fugacity of the gas* is equal to its partial pressure, and that the activity of the pure condensed reagents is unity,* we have

$$K'_{p_{1_I}} = p_{CO} = F'(T). \qquad (1)$$

Thus, the required relationship between the equilibrium pressure and the temperature can be readily found with the aid of the usual methods for calculating the temperature – equilibrium constant relationship.

We now consider the solution of this problem.

Integral solution of the Gibbs – Helmholtz equation is not possible in this case owing to the lack of reliable data on the temperature–heat capacity relationship for calcium carbide. It is therefore necessary to use an approximate entropy equation. The possibility of making the results so obtained more precise will be discussed later.

Given that the heat of sublimation of calcium = 47.8 kcal/mole; $\Delta H^{\circ}_{1,298} = 108.000$ cal/mole; $S_{CaO,\,298} = 9.5$; $S_{CaC_2,\,298} = 11.34$; $S_{C,298} = 1.36$; $S_{CO,298} = 47.32$ cal/degree · mole; $c_{p_{CaO,\,298}} = 10.23$; $c_{p_{CaC_2,298}} = 11.47$; $c_{p_{C,298}} = 2.06$; $c_{p_{CO,298}} = 6.95$ cal/degree · mole. We then have:

$$\log K'_{p_1} = \log p'_{CO} = -\frac{23620}{T} + 9.86 + 0.44\varphi(T). \qquad (2)$$

The above thermodynamic data are taken from Rostovtsev's monograph [11], apart from the data for calcium carbide, taken from the paper by Mauderli, Moser, and Treadwell [12], and the heat of sublimation of calcium, as given by Umansky, Finkelshtein, and Blanter [13].

If the temperature of the system lies above the liquidus line, calcium oxide and carbide will not be present in two independent phases, and will constitute a single phase – a melt of variable composition.

* At not very high pressures (P = 10 atm.).

$$(CaO) + 3C_s = (CaC_2) + CO. \qquad (I^*)$$

Under these conditions the equilibrium state of the three-component, three-phase system will be described not by two, but by four parameters – (P, T, N_{CaO} and N_{CaC_2}) of which, according to the phase rule, only two are independent. The other two may be found by means of the equations:

$$N_{CaO} + N_{CaC_2} = 1, \qquad (3)$$

$$K''_{p_I} = \frac{a_{CaC_2} f_{CO}}{a_{CaO} \cdot a_C} = \frac{N_{CaC_2} \cdot p''_{CO}}{N_{CaO}} = F''(T), \qquad (4)$$

the second of which is based on the assumption that the pressures are not too high and that calcium oxide and carbide form ideal solutions (i.e., $a_i = N_i$).

It follows from this second equation that

$$\log p''_{CO} = \log F''(T) + \log N_{CaO} - \log N_{CaC_2}. \qquad (5)$$

It must be noted that F'(T) is not equal to F"(T) because in the latter case the presence of liquid reactants must be taken into account. Assuming that the heats of fusion of calcium oxide and carbide are λ_{CaO} = 10 000 cal/mole and λ_{CaC_2} = 7680 cal/mole and their melting points are T_{CaO} = 2840° and T_{CaC_2} = 2573° K [14] respectively, we have

$$\log p''_{CO} = -\frac{23100}{T} + 9.53 + 0.44\varphi(T) - \log N_{CaC_2} + \log N_{CaO}. \qquad (6)$$

It must be emphasized that this equation is only valid for the liquidus region, and under the previously stated conditions regarding the ideality of the solution.

Comparison of these expressions with experimental data is somewhat difficult owing to the inadequacy and sometimes the unreliability of the latter.

Equation (2) is only valid for solid CaO and CaC_2 phases. The equilibrium in this system was investigated a long time ago by Tomson [15] who found that $p_{CO,\ 1718°\,K}$ = 0.44 mm Hg, and $p_{CO,1748°\,K}$ = 0.82 mm Hg. Equation (2) gives $p_{CO,1718°\,K}$ = 0.24 and $p_{CO,1748°\,K}$ = 0.437 mm Hg. This discrepancy may be diminished by applying a correction based on an experimental determination to Equation (2).

Geld [3] corrected equilibrium data for individual systems containing calcium carbide on the basis of the fact [10] that the reaction of calcium oxide with carbon up to 1400° does not yield CaC_2 – only calcium vapor is formed; conversely, at 1400° and over, calcium carbide is formed. This indicates that at 1400°

$$(p_{Ca})_{II} = (p_{Ca})_{IV}.$$

From this, and from the reasonably reliable data on the temperature relationship for the reacting substances in System II, he derived the equation

$$\log p'_{CO} = -\frac{23800}{T} + 10.55, \qquad (7)$$

which agrees satisfactorily with Tomson's data.

It is possible to modify Equation (2) in another way, by direct use of Tomson's data, such as the above value $p_{CO,1718°\,K}$ = 0.44 mm Hg. Then, by correcting the independent term of Equation (2), we have

$$\log K'_{p_I} = \log p'_{CO} = -\frac{23620}{T} + 10.12 + 0.44\varphi(T). \qquad (2')$$

No data are available for verification of the results obtained by means of Equation (6). Not only are Brunner's determinations [16] doubtful, but they cannot be used because the compositions of the melts to which they relate are not given.

Because of this, the applicability of the ideal solution laws to $CaO - CaC_2$ melts cannot be verified. We shall therefore confine ourselves to correction of the independent term on the assumption that Equation (6) contains the same systematic error as Equation (2), due to inaccurate thermochemical data on the reactants. This gives the equation

$$\log K''_{p_I} = \log p''_{CO} = -\frac{23100}{T} + 9.79 + 0.44\varphi(T) - \log N_{CaC_2} + \log N_{CaO}. \qquad (6')$$

Thus, the most probable equations describing equilibrium in the System (I) are Equation (2') for the solidus region and (6') for the liquidus region.

The equilibrium pressures of carbon monoxide in System (I) at a number of temperatures are given below.

T (°C)	1200	1500	1700	2000
$\log p_{CO}$ (in mm Hg)	− 2.76	0.07	1.44	3.096
p_{CO} (in mm Hg)	$1.74 \cdot 10^{-3}$	1.18	27.6	1250

As was stated earlier, at temperatures below 1400° reduction of calcium oxide by carbon does not yield CaC_2; in other words, equilibrium in the system is reached in accordance with the equation

$$CaO_{cond} + C_{cond} = Ca_g + CO_g. \qquad (II)$$

The three-component, three-phase system in question is bivariant. This means that of the four variables (T, P, p_{CO}, p_{Ca}), which characterize its equilibrium state, two are independent. The others can be found by means of the equation

$$P = p_{CO} + p_{Ca}, \qquad (8)$$

$$K'_{p_{II}} = \frac{f_{Ca} \cdot f_{CO}}{a_{CaO} \cdot a_C} \approx p_{CO} \cdot p_{Ca} = F_{II}(T), \qquad (9)$$

the second of which is valid at not very high pressures (< 10 atm.) and if the pure CaO phase is present.

Using the data quoted earlier, and also $S_{Ca,\ g,\ 298} = 37$ cal/degree · mole and $c_{p_{Ca,\ g,\ 298}} = 4.97$ cal/degree · mole, we have

$$\log K_{p_{II}} = p_{CO} p_{Ca} = -\frac{37800}{T} + 16.1 - 0.08\varphi(T). \qquad (10)$$

In the particular case when carbon monoxide and calcium are present in the gas phase in the stoichiometric ratio

$$\log p'_{CO_{II}} = -\frac{18900}{T} + 8.05 - 0.04\varphi(T). \qquad (11)$$

The last equation can be used for finding equilibrium partial pressures of the gaseous components at a given temperature. If $p_{CO} \neq p_{Ca}$, then p_{CO} and p_{Ca} can be found by solving Equations (8), (9), and (10) simultaneously.

Equation (11) can be corrected with the use of more accurate data on the thermal properties of the components, giving, for example [3], the following value at 1700° K $\log K_{p_{II}} = -6.936$. Correction of the independent term of Equation (11) gives:

$$\log p_{CO_{II}} = -\frac{18900}{T} + 7.665 - 0.04\varphi(T), \qquad (11')$$

$$\log K_{p_{II}} = -\frac{37800}{T} + 15.33 - 0.08\varphi(T). \qquad (10')$$

Equilibrium values of $p_{CO_{II}}$ for a number of temperatures in System II, calculated by means of Equation (11), are given below.

T (°C)	1200	1500	1700	2000
log p_{CO} (mm Hg)	−2.275	−0.18	0.91	2.16
$p_{Ca} = p_{CO}$ (mm Hg)	$5.31 \cdot 10^{-3}$	0.661	8.13	145
P (mm Hg)	$10.62 \cdot 10^{-3}$	1.322	16.26	290

Comparison of these results with direct experimental data is not possible as no such data are available.

It may be noted, however, that many workers reported the formation of considerable amounts of calcium in the reduction of calcium oxide, even under conditions (T < 1400°), when formation of calcium carbide is not possible.

The results obtained by Franck [9] and by Geld [3] are particularly significant in this respect; they found that below 1400° the reaction of CaO and C is accompanied by sublimation of calcium; since calcium is condensed in the cold parts of the apparatus as a pyrophoric deposit ($p_{Ca} \rightarrow 0$), equilibrium in System (II) does not become established, and the partical pressure of CO increases continuously (since $p_{Ca} \cdot p_{CO}$ = const. at equilibrium).

The above calculations and experimental data indicate that relatively considerable amounts of elemental calcium vapor are formed in the reaction between CaO and carbon. It will be shown below that it can also be formed by other reactions, and that it plays a significant role in the mechanism of the reduction of calcium oxide by carbon.

If CaO is reduced from solution, we have instead of (9)

$$K''_p \simeq \frac{p_{CO} \cdot p_{Ca}}{N_{CaO}} = F''_{II}(T), \qquad (9')$$

and the form of the relationship between $K''_{p_{II}}$ and the temperature can be found from Equation (10) with the heats of fusion and entropy changes in formation of the melt taken into account, giving

$$\log K''_{p_{II}} = \log p_{Ca} \cdot p_{CO} = -\frac{35600}{T} + 14.56 - 0.08\varphi(T) + \log N_{CaO}. \qquad (10'')$$

Thermodynamic Analysis of Systems Containing Calcium Carbide (Reactions III and IV)

Calcium carbide formed in Reaction (I), being a powerful reducing agent, can under suitable conditions reduce calcium oxide to the metal according to the equation

$$2CaO_{cond} + CaC_{2cond} = 3C_g + 2CO_g. \qquad (III)$$

Depending on the phase state of the condensed components, System (III) may either be bivariant (if two separate phases of CaO and CaC_2 are present) or it may have three degrees of freedom (if CaO and CaC_2 form a mutual solution).

In the first case, which is found when the multiple point for the system is below or on the liquidus line, two alternatives are possible.

Absence of a liquid phase, i.e., at temperatures below the eutectic point (1630°). Here the system is characterized by only four parameters (P, T, p_{CO} and p_{Ca}) of which the two dependent variables can easily be found from the two independent variables by means of the following equations:

$$P = p_{CO} + p_{Ca}, \tag{12}$$

$$K'_{p_{III}} = \frac{f_{Ca^3} \cdot f_{CO^2}}{a_{CaO^2} \cdot a_{CaC_2}} \approx p_{Ca^3} \cdot p_{CO^2} = F'_{III}(T). \tag{13}$$

To obtain the value of F'_{III} in explicit form no additional calculations are necessary since, as has already been stated, only two reactions are independent in the system Ca – C – O, and the others can be deduced from them. In fact, with the use of the Hess law we have

$$\begin{gathered} 3\,(CaO + C = Ca_g + CO);\ \ 3\Delta F^\circ_{II} \\ -(CaO + 3C = CaC_2 + CO);\ \ \Delta F^\circ_{I} \\ \hline 2CaO + CaC_2 = 3Ca_g + 2CO;\ \ \Delta F^\circ_{III} = 3\Delta F^\circ_{II} - \Delta F^\circ_{I} \end{gathered}$$

or, since $\Delta F^\circ = -RT \log K$, $\log K'_{p_{III}} \approx 3 \log K'_{p_{II}} - \log K'_{p_I}$.

From (2') and (10') we have

$$\log K'_{p_{III}} = p_{CO^2} - \log p_{Ca^3} = -\frac{89780}{T} + 35.87 - 0.68\varphi(T), \tag{14}$$

and from this, together with Equations (12) and (13), we can find the required dependent variables.

For the special case when the gaseous components are present in stoichiometric ratio in the system, that is, when $p_{Ca} = 1{,}5\ p_{CO} = \frac{3}{5}\ P$, we have

$$\log p_{CO} = -\frac{17956}{T} + 7.069 + 0.136\varphi(T), \tag{15}$$

$$\log p_{Ca} = -\frac{17956}{T} + 7.244 + 0.136\varphi(T), \tag{16}$$

$$\log P = -\frac{17956}{T} + 7.464 + 0.136\varphi(T). \tag{17}$$

These equations were used to obtain the following calculated data for the influence of temperature on the partial pressures (p_{CO} and p_{Ca}) and the total pressure in System (III).

T (°C)	1200	1500	1700	2000
p_{CO} (mm Hg)	$7.08 \cdot 10^{-3}$	0.205	9.13	159
p_{Ca} (mm Hg)	0.0106	0.306	13.7	238
P (mm Hg)	0.0176	0.511	22.83	396

If liquid, solid, and gaseous phases coexist, i.e., when the component systems are represented by one of the points in the solidus region, the number of variables is increased by two (N_{CaO} and N_{CaC_2} for the liquid phase), but the number of connecting equations increases by two at the same time. In this case, in addition to Equations (12), (13), and (14), we have also the following equations:

$$N_{CaO} + N_{CaC_2} = 1 \tag{18}$$

and

$$\frac{d \ln N_i}{dT} = \frac{\bar{H}_i - H_i}{RT^2} . \tag{19}$$

The latter equation can be simplified on the assumption that $\Delta H = \bar{H}_i - H_i$ – the heat of fusion of the solid – depends little on the temperature. We then have (assuming, of course, ideality of the solution),

$$\ln N_i = \frac{\Delta H}{R}\left(\frac{1}{T_i} - \frac{1}{T}\right), \tag{20}$$

where T_i is the melting point of the dissolved solid component (coexisting with the melt).

In practice, Equations (18) and (19) are not suitable for use because it is not certain whether the ideal solution laws are applicable to the system $CaO-CaC_2$, and because of the lack of reliable data on the value of ΔH. It is simpler and more exact to find N_i for a given temperature directly from an experimentally determined fusion diagram, such as that given by Ruff and Foerster.

In the second case, when the system contains only one condensed phase, a melt of CaO and CaC_2, the number of variables characterizing the state of the system is six (P, T, p_{CO}, p_{Ca}, N_{CaO}, N_{CaC_2}), and there are three degrees of freedom. This requires three connecting equations, namely

(12)

$$P = p_{Ca} + p_{CO_2},$$

$$N_{CaO} + N_{CaC_2} = 1, \tag{18}$$

$$\log K''_{p_{III}} = \frac{f_{Ca^2} \cdot f_{CO^2}}{a_{CaO^2} \cdot a_{CaC_2}} = \frac{p_{Ca^2} p_{CO^2}}{N_{CaO^2} N_{CaC_2}} = F''_{III}(T). \tag{21}$$

Here the last equation is valid only in so far as the ideal solution laws are applicable to $CaO-CaC_2$. F'_{III} differs from F''_{III} for the same reasons as were given earlier in relation to F'_I and F''_{II}, because of the different phase state of the reactants. The expression for it can be readily derived by combining Equations (6') and (10"), analogously to the procedure for calculation of $\log K'_{p_{III}}$. This gives the expression

$$\log K''_{p_{III}} \approx p_{Ca^2} \cdot p_{CO^2} = -\frac{83700}{T} + 33.89 - 0.68\varphi(T) + 2\log N_{CaO} + \log N_{CaC_2} . \tag{22}$$

The problem in question can be solved by simultaneous solution of Equations (12), (18), (21), and (22).

Reliable verification of these expressions is not possible owing to lack of experimental data for equilibrium conditions in System (III).

However, qualitative confirmation that Reaction (III) can be brought about is provided by the results of numerous investigations, both on thermal processes for the production of calcium, and on the condition for the stability of calcium carbide.

The most direct data on the reaction are given in Voinitsky's paper [17]. He showed that at 1300-1350° considerable amounts of calcium can be driven off from a mixture of CaO and CaC_2 under vacuum (0.02 mm Hg). For example, he obtained 5.6 g of Ca from a mixture of 64 g of CaO and 15 g of CaC_2.

The possibility of this reaction is also indicated by the results obtained by Geld and Mikulinsky, Franck [9], and others.

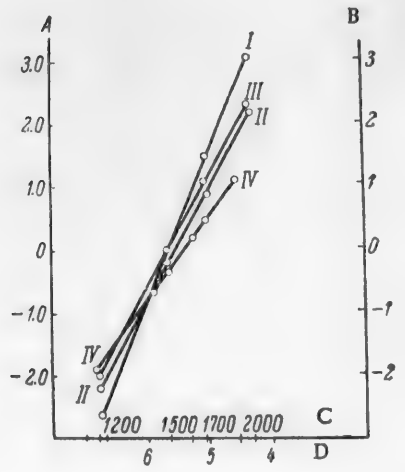

Fig. 2. Effect of temperature on the total pressure in Systems I-IV.
A) Log p_{Ca} mm Hg (II)-(IV), B) log p_{CO} mm Hg (I), C) temperature (°C) D) $\frac{1}{T} \cdot 10^4$.

In conclusion, we shall consider some characteristics of the dissociation of calcium carbide, which are very important both for understanding the mechanism of the reactions which develop in the production of calcium carbide, and in relation to its use as a reducing agent.

As before, two alternatives should be considered – the presence either of solid carbide, or of its solution in CaO, in the system.

In the first case we have a two-component, three-phase system, which therefore has one degree of freedom, while in the second the numbers of components and of the degrees of freedom are each greater by one.

If solid calcium carbide is present in the system

$$CaC_{2_s} = 2C_s + Ca_g, \qquad \text{(IV)}$$

then the two variables characterizing equilibrium in System (IV) (p_{Ca} = P and T) should be connected by an equation based on the expression for the equilibrium constant

$$K_{p_{IV}} \simeq p_{Ca_{IV}} = F'_{IV}(T). \qquad (23)$$

The form of this relationship can readily be found by combining Equations (2') and (10'):

$$\log K'_{p_{IV}} = \log K'_{p_{II}} - \log K'_{p_{I'}} = \log p_{Ca_{IV}} = -\frac{14180}{T} + 5.21 - 0.52\varphi(T). \qquad (24)$$

Thus, as shown in Fig. 2, for each temperature there will be a quite definite dissociation pressure of calcium carbide.

In dissociation of carbide dissolved in a slag phase (for example, in CaO), of the three variables (N_{CaC_2}, p_{Ca} and T) only one is dependent; as before, this can be found from the expression for the equilibrium constant, which in this case is of the form

$$K''_{p_{IV''}} = \frac{p_{Ca}}{N_{CaC_2}} = F''_{IV}(T). \qquad (25)$$

Combination of Equations (6') and (10") gives this relationship in analytical form.

Thus, we have

$$\log K''_{p_{IV}} = \log K''_{p_{II}} - \log K''_{p_I} = \log p''_{Ca_{IV}} = \frac{p_{Ca}}{N_{CaC_2}} = -\frac{12500}{T} + 4.77 - 0.52\varphi(T) + \log N_{CaC_2}. \qquad (26)$$

By means of this expression it is possible to calculate from two given parameters (the system is bivariant), such as N_{CaC_2} and T, the equilibrium dissociation pressure of calcium carbide dissolved in the oxide. The results of calculations carried out with the use of Equation (24) up to 2330°, and with Equation (25) above 2330° (the influence of temperature on the partial pressure of calcium in System IV) are given below.

T (°C)	1230	1430	1630	1930	2230	2530	2730	2930
log p_{Ca} (mm Hg)	−1.78	−0.73	+0.11	1.06	2.14	2.44	2.70	2.973
p_{Ca} (mm Hg)	0.0166	0.186	1.28	11.5	138	276	501	940

Our results, and in particular Equation (24), can be compared with the results of certain experimental and theoretical investigations.

According to Ruff and Foerster, the dissociation pressure of 82-94% calcium carbide can be represented by the expression

$$\log p_{Ca,\ air} = -\frac{26300}{T} + 9.65, \qquad (27)$$

shown in graphical form in Fig. 3. It follows from these results that the equilibrium pressure of calcium vapor in System (IV) is 1 mm Hg at 1825± 50°, and 1 atm at 2500± 50°. It is seen that these data lead to results which, for high pressures, differ considerably from the calculated values (see Fig. 3).

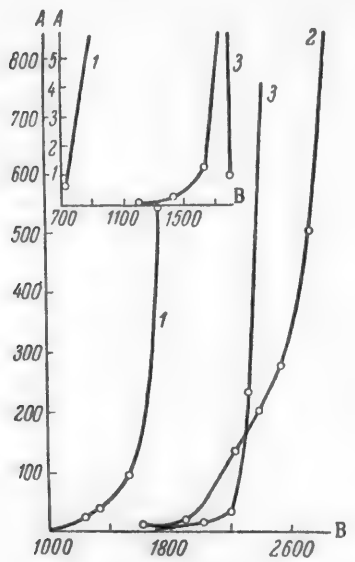

Fig. 3. Pressure of calcium vapor over calcium carbide at various temperatures.
A) Value of p_{Ca} over CaC_2 (in mm Hg),
B) temperature (°C).
Curves based on data of: 1) Mauderli, 2) the author, 3) Ruff and Foerster.

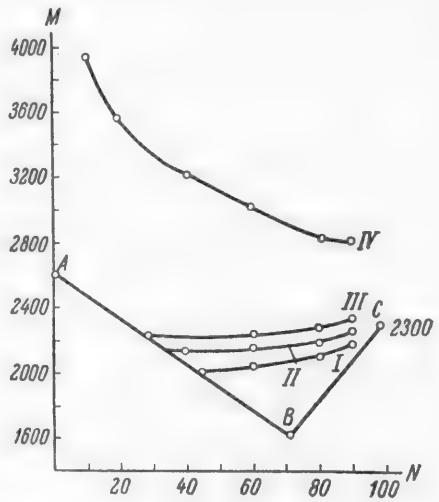

Fig. 4. Temperatures at which a total gas pressure of 1 atm is set up in System (I) - (IV) in the liquidus region.
M) Temperature T(°C), N) CaC_2 content (%).
Line ABC is the liquidus line from Ruff and Foerster's phase diagram.

It can be easily demonstrated that the results of Ruff and Foerster's dynamic experiments are unreliable. Numerous studies of the thermal stability of calcium carbide have shown that at low pressures (10^{-3}, 10^{-4} mm Hg)

it does not decompose up to 1100°. Conversely, at and above this temperature the dissociation of carbide can be clearly determined both from the sublimed calcium, and from the amount of carbon deposited. This is shown by the results obtained by Krase and Jee [18], by Geld's data [3], etc. However, it follows from Ruff and Foerster's data that at 1100° the dissociation pressure of CaC_2 is $2.7 \cdot 10^{-7}$ mm Hg. If their results were correct, dissociation of carbide at pressures of 10^{-3}, 10^{-4} mm Hg would be impossible at this temperature, and would begin only at about 1400°. This is clear contradiction to the above data.

Moreover, Ruff and Foerster's data give rise to doubt because their slope factor is extraordinarily high; in the first approximation it follows from Equation (27) that the heat of dissociation of carbide at high temperature is $\Delta H = 4.575 \cdot 26300 = 121000$ cal/mole, whereas the value determined from thermochemical data is about half this.

These facts indicate that Ruff and Foerster's data on the dissociation pressure of calcium carbide are erroneous, being too high; this is probably the consequence of a faulty experimental procedure (based on determinations of weight loss – temperature curves), applicable only to systems in which crystalline rearrangements do not present appreciable difficulties, i.e., applicable only when equilibrium in the system is established particularly rapidly.

The thermochemical calculations of Mauderli, Moser, and Treadwell [12] give higher values of the equilibrium pressure of calcium in System (IV). From the value of $S_{CaC_2} = 11.34$ cal/degree · mole they find $P_{Ca,\ 1000°\ K} = 0.765$ mm Hg and $P_{Ca,\ 1500°\ K} = 17.0$ mm Hg, likewise in contradiction to the experimental data given above.

Our calculated values are found to be in quite satisfactory agreement with the results of Krase and Jee [18], Geld [3], Franck [9], and others. In particular, Equation (24) gives $p_{Ca} = 7.42 \cdot 10^{-3}$ mm Hg for 1100°.

The effect of temperature on the total pressure P for Systems (I) - (IV) is shown in Fig. 2. It is seen that at low temperatures System (IV) has the highest equilibrium pressure. In the high-temperature region System I reaches the highest pressure. This is in good agreement with experimental data.

In conclusion, Fig. 4 shows a comparison of the temperatures at which a total gas pressure of 1 atm is set up over the systems in question (I) - (IV) in the liquidus region (i.e., in presence of melts). It follows from Fig. 4 that calcium oxide is reduced to calcium carbide at the lowest temperatures, and conversely, dissociation of liquid calcium carbide occurs at very high temperatures. These curves are limited by the liquidus curve ABC from Ruff and Foerster's phase diagram.

SUMMARY

A thermodynamic analysis of the most important reactions in the system Ca – C – O, has been carried out and it is shown that the maximum total gaseous pressure – of carbon monoxide and calcium vapor – is reached in the high-temperature region in the reduction of calcium oxide with formation of calcium carbide. At low temperatures (1400°) the reactions with the most favorable characteristics for reduction of calcium oxide are those which give rise to calcium vapor; namely, reduction of calcium oxide by calcium carbide, and dissociation of calcium carbide.

LITERATURE CITED

[1] P. V. Geld and F. S. Maron, J. Appl. Chem. 12, 11, 1160 (1949).

[2] F. S. Maron and A. S. Mikulinsky, Theory and Practice of Electrothermal Metallurgy (Metallurgy Press, 1948) p. 47.*

[3] P. V. Geld, Trans. S. M. Kirov Polytechn. Inst. Urals 37, 171 (1951).

[4] O. Ruff and E. Foerster, Z. allg. anorg. Ch., 131, 321 (1923).

[5] G. Flusin and Ch. Aall, J. du four electrique, 44, 317 (1935).

[6] Ch. Aall, Contribution a l'etude du Carbure de calcium industriel, Paris (1940).

[7] P. V. Geld, F. S. Maron, and N. N. Serebrennikov, Proc. Acad. Sci. USSR 1, 48, 123 (1949).

* In Russian.

[8] M. Stackelberg, Z. Phys. Chem., B 9, 437 (1930).

[9] H. Franck, Z. anorg. Chem., 232, 75 (1937).

[10] M. A. Bredig, J. Phys. Chem., 46, 801 (1942).

[11] S. T. Rostovtsev, Theory of Metallurgical Processes (Metallurgy Press, 1945).*

[12] B. Mauderli, E. Moser u. W. Treadwell, Helv. Chim. Acta., 27, 105 (1944).

[13] S. Ya. Umansky, B. I. Finkelshtein, and M. E. Blanter, Physical Principles of Metal Science (Metallurgy Press, 1949).*

[14] Allmand, Principles of Applied Electrochemistry (ONTI Chem. Theoret. Press, 1934).*

[15] K. Tomson, J. Russ, Metallurg. Soc. III, 5, 744 (1910).

[16] R. Brunner, Z. Elektroch., 38, 55 (1932).

[17] A. I. Voinitsky, Trans. VAMI 18, 152 (1939).

[18] Ch. D. Krase and D. K. Jee, J. Am. Chem. Soc., 46, 1358 (1924).

Received October 31, 1955

* In Russian.

CALCULATION OF BATCH RECTIFICATION COLUMNS

Fu Tszyui-fu

Chair of Chemical Fuel Technology, Tientsin Polytechnic Institute

There are two alternative methods of carrying out rectification with batch rectification columns. In the first, the reflux ratio must be varied in order to keep the distillate concentration constant. In the second, the reflux ratio remains constant while the distillate concentration varies continuously. In batch rectification, the conditions (concentration, temperature, flow rate) vary continuously along the column from the condenser to the still in the course of distillation. Therefore, calculations of batch rectification are in many respects more complicated than calculations of continuous rectification in steady conditions.

For binary mixtures (only these are considered here), the McCabe – Thiele graphical method is generally used for calculation of the number of theoretical plates, based on the equilibrium curve

$$y = f(x) \tag{1}$$

and the equation for the operating line

$$x_p = (R + 1) \cdot y_{n+1} - Rx_n \tag{2}$$

In these equations and in the figures, $\underline{y}$ is the molar concentration of the more volatile component in the vapor phase, $\underline{x}$ is the molar concentration of this component in the liquid phase, R is the reflux ratio (at the given instant), x_p is the molar concentration of the distillate (at the given instant), $\underline{n}$ is the number of plates (counted downward), $\underline{p}$ is the amount of distillate withdrawn per unit time, in kg-moles, and $\underline{l}$ is the amount of overflow in kg-moles per unit time.

In this way it is possible to calculate the operating conditions at different cross sections of the column (Fig. 1). It is also possible to determine the relationship between the instantaneous values of x_p, $\underline{x}$, and x_n, y_n, and R. It should be assumed that in any given section of the column the amounts of ascending vapor and overflowing liquid are constant. Otherwise it is necessary to use a heat diagram for graphical characterization of changes in the amounts of liquid and vapor phases and heat changes in the alternating processes of partial evaporation and condensation.

When the influence of the amount of liquid present on the plates (the plate holdup) cannot be neglected, certain corrections must be introduced into the equation for the operating line. Then

$$x_p = (R + 1) \cdot y_{n+1} - R \cdot x_n + \frac{H_{n+1}}{p} \Delta x_h, \tag{3}$$

where H_{n+1} is the holdup on the (n + 1)th plate (the total number of moles of liquid held up above the (n + 1)th plate, including the (n + 1) th plate); Δx_h is the change in the concentration of the liquid held up above the (n + 1)th plate during the production of $\underline{p}$ kg-moles of distillate per hour.

With these corrections the equation of the operating line will change its form and will no longer be a linear equation, so that calculation will be much more complicated. In some cases, when H is very small or the concentration change Δx_h differs little from 0, the effect of the retaining capacity may be neglected and the above simplified calculation method may be used.

In intermittent rectification with constant concentration of distillate and variable reflux ratio it is very important to determine the average numerical value of the reflux ratio. If this is known, it is possible to

calculate the quantity of heat required for heating, and also the amount of cooling water for the condenser. If the process is carried out at constant reflux ratio, determination of the amount and average concentration of the distillate is important. Moreover, in both cases it is necessary to know the duration of a single distillation (the time required for intermittent rectification). Some of these factors which influence the course of intermittent rectification may be calculated by means of the material balance equation. The literature also contains a number of equations for analytical calculations of rectification equipment. Because intermittent rectification occurs in nonsteady conditions, these equations are very complex and graphical integration is required. In some instances, however, algebraic integration is possible. The present paper contains a critical analysis of methods of algebraic integration described in the literature [1, 2].

Fundamental Calculation Equations

The analytical method of investigating the performance of periodic-action rectification columns is based on the following assumptions: 1) the influence of the column holdup may be neglected; 2) the amount of vapor ascending in the column is constant in any cross section of the column; 3) the number of theoretical plates is known.

1st alternative. Rectification at constant reflux ratio.

Amount of distillate. An equation analogous to the Rayleigh equation [3] can be used to determine the amount of distillate in this case. The value of x corresponding to x_p should be found by the method illustrated in Fig. 1. Graphical integration can then be performed:

$$\log W = \log F - \frac{1}{2.303}\int_{x_W}^{x_f}\frac{dx}{x_p - x}, \qquad (4)$$

where F is the amount of original feed mixture entering the column (in kg-moles), W is the amount of residue in the still (in kg-moles); x_p is the concentration of the distillate (mole fraction of the more volatile component), x is the instantaneous concentration of the liquid in the still (mole fraction of the more volatile component), x_f is the concentration of the original feed mixture (mole fraction of the more volatile component), and x_W is the concentration of the still residue (mole fraction of the more volatile component).

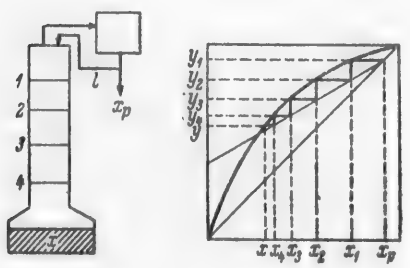

Fig. 1. Graphical method for calculation of the number of theoretical plates.

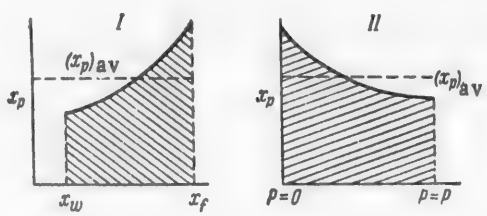

Fig. 2. Determination of the average distillate concentration.
I) Graphical solution of Equation (6), II) graphical solution of Equation (7).

Rose and Long [4] used this method to obtain a series of curves for the relationships between the reflux ratio, relative volatility, number of theoretical plates, and the amount of still residue.

Duration of rectification. The rectification time t (in the first alternative) can be calculated from the following equation:

$$t = \frac{(F-W)(R+1)}{v}, \tag{5}$$

where v is the amount of vapor ascending in the column, in kg-moles per unit time.

Since the reflux ratio R is constant, the value of v does not change. At the maximum column output the numerical value of v is determined by the permissible vapor rate.

Average concentration of distillate. Kasatkin [1, 2] uses the theorem for the near value of a function to express the average distillate concentration $(x_p)_{av}$ in the form of the equation

$$(x_p)_{av} = \frac{1}{x_f - x_W} \int_{x_W}^{x_f} x_p \cdot dx \tag{6}$$

However, in this instance this is not correct, as $(x_p)_{av}$ is not the true average concentration of the distillate, as is readily seen on examination of Fig. 2, I, in which Equation (6) is shown in graphical form.

In reality, the average concentration of the distillate $(x_p)_{av}$ should be calculated from the following equations:

$$P\,(x_p)_{av} = \int_0^P x_p dP$$

or

$$(x_p)_{av} = \frac{1}{P} \int_0^P x_p \cdot dP, \tag{7}$$

where P is the total amount of distillate, and dP is the differential amount of distillate (instantaneous value).

The physical meaning of Equation (7) is perfectly clear. It is evident from Fig. 2 II that the true average distillate concentration is found in this way.

In practice, for calculation of $(x_p)_{av}$ it is possible to avoid integration of Equation (7), by proceeding as follows.

Since

$$F \cdot x_f = W \cdot x_W + P\,(x_p)_{av}$$

then

$$(x_p)_{av} = \frac{Fx_f - Wx_W}{P} = \frac{Fx_f - Wx_W}{F - W}. \tag{8}$$

From Equation (4)

$$\ln \frac{F}{W} \int_{x_W}^{x_f} \frac{dx}{x_p - x}.$$

Hence

$$\frac{F}{W} = e^{\int_{x_W}^{x_f} \frac{dx}{x_p - x}}$$

or

$$W = \frac{F}{e^{\int_{x_W}^{x_f} \frac{dx}{x_p - x}}}. \tag{9}$$

Substitution of Equation (9) into Equation (8) gives:

$$(x_p)_{av} = \frac{x_f - \frac{x_W}{e^{\int_{x_W}^{x_f} \frac{dx}{x_p - x}}}}{1 - \frac{1}{e^{\int_{x_W}^{x_f} \frac{dx}{x_p - x}}}}. \tag{10}$$

At constant reflux ratio the average distillate concentration can be calculated by means of Equation (10); or Equation (4) may first be used to find the amount of distillate, and then $(x_p)_{av}$ is found directly from Equation (8).

2nd alternative. Rectification with constant distillate concentration.

Amount of distillate. From the material balance equation

$$Px_p = Fx_f - Wx_W$$

or

$$Px_p = Fx_f - (F - P)x_W$$

we have

$$P = \frac{F(x_f - x_W)}{x_p - x_W}, \tag{11}$$

where F, x_f, x_p, and the final composition of the liquid in the still, x_W, are predetermined. With regard to x_W it may be noted that in rectification of a definite solution, with a known number of theoretical plates, the numerical value of x_W should not be less than the value calculated for total reflux.

If the mixture is an ideal solution (i.e., if it obeys Raoult's law) and total reflux occurs at the end of the rectification process, the total amount of distillate can be calculated by means of the Edgeworth-Johnstone equation [5]

$$P = \left(F\frac{x_f}{x_p}\right)\frac{\alpha^{N+1} - \left(\frac{x_p}{1 - x_p}\right)\left(\frac{1 - x_f}{x_f}\right)}{\alpha^{N+1} - 1}. \tag{12}$$

Duration of rectification. In this case, the duration of rectification for maximum column output can be calculated by means of Bogart's equation [6]:

$$t = \frac{-F(x_p - x_f)}{v} \int_{x_f}^{x_W} \frac{dx}{\left(1 - \frac{l}{v}\right)(x_p - x)^2} \tag{13}$$

or

$$t = \frac{-F(x_p - x_f)}{v} \int_{x_f}^{x_W} \frac{(R+1)\,dx}{(x_p - x)^2}. \tag{14}$$

If this equation is used to find x corresponding to R, the graphical method shown in Fig. 1 can be used. It is then possible to find t by graphical integration.

Average reflux ratio. Kasatkin [1, 2] calculates the average value of the minium reflux ratio by means of the theorem for the mean value of the function:

$$R_{av} = \frac{1}{x_f - x_W} \int_{x_W}^{x_f} R\,dx \tag{15}$$

This is not correct. The average reflux ratio R_{av} is in this case calculated from the change of concentration of the liquid in the still, which has no practical significance.

To calculate the required total heat consumption and the consumption of cooling water in a single rectification, it is first necessary to determine the total reflux L for the whole process.

This can be found from the equation:

$$L = \int_0^L dL,$$

where dL is the instantaneous, infinitesimal amount of reflux.

However, since $R = \frac{dL}{dP}$, we have

$$L = \int_0^L dL = \int_{R_f}^{R_W} R\,dP,$$

where R_f and R_W are reflux ratios corresponding to liquid concentrations x_f and x_W. R_f and R_W are the initial and final reflux ratios.

Then the average reflux ratio can be represented as

$$R_{av} \cdot P = L = \int_{R_f}^{R_W} R\,dP \tag{16}$$

or

$$R_{av} = \frac{\int_{R_f}^{R_W} R \cdot dP}{P} \qquad (17)$$

After R_{av} has been found, it is multiplied by P to calculate the total amount of reflux L for a single batch rectification. It is then possible to calculate the amount of liquid to be evaporated and the amount of vapor to be condensed. In this way it is easy to determine separately the consumption of heating steam for evaporation of the liquid and the consumption of cooling water in the condenser.

After the rectification has continued until the concentration of the residue in the still is x, from the material balance equation

$$P = \frac{F(x_f - x)}{x_p - x}$$

we have after differentiation

$$dP = \frac{F(x_f - x_p)\,dx}{(x_p - x)^2}. \qquad (18)$$

Substitution of this expression into Equation (16) gives:

$$R_{av} = \frac{-F(x_f - x_p)}{P} \int_{x_W}^{x_f} \frac{R dx}{(x_p - x)^2}. \qquad (19)$$

We now substitute Equation (11) into Equation (19) to give

$$R_{av} = \frac{-(x_f - x_p)(x_p - x_W)}{x_f - x_W} \int_{x_W}^{x_f} \frac{R dx}{(x_p - x)^2}. \qquad (20)$$

Comparison of Equations (14), (15), and (19) shows that Equation (19) and the Bogart equation have the same form of integral, and differ in this respect from A. G. Kasatkin's equation.

All the equations derived or quoted above are collected in the Table.

Algebraic Integration of the Equations

Equations (a), (d), (f), and (g) given in the Table were derived by graphical integration. Algebraic integration can give solutions of great practical importance.

For analysis of the performance of a rectification column, and for calculation of its characteristics, it is first necessary to determine the functions of many variables.

For ideal solutions, we have the general relationship

$$\Phi(R,\ n,\ x_p,\ x,\ \alpha) = 0, \qquad (21)$$

where α is the relative volatility of a binary mixture.

With the use of α the phase equilibrium function y = f (x) can be expressed algebraically in the form of the equation

	Distillate, P	Rectification time, t	Average reflux ratio, R_{av}	Average concentration of distillate, $(x_p)_{av}$
1st alternative Distillation at constant reflux ratio	$P = F - W$ $\log W = \log F - \frac{1}{2.303}\int_{x_W}^{x_f} \frac{dx}{x_p - x}$ (a)	$\frac{(F-W)(R+1)}{v}$ (b)	R (c)	$x_f - \frac{x_W}{\int_{x_W}^{x_f} \frac{dx}{x_p - x}}$ $\frac{e}{1 - \frac{1}{\int_{x_W}^{x_f} \frac{dx}{x_p - x}}}$ (d)
2nd alternative Distillation with const. distillate concentration	$\frac{F(x_f - x_W)}{x_p - x_W}$ (e)	$\frac{-F(x_p - x_f)}{v}\int_{x_f}^{x_W} \frac{(R+1)\,dx}{(x_p - x)^2}$ (f)	$\frac{(x_f - x_p)(x_p - x_W)}{x_f - x_W}\int_{x_f}^{x_W} \frac{Rdx}{(x_p - x)^2}$ (g)	x_p (h)

$$y = \frac{\alpha x}{1 + (\alpha - 1)x}. \qquad (22)$$

For nonideal solutions the function y = f(x) may be algebraically expressed as

$$\Phi[n,\ R,\ x_p,\ x, f(x)] = 0. \qquad (23)$$

In Kasatkin's [1, 2] algebraic solution of this equation there is an error. He considers that the equation

$$R_{\min} = \frac{x_p - y}{y - x} \qquad (24)$$

and the equation

$$R = \frac{x_p - y_0}{y_0 - x} \qquad (25)$$

are of analogous construction, and, since the composition of the vapor over the liquid, as a function of the liquid composition, y = f(x) may be represented as

$$y = \frac{\alpha x}{1 + (\alpha - 1)x},$$

it is therefore possible to represent the relationship between $\underline{x}$ and y_0 in an analogous manner:

$$y_0 = \frac{\alpha' x}{1 + (\alpha' - 1)x}, \qquad (26)$$

where R_{min} is the minimum reflux ratio; $\underline{y}$ is the equilibrium concentration of vapor over the solution with concentration $\underline{x}$ in the still; y_0 is the ordinate corresponding to the abscissa $\underline{x}$ of the point at which the operating reflux ratio is $\bar{R}$ (as shown in Fig. 3).

Thus, by elimination of y_0 from Equations (25) and (26) it is possible to derive a functional relationship between x_p, $\underline{x}$ and R

$$R = \frac{x_p - [\alpha' - (\alpha' - 1)x_p]x}{x(\alpha' - 1) - (\alpha' - 1)x^2}. \qquad (27)$$

Hence, direct algebraic integration of Equations (6) and (15) is possible. We then have:

$$R_{av} = \frac{\alpha'(1-x_p)\log\frac{1-x_f}{1-x_W} + x_p\log\frac{x_f}{x_W}}{0.435(\alpha'-1)(x_f-x_W)} \quad (28)$$

and

$$(x_p)_{av} = \frac{(R+1)\alpha'}{(\alpha'-1)^2}\left[\alpha'-1-\frac{2.3}{x_f-x_W}\log\frac{1+(\alpha'-1)x_f}{1+(\alpha'-1)x_W} - \frac{R(x_f+x_W)}{2}\right]. \quad (29)$$

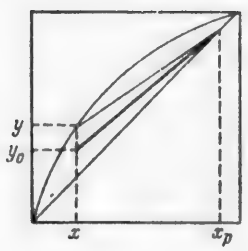

Fig. 3. Calculation of the operating concentration line.

Thus, by plotting a graph (Fig. 3) for a definite number of plates n and a definite value of x_p found for a single selected value of the reflux ratio R, we can find the value of y_0 corresponding to $\bar{x}$.

Substitution of y_0 and $\bar{x}$ into Equation (26) gives α'. By substitution of the value found for α' into Equation (28) with the number of plates n and the reflux ratio R known, y_0 corresponding to the value of $\bar{x}$ is found graphically. By using the values found for $\bar{x}$ and y_0 in Equation (26) we can calculate α' for Equation (29).

It was pointed out earlier that the derivation of Equation (6) and (15) contains an error; therefore, the equations obtained by integration also contain an error, even if Kasatkin's integration method is correct. If the algebraic integration is performed correctly, Kasatkin's Equation (27) can be used for direct integration of Equations (a), (d), (f), and (g) in the Table, as Equation (27) is the simplest form of the function represented by Equation (21).

Thus, if Kasatkin's algebraic integration method was correct, many complex calculations of the rectification process could be simplified considerably. It is therefore very important to detect and discuss the error inherent in the integration method itself. The essence of Kasatkin's theory [1, 2] is that the terminal point (y_0, x) of the operating line lies on a line similar to the equilibrium curve y = f(x), and therefore in the equations for the two curves α' differs from α.

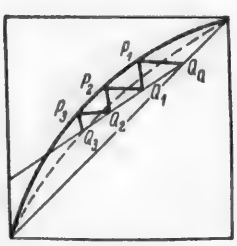

Fig. 4. Determination of the operating concentration path.

However, despite the fact that the operating line for the minimum reflux ratio and the operating line for the actual reflux ratio are straight lines and are even analogous in their construction, there is no reason for assuming that the path of the terminal point (x, y_0) and the path of the point of intersection of the operating line for the minimum reflux ratio with the equilibrium curve belong to the same family of curves.

From the mathematical aspect the following inaccuracies in Kasatkin's derivation may be pointed out. The equilibrium curve $y = \frac{\alpha x}{1+(\alpha-1)x}$ may be written in the form:

$$x = \frac{y}{\alpha-(\alpha-1)y}. \quad (30)$$

The operating line can be represented as

$$y = x_p + \frac{R}{R+1}(x-x_p). \quad (31)$$

If we take n = 3, then in Fig. 4 we can consecutively determine the points $p_1(x_1, y_1)$, $p_2(x_2, y_2)$, $p_3(x_3, y_3)$, $Q_1(x_1, y_2)$, $Q_2(x_2, y_3)$, $Q_3(x_3, y_4)$.

We find the coordinates of these points:

$$y_1 = x_p$$

$$x_1 = \frac{x_p}{\alpha - (\alpha - 1)\, x_p} = \frac{x_p}{K_1},$$

where $K_1 = \alpha - (\alpha - 1)x_p$.

Substituting the value of x_1 into Equation (31), we have:

$$y_2 = x_p + \frac{R}{R+1}\left(\frac{x_p}{K_1} - x_p\right) = x_p \frac{R + K_1}{K_1 R + K_1};$$

$$x_2 = x_p \frac{R + K_1}{K_2 R + K_1^2},$$

where

$$K_2 = \alpha K_1 - (\alpha - 1)\, x_p = \alpha^2 - (\alpha^2 - 1)\, x_p.$$

Further

$$y_3 = x_p + \frac{R}{R+1}\left(x_p \frac{R + K_1}{K_2 R + K_1^2} - x_p\right) =$$

$$= x_p \frac{R^2 + (K_1 + K_2) R + K_1^2}{K_2 R^2 + (K_2 + K_1^2) R + K_1^2};$$

$$x_3 = \frac{x_p \dfrac{R^2 + (K_1 + K_2) R + K_1^2}{K_2 R^2 + (K_2 + K_1^2) R + K_1^2}}{\alpha - (\alpha - 1)\, x_p \dfrac{R^2 + (K_1 + K_2) R + K_1^2}{K_2 R^2 + (K_2 + K_1^2) R + K_1^2}} =$$

$$= x_p \frac{R^2 + (K_1 + K_2) R + K_1^2}{K_3 R^2 + K_1 K_2 R + K_1^3};$$

$$y_4 = x_p + \frac{R}{R+1}\left(x_p \frac{R^2 + (K_1 + K_2) R + K_1^2}{K_3 R^2 + K_1 K_2 R + K_1^3} - x_p\right) =$$

$$= x_p \frac{R^3 + (K_1 + K_2 + K_3) R^2 + (K_1 K_2 + K_1^2) R + K_1^3}{K_3 R^3 + (K_1 K_2 + K_3) R^2 + (K_1 K_2 + K_1^3) R + K_1^3},$$

where $K_3 = \alpha K_2 - (\alpha - 1)x_p = \alpha^3 - (\alpha^3 - 1)x_p$.

The coordinates of the point Q_3 vary with R (and with the number of plates n). In the present instance the value of the reflux ratio R is variable. The path of the point Q_3 may be represented by the following parametric equation:

$$\left.\begin{aligned} x &= x_p \frac{R^2 + (K_1 + K_2) R + K_1^2}{K_3 R^2 + K_1 K_2 R + K_1^3} \\ y &= x_p \frac{R^3 + (K_1 + K_2 + K_3) R^2 + (K_1 K_2 + K_1^2) R + K_1^3}{K_3 R^3 + (K_1 K_2 + K_3) R^2 + (K_1 K_2 + K_1^3) R + K_1^3)} \end{aligned}\right\} \quad (32)$$

Equation (32) cannot be reduced to the form of Equation (26)

$$y = \frac{\alpha' x}{1 + (\alpha' - 1) x} .$$

In order to modify Equation (32) to give an equation of the type of (26), it is necessary to introduce a constant α', to obtain the following identity:

$$x_p = \frac{R^3 + (K_1 + K_2 + K_3) R^2 + (K_1 K_2 + K_1^2) R + K_1^3}{K_3 R^3 + (K_1 K_2 + K_3) R^2 + (K_1 K_2 + K_1^3) R + K_1^3} \equiv$$

$$\equiv \frac{\alpha' x_p \cdot \dfrac{R^2 + (K_1 + K_2) R + K_1^2}{K_3 R^2 + K_1 K_2 R + K_1^3}}{1 + (\alpha' - 1) x_p \cdot \dfrac{R^2 + (K_1 + K_2) R + K_1^2}{K_3 R^2 + K_1 K_2 R + K_1^3}} \equiv$$

$$\equiv \frac{\alpha' x_p \left[R^2 + (K_1 + K_2) R + K_1^2\right]}{\left[K_3 + (\alpha' - 1) x_p\right] R^2 + \left[K_1 K_2 + (\alpha' - 1)(K_1 + K_2) x_p\right] R + \left[K_1^3 (\alpha' - 1) x_p K_1^2\right]} . \quad (33)$$

Reducing Identity (33) to a common denominator, we obtain an equation of the 5th degree. Introduction of α' results in inequality of the coefficients in the left and right sides of Equation (6).

We compare the coefficients of the highest and of the independent terms.

The highest term (5th power)

$$K_3 + (\alpha' - 1) x_p = \alpha' K_3$$
$$K_3 - x_p = \alpha' K_3 - \alpha' x_p$$

The independent term:

$$K_1^3 \left[K_1^3 + (\alpha' - 1) x_p K_1^2\right] = K_1^3 \alpha' K_1^2$$
$$K_1 + (\alpha' - 1) x_p = \alpha'$$
$$K_1 = \alpha' - (\alpha' - 1) x_p$$
$$\alpha' = \alpha$$

Not only do the two results fail to coincide, but they have no practical meaning. This means that Equation (32) cannot be reduced to the form of Equation (26).

For ideal solutions, Kasatkin gives another method for analytical calculation of R_{av} and $(x_p)_{av}$. By using the equations

$$R_{min} = \frac{x_p - y}{y - x}$$

and

$$y = \frac{\alpha x}{1 + (\alpha - 1)\, x}$$

we obtain

$$R_{\min} = \frac{x_p + [x_p (\alpha - 1) - \alpha]\, x}{(\alpha - 1)\, x - (\alpha - 1)\, x^2} \cdot \tag{34}$$

Integration of the equations

$$(R_{\min})_{av} = \frac{1}{x_f - x_W} \cdot \int_{x_W}^{x_f} R_{\min} \cdot dx \tag{35}$$

and

$$(x_p)_{av} = \frac{1}{x_f - x_W} \int_{x_W}^{x_f} x_p \cdot dx = \frac{1}{x_f - x_W} \int_{x_W}^{x_f} [(R_{\min} + 1)\, y - R_{\min} x]\, dx \tag{36}$$

gives equations analogous to Equations (28) and (29). Only α' and R in Equations (28) and (29) are replaced by α and R_{min}.

Multiplication of the calculated average minimum reflux ratio $(R_{min})_{av}$ by the coefficient b gives the practical average reflux ratio

$$R_{av} = b\, (R_{\min})_{av} \tag{37}$$

In the above equations the algebraic integration is carried out correctly.

However, only the average minimum reflux ratio can be found from Equation (37), while the practical values of R_{av} and $(x_p)_{av}$ cannot be determined, as to determine the coefficient b it is first necessary to calculate R_{av} from (21) or (23). Then, by means of Equation (37), with the value of $(R_{min})_{av}$ known, the value of b can be found.

The next stage is to find the actual functional relationship (21) or (23).

For ideal solutions, Smoker [7] derived the equation

$$x = K + \frac{(mc^2)^n\, (x_p - K)}{\alpha^n - (mc)\, (\alpha - 1)\, (x_p - K) \left[\dfrac{\alpha^n - (mc^2)^n}{\alpha - mc^2} \right]}, \tag{38}$$

where $m = \frac{R}{R+1}$, $c = 1 + (\alpha - 1)\, K$, $b = \frac{x_p}{R+1}$.

The value of K ranges between 0 and 1.

K is the root of the following quadratic equation:

$$m(\alpha - 1)\, K^2 + [m + b(\alpha - 1) - \alpha]\, K + b = 0.$$

In the derivation of this equation it was assumed that the equilibrium curve coincides with the functional relationship $y = \frac{\alpha x}{1 + (\alpha - 1)x}$. No other assumptions were made. This equation can therefore be regarded as sufficiently rigid and accurate. Comparison of results calculated by means of Smoker's and Kasatkin's equations clearly reveals considerable discrepancies between the two.

For example, if the number of theoretical plates n = 4, the reflux ratio R = 19, the relative volatility $\alpha = 2$, and the distillate concentration $x_p = 0.9$. Smoker's equation gives x = 0.4 for the concentration of the solution in the still.

Substituting the values of R, x_p and x into Equation (25), we find $y_0 = 0.425$. Further, substituting the calculated values $y_0 = 0.425$ and x = 0.4 into Equation (26), we find $\alpha' = 1.11$.

Then, for definite values of n, R, α, and $x_p = 0.98$, Smoker's equation gives x = 0.6. For the same conditions (and at x = 0.6) Equation (27) gives $x_p = 1.15$.

This illustrates the discrepancy between the results of calculations by the two methods, and demonstrates the erroneous nature of A. G. Kasatkin's derivation.

In theory, by integration of Equations (a), (d), (f), and (g) with the aid of Smoker's equation, it is possible to find algebraic solutions.

However, as the functional relationship in this case is very complex, algebraic integration is very difficult, and the algebraic solution is a complex expression. Therefore, the use of these equations does not in any way simplify calculations of rectification columns as compared with the graphical method.

In addition to Equation (38), Lewis [8], Underwood [9, 10], Harbert [11], Stoppel [12], Clark [13], Eshaya [14], Amundson [15], Mitsuho Hirata [16], and others have proposed various algebraic expressions for relationships between the number of theoretical plates n, the reflux ratio R, the distillate concentration x_p, the concentration in the still x, and the functional phase equilibrium relationship y = f(x). Some of these, such as Clark's and Eshaya 's equations, are algebraic formulas for nonideal solutions. However, all these functional relationships are very complex. Therefore, direct integration of Equations (a), (d), (f), and (g) with the aid of these formulas is difficult.

For total reflux, the functional relationship (21) or (23) is very simple, and when the value of the relative volatility shows only small deviations the number of theoretical plates can be determined by means of the Fenske equation [17]

$$n = \frac{\log\left(\frac{x_p}{1-x_p}\right)\left(\frac{1-x_W}{x_W}\right)}{\log_{\alpha}} . \qquad (39)$$

Gilliland [18] used this relationship and integrated Equation (a) to obtain the following equation

$$\ln \frac{W}{F} = \frac{1}{\alpha^{N+1} - 1} \ln \frac{x_W(1-x_f)}{x_f(1-x_W)} + \ln \frac{1-x_f}{1-x_W} . \qquad (40)$$

Equation (40) represents the general relationship between the relative volatility, the maximum degree of separation, and the minimum number of theoretical plates. However, in practical rectification this equation also is of no help in integration of Equations (a), (d), (f), and (g) for determination of the amount of distillate $(x_p)_{av}$, reflux ratio R_{av}, and the time required for intermittent distillation.

In some special instances of practical rectification the functional relationship (21) and (23) may be expressed in simpler form, and the basic Equations (a), (d), (f), and (g) are easier to integrate. This matter is considered in the following section.

Analytical Calculation When the Concentration of the Distillate is Close to 1

Under such conditions we can use Underwood's equation [19]

$$(k\alpha)^{n-1}\left[\frac{1}{1-x}-\frac{k(\alpha-1)}{(k\alpha-1)}\right]=\frac{1}{\alpha(1-x_p)}\,, \tag{41}$$

where $k=\frac{R}{R+1}$.

Integration of Equation (a) then gives:

$$\log W=\log F-\frac{1}{(k^{n-1}\alpha^n-1)}\left[-k^{n-1}\alpha^n\log(1-x)+\right.$$
$$\left.+\log\left\{k^n\alpha^n(\alpha-1)x+k^{n-1}\alpha^n(k-1)-(k\alpha-1)\right\}\right]_{x_W}^{x_f} \tag{42}$$

Equation (d) is simplified and reduced to the fonn

$$(x_p)_{av}=\frac{x_f\cdot e^{\ln\frac{F}{W}}-W}{e^{\ln\frac{F}{W}}-1}\,. \tag{43}$$

The value $\ln\frac{F}{W}$ in Equation (43) is detennined by Equation (42).

In theory, Equations (f) and (g) may also be integrated to give an algebraic solution. However, algebraic integration of these equations is very difficult.

The following assumptions must be valid in calculations with the use of Equations (42) and (43): x_D approaches 1; α is constant.

Analytical Calculation for Cases in Which the Functional Relationship for the Phase Equilibrium is Linear

For some solutions, usually within fairly wide limits, the equilibrium line may be represented by the equation y = ax + m. For very dilute solutions m = 0 (a and m are constants). Thomann [20] derived the following equation for such conditions:

$$\left[\frac{R}{a(R+1)}\right]^{n-1}\left[\frac{m-\frac{x_p}{R+1}}{\frac{R}{R+1}-a}-\frac{x_p-m}{a}\right]=\frac{m-\frac{x_p}{R+1}}{\frac{R}{R+1}-a}-x. \tag{44}$$

Equation (44) can be simplified and reduced to:

$$x_p\left\{\left[\frac{R}{a(R+1)}\right]^{n-1}\left(a-\frac{a+R}{R+1}\right)+\frac{1}{R+1}\right\}=x\left(a-\frac{R}{R+1}\right)+m\left\{1-\frac{R}{R+1}\left[\frac{R}{a(R+1)}\right]^{n-1}\right\}. \tag{45}$$

Equation (a) (see Table) can then be integrated:

$$\log W=\log F-\frac{1}{2.303}\left\{\frac{A}{B-A}\log\left[x\left(\frac{B}{A}-1\right)+\frac{C}{A}\right]\right\}_{x_W}^{x_f}, \tag{46}$$

where

$$A = \left[\frac{R}{a(R+1)}\right]^{n-1}\left(a - \frac{a+R}{R+1}\right) + \frac{1}{R+1}, \quad B = a - \frac{R}{R+1},$$

$$C = m\left\{1 - \frac{R}{R+1}\left[\frac{R}{a(R+1)}\right]^{n-1}\right\}.$$

The solution of Equation (d) resembles Equation (43), but the value $\ln \frac{F}{W}$ in it is determined by Equation (46).

It is similarly possible to integrate Equations (f) and (g) in order to obtain algebraic solutions. However, algebraic integration here is also very difficult.

In addition, Suen [21], and Thomson and Beatty [22], proposed calculation methods for the case when the equilibrium curve is a straight line. These calculation methods are essentially analogous to Thormann's method. They can also be used to integrate Equations (a), (d), (f), and (g).

Dodge and Huffman [23] made a different approach to the calculation; if y = ax, simplification of Lewis's equation [8] gives the following equation:

$$n = \frac{2.303}{A}\log\frac{Ax_p + B}{Ax + B}, \tag{47}$$

where $A = a - 1 + \frac{a}{R}$, $B = -\frac{x_p}{R}$

Equation (47) can be used for integration of Equation (a) (see Table)

$$\log W = \log F - \frac{1}{2.303(M-1)}\log\frac{x_f}{x_W}, \tag{48}$$

where $M = \dfrac{e^{nA}A}{A - \frac{1}{R} + \frac{e^{nA}}{R}}$.

This equation is less complicated, but accurate calculation results can only be obtained if the functional relationship for the phase equilibrium is of the form y = ax and if the column contains a large number of plates.

LITERATURE CITED

[1] A. G. Kasatkin, Processes and Equipment in Chemical Technology (GONTI, 1950) p. 533.*

[2] A. G. Kasatkin, Processes and Equipment in Chemical Technology (1955) p. 547.*

[3] Rayleigh, Phil. Mag., 4, 521 (1902).

[4] A. Rose, H. H. Long, Ind. Eng. Ch., 33, 684 (1941).

[5] R. Edgeworth-Johnstone, Ind. Eng. Ch., 35, 408 (1943).

[6] M. T. P. Bogart, Trans. Am. Inst. Chem. Engrs. 33, 139 (1931).

[7] E. H. Smoker, Trans. Am. Inst. Chem. Engrs., 34, 165 (1938).

[8] W. K. Lewis, Ind. Eng. Ch., 14, 492 (1922).

[9] A. T. V. Underwood, J. Inst. Petroleum, 29, 147 (1943); 30, 325 (1944).

[10] A. T. V. Underwood, J. Soc. Chem. Ind. (London), 52, 232 (1933).

[11] W. H. Harbert, Ind. Eng. Ch., 37, 1162 (1945).

* In Russian.

[12] A. E. Stoppel, Ind. Eng. Ch., 38, 127 (1946).

[13] A. M. Clark, Trans. Faraday Soc., 41, 138 (1945).

[14] A. M. Eshaya, Chem. Eng. progress, 43, 10, 555 (1947).

[15] N. Amundson, Trans. Am. Inst. Chem. Engrs., 42, 939 (1946).

[16] Mitsuho Hirata, Chem. Eng. (Japan), 15, 267 (1950).

[17] M. R. Fensky, Ind. Eng. Ch. 36, 482 (1932).

[18] C. S. Robinson and E. R. Gilliland, Elements of Fractional Distillation (McGraw Hill, New York, (1950).

[19] A. T. V. Underwood, Trans. Inst. Chem. Engrs., (London) 10, 112 (1932).

[20] K. Thormann, Destillieren und Rektifizieren. Leipzig, Otto Spämer (1929).

[21] T. T. Suen, Ind. Eng. Ch., 33, 656 (1941).

[22] G. W. Thomson, H. A. Beatty, Ind. Eng. Ch., 34, 1124 (1942).

[23] B. F. Dodge, T. R. Huffman, Ind. Eng. Ch., 29, 1434 (1937).

Received November 27, 1956

HARD GOLD PLATING

A. G. Atanasyants, N. T. Kudryavtsev, and V. M. Karataev

One of the disadvantages of gold coatings is their low resistance to wear. Gold-plated parts working under friction (moving current collectors, etc.) quickly become unserviceable owing to abrasion of the gold coating. It was therefore very desirable to study the possibility of producing gold coatings of higher hardness and wear resistance.

Very little information is available in the literature on hard gold electroplating. According to literature data [1], small amounts of nickel in the form of a complex cyanide salt should be added to the gold cyanide electrolyte for this purpose. The cathodic deposit formed contains only 0.17% nickel. It is stated, however, that this is enough to increase the hardness of the gold coating appreciably without affecting its external appearance. According to Billiter [2], 0.6-1.0 g of nickel per liter can be added to the electrolyte in the form of carbonate. Krause [3] recommends the addition of 2 to 3% of nickel in the form of a complex nickel and potassium cyanide salt. The electrolyte is warmed to 30-50°. Winkler's process [4,5] described in foreign patents (Germany, France, Canada, Italy, Switzerland, England, and U.S.A.) in 1931-1932 is based on the use of a pulsating current and commutator. According to this author, it is possible to introduce up to 1.7% of nickel into the gold deposit and to obtain a ternary copper–nickel–gold alloy by this method. Boitsov et al. [6] report that copper, deposited in large amounts together with gold, also increases the hardness of the coatings.

Production of gold – nickel and gold – cobalt alloys is difficult because the potentials of nickel and cobalt in cyanide solutions differ considerably from the cathode potential of gold. The deposition potentials of nickel and cobalt are more electronegative than the deposition potential of gold. Therefore for joint deposition of nickel or cobalt with gold it is necessary to use considerably higher current densities than for deposition of gold alone. At high current densities, however, gold is deposited in powder form.

It was necessary to find electrolysis conditions in which the cathode potentials of the deposited metals, gold and nickel or cobalt, are similar at relatively low current densities, suitable for deposition of gold.

EXPERIMENTAL

The effects of electrolyte composition and electrolysis conditions on the composition, structure, and hardness of the deposits were studied. Deposits of the maximum hardness obtained from various baths were subjected to comparative tests for wear resistance, contact continuity, corrosion resistance, porosity, adherence, etc. The composition of the deposits was determined by chemical analysis, and the quality of the deposits was evaluated by visual inspection under 10-fold magnification and from photographs of individual specimens under 487-fold magnification to reveal the microstructure.

The hardness of the coatings was determined by means of the PMT-3 instrument at 10 and 20 gram loads.

The wear resistance of the coatings was tested by two methods: 1) by rotation of gold-plated collectors against stationary brushes at a pressure of 35 ± 5 g, with the rings rotating at 60 r.p.m.; 2) by abrasion of stationary specimens against a vibrating slider at a pressure of 0.2 g. The groove formed by friction against the slider was measured after 500,000 oscillations. MIS-11 and MBS-1 microscopes were used as measuring instruments. The continuity of contact was determined oscillographically after each 20,000 oscillations.

The porosity of the coatings was determined by the action of Walker's reagent on the copper basis metal. The adherence of the coating to the basis metal was tested by the usual method, by peeling after fracture.

The electrolyte for hard gold plating was made by addition of complex potassium – nickel cyanide salt to the gold cyanide electrolyte. The nickel cyanide salt was made by dissolving nickel sulfate in excess of potassium cyanide. The anodes were plates of sheet gold (99.99%), and the cell was a porcelain beaker 0.5 liter in capacity. The liquid was agitated mechanically by means of screw and blade stirrers. The thickness of the coatings was about 10 μ. The coating thickness was found from the difference between the weights of the plate before and after electrolysis.

To determine the optimum electrolysis conditions in the electrolyte of the chosen composition, cathodic polarization and current efficiency were studied. Cathodic polarization was also determined in gold and nickel electrolytes separately, and hydrogen overvoltage at gold and nickel electrode was studied. The current efficiency in different electrolytes was determined. Specimens of brass, grade L-62, 7 cm^2 in area, were used for the experiments. Some specimens were coated with a layer of copper 10 μ thick before the gold plating.

Data for the polarization curves were obtained with the aid of the LP-5 potentiometer. The cathode was platinum, coated with the metal to be studied in a layer 2 μ thick before each determination. For polarization measurements in the mixed electrolyte, the platinum was coated with gold. A standard calomel half-cell was used as the standard electrode. Each current density was applied for 0.5 minute; the cathode potential did not change during this time.

Experiments on the separate deposition of gold, nickel, and cobalt. The cyanide electrolyte for gold plating had the following composition (in g/liter): gold 4.65, potassium cyanide (free) 5.15, potassium carbonate 32; electrolyte temperatures, 18 and 60°.

The thickness of the gold plating was 8 ± 2 μ.

Dense gold deposits, quite satisfactory in external appearance, were obtained at current densities up to 0.2 amp/dm^2 in the hot electrolyte, and up to 0.1 amp./dm^2 in the cold.

The current efficiency in an electrolyte containing 7.6 g of potassium cyanide (free) per liter at 60° and D_c = 0.2 amp./dm^2 was about 75%; at room temperature and D_c = 0.1 amp./dm^2, it was 65%. The current efficiency in an electrolyte with a higher cyanide content (up to 15 g/liter) fell by 10%. The hardness of the deposits was in the range of 95-110 kg/mm^2 in both cases. Gold deposits obtained at room temperature were harder than those from the hot electrolyte. Increase of the free cyanide concentration from 7.5 to 15 g/liter raised the hardness of the deposit from 96-110 to 110 kg/mm^2.

The nickel electrolyte had the following composition (in g/liter): nickel 4.65, potassium cyanide (free) 15, potassium carbonate 32; electrolyte temperatures, 18-20 and 60°.

Experiments at the higher temperature showed that electrodeposition of nickel only begins at a current density of 0.6 amp./dm^2; at lower current density only hydrogen is liberated. The current efficiency is only 1.5%.

At room temperature, in an electrolyte of the same condition, deposition of nickel on the cathode began at a lower current density, about 0.4 amp./dm^2.

The cobalt electrolyte had the following composition (in g/liter): cobalt 3.5, potassium cyanide (free) 15, potassium carbonate 32; electrolyte temperatures, 20 and 60°.

Platinum anodes were used. The elctrolysis was carried out at current densities up to 10 amp./dm^2; in no case was cobalt deposited.

Investigation of conditions for simultaneous deposition of gold and nickel from cyanide electrolytes. For determination of the optimum electrolyte composition for simultaneous deposition of gold and nickel, solutions with equal contents of the metals by weight (5 g/liter) and of free cyanide (KCN_{free} = 15 g/liter) were prepared. These solutions were mixed in such a way that the concentration of each metal varied from 0.5 to 4.5 g/liter while the total content of the two metals remained at about 5 g/liter. The free cyanide concentration was constant at 15 g/liter in all the electrolytes. The electrolysis was performed at electrolyte temperature of 60° and current density 0.2 amp./dm^2.

These experiments showed that the nickel contents of the deposits were low, and varied irregularly with the relative concentrations of the two metals in solution. A considerable increase in the hardness of the deposits

was found with about 1.5% of nickel in the solution, corresponding to a concentration of 3.5 g/liter or about 70%.

The nickel content and hardness of the deposit increased with increase of current density up to 0.6 amp./dm^2. However, the structure of the deposit was irregular and it was spongy at the the edges of the plates.

Dense deposits could not be obtained from an electrolyte containing (in g/liter): cobalt 3.5, gold 1.5, potassium cyanide (free) 15, and potassium carbonate 32. Spongy deposits were formed on the cathode, both at room temperature and at the higher temperature, even at a current density of 0.5 amp./dm^2.

A change of the free cyanide concentration from 7.5 to 20 g per liter in an electrolyte containing 1.5 g of gold and 3.5 g of nickel per liter did not have any appreciable influence on the external appearance and hardness of the deposits. With over 20 g of free cyanide per liter the deposits became spongy.

A decrease of the electrolyte temperature to 18-20° at D_c = 0.2 amp./dm^2 resulted in an increase of hardness of the deposits to 190 kg/mm^2 as compared with 160-170 kg/mm^2 for deposits obtained from hot electrolytes under the same conditions. The greater hardness of the deposits formed at room temperatures is probably the consequence of a more finely granular structure, as they have somewhat lower nickel contents than deposits from hot electrolytes. Stirring of either the hot or the cold electrolytes had no effect on the permissible cathodic current density.

The current efficiency was calculated only for the gold, as nickel was present in insignificant amounts in the deposits. At an electrolyte temperature of 60°, the cathodic current efficiency at D_c = 0.2 amp./dm^2 was 65%; at room temperature and the same current density, it was 25%. The anodic current efficiency was equal to the cathodic at 3 : 1 ratio of anode to cathode surface in the hot electrolyte, and at 2 : 1 ratio in the cold. Under these conditions the composition of the electrolyte is fairly stable, and the main adjustment necessary is of the free cyanide content.

The following electrolysis conditions for the production of gold deposits of increased hardness can be recommended on the basis of these results. Electrolyte composition (in g/liter): gold 1.5, nickel 3.5, potassium cyanide (free) 15, potassium carbonate up to 35; current density D_c = 0.2 amp./dm^2. The current efficiency is between 25 and 60% for electrolyte temperatures from 20 to 60° respectively.

Gold anodes are used. The ratio of anode to cathode area is 2 : 1 at 20° and 3 : 1 at 60°. The gold deposit contains up to 1.8% nickel, which increases its hardness to 150-190 kg/mm^2, according to the temperature (60 or 20°). Electrolyte composition is adjusted mainly by additions of nickel cyanide and potassium cyanide. The laboratory results were tested in a larger cell with the same results.

Investigation of cathodic polarization. The cathode potential as a function of the current density was determined in cyanide electrolytes in simultaneous and separate deposition of gold and nickel at 20 and 60°.

The graph shows that at very low current densities the cathode potential is considerably more negative in the nickel electrolyte (Curves 1 and 4) than in the gold electrolyte (Curves 2 and 5) under the same conditions. For example, at D_c = 0.1 amp./dm^2 and electrolyte temperature 60° the difference between the potentials is 0.45 v, and at 20°, about 0.2 v.

At current densities of about 0.15 amp./dm^2 at 20° and 0.35 amp./dm^2 at 60° the polarization curves for nickel and gold intersect, and at higher current densities the relationship between the potentials is reversed, but gold is deposited in spongy form.

The very low current efficiency in the nickel electrolyte in the operating current density range (0.15-0.3 amp./dm^2) can be attributed to the low hydrogen overvoltage on nickel. The curves show that the potential of hydrogen evolution is lower than the cathode potential of nickel under the same conditions (Curves 1 and 7). For example, at D_c = 0.2 amp./dm^2 the hydrogen evolution potential is 0.97 v, and the cathode potential of nickel is 1.4 v.

In the mixed electrolyte at low current densities (D_c = 0.1-0.3 amp./dm^2) the cathode potential of the alloy approaches the values of the cathode potential of nickel at both temperatures (Curves 1 and 3, 4 and 6). At higher current densities the polarization curves for the alloy are shifted considerably in the direction of less negative values relative to gold, indicating that nickel exerts a depolarizing action. The curve for hydrogen overvoltage at a nickel cathode (Curve 7), in contrast to the curve for hydrogen overvoltage at a gold cathode

(Curve 8), lies to the left of the curve for the potentials of the simultaneous deposition of gold and nickel (Curve 3). This is the probable reason for the low nickel content in the alloy deposit. Increase of the electrolyte temperature results in a relatively small decrease of cathodic polarization in all cases.

Tests of the deposits. The deposits formed from the mixed electrolyte of optimum composition were tested for hardness, porosity, adherence, wear resistance, contact quality, and protective properties.

Porosity tests showed that coatings about 10 μ thick on polished copper surfaces have between 1 and 3 pores per 3 cm^2, mainly at the edges of the specimens and at contact points.

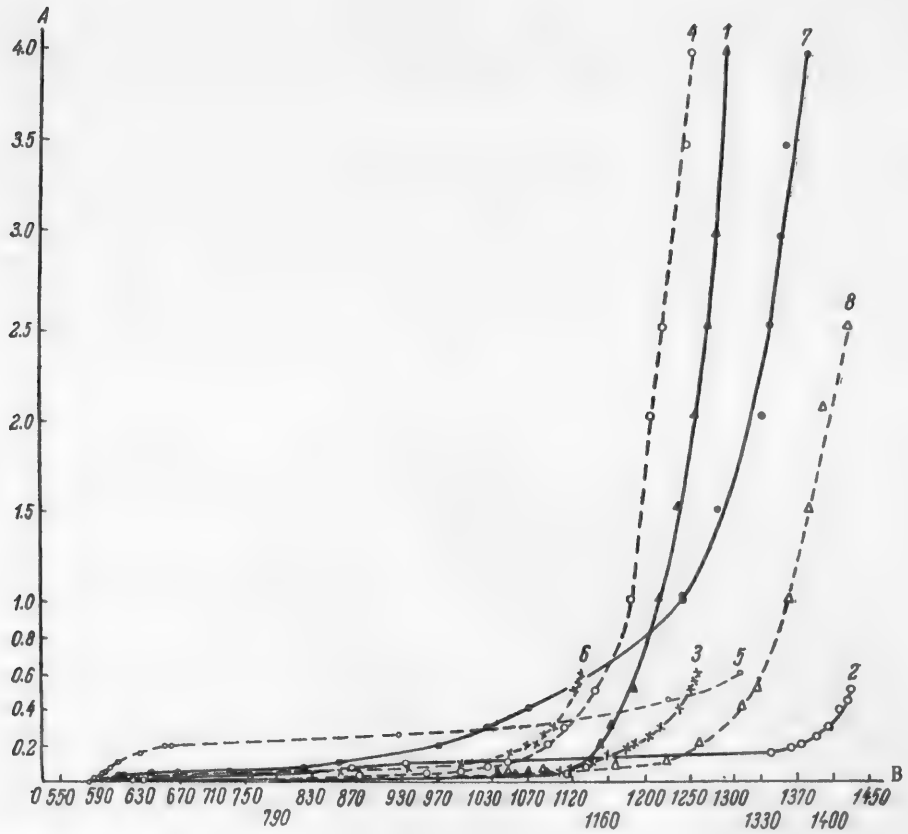

Polarization curves.
A) Cathode current density D_c (in amp./dm^2), B) cathode potential (mv).
Electrolyte compositions (in g/liter) and temperatures (°C) respectively: 1) 5Ni + 15KCN_{free} + + 25K_2CO_3, 20°; 2) 5Au + 15KCN_{free} + 25K_2CO_3, 20°; 3) 3.5Ni + 1.5Au + 15KCN_{free} + 25K_2CO_3, 20°; 4) 5Ni + 15KCN_{free} + 25K_2CO_3, 60°; 5) 5Au + 15 KCN_{free} + 25K_2CO_3, 60°; 6) 1.5Au + 3.5Ni + + 15KCN_{free} + 25K_2CO_3, 60°; 7) 15KCN_{free} + 25K_2CO_3, 20°, Pt anode, Ni cathode; 8) 15KCN_{free} + + 25 K_2CO_3, 20°, Pt anode, Au cathode.

Tests for adherence of the coatings to the basis metal showed that the deposits do not peel off when the specimens are fractured.

Comparative tests of wear resistance and contact properties of specimens coated with pure gold and specimens coated with gold – nickel alloys deposited from hot and cold electrolytes gave the following results. In tests under 0.2 g pressure on the rubbing surface, the depth of the groove rubbed out by the current collector in

a gold coating of the usual type was 1.25 μ, whereas no changes were found on the surface of hard gold (gold – nickel alloy coating).

Very minute gold particles were found on the slider moving on the pure gold coating. No gold was detected on sliders moving on hard gold (deposited both from hot and cold electrolytes).

The contact quality of hard gold deposits formed from cold or hot electrolytes does not differ from that of ordinary gold deposits – the contact continuity is the same.

The following results were obtained in tests under 35 ± 5 g pressure at the rubbing surface. The groove depth in a pure gold deposit was 4.8 μ, in a deposit of Au – Ni alloy formed at 20°, it was 1.15 μ, and at 60°, 2.5 μ. The contact properties were unchanged.

Corrosion tests were carried out on specimens coated with pure gold and with Au-Ni alloy deposited from hot and cold electrolytes.

The tests were performed: 1) in an industrial gas atmosphere, 2) in a mist chamber, 3) in a humidity chamber, 4) in a hydrogen sulfide atmosphere, 5) in a cold and warm chamber consecutively. The tests were performed on 3 specimens from each electrolyte, with coatings 10 ± 2 μ thick. The results of the tests showed that:

1) the protective properties of hard gold (Au – Ni) deposits tested in an industrial gas atmosphere, in a humidity chamber, and in cold and warm chambers consecutively, are somewhat better than those of pure gold deposits;

2) the protective properties of hard Au – Ni deposits tested in a mist chamber and in hydrogen sulfide are equivalent to those of ordinary gold;

3) the protective properties of Au – Ni deposits from cold electrolytes are somewhat better than those of Au – Ni deposits from hot electrolytes.

SUMMARY

1. An electrolyte composition has been found for producing gold – nickel (gold-based) alloy coatings of higher hardness, 160-190 kg/mm^2, than that of ordinary gold coatings, about 100 kg/mm^2. The nickel content of the gold – nickel alloy deposit does not exceed 2%.

2. The optimum electrolysis conditions for deposition of gold – nickel alloy coatings and a method for adjusting the electrolyte composition are given.

3. Gold – nickel alloy deposits have high wear resistance when used in special current-collecting equipment at pressures up to 35 ± 5 g, the abrasion loss of "hard gold" deposits from cold electrolytes being one quarter, and that of deposits from hot electrolytes one half, of the abrasion loss of ordinary gold deposits. The contact quality is fully retained.

4. The corrosion resistance of "hard gold" is not inferior to the corrosion resistance of ordinary gold.

LITERATURE CITED

[1] V. I. Lainer and N. T. Kudryavtsev, Fundamentals of Electroplating, II (Metallurgy Press, 1946).*

[2] J. Billiter, Fundamentals of Electroplating Technology (ONTI, 1937). * *

[3] H. Krause, Galvanotechnology (Nonferrous Metallurgy Press, 1933).* *

[4] J. Winkler, French Patent 737 031.

[5] J. Winkler, DRP, 576 685.

[6] A. V. Boitsov, G. F. Voinova, and N. A. Avdonina, The Noble Metals (Metallurgy Press, 1946).*

Received December 2, 1955.

* In Russian.

* * Russian translation.

ELECTROCHEMICAL METHODS FOR DECORATIVE SURFACE TREATMENT OF ALUMINUM ARTICLES

P. V. Shchigolev

Electrochemical and chemical methods for decorative surface treatment of articles made of aluminum and its alloys are undoubtedly destined for extensive practical use in industry. The use of aluminum and its alloys for production of a wide range of extensively used articles, with surface finish imitating gold or brass, and for instrument parts, will make it possible to effect considerable savings of scarce and costly metals and alloys (gold, silver, brass, etc.).

The production of aluminum articles with an attractive external appearance (combined luster and color) is based on three consecutive technological stages: electropolishing (or chemical polishing), anodizing, and coloring with organic dyes or inorganic colored compounds.

The present investigation consisted of studies of electropolishing, chemical polishing, and anodizing of technical aluminum (AI and AO grades), and coloration of the anodic films to give gold and other colors.

EXPERIMENTAL

Electrolytic and chemical polishing of aluminum. Specimens in the form of plates and wire spirals (2 mm in diameter), and also finished articles – bottle caps – were used for the electropolishing. The specimens were merely degreased in dichloroethane before the electropolishing, and were not subjected to any mechanical treatment. The quality of the polished surface was evaluated by the value of the relative reflectivity coefficient and by inspection under the microscope. The reflectivity coefficient was determined by means of the apparatus described by Chertavskykh [1]. The comparison standard was a mirror made by vacuum condensation of aluminum on a flat, carefully polished glass plate.

Experiments were carried out to determine the optimum conditions for polishing aluminum in a sulfuric – – phosphoric – chromic acid electrolyte. It was found that the following electrolyte has good polishing power: H_2SO_4 (d = 1.6) 500 cc, H_3PO_4 (d = 1.55) 500 cc, CrO_3 60 g; % by weight: H_2SO_4 34, H_3PO_4 34, CrO_3 3.6, H_2O 28.4. The electropolishing conditions are: anodic current density 20-30 amp/dm^2, electrolyte temperature 80-90°, time 3-6 minutes, potential 10-15 v. A lead cathode was used.

This electrolyte can also be successfully used for polishing aluminum – magnesium and aluminum – magnesium – zinc alloys. Articles with curved or spherical surfaces acquire an excellent polish, but flat specimens exhibit occasional stripiness, especially after long exposures.

In our earlier publications we considered the theory of the electropolishing process [2], and the physicochemical, corrosion, and electrochemical properties of electropolished aluminum [3, 6].

The alkaline electrolyte proposed by Pullen (for the so-called Brital process) [7] can also be used for electropolishing of pure aluminum; this contains 150 g Na_2CO_3 (anhydrous), 80 g of Na_3PO_4 (anhydrous), and H_2O to 1 liter. Our experiments showed that increase of the Na_3PO_4 content of this electrolyte has a favorable effect on the quality of the polishing. The electropolishing conditions are: anodic current density 2.5-5 amp/dm^2, cell potential 12-14 v, electrolyte temperature 90°, treatment time 10-15 minutes.

The chemical method of aluminum polishing is of particular interest in practice. The advantage of chemical polishing is that an electric current or contact devices are not needed, and the productivity of the process is very high, being limited in practice only by the bath dimensions. The following disadvantages may be mentioned: harmful gases are liberated during dissolution of aluminum (NO_2, NO, etc.), it is difficult to maintain

a high temperature (100-120°), exact control of the bath composition is required during use, and the reflectivity of chemically polished specimens is somewhat inferior to that of electropolished. Recently there have been many publications (especially patents) in the foreign literature on chemical polishing of aluminum [8-16]. We tested some of the solutions suggested, in order to select the most suitable.

Solutions of the following compositions[8, 9], in vol. %, give good chemical polishing of aluminum: 1) H_3PO_4 (d = 1.7) 80, CH_3COOH (conc) 15, HNO_3 (d = 1.5) 5; 2) H_3PO_4 (d = 1.7) 75, H_2SO_4 (d = 1.84) 20, HNO_3 (d = 1.4) 5; in wt. %: 3) H_3PO_4 (d = 1.7) 77.5, H_2SO_4 (d = 1.84) 15.5, HNO_3 (d = 1.52) 6.0, H_3BO_3 (cryst) 0.5, $Cu(NO_3)_2$ (cryst) 0.5; 4) HNO_3 13, NH_4HF_2 16, H_2O 71.

In Solutions 1, 2, and 3 chemical polishing is carried out at 100-110° for 1-5 minutes, and in Solution 4, at 60 ± 5° for 20-60 seconds. After polishing in Solution 3, the specimens must be treated in 30-40% HNO_3 solution at room temperature for a few seconds to remove small pinpoint deposits of metallic copper.

The above solutions are also quite satisfactory for polishing aluminum – magnesium alloys containing 0.5-5% of magnesium.

Anodizing of electropolished aluminum. The anodizing process consists of electrochemical oxidation of aluminum acting as anode in certain electrolytes. The thickness of the oxide film formed, its composition, porosity, hardness, elasticity, and other properties depend on the composition of the electrolyte, anodic current density, bath temperature, and duration of treatment. Either direct or alternating current can be used for anodizing aluminum. In decorative anodizing of aluminum two important conditions must be satisfied: first, the anodic coatings must adsorb colors satisfactorily, and second, the reflectivity of the electropolished aluminum should not be appreciably diminished by the anodizing treatment. Oxalic and chromic acids are unsuitable for anodizing aluminum, as fairly high potentials must be used (~40 – 60 v), which involves certain technical difficulties, and, moreover, films formed in these electrolytes are self-colored (yellow to brown) and therefore, pure hues are not obtained by subsequent coloration with organic dyes.

The most suitable electrolyte for anodizing electropolished aluminum is H_2SO_4 solution.

We carried out experiments on anodizing of electropolished aluminum in 20% H_2SO_4 solution, with direct and alternating current (frequency 50 cycles/second) at 18 and 30° and current densities from 1 to 4 amp/dm^2.

The following results were obtained: 1) increases of the electrolyte temperature, treatment time (up to a definite limit), and current density favor formation of anodic films with higher adsorptive capacity for dyes, but the reflectivity (luster) of the anodized specimens decreases appreciably, which is highly undesirable; 2) anodizing by means of alternating current yields anodic coatings of better adsorptive capacity than coatings produced by means of direct current; 3) anodizing by means of alternating current causes somewhat less loss of luster in the electropolished aluminum than anodizing by means of direct current.

The above finds also apply to aluminum – magnesium alloys.

Anodic treatment of aluminum – magnesium – zinc and aluminum – silicon alloys, either by direct or by alternating current, yields dark gray opaque oxide films, unsuitable for decorative coloration.

We recommend the following conditions for anodizing of electropolished aluminum for decorative purposes: electrolyte, 20% H_2SO_4 solution; current density 2 amp/dm^2; electrolyte temperature 18-20°; time 20-30 minutes; alternating current.

Anodizing by means of direct current can be carried out under the same conditions, with a time of 15-20 minutes.

Anodic films of varying thickness, depending on the purpose of the articles and the conditions in which they are to be used, can be obtained by suitable variations of current density and treatment time.

Coloration of anodized aluminum. The coloration of porous anodic coatings is similar in some respects to the dyeing of various fibrous materials of plant and animal origin.

The adsorption of a dye by a fiber and the strength of the bonds between them depend to a considerable extent on the charge on the fiber surface, the structure of the double layer at the fiber – dye solution interface [17], and the degree of dispersion of the dye on solution. Moreover, an important part in dyeing processes is played by the molecular structure of the dye and the material, and by the chemical reactions between them.

The problem of dye fading is extremely complex, and has not yet been solved even in general terms. The action of solar or artificial radiation on presence of moisture induces complex photochemical reactions accompanied by destruction of the dyes [18].

Anodic coatings can be dyed either with organic dyes of different classes, or with inorganic soluble or insoluble colored compounds (pigments). The correct selection of organic dyes and the optimum dyeing conditions (dye concentration, pH, temperature of the dye bath, dyeing time), as well as the anodizing conditions, are important for the production of attractive and stable colors.

Several methods may be used for coloration of anodic coatings with inorganic compounds.

1. Formation of a colored insoluble compound (salt) by double decomposition in the pores of the coating [19-22]. For example, different shades of blue can be produced in anodic coatings by immersion first in 1% ferric chloride ($FeCl_3$) solution for a few minutes, followed, after rinsing in water, by immersion in 1% solution of potassium ferrocyanide ($K_4[Fe(CN)_6]$). An insoluble blue precipitate of Prussian blue is formed in the pores of the coating.

2. Reduction or oxidation of various metallic salts directly within the pores of the coating to give colored compounds [20, 22]. For example, salts of copper, silver, and gold are easily reduced in the coatings, which become colored reddish brown, violet-brown, and black. Lead salts are oxidized by potassium permanganate to give brown lead peroxide, and cobalt salts give the dark brown hydroxide.

3. Precipitation of colored hydroxides in the pores, by hydrolysis of heavy-metal salts [20, 22]. An attractive gold color may be produced by immersion of anodized articles for 10-15 minutes into 1.5% ferric ammonium oxalate solution [$(NH_4)_3Fe(C_2O_4)_3 \cdot 3H_2O$] at 60°. The salt is hydrolyzed with formation of ferric hydroxide which is deposited in the pores of the coating and colors it.

4. Filling of the anodic coating with photosensitive salts which decompose under the action of light to give colored products. This method can be used for the production of photographic plates after the anodic coating has been filled with silver bromide [20, 23, 24].

5. Treatment of the coatings with solutions of colored salts, which color the coatings by adsorption or chemical reaction with them. An example is the chromate treatment used as a protection against corrosion, which confers a yellow color to the coating. The treatment is carried out in 5-10% $K_2Cr_2O_7$ solution at 95° for 15-25 minutes, or in $K_2Cr_2O_7$ solution with additions of Na_2CO_3 or NaOH [25].

Experiments were carried out to determine the optimum conditions for dyeing anodized aluminum with mordant dyes. These organic dyes contain hydroxyl, carboxyl, and other groups capable of taking part in the formation of stable complex compounds with metallic salts (known as mordants) with which the fabrics are impregnated. Salts of aluminum, chromium, iron, etc., are used as mordants. As the pore surface of the anodic coating is strongly hydrated, and the pores may contain appreciable amounts of H_2SO_4, which forms aluminum sulfate (or possibly the basic salt) with $Al(OH)_3$, such a coating is a very suitable basis for the application of mordant dyes.

We recommend the following formulations for gold coloration of anodized aluminum: 1) Mordant Yellow 1 g, Alizarin Red C 0.14-0.3 g, water (distilled) 1 liter; 2) Mordant Yellow 1 g, Alizarin Orange P 0.15-0.3 g, water 1 liter. Dye bath temperature 70-80°, time 3-10 minutes.

These dye mixtures color the anodic coatings in various shades (from yellow to reddish) according to the anodizing conditions and the dyeing time. Oxide films formed by anodizing with direct current at 0.5-1 amp/dm^2 at 20° are colored in redder shades (the color of red gold). Definite standard anodizing and dyeing conditions must be carefully maintained in order to obtain particular shades.

For production of red, orange, and yellow colors the above-named dyes can be used singly. The dye concentration should be 1 g/liter, t = 70-80°, time 3-10 minutes.

Experiments were then carried out in order to determine the influence of various treatments of the anodized specimens, before and after dyeing, on the fastness of the colors to alcohol and tap water at room temperature, and to boiling water.

Alternating current was used for the anodizing (t = 18°, I_a = 2 amp/dm^2, time 20 minutes), and a mixture of Mordant Yellow + Alizarin Red C was used for dyeing, the time being 6 minutes.

The following treatments were tested: 1) dyeing of the anodized specimens immediately after washing in water; 2) dyeing of specimens heated in a drying oven at 120° for 3 hours; 3) dyeing after treatment in distilled water at 98-100° for 5 minutes; 4) dyeing after treatment in 10% $K_2Cr_2O_7$ solution at 95° for 5 minutes; 5) dyeing in the dye mixture followed by treatment of the dyed specimens in 10% $BaCl_2$ solution at 75° for 5 minutes; 6) dyeing in the mixture followed by treatment of the dyed specimens in 5% $NiSO_4 \cdot 7H_2O$ solution at 75° for 5 minutes.

It was found that: 1) anodized specimens treated in boiling water cannot be dyed (they only acquire a pale reddish tinge); 2) anodic coatings treated in $K_2Cr_2O_7$ solution retain their dyeability to a considerable extent; 3) the dyeability of anodized specimens is not influenced significantly by preliminary heating in air; 4) specimens dyed by all the above methods (except Method 3) retain their color completely in alcohol and in tap water at room temperature for 3.5 months; 5) all the dyed specimens, with the exception of those treated in $NiSO_4$ solutions, are completely decolorized in boiling water in 2.5-3 hours. Fixation of the dye in $NiSO_4$ solution considerably increases the fastness of the dye to hot water.

Anodic coatings can be dyed to various shades of yellow with tartrazine, Direct Chrysophenine, and dibromofluorescein; red colors can be produced with Bengal Rose, fuchsine, rhodamine, and erythrosine; dark and light blues, with Aniline Pure Blue, Patent Blue; greens, with Partaline Green and Emerald Green.

SUMMARY

1. The optimum conditions for electrolytic and chemical polishing of aluminum have been determined.

2. A procedure is recommended for anodizing treatment of electropolished aluminum in H_2SO_4 solution, which yields transparent oxide coatings which diminish the luster of aluminum only very slightly.

3. Dye bath compositions for coloration of anodized aluminum to gold and other shades are given.

LITERATURE CITED

[1] A. K. Chertavskikh, Factory Labs. 2, 222 (1936).

[2] P. V. Shchigolev and N. D. Tomashov, Proc. Acad. Sci. USSR 100, 2, 327-330 (1955).

[3] P. V. Shchigolev, Factory Labs. 21, 12, 1474-1476 (1955).

[4] P. V. Shchigolev and G. V. Akimov, Proc. Acad. Sci. USSR 100, 3, 499-502 (1955).

[5] P. V. Shchigolev, J. Phys. Chem. 29, 4, 682-684 (1955).

[6] I. L. Rozenfeld and P. V. Shchigolev, J. Phys. Chem. 29, 4, 668-670 (1955).

[7] N. D. Pullen, J. Inst. Metals, 59, 2, 151-158 (1936).

[8] H. Spähn, Metalloberfläche, 6, 2, B17-B26 (1954).

[9] R. Lattey, H. Neunzig, Metalloberfläche, 9, 7, A97-A103 (1955).

[10] H. Ginsberg, F. Baumann, Metall, 9, 5/6, 159-163 (1955).

[11] L. Koch, S. Keste, Metall, 7, 15/16, 577-581 (1953).

[12] R. Lattey, Metall, 7, 15/16, 582-586 (1953).

[13] H. Baur, Metalloberfläche, 9, 2, A22-A28 (1955).

[14] H. Mäurer, Metallwaren-Ind u. Galvanotechn., 46, 7, 10, 11, 12 (1955).

[15] R. Pinner, Electroplating a. Metal Spraying, 6, 11, 401-410 (1953).

[16] M. Schenk, Techn. Rundschau, 45, 33, 1-3, 5, 6 (1953).

[17] F. I. Sadov, Sci. Res. Trans. Moscow Text. Inst. 13, 3-13 (State Light Ind. Press, Moscow, 1954)*

[18] F. I. Sadov and E. S. Shatrova, ibid, 32-46.

[19] G. A. Zubova and N. T. Kudryavtsev, Corrosion and its Prevention 6, 5-6, 45-52 (1940).

* In Russian.

[20] M. Schenk, Werkstoff Aluminium und seine anodische Oxydation. Francke A. G. Verlag Bern, 809-838 (1948).

[21] A. V. Tukovskaya and N. A. Lukyanova, Jubilee Coll. Sci. Trans. Moscow Inst. Nonferrous Metals and Gold (Metallurgy Press, 1950) p. 237. *

[22] E. Hermann, W. Hübner, Aluminium (Suisse), 5, 4, 134-138 (1955).

[23] N. P. Fedotyev and S. Ya. Grilikhes, Trans. Lensoviet Technol. Inst. Leningrad 10, 9-19 (Goskhimizdat, 1941). *

[24] N. I. Kirillov and A. S. Kheinman, J. Appl. Chem. 24, 10, 1019-1025 (1951).* *

[25] N. D. Tomashov and M. N. Tyukina, Accelerated Methods of Corrosion Protection (Collected Papers) (Izd. AN SSSR, Moscow – Leningrad, 1946) pp. 45-70. *

Received August 1, 1955

* In Russian.

** Original Russian pagination. See C. B. translation.

INVESTIGATION BY AN ULTRASONIC METHOD OF THE FORMATION OF A SOLID PHASE IN A PARAFFINIC DISTILLATE

A. P. Grishin

Ultrasonic methods are being increasingly used for the solution of a great variety of physicochemical problems and of individual questions [1] both of theoretical and of applied significance. Investigations of the propagation of ultrasonic vibrations are used in analysis of the state of crystalline substances and in studies of the crystallization process [2-6]. Ultrasonic methods may prove very valuable in investigations of the processes involved in the formation of solid phases in solutions, and hence for determination of important physicochemical parameters used in industrial processes and in control and automation of such processes.

Our investigation of the formation of a solid phase in paraffinic distillates, carried out on a large number of distillate samples from the Grozny oil refinery, revealed an abrupt change in the propagation of ultrasonic waves in paraffinic distillates under certain temperature conditions.

It was found that the nature of this change in the propagation of ultrasonic vibrations in the distillates is characteristic for each different sample, and depends on the nature of the petroleum product and the degree of dispersion and structure of the nuclei of the new phase. In the separation of a solid phase, the formation of nucleation centers is accompanied by their growth. As the result of the growth of nuclei in a medium through which weak ultrasonic vibrations are propagated, at a certain instant the solution becomes, in a sense, a bad conductor of ultrasonic waves.

The propagation of ultrasonic waves in paraffinic distillates was also used for evaluation of the distillate quality and determination of its highly important industrial characteristic – filterability.

EXPERIMENTAL

A sample of paraffinic distillate, warmed until completely melted, was placed in a thermostat. The sample was kept in the thermostat for an invariably constant time at 35°. It was then poured into the experimental vessel at the same temperature. After equalization of the temperature, a periodic beam of low-power ultrasonic vibrations was passed through the vessel.

The temperature of the distillate was lowered to 20-15°, i.e., to the point of crystallization and loss of mobility of the sample, the intensity of propagation of the vibrations being measured at half-degree intervals. The temperature must always be varied at the same rate.

The experimental vessel was a special thick-walled hollow glass cylinder, polished internally and of constant internal diameter throughout its length, with metal ends mounted on supports.

The metal ends were used for mounting all the necessary equipment for producing the ultrasonic vibrations, the quartz crystal, and piezoelectric receiver, inside the vessel. The construction of the vessel is shown in Fig. 1.

The use of glass for construction of the vessel ensured good insulation of the instrument when high-frequency currents were used, made direct visual observation of the crystallization process possible, and also ensured mutually independent operation of the generating and receiving quartz plates. The generating and receiving plates had the same fundamental frequency. The receiving plate could be moved with its holder, by means of a micrometer screw, parallel to the generator. The displacement of the receiving plate could be carried out to an accuracy of 0.005 mm.

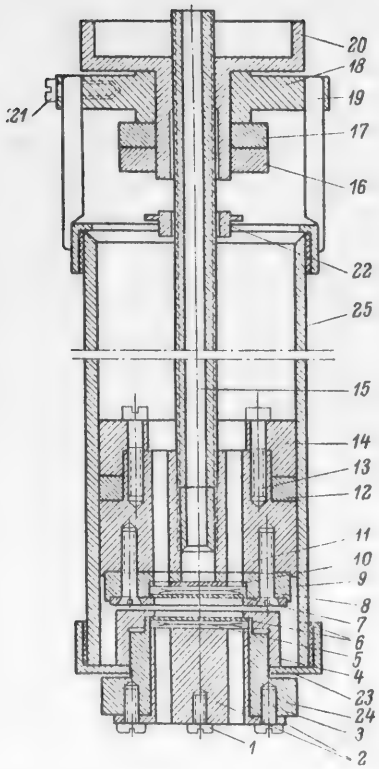

Fig. 1. Diagram of the experimental vessel.
1, 3, 8, 13, 21) Contact bolts and fixing bolts; 2) base of generating quartz crystal holder; 4) brass collar; 5) spring washer; 6) quartz plates; 7) brass clamping ring; 9) ebonite insert; 10) contact washer; 11) body of receiving quartz crystal holder; 12) cork ring; 14) collar; 15) directing shaft of micrometer screw; 16, 17) nuts; 18) end flange; 19) support; 20) graduated head of micrometer screw; 22) bushing; 23) chromed brass end plate; 24) insulating insert; 25) glass experimental vessel.

A block diagram of the whole apparatus is shown in Fig. 2.

The electrical impulses from the quartz plate were fed into a receiving and amplifying device of the superheterodyne type, and then to an electronic indicator.

Either a tube voltmeter or an oscillograph can be used as an indicator for the vibrations, which are now electrical amplified vibrations and not ultrasonic waves. The generating quartz plate was connected to an electromagnetic oscillator with a dual excitation circuit. The quartz crystal was inductively coupled. The oscillation frequency was regularly checked by means of a heterodyne wavemeter and maintained constant. The operating frequency was 6 megacycles per second.

Our superheterodyne receiver 3 (Fig. 2) minimized all possible interference and made it possible to select only the fundamental harmonic of the oscillator. The power of the ultrasonic oscillations was reduced to the lowest permissible level, so that the oscillations and the action of the oscillating quartz crystal did not exert a heat effect on the distillate.

The problem of studying the formation of a solid phase in the solution involved certain difficulties in evaluation of the intensity maximum in the propagation of the ultrasound through the distillate. These difficulties were due to the need to vary the temperature. Temperature variations influence the rate of propagation of ultrasonic vibrations and therefore lead, at constant frequency, to changes of wave length and phase shift. The combined effect is to displace the intensity maximum in measurements of the propagation of ultrasonic vibrations in the system. These difficulties were overcome by means of very small displacements of the receiving plate parallel to the generator at each decrease of temperature in the direction of the wave length change of the ultrasonic vibrations. In this way it was possible to follow, more or less continuously, the intensity maximum of the ultrasonic vibrations propagated through the distillate.

The total displacement of the receiver throughout an experiment, up to the time when the distillate lost mobility with decrease of temperature, was small, measurable in fractions of a millimeter. As the absorption of ultrasound in liquids is relatively low, this variation of the distance between the oscillator and receiver could not influence the accuracy with which the intensity of the ultrasound was measured.

The results of measurements of the intensity of propagation of ultrasound through paraffinic distillates of different filterabilities at various temperatures are plotted in Fig. 3.

The ordinates represent the intensity of propagation of ultrasound in arbitrary units on a 100-point scale. Each curve corresponds to a different distillate sample, characterized by its percentage filterability. It is seen

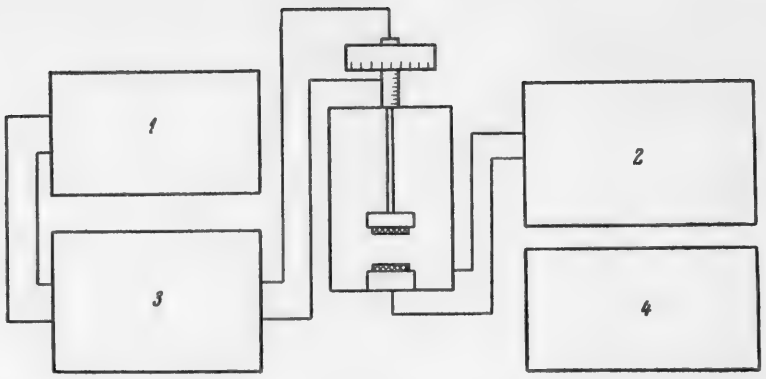

Fig. 2. Block diagram of ultrasonic equipment for investigation of paraffinic distillates.
1) Electronic indicator; 2) oscillator; 3) receiver, 4) heterodyne wavemeter.

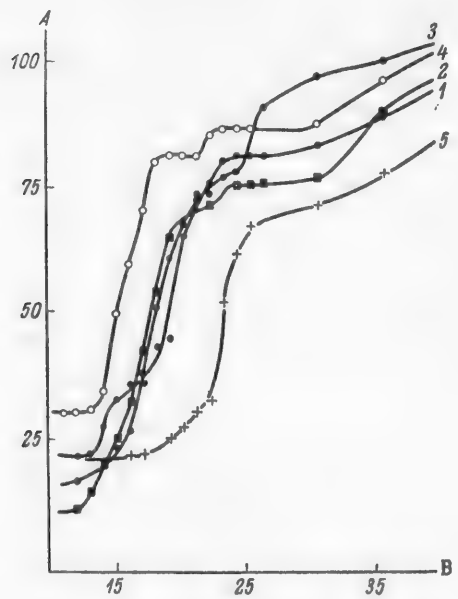

Fig. 3. Propagation of ultrasound in paraffinic distillates.
A) Propagation intensity I, B) temperature (°C).
Distillate characteristics (% filterability): 1) 60.79; 2) 59.64; 3) 61.19; 4) 52.47; 5) 65.67.

that all the intensity – temperature curves show a well-defined jump, as noted earlier. This is caused by formation of a solid phase in the solution with decrease of temperature, and the formation and growth of micronuclei of the disperse phase. The most abrupt change of intensity corresponds to the instant at which the average size of the microcrystals becomes comparable with the wave length or even exceeds the latter somewhat. At this instant the solution becomes "opaque" to ultrasound. Further decrease of temperature below 15° has little

influence on the intensity, and in consequence horizontal regions appear on the curves. Before the actual jump, some of the curves show signs of a bend with decrease of temperature, in the 20-30° region; this is probably attributable to specific characteristics of the crystallization process in distillate samples differing in composition and nature. This probably provides additional possibilities in studies of the mechanism of solid phase formation and of the state of the liquid near the crystallization temperature.

DISCUSSION OF RESULTS

Various workers have shown that different impurities and inclusions have a considerable influence on crystallization of paraffin wax and distillates [7-11]. The nature and amounts of the impurities influence the degree of dispersion of the nuclei, and, in the subsequent stage, the size and shape of the solid hydrocarbon crystals deposited in the solution on decrease of temperature. Much the same impurities and inclusions determine the filterability of paraffinic distillates. The action of ceresins and petroleum tars is exceptionally important. They give rise to a highly disperse and badly filtering solid phase. Our supplementary experiments, intended mainly to study the quantitative effects of these impurities, confirmed that the filterability is decreased sharply, especially in the presence of even very small amounts of ceresin in the distillate. The presence of 0.05-0.10% of ceresin in the crude distillate lowers filterability by 10-15%, while 0.25-0.50% of ceresin makes it unsuitable for processing, from the filterability aspect. The microstructure of the paraffin crystals formed is quite unsatisfactory in this case, and the solid phase is very finely dispersed.

Thus, the filterability of crude paraffinic fractions is largely determined, apart from other causes, by the degree of dispersion and the form of the paraffin crystals formed.

Propagation of ultrasonic vibrations in paraffinic distillates shows that, under equal conditions, the intensity of the propagated ultrasound is higher in distillates in which the paraffin crystals formed are more finely dispersed. Consequently, such a distillate will become "opaque" to ultrasound at its own specific temperature. Samples with larger and better-formed crystals will be more "opaque" to ultrasound, and will become totally opaque under different conditions. In other words, under given constant conditions the propagation of ultrasound will be less intense in distillates of good filterability and considerably more intense in distillates of poor filterability.

The nature and magnitude of the jump on the "intensity – temperature" curves will differ for different distillates, and convincingly confirm the foregoing views on the relationship between the formation of the solid phase and the propagation of ultrasound. Thus, it follows from an examination of the curves in Fig. 3 that the intensity of propagation of ultrasound is considerably less in a distillate of high filterability (Curve 5), and the curve lies below the others, whereas most of the curve for a sample of low filterability (Curve 4) lies above the others. Curves for samples with filterability values of 60.79, 59.64 and 61.19% occupy an intermediate position, and are close to each other. The jump in Curve 5 lies in the region of relatively high temperatures, and that in Curve 4, on the contrary, in the low-temperature region. This last fact indicates that a highly disperse crystalline phase is formed in the distillate with 52.47% filterability on decrease of temperature.

The horizontal regions of the curves also show specific characteristics, the relationships following the same sequence as previously.

It proved possible to evaluate the quality of the paraffinic distillate from the propagation intensity of ultrasound, the magnitude of the jump with change of temperature, and the temperature region in which the jump occurs. This subject, however, is outside the scope of the present paper, it is of technological and industrial significance, and it is our intention to discuss it separately in one of the petroleum journals.

For verification, the propagation of ultrasound in synthetic mixtures was compared with that in paraffinic distillates.

The results of the experiments on the propagation intensity of ultrasound in synthetic mixtures are shown graphically in Figs. 4, 5, and 6. The curves are plotted in the same coordinates as before, and represent the "intensity – temperature" relationship.

The graphs show that the jump in the intensity of the transmitted ultrasound is even more pronounced in the synthetic mixtures, and that all the other effects due to the nature of the solid phase, its composition, and the degree of dispersion, are fully confirmed.

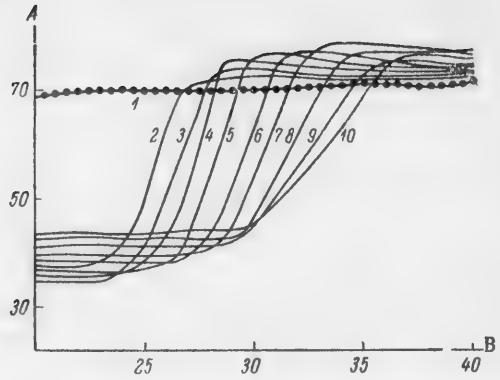

Fig. 4. Effect of temperature on the propagation intensity of ultrasound in synthetic mixtures with different contents of solid paraffins.
A) Intensity I, B) temperature (°C).
Paraffin wax contents of mixtures (%): 1) 3.85; 2) 11.85; 3) 12.85; 4) 13.85; 5) 14.85; 6) 15.85; 7) 16.85; 8) 17.85; 9) 18.85; 10) 19.85.

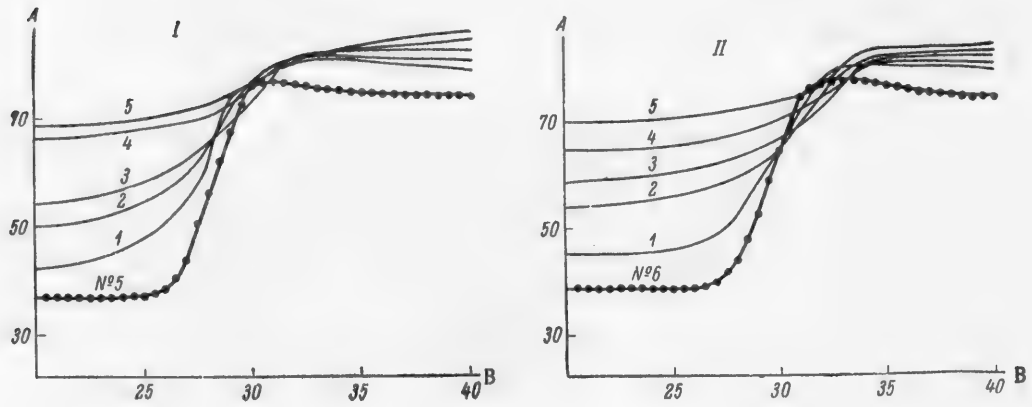

Fig. 5. Effect of temperature on the propagation intensity of ultrasound in Mixtures Nos. 5 and 6 (Fig. 4) after addition of ceresin.
A) Intensity I, B) temperature (°C).
No. 5) Curve for mixture containing 14.85% of paraffin wax; No. 6) curve for mixture containing 15.85% of paraffin wax.

The intensities for ten synthetic mixtures with different contents of paraffin wax are plotted in Fig. 4.

The mixtures were made up by weight, highly purified grade "A" paraffin wax being dissolved in filtered distillate.

The ultrasound propagation intensity was measured at half-degree intervals. It follows from Fig. 4 that apart from the first curve, which corresponds to a mixture with very low paraffin wax content, a solid phase was not formed in the given temperature conditions. All the curves show a sudden decrease of the intensity on formation of the solid phase, such as was found earlier for paraffinic distillates.

Fig. 5 gives the results of determinations of the intensity of ultrasound in the same separate mixtures, but after additions of 0.1, 0.2, 0.3, 0.4, and 0.5% of ceresin to each. Curves are given for Mixtures Nos.5 and 6, containing 14.85% and 15.85% paraffin wax respectively, and also for these mixtures containing ceresin in the amounts stated. For brevity, the changes in the decrease of the intensity of ultrasound caused by addition of ceresin are given for only two mixtures, although measurements were carried out for all ten mixtures, as all the results were quite similar and it is not necessary to repeat them here.

Examination of the curves in Fig. 5 clearly reveals the whole course of the decrease in the intensity of ultrasound transmitted through a medium in which a solid phase with particles of different degrees of dispersion is formed. As has been conclusively proved and noted earlier, ceresin assists the formation of a finely crystalline structure and of a highly disperse solid phase, and this is clearly reflected in the curves in Fig. 5. Curve No. 5 corresponds to a mixture without ceresin, and it shows an abrupt and large decrease of intensity of the transmitted ultrasound, but with increasing ceresin content in the mixture the degree of damping of the ultrasound diminishes, and the curves for mixtures containing 0.4 and 0.5% of ceresin are almost without jumps; they represent a relatively smooth decrease of intensity during crystallization, with good conductivity for ultrasound in the solid phase.

Thus, the great possibilities of the ultrasonic method for studying the process of solid phase formation are revealed even more clearly in synthetic mixtures.

SUMMARY

1. A study of the propagation of ultrasonic vibrations in paraffinic distillates and in solutions of paraffin wax and ceresin showed that the intensity of the ultrasonic vibrations changes abruptly at the instant when a disperse phase is deposited. The nature and magnitude of this jump depends on the nature of the distillate and the degree of dispersion of the paraffin crystals formed.

2. Studies of the propagation of ultrasound in paraffin wax and ceresin solutions and in paraffinic distillates show that ultrasonic methods have great possibilities for investigations of solid phase formation in solutions of all kinds on decrease of temperature.

LITERATURE CITED

[1] B. B. Kudryavtsev, Applications of Ultrasonic Methods in Physicochemical Research Practice (GITTL, 1952).*

[2] S. Ya. Sokolov, Proc. Acad. Sci. USSR 59, 59, 883 (1948).

[3] W. Roth, J. Appl. Phys., 19, 901 (1948).

[4] W. P. Mason and H. J. McSkimin, J. Appl. Phys., 19, 940 (1948).

[5] S. Ya. Sokolov, Proc. Acad. Sci. USSR 64, (4), 503 (1949).

[6] S. Ya. Sokolov, Progr. Phys. Sci. 40, 3 (1950).

[7] A. N. Sakhanov and L. G. Zherdeva, Trans. Grozny Sci. Res. Inst. 231 (1931).

[8] A. N. Sakhanov and N. A. Vasilyev, Trans. Grozny Sci. Res. Inst. 246 (1931).

[9] A. N. Sakhanov and L. G. Zherdeva, Petroleum Economy 11-12 (1928).

[10] Padgett, Hefley and Henriksen, Ind. Eng. Ch., 19, 935 (1927).

[11] T. P. Zhuze, Colloid J. 13, 1, 27 (1951).

Received December 15, 1955

* In Russian.

PRODUCTION OF ETHYL ALCOHOL ON THE BASIS OF ELECTROCRACKING OR METHANE GASES

M. G. Tereknova, E. N. Eremin, and N. I. Kobozev

This investigation consisted of a study of the principles of a continuous process for the production of ethyl alcohol from methane, by electrocracking of natural Saratov gas, containing about 95% of methane, to acetylene, followed by catalytic hydration of acetylene to acetaldehyde and catalytic reduction of acetaldehyde to ethyl alcohol. A combined unit was designed for this purpose, and used for carrying out successively the above-named three stages in the synthesis of ethyl alcohol from methane.

The advantage of the use of acetylene made by cracking of natural gas, over acetylene made from calcium carbide, lies in the fact that in the cracking of methane, hydrogen is formed together with acetylene, and this is necessary for the reduction of acetaldehyde to ethyl alcohol. It is thus not necessary to introduce hydrogen into the system from outside, and the additional costs for the production of hydrogen are eliminated.

A second, no less important advantage of acetylene obtained by electrocracking of methane, over acetylene from calcium carbide, is the purity of the former, whereas acetylene from calcium carbide is contaminated with large amounts of hydrogen sulfide and phosphine.

Extensive and complete information on the production of acetylene by electrocracking of methane is available in the recent literature. In work on this problem a leading part was played by Soviet physical chemists, among whom special mention must be made of Vasilyev, Bozhko, Koller, and others [1]. They studied the effects of the following conditions on the yield of acetylene: pressure, gas flow rate, current strength, discharge power, etc. The results show that the problem of the electrocracking of methane has been satisfactorily solved from the technological aspect.

The second stage in the conversion of acetylene into ethyl alcohol is the production of acetaldehyde by hydration of acetylene. Acetylene can be converted into acetaldehyde: a) by way of vinyl alkyl ethers (Favorsky and Shostakovsky [2]), b) by direct hydration in presence of catalysts.

The method of Favorsky and Shostakovsky is not used industrially, as it is necessary to use acetylene under pressure (5-12 atm).

Direct catalytic hydration of acetylene to acetaldehyde can be effected in three different ways: in the liquid phase (in presence of mercury salts, by Kucherov's method [3]), in the vapor phase, and by various combinations of these two methods. A disadvantage of the first method is the high consumption of mercury compounds. A valuable feature of the vapor-phase catalytic hydration of acetylene is the possibility of using dilute acetylene (5-15%) for the production of acetaldehyde. Yakubovich, Danilevich, and Medzykhovskaya [4] found that good yields of acetaldehyde are obtained in this process with the use of phosphoric acid catalyst with traces of copper phosphate as promoter, or with mixtures of phosphoric acid and zinc phosphate on activated "AG" carbon at 350°.

The literature does not contain any original papers on the third stage of the process – the reduction of acetaldehyde to ethyl alcohol. However, many patents deal with this question, indicating a considerable degree of technical interest. The catalysts most frequently specified in patents for this reaction are the usual hydrogenation catalysts – nickel, copper, iron. Reaction temperatures in the range of 100-200° are specified. The favorable influence of a large excess of hydrogen (up to 30-fold amounts) is noted in many patents.

A characteristic feature of the process in question is that at the second and third stages a complex mixture of cracking gases, consisting of acetylene, ethylene, hydrogen, unchanged methane, and other gases, with

large amounts of water vapor, is passed over the catalysts. A great variety of reactions is possible in such a complex mixture, and the principal task in the present investigation was to find the conditions for selective acceleration of the processes in the desired direction.

In order to determine the possible degrees of conversion of the starting substances into the desired final products, and to evaluate the probability of certain side reactions, we calculated the equilibrium constants of the reactions which may occur in the given experimental conditions.

The equilibrium degrees of conversion were determined for the following reactions: 1) reduction of acetaldehyde to alcohol; 2) hydration of acetylene to acetaldehyde; 3) hydrogenation of acetylene to ethylene; 4) hydration of ethylene to ethyl alcohol; 5) formation of acetone from acetylene and water; 6) conversion of acetylene into carbon monoxide and hydrogen; 7) conversion of acetaldehyde into carbon monoxide and hydrogen; 8) equilibrium in the system: copper oxide + hydrogen $\rightleftharpoons$ copper + water, which determines the state of the copper used as hydrogenation catalyst in the third stage of the process, under quite unusual conditions – in the presence of a large amount of water vapor.

The theoretical degrees of conversion of acetaldehyde into ethyl alcohol at various temperatures are given in Table 1. The calculations were made for the conditions of Experiment 74 (see Table 4), for which (in moles): $\Sigma n = 0.4071$, $n_{CH_3CHO} = 0.0332$, $n_{H_2} = 0.18197$, $n_{H_2O} = 5.833$, where n is the mole fraction of a given component in the reaction, and Σn is the total amount of gases passed through, in moles.

The corresponding equilibrium yields for the other reactions listed above are given in Table 2. The equilibrium concentrations of the reactants were calculated for the conditions of Experiment 43 (see Table 4), in which (in moles): $\Sigma n = 0.355$, $n_{CH_3CHO} = 0.0211$, $n_{H_2O} = 3.22$, $n_{C_2H_2} = 0.0270$, $n_{C_2H_4} = 0.00852$, $n_{H_2} = 0.144$.

TABLE 1

Theoretical Degrees of Conversion of Acetaldehyde into Ethyl Alcohol

Reaction temperature (°C)	Equilibrium yield of alcohol (%)
150	87
175	69
200	45
225	25
250	13.5

It follows from the data in Table 2 that all the above-named side reactions which accompany the hydration of acetylene to acetaldehyde and reduction of the latter to ethyl alcohol are not only thermodynamically possible, but may, in conditions of vapor phase hydration and reduction, occur with very high yields (99.9-100.0%), with the exception of the hydration of ethylene to ethyl alcohol, which can only give a 2.9% yield in the experimental conditions used. Therefore, in selection of catalysts and process conditions, it is necessary to find catalysts with a selective action on the principal reaction without activation of the side processes. This was the main task in the present investigation.

It proved possible to find catalysts which gave 92% conversion in the hydration of acetylene to acetaldehyde, calculated on the acetylene passed, while approximately 30% conversion of the acetaldehyde, formed in the second stage, into ethyl alcohol was obtained, the remaining acetaldehyde passing out unchanged from the reaction vessel. Thus, it proved possible to eliminate all the parasitic reactions listed above.

TABLE 2

Equilibrium Yields of Reaction Products

Reaction	Reaction temperature (°C)	Equilibrium yield of reaction product (%)
$C_2H_2 + H_2O \rightleftharpoons CH_3CHO$	350	97.7
$C_2H_2 + H_2 \rightleftharpoons C_2H_4$	200	100.0
$C_2H_4 + H_2O \rightleftharpoons C_2H_5OH$	200	2.9
$C_2H_2 + 2H_2O \rightleftharpoons 2CO + 3H_2$	350	100.0
$CH_3CHO + H_2O \rightleftharpoons 2CO + 3H_2$	200	99.9
$2C_2H_2 + 3H_2O \rightleftharpoons CH_3COCH_3 + 2H_2 + CO_2$	350	100.0

The equilibrium constant for the reaction $Cu + H_2O \rightleftharpoons CuO + H_2$, which was found to be $K_p = \frac{p_{H_2}}{p_{H_2O}} = 3.83 \cdot 10^{-25}$, shows that copper is present as the metal in the system, so that the hydrogenation catalyst II, used for reduction of acetaldehyde to alcohol, consists of copper and not its oxide, supported on silica gel.

EXPERIMENTAL

The apparatus used for the production of acetylene and its catalytic hydration and reduction to acetaldehyde and alcohol is shown schematically in Figs. 1 and 2.

Acetylene was made in the electric arc under reduced pressure in dynamic conditions (Fig. 1).

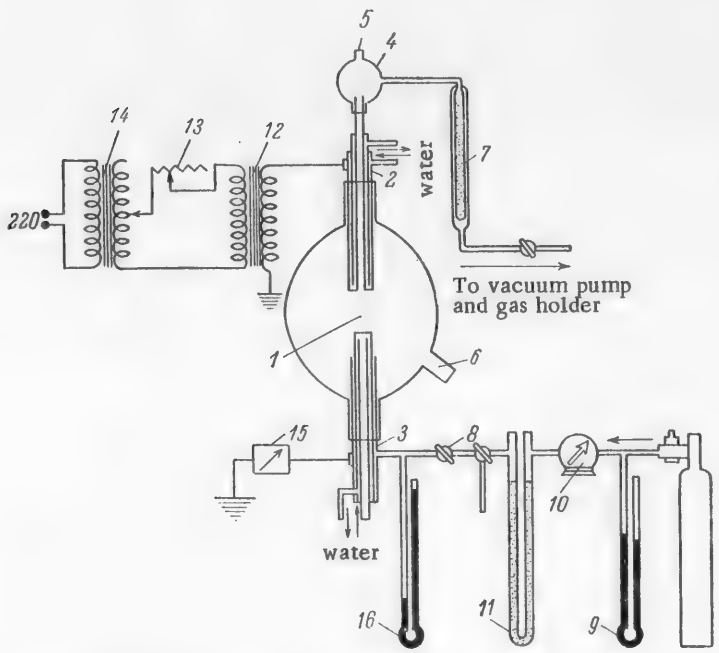

Fig. 1. Apparatus for production of acetylene by electrocracking of methane.
Explanation in text.

The reaction vessel 1 was an ellipsoidal flask of Pyrex glass, 0.5 liter in capacity. The electrodes 2 and 3, made from brass tubes, had canals for the passage of gas and were water cooled. The distance between them was 50 mm. The flask 4 with ground-glass stopper 5, and the side tube 6 of the reaction vessel, were used to remove carbon from the electrodes. The filter 7, of closely woven fabric, retained carbon entrained in the gases leaving the reaction vessel; the stopcock 8 was used to regulate the supply of gas into the reaction vessel; the mercury manometer 9 served to measure the pressure in the gas meter 10; the U tube 11, filled with calcium chloride, was used to dry the original methane.

The cracking gases, after passing through an oil pump, were collected in gas holders over saturated calcium chloride solution.

The electrical section of the apparatus consisted of a 110/15000 v 350 w transformer 12, a rheostat 13, a variable-ratio transformer 14,and a milliameter 15 for measurement of the discharge current.

The methane feed rate into the system, measured by means of the gas meter was 12-13 liters per hour. The pressure in the system, measured by means of the vacuum gage 16, was kept at 35-40 mm Hg, and the current strength was 100 ma.

The acetylene content of the cracking gases was 8-10%, which is quite suitable for the subsequent catalytic hydration and reduction to acetaldehyde and alcohol. In addition to acetylene, the cracking of methane yielded 44-47% of hydrogen, which was used for reduction of acetaldehyde to alcohol without the need for addition from outside.

Samples for analysis were taken from the cracking gases collected in the gas holder, and the gases were then passed to catalytic conversion into acetaldehyde and alcohol.

Catalytic hydration of acetylene to acetaldehyde and reduction of acetaldehyde to ethyl alcohol was carried out in the vapor phase in a flow system, in consecutive stages in the same unit, shown diagrammatically in Fig. 2.

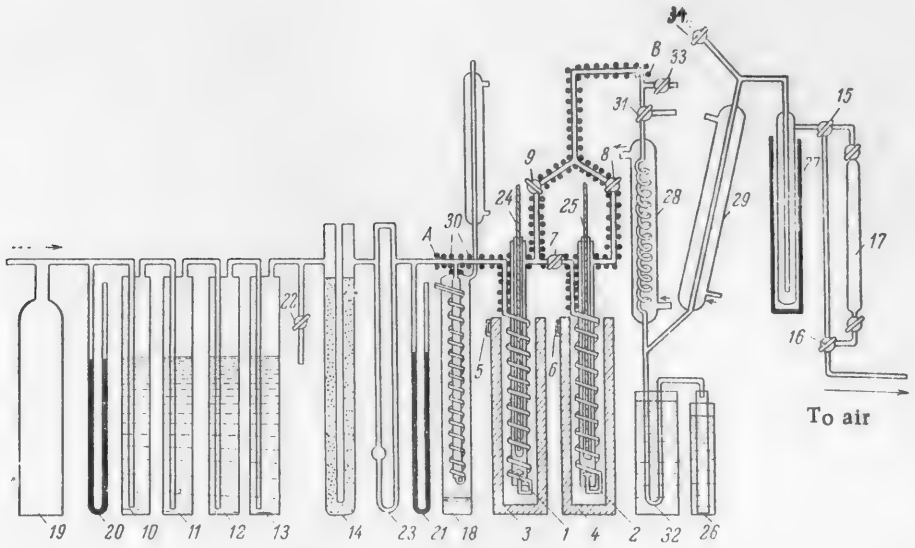

Fig. 2. Apparatus for catalytic production of ethyl alcohol. Explanation in text.

Acetaldehyde and ethyl alcohol were formed in the reactors 1 and 2 respectively, contained in vertical electric heaters 3 and 4, the temperature in which was regulated by means of thermoregulators of the usual type, with mercury contact breakers.

The stopcocks 7, 8, and 9 could be used to isolate reactor 2 from the system.

The wash bottles 10, 11, 12, and 13, filled with alkaline pyrogallol solution, chromic acid mixture, concentrated sulfuric acid, and 50% alkali respectively, were used to purify the original gas.

The U tube 14, filled with calcium chloride, was used to dry the original gas. The three-way stopcocks 15 and 16 served to isolate the gas pipet 17 from the system. The evaporator 18 was used to supply water vapor [5]. Water was fed into the evaporator by means of a special metering device, described by Shpolyansky and Likhacheva [6]. The gas holder 19 contained the original cracking gas.

For observations of the course of the process, and for control measurements, the system contained: two mercury manometers, one of which, 20, was next to the gas holder, and the other, 21, before the water evaporator; a sampling cock 22, for checking the degree of purity of the gas fed into the reactor; a rheometer 23 filled with dibutyl phthalate (calibrated against cracking gas) to measure the gas feed rate; 500° thermometers 24 and 25, for temperature measurements in reactors 1 and 2; a graduated receiver 26, for the aqueous condensate of acetaldehyde and alcohol; a gas pipet 17, for sampling the exit gas; and a trap 27, for freezing out traces of aldehyde not liquefied in condensers 28 and 29.

The system was made from ordinary glass tubing sealed together, with the exception of the region between A and B, which was made of quartz and connected to the rest of the system by means of ground-glass joints. The quartz section of the system was provided with the electric heater 30, which maintained a temperature of about 150° inside the tubes, in order to prevent condensation of the water vapor entering from the evaporator 18.

The original gas mixture was supplied from the gas holder 19 into the system through a rubber tube.

The two reactors 1 and 2 were of the same design, consisting of tubes with side tubes for exit gases and for addition of catalyst. A thermometer socket was sealed into the top of each tube; the thermometer bulb was located in the center of the catalyst mass. The original steam – gas mixture entered through the inlet tube, passed through the coil, and entered the contact mass from below. The reactors were made of quartz and were connected to the system by ground joints.

Experimental procedure in the catalytic production of alcohol. After the system (Fig. 2) had been tested for air tightness, it was rinsed out with 6-8 liters of the cracking gas, which escaped into the air through the three-way cock 31. During the rinsing,the required temperature was established in the heaters 3 and 4, the gas feed rate into the reactor was regulated with the aid of the rheometer 23, and the steam feed rate was regulated by means of the metering device for water.

When a constant gas rate and the necessary temperatures in heaters 3 and 4, had been established, and a small amount (10-15 ml) of condensate had been collected through the stopcock 31, the experiment was started; the stopcock 31 was switched over to the condenser 28, the gas level in the gas holder was noted, and a time reading was taken.

The original gas mixture from the gas holder passed through the purification system and entered the T-joint connected to the water evaporator 18. The mixture of cracking gases and water vapor entered the reactor 1 through an electrically heated quartz inlet tube. The gas containing acetaldehyde then passed through the stopcock 7 (with the cock 9 closed) into the reactor 2. Ethyl alcohol, unreacted acetaldehyde, and excess water vapor were condensed in the condensers 28 and 29, and collected, through the hydraulic seal cooled with ice, in the graduated receiver 26, also cooled with ice. Any acetaldehyde not condensed in condensers 28 and 29 was frozen out in the trap 27, cooled to – 78°. Any unreacted cracking gas escaped into the air through the pipet 17.

At the end of the experiment the gas level in the gas holder and the amount of condensate collected in the receiver 26 were noted, and condenser 28 was disconnected from the system by opening the cock 31 to the atmosphere. Condensers 28 and 29 and the seal 32 were rinsed out with a small amount (10 ml) of distilled water, which was then combined with the condensate, through the tubes 33 and 34.

The condensate, liquid in the trap, and the original cracking gas in pipet 17 were analyzed on the day of the catalytic experiment, by the methods described below.

The alcohol content of the condensate was determined by the All-Union Scientific Research Institute of Hydrolysis and Sulfite Alcohol Industry photoelectric method [7] the principle of which is the formation of an azo dye in an amount proportional to the alcohol content. The color intensity of the solution was measured by means of a photoelectrocolorimeter (FEK-1) immediately after formation of the dye. The standard liquid used was distilled water. Repeated checks of the calibration curve against standard alcohol solutions showed that the most reliable region of the curve is between 0.005 and 0.010%, and this region was used for the determinations. The error is 1-2%.

Hydroxylamine hydrochloride [8] was used for determinations of acetaldehyde in the condensate. The acid liberated in the reaction was titrated with 0.1 N KOH solution with bromophenol blue indicator. A correction was applied to the titration results, as the end point of the indicator is at pH = 3.0-4.6. A check of the accuracy of the method against known solutions of aldehyde in water gave good results – the error did not exceed 1.2%.

Analysis of the original natural gas, of the cracking gases collected in the gas holder, and of the exit gas in pipet 17 (Fig. 2) was carried out by means of the VTI gas analysis apparatus. The gases were determined in the following sequence: carbon dioxide was absorbed in 50% alkali solution; acetylene, in a solution of 40 g of mercuric cyanide in 200 ml of 2 N alkali solution; ethylene, in 16% solution of mercuric oxide in 29% sulfuric acid; oxygen, in a solution of 10 g of pyrogallol in 200 ml of 60% alkali; carbon monoxide, in ammoniacal cuprous chloride solution; hydrogen and methane were burned over copper oxide in a quartz coil.

Hydrogen was burned at 300°, and methane, at 800°.

The original Saratov gas contains methane (95% on the average), carbon dioxide (0.5%), hydrogen (0.5--1.5%); unsaturated compounds, oxygen, and carbon monoxide are absent; 4-5% is nitrogen. Some typical compositions of the cracking gases and exit gases after experiments on the production of alcohol are given in Table 3; the presence of oxygen is explained by leakage of air into the cracking gases during collection in the gas holder through the oil pump.

TABLE 3

Composition of Cracking Gases and Exit Gases

Experiment No.	Contents (%)															
	cracking gases								exit gases							
	C_2H_2	C_2H_4	CH_4	H_2	CO_2	CO	O_2	N_2	C_2H_2	C_2H_4	CH_4	H_2	CO_2	CO	O_2	N_2
82	8.90	2.35	33.55	46.90	0.20	0.05	0.75	7.30	0.10	2.55	36.50	51.60	1.00	0.40	0.35	7.50
84	9.80	1.95	35.90	43.80	0.05	0	0.40	8.10	0.50	2.40	38.55	48.05	0.40	0	0.10	10.00
87	7.65	2.40	35.20	45.60	0.20	0.05	1.20	7.70	0.25	2.50	37.65	49.35	0.50	0.40	0.15	9.20
89	8.50	2.35	36.20	45.30	0.15	0	0.60	6.90	0.75	2.60	39.50	48.25	0.60	0.75	0.30	7.25
90	8.25	2.30	34.85	46.05	0.10	0	0.65	7.80	0.20	2.50	39.25	48.65	0.40	0.30	0.20	8.50
91	8.40	2.25	31.65	46.95	0.10	0.40	0.75	9.50	0.15	2.35	36.15	50.50	0.40	0.15	0.20	10.10

Preparation of catalysts. The following reagents were used for catalytic hydration of acetylene to acetaldehyde: phosphoric acid, chemically pure grade, $d_4^{25} = 1.628$, 80% orthophosphoric acid; basic copper carbonate, precipitated from cupric chloride with sodium carbonate [9]; zinc carbonate, precipitated from zinc chloride with sodium carbonate [10]; zinc oxide, chemically pure grade; carriers: "AG" activated carbon, "BAU" steam-activated birchwood charcoal, sugar carbon, and silica gel. The silica gel used as carrier was throughly purified by prolonged boiling with dilute hydrochloric acid to a negative thiocyanate reaction for iron, and by washing with distilled water to a negative chloride reaction with silver nitrate.

Catalyst "A," phosphoric acid with copper phosphate on "AG" carbon. This catalyst, containing 15% of contact mixture of the composition: 0.01 g-atom of copper per 1 mole of phosphoric acid (0.64% by weight), supported on "AG" activated carbon, was prepared as follows: 0.34 g of basic copper carbonate was dissolved in 37.6 g of phosphoric acid (80%), previously diluted with 50 ml of water, and water was then added to 250 ml. 170 g of "AG" carbon was put into this solution and left overnight at room temperature. The mixture was then evaporated to dryness on the water bath in a porcelain basin, with continuous stirring with a glass rod. The catalyst was dried at 90-95° under vacuum (10-20 mm) to constant weight.

Catalyst "B," phosphoric acid with copper phosphate on sugar carbon, and Catalyst "I," phosphoric acid with copper phosphate on "BAU" carbon, were prepared similarly, and differed from Catalysts "A" only by the nature of the carrier.

Catalyst "C," phosphoric acid with zinc phosphate on "AG" carbon. This catalyst, containing 15% of contact mixture with the composition: 11.5 moles of phosphoric acid per 1 g-atom of zinc, was prepared as described above, from 3.0 g of zinc carbonate, 33.8 g of phosphoric acid (80%), and 170 g of "AG" carbon.

Catalyst "D," zinc oxide on silica gel. Catalysts of zinc oxide on silica gel were prepared with different degrees of filling α of the carrier surface, from 0.1 to 0.3 (calculated as a fraction of a monomolecular layer). A weighed amount of zinc oxide corresponding to the required degree of surface filling α was dissolved in dilute nitric acid (1 : 1). A weighed amount of silica gel was put into this solution and left overnight at room temperature. The mixture was then evaporated to dryness on a water bath in a porcelain basin with continuous stirring with a glass rod. The catalyst was then heated in a muffle furnace at 450° for 6.5 hours.

The following catalysts were tested for catalytic reduction of acetaldehyde to alcohol: Catalyst "N," nickel on silica gel, and Catalyst "H," copper on silica gel.

Of the original reagents, the ammine $[Ni(NH_3)_6]Cl_2$ was prepared by the action of excess concentrated ammonia solution on concentrated nickel chloride solution of chemically pure grade. The precipitated violet crystals of the nickel ammine were filtered off on a Buchner funnel and dried between sheets of filter paper. Basic copper carbonate was prepared from copper chloride by precipitation with sodium carbonate [9]. The carrier was silica gel, purified as described earlier.

Catalyst "N," nickel on silica gel. This catalyst, with degree of surface filling $\alpha = 0.1$, was prepared from the nickel ammine on silica gel. A weighed quantity of the nickel ammine was dissolved in aqueous ammonia solution (1:1). The required amount of silica gel was put into this solution and left overnight at room temperature. The mixture was then evaporated to dryness on a water bath with continuous stirring with a glass rod. The catalyst was reduced with hydrogen at 450°.

Catalyst "II," copper on silica gel. This catalyst was prepared from basic copper carbonate on silica gel with different degrees of surface filling α, from 0.1 to 0.3. A weighed quantity of basic copper carbonate corresponding to the required degree of surface filling was dissolved in concentrated ammonia. A definite quantity of silica gel was put into this solution and left overnight at room temperature. The mixture was then evaporated to dryness on a water bath with continuous stirring. The catalyst was then put into the reactor for reduction with hydrogen at 200°.

Results of the Experiments

The results of separate experiments on hydration of acetylene showed that at 350°, with 1:11 and 1:17 acetylene: water ratios in the gas mixture, Catalyst "B" causes only a slight reaction to occur; Catalyst "D" is considerably more active, but its activity is not adequate, as acetylene is hydrated to less than 50%.

Quite satisfactory results were obtained with Catalysts "A," "I," and "C." However, catalysts obtained by deposition of the contact material on "AG" activated carbon had to be rejected because "AG" anthracite carbon contains sulfur, which poisons the catalyst used for subsequent hydrogenation.

It was also found that, in contrast to acetylene made by electrocracking, acetylene made from calcium carbide was only 19% hydrated in presence of catalyst "A," and the catalyst activity diminished so rapidly as the result of poisoning that after 8-10 hours the conversion of acetylene to aldehyde fell to 1.0-1.5%. This, as has already been mentioned, is evidence of the considerable advantage of acetylene from methane over carbide acetylene for catalytic processes. Carbide acetylene evidently needs much more thorough purification.

The best of the hydration catalysts tested was phosphoric acid with copper phosphate promoter, supported on steam-activated birchwood charcoal "BAU" (Catalyst "I"). With this catalyst, a yield of 89-92% of acetaldehyde was obtained, calculated on the acetylene passed. The catalyst was selective in action, and side reactions such as hydrogenation of acetylene to ethylene, conversion of acetylene to carbon monoxide and hydrogen, etc., did not occur. A disadvantage of this catalyst is its relatively low stability.

No special investigations were made of possibilities of decreasing catalyst fatigue and increasing its service life, as the principal aim was to establish the possibility of obtaining maximum equilibrium yields of alcohol.

The last state of the process – reduction of acetaldehyde to ethyl alcohol – was studied with nickel and copper on silica gel as catalysts.

As before, selection of the hydrogenation catalyst was complicated by the diversity of the possible directions of the process.

It was found that at 200° only traces of alcohol are formed in presence of nickel on silica gel (Catalyst "N"); copper on silica gel (Catalyst "II") gives satisfactory reduction of acetaldehyde to alcohol; the alcohol yield is 25-33% on the acetylene passed.

The inactivity of the nickel catalyst is probably caused by oxidation of nickel in presence of large amounts of water vapor. In the case of the copper catalyst, calculation of the equilibrium constant for the system copper oxide + hydrogen (see above) shows that at 200°, even in presence of large amounts of water vapor, copper is present in the form of catalytically active metal. The action of the copper catalyst is selective and side reactions are practically eliminated.

TABLE 4

Results of Experiments on Hydration of Acetylene and Reduction of Acetaldehyde to Alcohol

Experiment No.	Catalyst		Composition of original gas								Feed rate of original gas (liters/hour)	Water feed (g/hour)	Volume of water vapor / volume of gas
	Aldehyde	Alcohol	C_2H_2	C_2H_4	CH_4	H_2	CO_2	CO	O_2	N_2			
43	I	—	7.60	2.40	39.90	40.60	0.20	0.10	0.90	8.30	2.66	19.3	8.1
65	I	—	9.45	1.45	24.90	56.30	0.05	0.15	0.70	7.00	1.78	15.0	9.6
74	I	—	8.85	2.40	36.80	44.70	0.20	0	0.45	6.60	1.52	17.5	13.0
84	I	II	9.80	1.95	35.90	43.80	0.05	0	0.40	8.10	1.47	14.7	11.0
87	I	II	7.65	2.40	35.20	45.60	0.20	0.05	1.20	7.70	1.30	18.0	15.0
89	I	II	8.50	2.35	36.20	45.30	0.15	0	0.60	6.90	1.25	14.3	12.5
90	I	II	8.25	2.30	34.85	46.05	0.10	0	0.65	7.80	1.03	13.8	14.7
91	I	II	8.40	2.25	31.65	46.95	0.10	0.40	0.75	9.50	0.92	14.5	17.5

The alcohol yield obtained, about 30%, is fairly close to the thermodynamic equilibrium concentration of alcohol at this temperature (200°). It follows from Table 1 that the equilibrium yield of alcohol is 45% at 200°, and 25% at 225°. If allowance is made for certain temperature variations which were not excluded in our experiments, as the temperature at the reactor walls nearer to the heater might have been somewhat higher than at the center of the reactor where it was measured, the actual yield of 30% is very close to the theoretically possible.

These experiments represent the first stage of the investigation, which should be continued in order to increase the yield of alcohol by a decrease of the temperature at the aldehyde reduction stage, with a displacement of the reaction equilibrium in the desired direction.

The results of certain experiments are given in Table 4. Of these, Experiments 43, 65, and 74, performed with 25 cc of Catalyst "I" at 350° for 6 hours, were on hydration of acetylene only. Experiments 84 to 91 on the production of alcohol were carried out with the same amounts of hydration Catalyst "I," and with Catalyst "II" at the reduction stage. 100 cc of Catalyst "II" was used; the reduction temperature was 200°.

SUMMARY

1. It has been demonstrated that ethyl alcohol can be produced from acetylene and hydrogen made by electrocracking of methane, by a continuous vapor-phase catalytic process, without costly separation of the cracking gases; catalysts have been found for both stages of the process, with side reactions practically eliminated.

2. With cracking gas containing 8-10% of acetylene by volume, the best yields of acetaldehyde were obtained at 350°, with phosphoric acid catalyst containing traces of copper phosphate promoter supported on "AG" and "BAU" carbons, and with mixtures of phosphoric acid and zinc phosphate on "AG" carbon. With these catalysts, acetaldehyde was obtained in 85-92% yields calculated on the acetylene passed, with an average output of 0.20-0.22 mole of acetaldehyde per hour per liter of catalyst, with a catalyst service life of 25-30 hours. The action of the catalyst is selective, and side processes are practically eliminated.

The best catalyst for reduction of acetaldehyde to ethyl alcohol was copper on silica gel (Catalyst "II") which gave average alcohol yields of about 30% calculated on the acetylene passed, with an average output of 0.015-0.020 mole of ethyl alcohol per hour per liter of catalyst. The alcohol yield obtained is close to the thermodynamic equilibrium value.

3. By a decrease of the reduction temperature by 60-70°, the yield of alcohol can be raised to 80-90%.

Yield of acetaldehyde		Conversion of acetylene to aldehyde (%)		Amount of alcohol in condensate (g)	Conversion of acetylene to alcohol (%)		Composition of final gas (%)							
in condensate (g)	in trap (g)	on reacted C_2H_2	on C_2H_2 passed		on reacted C_2H_2	on C_2H_2 passed	C_2H_2	C_2H_4	CH_4	H_2	CO_2	CO	O_2	N_2
0.745	0.183	89	78	—	—	—	0.90	2.50	45.35	43.05	0.40	0.10	0.45	7.25
1.338	0.174	98.8	89	—	—	—	0.95	1.60	26.80	60.90	0.30	0.60	0.35	8.50
1.100	0.538	99	92	—	—	—	0.50	2.55	39.85	49.85	0.20	0.10	0.25	6.70
0.420	0.084	32.3	31.0	0.564	34.5	33.2	0.50	2.40	38.55	48.05	0.40	0	0.10	10.00
0.338	0.043	35.6	34.5	0.263	23.5	23.0	0.25	2.50	37.65	49.35	0.50	0.40	0.15	9.20
0.454	0.019	44.5	40.5	0.368	33.0	30.0	0.75	2.60	39.50	48.25	0.60	0.75	0.30	7.25
0.305	0.026	36.2	35.3	0.261	27.2	26.6	0.20	2.50	39.25	48.65	0.40	0.30	0.20	8.50
0.416	0.080	62.0	61.0	0.174	21.0	20.5	0.15	2.35	36.15	50.50	0.40	0.15	0.20	10.10

LITERATURE CITED

[1] S. S. Vasilyev, N. I. Kobozev, and E. N. Eremin, J. Phys. Chem. 7, 5, 619 (1936); N. I. Kobozev, S. S. Vasilyev, and E. E. Galbraikh, Proc. Acad. Sci. USSR 2, 236 (1935); E. N. Eremin, M. Z. Altshuler, Z. I. Kiryashkina, and V. V. Igonin, J. Appl. Chem. 22, 4 (1947); N. I. Kobozev, S. S. Vasilyev, and M. S. Selivokhina, Annals Moscow State Univ. 86, 2 (1946); E. N. Eremin, Doctorate Dissertation (Moscow, 1950); E. N. Eremin and N. I. Kobozev, Authors' Certif. 80, 290 (1949); S. S. Vasilyev, N. I. Kobozev, and E. N. Eremin, Chemistry of Solid Fuel 8, 70 (1937); A. B. Tsentsiper, Author's Summary of Candidate's Dissertation (Moscow, 1954); S. S. Vasilyev, J. Moscow Univ. 12, 63 (1947); N. P. Bozhko and D. L. Orshansky, Chemistry of Solid Fuel 7, 59 (1936); N. P. Bozhko and I. A. Kosyakova, J. Appl. Chem. 11, 43 (1938); D. K. Koller, Chemistry of Solid Fuel 7, 808 (1936).

[2] A. Favorsky and M. Shostakovsky, J. Gen. Chem. 13, 1 (1943).

[3] M. Kucherkov, Ber., 14, 1532; 1540 (1881); 42, 2759-2762 (1909).

[4] A. Ya. Yakubovich, A. A. Danilevich, and N. A. Medzykhovskaya, J. Appl. Chem. 19, 9, 973 (1946).

[5] M. A. Shpolyansky, Factory Labs 2, 252 (1951).

[6] M. A. Shpolyansky and A. S. Likhacheva, Factory Labs. 12, 1500 (1950).

[7] V. K. Nizovkin, Photoelectric Determination of Alcohol by the All-Union Scientific Research Institute of Hydrolysis and Sulfite Alcohol Industry Method (1941).

[8] M. A. Joslyn, C. L. Comar, Ind. Eng. Ch., Anal. Ed, 10, 364 (1938); H. Schultes, Ang. Ch., 47, 258 (1934); Neuberg, Gottschalk, Bioch. Zts., 146, 164 (1924); Treadwell and Hall, Analytical Chemistry, II (1935) p. 73.

[9] G. Bornemann, Inorganic Preparations (1934) p. 152.

[10] Ibid (1934) p. 163.

Received September 8, 1955

RESIN IN SPRUCE WOOD*

S. S. Malevskaya

Chair of Organic Chemistry, the S. M. Kirov Academy of Forestry Technology

As reported earlier [1], spruce wood contains resin which partially remains in the cellulose fibers after sulfite cooking. During processing of the cellulose the resin may be deposited on the equipment in various amounts which depend on the degree of oxidation of its constituents. Not enough is known about the autoxidation products formed in the resin. We studied oxidized resin acids from ether and dichloroethane extracts and showed that oxygen atoms enter the resin acid molecules on exposure to air. In the main, oxygen is not added at the double bonds. The formula of such acids is $C_{20}H_{28}O_5$.

It was thought that the resin should also contain acids of a higher degree of oxidation, insoluble in ether and in dichloroethane but soluble in solvents such as acetone. The following experiments were carried out for extraction of such acids. Sawdust from seasoned wood (stored for 5 months) was extracted with dichloroethane to yield a dichloroethane resin extract the composition of which was given in the preceding communication [1]. After extraction of the resin soluble in dichloroethane, the sawdust was additionally extracted with acetone, 19.6 g of acetone extract being obtained. The contents of resin soluble in dichloroethane and in acetone were determined in a Soxhlet apparatus with sawdust of standard particle size [2]. Determinations of the extractable resin were repeated a year later. The sawdust was kept in the laboratory in a stoppered bottle.

TABLE 1

Results of Experiments on Extraction of Resin from Wood

Wood	Amount of resin extracted (%)		
	by dichloroethane	additionally by acetone	total
Freshly felled	2.14	–	–
After 5 month of storage	1.63	0.63	2.26
After 20 month.	1.11	0.29	1.40

The results of the experiments are given in Table 1.

The contents of resin extracted by these solvents decrease during storage. As we were interested in the composition of the acetone extract, it was separated by the method described previously [1].

The results of these experiments are given in Table 2.

The acetone extract consists predominantly of acids, which represent 81.6% of the total resin; of these, 60.4% consists of oxidized resin acids of formulas $C_{20}H_{26}O_{6.5}$ and $C_{20}H_{26}O_7$. These acids were analyzed; double bonds were determined by Kaufmann's method [3], hydroxyl groups by Tserevitinov's (Zerevitinov's) method in quinoline solution, carboxyl groups by titration at room temperature and after boiling with alkali (lactones); quinoid groups were also determined, and the molecular weight was found by the Rast method. The results are are given in Table 3. It follows from these experiments that oxygen was not added at the double bonds. The acid with the composition $C_{20}H_{26}O_{6.5}$ contains about 3 OH groups in the molecule, and the acid with the

* Communication II.

TABLE 2

Results of Experiments on Separation of the Acetone Extract

Weight of resin	Amount of acids		Amount of acids soluble in ether						Amount of acids soluble in acetone						Amount of neutral substances					
			total		resin acids		fatty acids		total		resin acids		fatty acids		total		unsaponifiable		saponifiable	
g	g	%	g	%	g	%	g	%	g	%	g	%	g	%	g	%	g	%	g	%
19.60	16.0	81.6	8.17	41.7	5.17	26.4	3.0	15.3	7.82	39.9	6.67	34.0	0.4	2.1	3.60	18.4	1.46	7.5	2.04	10.4

composition $C_{20}H_{26}O_7$ contains 3.4-3.8 (3.5) hydroxyl groups. Titration at room temperature gives 0.6 carboxyl groups for the first acid, and 0.5 for the second. After boiling with alkali this is increased by 0.4-0.5 carboxyl groups. The overall content is one carboxyl group per molecule of each acid.

Half the carboxyl groups are present in the free state, and half probably in the form of lactones. In view of the high molecular weight of the acids, the presence of a small proportion of dimeric molecules, linked by ester linkages, may be postulated. The existence of dimeric molecules of this type is reported in the literature [4]. In addition, when the acetone extract was separated, the residue contained a small amount of an acid which was insoluble in acetone but dissolved in acetic acid; its molecular weight determined by the Rast method was 1289. The nature of this substance requires further investigation.

The molecule of the $C_{20}H_{26}O_7$ acid was found to contain one quinoid group, and that of the $C_{20}H_{26}O_{6.5}$ acid, 0.76 of a quinoid group. For confirmation of the presence of lactones in the oxidized acids, the $C_{20}H_{26}O_7$ acid isolated from an acetone extract of resin obtained without preliminary extraction with dichloroethane was titrated in the cold and after boiling with alkali.

COOH groups found

By titration in the cold	0.5	0.4
By titration after boiling with alkali	0.6	0.6

These results agree with those given earlier.

These results suggest that as the number of oxygen atoms in the resin acid molecules increases, quinoid groups and hydroxyl groups are formed; formation of the latter leads to formation of lactones and probably also of dimeric molecules. The latter are insoluble in the organic solvents used for the extraction of resin from wood. This reaction converts the resin into a form which is harmless in pulp and paper production, and leads to an apparent decrease of the resin content in seasoned wood.

Since the most easily oxidized acid in wood resin is α-sapinic, on the basis of the foregoing the following structural formula is proposed for the $C_{20}H_{26}O_7$ acid:

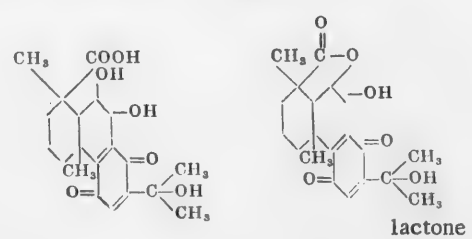

lactone

To establish the structure of the $C_{20}H_{26}O_7$ acid, an ozonation experiment was carried out.

TABLE 3

Analytical Data for Resin Acids

Type of resin acids	Formula nearest to elementary composition	Analysis found % C	Analysis found % H	Analysis calculated (%) C	Analysis calculated (%) H	Molecular weight, Rast method	Bromine added (in g/mole)	Content of OH groups	Carboxyl group content by titration: at room temperature	Carboxyl group content by titration: after boiling with alkali	Carboxyl group content by titration: total	Quinoid group content
Soluble in ether	$C_{20}H_{26}O_{8.5}$	64.46	7.08	64.83	7.07	391	2.3	2.8	0.6	0.49	1.09	0.78
Insoluble in ether, soluble in ethyl acetate	$C_{20}H_{26}O_{8.5}$	64.87	7.23	64.83	7.07	—	2.3	2.6	0.6	0.4	1.0	0.74
	$C_{20}H_{26}O_7$	63.52	7.05	63.46	6.92	445	2.3	3.8	0.57	0.52	1.09	1.0
	$C_{20}H_{26}O_7$	63.40	7.02	63.46	6.92	439	2.4	3.4	0.51	0.49	1.0	1.0

A solution of the acid in ethyl acetate had a dark cherry color, and it became yellow at the end of ozonation, but after removal of the solvent the ozonide was dark in color. Analysis of the ozonide showed that a little more than two molecules of ozone were added on per acid molecule. The ozonide had the formula $C_{20}H_{28}O_{13.5}$.

Found %: C 49.46, 49.33; H 5.84, 5.91. $C_{20}H_{28}O_{13.5}$. Calculated %: C 49.56, H 5.82.

The ozonide was decomposed with steam. Hardly any volatile acids were obtained. The decomposition product was not soluble in ether, and was extracted from aqueous solution with butyl alcohol. Analysis of the decomposition product gave:

Found %: C 58.47, 58.38; H 6.57, 6.54. $C_{20}H_{23}O_9$. Calculated %: C 58.50, H 6.38.

The ozonide decomposition product was analyzed for hydroxyl group content by Tserevitinov's method, in quinoline solution.

OH groups found	3.3,	3.4.
Carboxyl groups		
titration in the cold	0.83	0.83
after boiling with alkali	1.28	1.3

The results of the ozonation experiment confirm the presence of two double bonds in the acid molecule. Decomposition of the ozonide gave a dibasic hydroxy acid, one carboxyl group of which is present mainly in lactone form. The acid molecule contains about three hydroxyl groups, which agrees with the expected structure of the ozonide decomposition product. The presence of 9 oxygen atoms in the decomposition product is a discrepancy, as theoretically 11 oxygen atoms should be present.

The study of the oxidized resin acid with the composition $C_{20}H_{28}O_{4.6}$ from the dichloroethane extract [1] was continued. The hydroxyl group content determined by Tserevitinov's method in quinoline solution was found to be 2.6, 2.8.

Titration showed the presence of one carboxyl group (0.97, 0.95). The quinoid group content was found to be 0.53-0.6.

To establish the structure of the acid, an ozonation experiment was carried out. The initially dark solution was decolorized during ozonation, and a straw-yellow ozonide was obtained.

Analysis of the ozonide.

Found %: C 56.55, 56.50; H 7.24, 7.26. $C_{20}H_{30}O_{9.5}$. Calculated %: C 56.84, H 7.15.

About 2 molecules of ozone (5 oxygen atoms) were added, which corresponds to the number of double bonds in the acid molecule, found to be 1.6, 1.7 [1].

The decomposition of the ozonide by steam was extremely slow. The yield of volatile acids, calculated as acetic, was 0.32 g. A part of the ozonide decomposition products was soluble in ether, while a part could be extracted only after preliminary treatment with butanol.

Analysis of the ether-soluble decomposition product of the ozonide.

Found %: C 60.47, 60.53; H 8.18, 7.70. $C_{20}H_{30}O_{7.8}$. Calculated %: C 60.76, H 7.64.

The hydroxyl group content of the decomposition product was determined by Tserevitinov's method (in quinoline). This gave 3.5, 3.4 OH groups.

These results lead to the conclusion that the less oxidized the substance, the lower is its quinoid group content. The acid with the composition $C_{20}H_{28}O_{4.6}$ may be a mixture of two isomers with the structures:

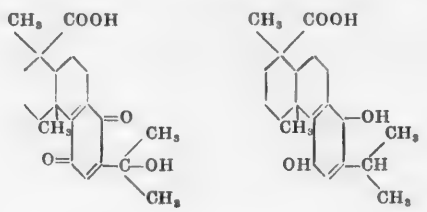

EXPERIMENTAL

Investigation of the Acid of Composition $C_{20}H_{26}O_{6.5}$

Analysis.

Found %: C 64.46, 64.87; H 7.08, 7.23. $C_{20}H_{26}O_{6.5}$. Calculated %: C 64.83, H 7.07.

Molecular weight, by the Rast method: 0.0506 g substance; 0.5072 g camphor, $\Delta t^\circ = 10.2$, M = 391.

Double Bond Content, by Kaufmann's Method

	Br_2 added calculated as I_2	Number of double bonds
0.1028 g substance	0.1662 g	2.3
0.1048 g substance	0.1675 g	2.3

Number of OH groups, by Tserevitinov's method. The determinations were carried out in quinoline solution. The organomagnesium compound was prepared in butyl ether solution.

	v_0	Number of OH groups
0.1040 g substance	19.3 ml	2.8
0.1144 g substance	18.2 ml	2.6

Carboxyl content, by titration. The acids were dissolved in alcohol.

Experiment 1. 0.1038 g substance, titration took 1.6 ml of 0.1 N NaOH solution, corresponding to 0.6 of a COOH group. 5 ml of 0.1 N NaOH solution was added and the solution was boiled for an hour. After cooling the excess alkali was titrated with 0.1 N HCl solution. A further 1.3 ml of 0.1 N NaOH solution was required for titration, corresponding to 0.49 of a COOH group. The two titrations together gave 1.09 COOH. The procedure was similar in all the experiments.

Experiment 2. 0.0859 g substance, titration took 1.3 ml of 0.1 N NaOH solution, corresponding to 0.6 of a COOH group. After boiling, 0.9 ml of 0.1 N NaOH was required for titration, corresponding to 0.4 of a COOH group. Altogether the acid molecule contained 1 COOH group.

Quinoid group determination. A weighed sample of the acid was dissolved in 10 ml of glacial acetic acid, the solution was heated to boiling, and zinc dust was added. The cherry-red solution became yellow. The excess zinc was filtered off and washed. The solution was neutralized with caustic soda until neutral to phenolphthalein, and titrated with iodine in presence of starch. The quinoid group contents were 0.78, 0.74. 0.1046 g of substance, 0.0533 g of iodine required for titration. 0.1028 g of substance, 0.0495 g of iodine required for titration.

The reaction proceeds according to the equation:

$$C_{20}H_{28}O_{6.5} + I_2 = 2HI + C_{20}H_{26}O_{6.5}.$$

Investigation of the Acid of Composition $C_{20}H_{26}O_7$.

Analysis.

Found %: C 63.52, 7.02; H 7.07, 7.02. $C_{20}H_{26}O_7$. Calculated %: C 63.46, H 6.92.

Molecular weight, by the Rast method

	Camphor	Δt°	M
0.0100 g substance	0.1654 g	7.5	439
0.0116 g substance	0.2082 g	5	455
		M_{av}	442

Double Bond Content, by Kaufmann's Method

	Br_2 added calculated as I_2	Number of double bonds
0.1036 g substance	0.1599 g	2.3
0.1032 g substance	0.1674 g	2.3

Number of OH groups, by Tserevitinov's method

	v_0	Number of OH groups
0.1080 g substance	24.5 ml	3.8
0.0993 g substance	19.7 ml	3.4

Carboxyl content, by titration

	0.1 N NaOH taken for titration	Carboxyl groups
0.1038 g substance	1.34 ml (in the cold)	0.57
	1.3 ml (after boiling	0.52
0.1076 g substance	1.23 ml (in the cold)	0.51
	1.2 ml (after boiling)	0.49

Quinoid group determination

	Iodine taken for titration	Number of quinoid groups
0.1042 g substance	0.0604 g	1.0
0.1042 g substance	0.0623 g	1.0

Ozonation experiment. 2 g of the acid with composition $C_{20}H_{26}O_7$ was taken for ozonation. 29 liters of oxygen was passed through. The ozone concentration was 3.1%. The solvent was ethyl acetate. At the end of ozonation the solvent was distilled off and the ozonide dried under vacuum.

Analysis of ozonide.

Found %: C 49.46, 49.33; H 5.84, 5.91. $C_{20}H_{28}O_{13.5}$. Calculated %: C 49.56, H 5.82.

The ozonide was decomposed by steam for 12 hours. Most of the ozonide went into aqueous solution, which was cooled and extracted with ether and butanol. Only 0.12 g of a substance, which was not investigated, was extracted in ether. The acid soluble in butanol was analyzed.

Analysis of acid soluble in butanol.

Found %: C 58.47, 58.38; H 6.57, 6.54. $C_{20}H_{26}O_9$. Calculated %: C 58.50, H 6.38.

Hydroxyl and carboxyl groups were determined in the decomposition product of the ozonide.

Number of OH Groups, by Tserevitinov's Method

Determinations in quinoline solution

	v_0	Number of OH groups
0.1060 g substance	19.1 ml	3.3
0.1210 g substance	28.8 ml	3.4

Acid groups were determined by titration, and lactones by titration after boiling with alkali.

Carboxyl content, by titration

	0.1 N NaOH taken for titration	Carboxyl groups
0.0980 g substance	2.0 ml (in the cold)	0.83
	3.1 ml (after boiling)	1.28
0.0984 g substance	2.0 ml (in the cold)	0.83
	3.2 ml (after boiling)	1.30

Substances volatile in steam. The volume of the first distillate was 715 ml. Its titration required 7.6 ml of 0.1 N NaOH. No volatile substances were found in the second distillate.

Investigation of the Acid of Composition $C_{20}H_{28}O_{4.6}$

The hydroxyl, carboxyl, and quinoid group contents of this acid were determined.

Number of OH groups, by Tserevitinov's Method

Determinations in quinoline solution

	v_0	Number of OH groups
0.1012 g substance	20 ml	3.0
0.1051 g substance	17.7 ml	2.6

Carboxyl content, by titration

	0.1 N NaOH taken for titration	Carboxyl groups
0.2032 g substance	5.8 ml	0.97
0.1756 g substance	4.7 ml	0.95

Quinoid group determination

	Iodine taken for titration	Number of quinoid groups
0.1031 g substance	0.0406 g	0.53
0.1001 g substance	0.0444 g	0.6

Ozonation experiment. 10 g of the substance, dissolved in ethyl acetate, was taken for ozonation. 47 liters of O_2 containing 3% ozone was passed through. After removal of the solvent a pale yellow ozonide remained.

Analysis.

Found %: C 56.55, 56.50; H 7.24, 7.26. $C_{20}H_{30}O_{9.5}$. Calculated %: C 56.84, H 7.15.

The ozonide was extremely difficult to decompose by steam.

The volume of the first distillate was 1056 ml, and its titration took 53.5 ml of 0.1 N NaOH, which is equivalent to 0.32 g of acetic acid.

Subsequent distillates contained no volatile acids. Decomposition of the ozonide gave 2.4 g of a substance soluble in ether; a further 2.53 g of substance was extracted with butanol, and the residue was 2.15 g. The residue was analyzed and it was found that it was mainly the original unchanged acid.

Analysis of the ether-soluble decomposition product of the ozonide.

Found %: C 60.47, 60.53; H 8.19, 7.70. $C_{20}H_{30}O_{7.8}$. Calculated %: C 60.76, H 7.64.

Carboxyl content, by titration

	0.1 N NaOH taken for titration	Carboxyl groups
1844 g substance	7.5 ml	1.6
1696 g substance	6.7 ml	1.6

Number of OH groups, by Tserevitinov's method

		Number of OH groups
0.1032 g substance	19.6 ml	3.5
0.0980 g substance	18.4 ml	3.4

Analysis of decomposition product of ozonide, soluble in butanol.

Found %: C 60.27, 60.60; H 7.41, 7.37.

SUMMARY

1. Experimental data obtained in a study of oxidized resin acids of the composition $C_{20}H_{26}O_{6.5}$ and $C_{20}H_{26}O_7$ (isolated from spruce wood by acetone extraction after preliminary treatment of the sawdust with dichloroethane) suggest that as the number of oxygen atoms in the resin acids increases, a quinoid group and hydroxyl groups are formed in the molecule. The formation of these groups leads to lactone formation and probably to dimerization of the molecules.

2. As the most readily oxidizable acid in wood resin is α-sapinic, a structural formula is proposed for the acid of composition $C_{20}H_{26}O_7$, on the basis of the experimental data.

3. Study of the oxidized resin acid of the composition $C_{20}H_{28}O_{4.6}$, obtained from dichloroethane extract of wood, has been continued. The experimental results suggest that this acid is a mixture of isomers; a proposed structure of these is given.

LITERATURE CITED

[1] S. S Malevskaya and V. D Karnaukhova, J. Appl. Chem. 29, 3, 401 (1956).*

* Original Russian pagination. See C. B. Translation.

[2] F. L. Komarov, Laboratory Manual of Wood and Cellulose Chemistry (1934) p. 26.*

[3] Kaufmann, Arch. Pharm., 267 (1923).

[4] Simonsen, The Terpenes, III (1950).

Received July 12, 1955

* In Russian.

AROMATIZATION OF TREE-STUMP TURPENTINE

V. G. Plyusnin, S. I. Chertkova, E. P. Babin, and M. A. Mikhailova

Dehydrogenation of the terpenes in turpentine over activated carbon yields mainly p-cymene, p-menthane, and toluene [1, 2]. In view of the large available resources of tree-stump turpentine, of which not nearly enough use is being made at the present time, and of the availability and relative cheapness of activated carbon, the conversion of tree-stump turpentine into a more valuable chemical raw material is of interest. The product may be used as an additive to aviation gasoline or as a raw material rich in aromatic hydrocarbons.

EXPERIMENTAL METHODS

Characteristics of the raw material. The raw material used was tree-stump turpentine with the following characteristics: boiling range 138-207°; n_D^{20} 1.4770; d_4^{20} 0.8627; iodine number 241.

Apparatus and experimental procedure. The dehydrogenation of turpentine terpenes was studied in a large-scale unit shown diagrammatically in Fig. 1.

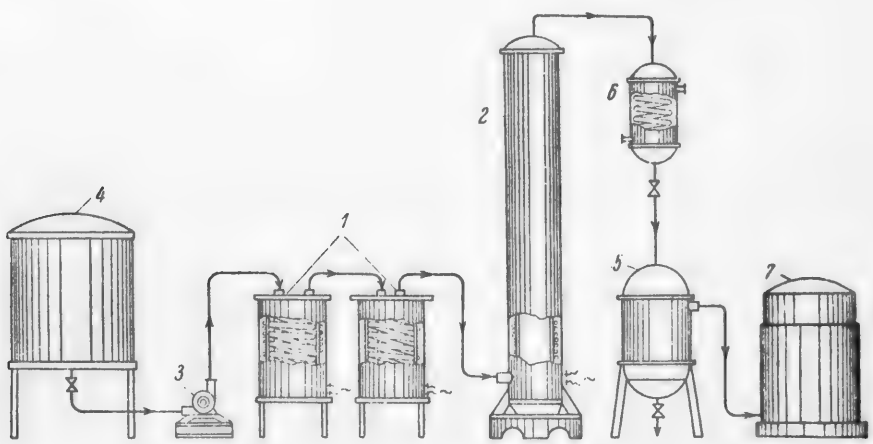

Fig. 1. Apparatus for aromatization of tree-stump turpentine.
1) Lead tanks; 2) catalytic chamber; 3) pump; 4) raw material tank; 5) receiver; 6) condenser; 7) gas holder.

The temperature of the lead tanks 1 with coil heaters was kept at 425°. The catalytic chamber 2 was 100 mm in diameter and 2200 mm high. It was filled with activated carbon (about 7 liters) and its temperature was kept constant. The throughput of the unit was regulated by means of the pump 3 (in the range of 5-10 liters per hour).

The liquid products obtained by dehydrogenation of the tree-stump turpentine were termed catalyzates; the catalyzates purified to remove unsaturated hydrocarbons were termed "uratols" (Ural toluene).

The effects of various factors on dehydrogenation of terpenes were judged by the yields of the catalyzates, their physicochemical characteristics, and the composition of the gas (contents of olefins and hydrogen).

The unsaturated hydrocarbon contents of the catalyzates were found from the iodine numbers, the unsaturated hydrocarbons in the gases were determined by absorption in sulfuric acid, by Dobryansky's method, and the hydrogen content was found by combustion over spongy palladium.

The apparatus described was used to study the effect of the raw feed rate (in volumes of raw feed per unit volume of catalyst per hour) at 425°, and the effect of reaction temperature at a constant feed rate of 1.

The results are given in Tables 1 and 2.

TABLE 1

Effect of the Raw Feed Rate on the Yields and Compositions of Catalyzate and Gas

V_r*	Yield		Catalyzate		Composition of gas				
	of catalyzate (%)	V_g**	n_D^{20}	iodine number	CO_2	n-C_4H_8	C_3H_8	C_2H_4	H_2
0.5	86.5	96	1.4970	125.0	0.4	1.6	6.4	6.0	18.5
1.0	88.7	78	1.4955	133.5	0.6	1.2	6.8	5.8	18.3
1.5	90.0	70	1.4890	156.8	0.5	1.6	6.2	5.8	18.8
2.0	91.0	65	1.4860	165.4	0.6	2.0	7.0	6.2	19.0
2.5	92.3	52	1.4805	174.6	0.5	1.6	6.3	5.9	18.7

* $V_r = \frac{\text{volume of raw feed}}{\text{volume of catalyst} \cdot \text{hour}}$

** $V_g = \frac{\text{volume of gas}}{\text{volume of raw feed}}$

TABLE 2

Dehydrogenation of Turpentine Terpenes at Constant Raw Feed Rate ($V_r = \frac{1 \text{ liter raw feed}}{\text{liter catalyst} \cdot \text{hour}}$) and Various Temperatures.

Temperature, (°C)	Yield		Catalyzate			Composition of gas				
	of catalyzate (%)	$\frac{V_g}{V_r}$	d_4^{20}	n_D^{20}	iodine number	CO_2	n-C_4H_8	C_3H_8	C_2H_4	H_2
425	94.5	34.0	0.8528	1.4720	208.0	0.2	4.0	5.4	8.4	17.2
450	90.0	66.0	0.8594	1.4869	130.0	0.2	4.4	5.6	7.5	17.2
500	82.0	168.0	0.8705	1.4990	98.0	0.2	6.8	8.0	8.2	17.0
550	70.0	236.0	0.8766	1.5090	47.0	0.3	6.4	7.0	7.4	17.8
580	68.0	248.0	0.8778	1.5120	40.0	0.2	7.8	7.2	8.1	17.9

It follows from the data in Table 1 that at 425° and volume feed rates between 0.5 and 2.5 the iodine numbers of the catalyzate remain high at all feed rates. However, depending on the composition of the gas, terpene dehydrogenation is accompanied by loss of side chains, leading to the formation of an aromatic product lighter than cymene.

The data in Table 2 show that although increase of temperature leads to a decrease of iodine number, the catalyzate contains considerable amounts of unsaturated hydrocarbons even at 580°.

The yields and physicochemical constants of "uratols" obtained by purifications of catalyzates with sulfuric acid at different concentrations are given in Table 3. It is seen that even 70% sulfuric acid has an effect on the unsaturated compounds in the catalyzate, as the process is accompanied by a considerable decrease of "uratol" yield and a decrease of the iodine number of the fraction boiling up to 200°. As the sulfuric acid concentration is increased from 70 to 96%, the decrease of the "uratol" yield reaches 10% calculated on the turpentine; the highest loss of "uratol" is 26.8%, which occurs on purification with 96% H_2SO_4. As was to be expected, the decrease of "uratol" yield with increasing acid concentration is due mainly to the amount of hydrocarbons passing into the acid tar rather than to an increased polymer content.

TABLE 3

Purification of Catalyzate from Tree-Stump Turpentine with Sulfuric Acid of Different Concentrations

H_2SO_4 conc. (%)	Amt. of 100% H_2SO_4 (in wt. %)	Yield (% on the turpentine)	d_4^{20}	n_D^{20}	Iodine number	Start of boiling (°C)	Proportion of material (in %) boiling at (°C)					
							100	120	140	160	180	200
0	0	81.0	0.8596	1.4902	82.5	85	1.5	5	13.8	40.2	80.0	91.0
70		64.0	0.8578	1.4852	60.7	95	0.2	2.5	10.0	37.8	86.0	95.8
70		62.0	0.8580	1.4834	58.7	93	0.2	3.0	13.0	48.0	94.0	98.0
75		60.0	0.8586	1.4850	50.1	93	0.3	2.5	8.8	39.0	84.5	94.0
75		61.0	0.8574	1.4845	49.0	96	0.2	2.4	12.0	45.0	92.0	96.0
80	14.0	58.5	0.8566	1.4850	39.1	105	—	0.8	7.8	38.1	85.5	95.0
80		56.3	0.8570	1.4865	41.0	106	—	0.5	16.0	47.0	81.0	97.0
90		55.0	—	1.4874	30.4	115	—	1.0	4.0	37.0	87.0	94.5
90		54.0	—	1.4870	29.5	110	—	0.4	5.0	39.0	88.1	96.0
96		52.2	—	1.4873	26.3	120	—	—	4.8	38.0	87.2	96.0

Purification with 96% sulfuric acid gave a yield of 52.2% of "uratol" with iodine number 26.3. Evidently, "uratol" free from olefins can be obtained by increasing the amount of acid, but the yield of "uratol," according to the data in Table 3, will decrease as the result of losses, not only of unsaturated compounds, but also of aromatic hydrocarbons. This is shown by the results of standard distillations, in which the contents of benzene – toluene – xylene fractions decrease with increasing sulfuric acid concentration. It is therefore evident that sulfuric acid is an unsuitable catalytic reagent for the production of pure aromatic hydrocarbons.

The stability of "uratols" was tested by determinations of the residual tar contents of a mixture consisting of 90% B-70 aviation gasoline and 10% "uratol." It was found that "uratol" purified by means of sulfuric acid of over 75% concentration gives a residual tar value of not over 2 mg per 100 ml of mixture with B-70 gasoline. "Uratol" purified by means of 70% sulfuric acid gives up to 7 mg residual tars, and products distilled from the catalyzate at a final boiling temperature of 200°, 10-12 mg. Thus, to obtain a stable "uratol," the concentration of sulfuric acid used for purification of the catalyzate should evidently be at least 75%. For this reason 80% sulfuric acid was used for subsequent purification of catalyzates.

The "uratol" obtained by purification with 14% of 80% sulfuric acid and distilled in steam had the following characteristics: yield of "uratol" calculated on turpentine 68%, density d_4^{20} 0.8651, refractive index n_D^{20} 1.4952, iodine number 42.8.

The results of fractionation of "uratol" through a column of 24 theoretical plates are given in Table 4 and plotted in Fig. 2. A curve for the fractional composition of the catalyzate distilled through the same column is also given.

The antiknock properties of the catalyzate and "uratol" in mixtures with B-70 gasoline were evaluated by determinations of octane numbers by the engine method.

It follows from the data in Table 5 that 10 to 30% additions of catalyzate and of "uratol" to B-70 aviation gasoline produce almost equal increases of octane numbers.

TABLE 4

Fractional Composition of "Uratol" With Iodine Number 42.8.

Fraction (boiling range, °C)	Yield (%)	n_D^{20}	d_4^{20}	Iodine number
Up to 100	2.8	1.4682	0.8082	102.8
100—130	20.6	1.4938	0.8654	18.9
130—140	14.8	1.4960	0.8667	20.5
140—150	15.3	1.4960	0.8664	31.2
150—160	10.6	1.4958	0.8695	37.1
160—170	16.1	1.4960	0.8703	44.4
170—175	7.0	1.4986	0.8733	32.0
175—183	3.6	1.5000	0.8776	41.9
Residue and losses	9.2	1.5100	0.9096	121.9
"Uratol"	100	1.4952	0.8651	42.8

Table 5 also gives the octane numbers of the pure products, catalyzate and "uratol," calculated by means of the formula for mixtures: the octane number of the mixture $= \frac{70 \cdot P_g + xP_q}{100}$, where x is the octane number of the pure component, P_q is the content of the pure component in the mixture (in %), and P_g is the content of B-70 gasoline in the mixture (in %).

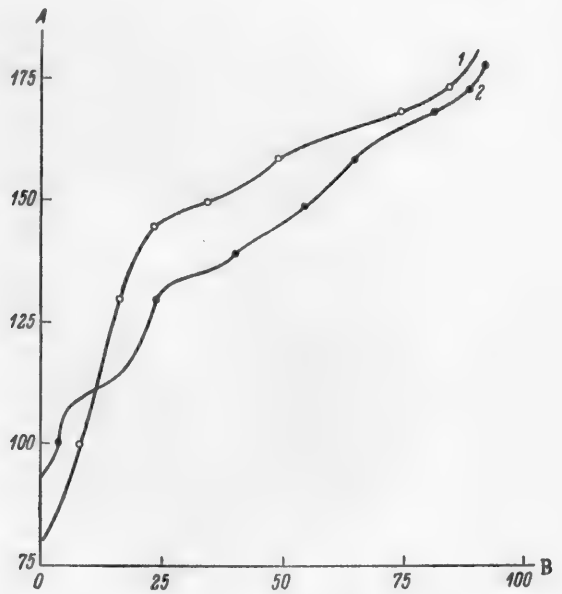

Fig. 2. Fractionation curves for catalyzate (1) with iodine number 130, and "uratol" obtained from it (2) with iodine number 42.8.

A) Temperature (°C); B) yields of fractions (%).

It follows from these data that in a mixture containing 10% of "uratol" the octane number of the "uratol" itself is very high, differing by 89 units from the value for the terpenes in the original raw material and by 12 units from the value for the catalyzate.

TABLE 5

Octane Numbers of B-70 Gasoline with Additives

Hydrocarbon mixture	Octane numbers with additives (%)			Octane no. with addition of 10% "uratol" (3 ml e.l.)	Calculated octane no. after addition of mixture (%)	
	10	20	30		10	30
Turpentine	67.3	64.2	—	—	43	—
Catalyzate	75.1	75.3	76.2	88.0	120	90.7
"Uratol"	76.2	76.0	76.4	89.6	132	91.3

However, the difference of octane values between "uratol" and the catalyzate diminishes with increase of the amounts added to B-70 gasoline, and at 30% contents it becomes close to zero.

Thus, if the high-octane component obtainable from turpentine by dehydrogenation is regarded as a component for raising the octane number of automobile and not of aviation fuel, sulfuric acid purification of the catalyzate evidently becomes unnecessary. Only steam distillation for removal of tars is needed.

TABLE 6

Fractional Composition of "Uratol" and Physicochemical Constants of Individual Fractions

Fraction (boiling range, °C)	Yield of fraction (wt. %)		n_D^{20}	d_4^{20}	Iodine number
	on the catalyzate	on the turpentine			
80 —100	2.5	0.4	1.4870	—	0
100 —110	0.1	—	—	—	—
110 —111	14.7	7.1	1.4960	0.9651	0
111 —136	0.2	—	—	—	—
136.5—141	32.2	15.7	1.4971	0.8659	0
141 —143	0.5	—	—	—	—
143 —150	1.3	0.6	1.4969	0.8661	0
150 —160	5.7	2.8	1.4948	0.8663	0
160 —170	16.6	8.0	1.4956	0.8681	0
170 —176	9.8	4.8	1.5018	0.8689	0
Residue, b. p. 176 . .	15.2	7.1	1.5048	0.8719	0

For the production of pure aromatic hydrocarbons, free from unsaturated hydrocarbons, a catalyst must be found which would remove unsaturated hydrocarbons without influencing aromatic hydrocarbons.

Consideration of the chemical and catalytic properties of a number of compounds used for removal of unsaturated hydrocarbons ($ZnCl_2$, $AlCl_3$, BF_3, H_3PO_4, HF, etc.) suggests that anhydrous hydrogen fluoride is the most suitable. Its low boiling point, in conjunction with its chemical properties, makes it easily and completely recoverable by simple distillation.

The apparatus used for purification of the catalyzate with hydrogen fluoride consisted of a copper reactor with a jacket for circulation of cold or hot water. The reactor was equipped with a blade stirrer driven by means of a pulley connected to an electric motor.

The experimental procedure was as follows. The required amount of hydrogen fluoride was introduced into the reactor from a special cylinder. Crude catalyzate from which unsaturated hydrocarbons were to be removed was then added through a copper funnel at the top of the reactor. The stirrer was switched on. At the end of the experiment the stirrer was switched off and the reaction product, together with the catalyst, was discharged into a copper flask through a special opening at the bottom of the reactor. The amount of hydrogen fluoride taken was 10% on the weight of catalyzate in all cases. The stirring was continued for 30 minutes. The hydrogen fluoride was separated off by distillation out of the copper flask, through a small column. Most of the hydrogen fluoride distilled at 30-60°, and the hydrogen fluoride was completely recovered by distillation up to 150°.

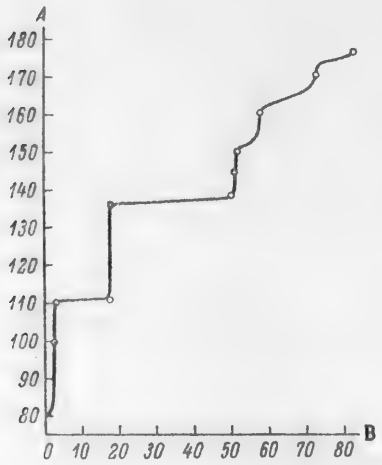

Fig. 3. Fractional composition of "uratol" after purification of the catalyzate with anhydrous hydrogen fluoride.
A) Boiling point (°C); B) yields of fractions (%).

The product was then distilled out of the copper flask, the fraction up to 200° being collected and designated as "uratol." The residue of the flask ("polymers") did not require washing, as it was quite neutral, while the distillate, "uratol," was washed with water, alkali, and water again to a neutral reaction.

Figure 3 shows a graph representing the fractionation of "uratol" after purification with hydrogen fluoride. It is evident from this graph and from the data in Table 6 that "uratol" contains very little benzene. The physicochemical constants of the narrow 110-111° fraction, obtained in 14.7% yield, correspond to toluene. The 136-141° fraction probably consists of xylenes. The 150-160° fraction can only contain propylbenzenes, which boil at 152 and 154°. The predominant component in this fraction is probably isopropylbenzene, which may be formed by demethylation of cymenes. The 160-170° and 170-176° fractions are complex mixtures of alkyl benzenes, which may be expected to contain homologs of cymene and menthane.

Since it was impossible to analyze the individual fractions spectroscopically, while chemical methods of analysis are complex and inaccurate, the contents of individual benzene homologs in "uratol" were not determined.

However, the foregoing data show fairly convincingly that turpentine can be regarded as a source of toluene and higher benzene homologs, which may be used for various purposes, such as high octane additives for aviation gasolines. The yield of additive obtainable from turpentine can be raised to 50%, the yield of toluene to 7%, and xylenes to 16%.

The yield of crude toluene obtained by dehydrogenation of turpentine is approximately 2-2.5 times the yield obtainable by pyrolysis of kerosene.

SUMMARY

1. The results show that terpenes from turpentine can be used as a raw material for the production of high-octane additives for aviation fuel. The additive has been named "uratol."

2. The maximum yield of low-boiling aromatics (up to 200°), termed "uratol," obtainable by dehydrogenation of turpentine over activated carbon can be raised to 50%.

3. From the catalyzate after removal of olefins, benzene, toluene, and xylene were isolated in yields of 0.45, 7.1, and 15.7% by weight, calculated on the raw material (turpentine).

4. It was found that hydrogen fluoride is a good catalyst for removal of unsaturated compounds from aromatic hydrocarbons, by conversion of the former into high-boiling polymers. The catalyst itself (HF) can be completely recovered.

LITERATURE CITED

[1] G. A. Rudakov, N. P. Borisova, O. K. Emelyanova, et al., J. Appl. Chem. 22, 2, 180 (1949).

[2] O. Hildani and K. Bergstrom, Swiss Patent 87706 (1934).

Received July 25, 1955.

ACTION OF METAL OXIDES AS VULCANIZATION ACTIVATORS OF SODIUM BUTADIENE RUBBER

M. Feldshtein, P. Orlovsky, and B. Dogadkin

Scientific Research Institute of the Tire Industry

The vulcanizing group in rubber mixes is a complex system consisting of vulcanizing agents, accelerators, and vulcanization activators. Activation of vulcanization consists of additional acceleration of the process (apart from the effects of accelerators) and improvement of the technical properties of the resultant vulcanizates. Until recently, the most usual vulcanization activator has been zinc oxide. In the opinion of some investigators the activating action of zinc oxide depends in some measure on the fact that reactions between accelerators and metallic oxides give rise to salts [1] which are more soluble in the rubber than the accelerators themselves. According to other workers, disulfides [2] or polysulfides [3] are formed during vulcanization in presence of accelerators and metallic oxides (especially zinc oxide), and these decompose to liberate active sulfur. It has also been suggested that zinc oxide exerts an oxidizing action [4] on the rubber thiols formed at the first stage of vulcanization:

$$RH + S_x \xrightarrow{\text{accelerator}} RSH + S_{x-1}, \quad (1)$$

$$2RSH + Zn^{++} \rightarrow RSZnSR + 2H^+, \quad (2)$$

$$RSZnSR + S_x \rightarrow RSSR + ZnS + S_{x-1}. \quad (3)$$

The oxidizing action of the activator may be replaced by the analogous action of certain types of accelerators when the latter give rise to free radicals under the heat conditions of vulcanization [5]. In particular, we have shown that 2-(diethylaminothio)-benzothiazole (sulfenamide BT) can be used for vulcanization of natural rubber in absence of zinc oxide. For example, with 1.5 parts by weight of sulfenamide BT to 100 parts of natural rubber, 10 minutes of heating at 143° gave a vulcanizate of tensile strength 260 kg/cm^2, as compared with 224 kg/cm^2 for the vulcanizate obtained in presence of Captax and zinc oxide.

It is reasonable to assume that the nature of the action of vulcanization activators depends to a considerable extent on the chemical nature of the rubber – on the reactivity of its molecular chains in reactions of the type described. Indeed, repeated attempts to replace in the vulcanization of natural rubber, zinc oxide by other less scarce metallic oxides have not proved successful. Since the introduction of synthetic rubber, for which the role of zinc oxide as vulcanization activator is less pronounced, there have been reports [6, 7] that it is possible to decrease the concentration of zinc oxide considerably or even to eliminate it completely from rubber compositions. However, the data available on this subject are contradictory, and in consequence a number of important practical and theoretical questions relating to the use and action of vulcanization activators have remained unsolved. This situation is probably the consequence of a lack of adequate experimental data on the role of the principal components of rubber mixes in activation of the vulcanization process. It was therefore desirable to study the action of various metallic oxides as vulcanization activators in relation to the type of rubber, vulcanization accelerators, and active fillers.

The present communication is confined to an account of experimental data on the influence of various metallic oxides (zinc oxide, magnesium oxide, calcium oxide, and calcium hydroxide) on the vulcanization kinetics of sodium butadiene rubbers. Two types of sodium butadiene rubber were studied: SKB polymerized by the rod method (SKB-r) and SKB polymerized by the rodless (vapor phase) method (SKB-v). The mixes studied contained different amounts of accelerators and activators. However, they were all based on 100 parts by weight of rubber, 2.0 parts of sulfur, and 2.0 parts of stearic acid. Stearic acid was not added to mixes which did not contain metallic oxides. The amounts of activators used were 1.0, 3.0, and 5.0 parts by weight.

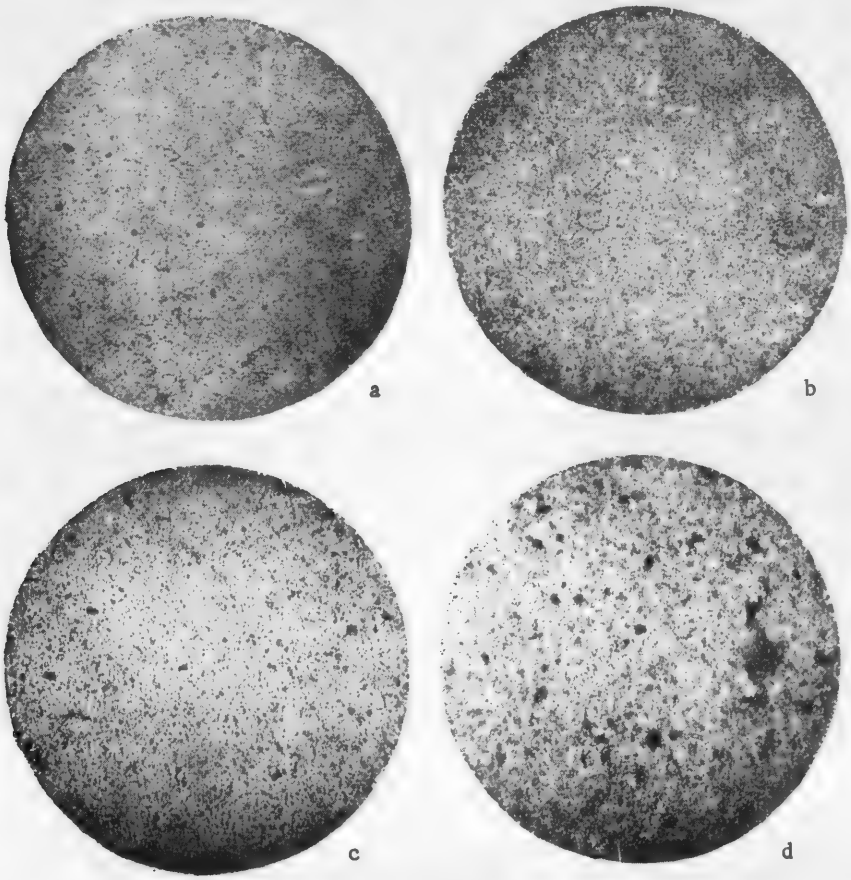

Fig. 1. Distribution of activators in sodium butadiene rubber. Contents of activators (in parts by weight): ZnO, a) 1, b) 5; $Ca(OH)_2$, c) 1, d) 5.

In a number of cases 1.0 part of activator gives a better vulcanizing effect, as shown by the mechanical properties, than 5.0 parts by weight. Microscopic investigations of raw mixes (Fig. 1) showed that this type of action of activators is the consequence of less effective distribution of the metallic oxides in mixes with increasing concentration. This effect is often found for such activators as calcium oxide, calcium hydroxide, and less often for magnesium oxide. Zinc oxide is distributed better, and therefore, in most cases 5 parts of it by weight are more effective.

The mixes were vulcanized at 143°.

The results, plotted in Fig. 2, show the effects of activators on the course of variation of the modulus for mixes based on rod-polymerized SKB containing mercaptobenzothiazole (Captax). Zinc oxide and magnesium oxide exerted the greatest activating action.*

Data on variations of the modulus (Fig. 3) show that in absence of metallic oxides the presence of dibenzothiazole disulfide (Altax) in the mix gives a vulcanization effect considerably greater than that produced by mercaptobenzothiazole under the same conditions.

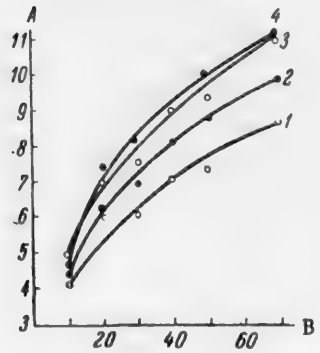

Fig. 2. Vulcanization of rod-polymerized sodium butadiene rubber in presence of Captax (0.6 part by weight). A) Modulus at 400% elongation (in kg/cm^2), B) vulcanization time (minutes). Contents of activators (in parts by weight): 1) without activator, 2) calcium oxide, 1.0, 3) zinc oxide 5.0, 4) magnesium oxide 5.0.

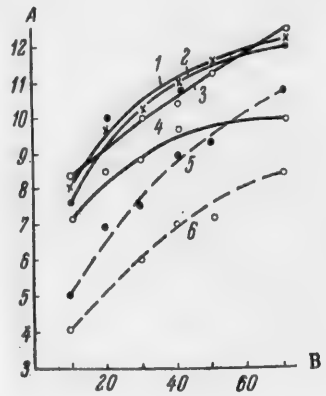

Fig. 3. Vulcanization of rod-polymerized sodium butadiene rubber in presence of Altax (0.8 part by weight). A) Modulus at 400% elongation (in kg/cm^2), B) vulcanization time (minutes). Contents of activators (in parts by weight): 1) zinc oxide 5.0, 2) magnesium oxide 5.0, 3) calcium oxide 5.0, 4) without activator, 5) Captax, zinc oxide 5.0, 6) Captax, without activator.

This effect of dibenzothiazole disulfide is a consequence of the fact that this accelerator has an independent vulcanizing (structurizing) influence on rubber [8]. In mixtures containing Altax, the vulcanizing effects of magnesium oxide and calcium oxide approach that of zinc oxide.

The effect of 2-(diethylaminothio)-benzothiazole (sulfenamide BT) on vulcanization of mixes based on rod-polymerized SKB is similar to the effect of Altax, both in presence and in absence of activators.

In mixes with thiuram, zinc oxide is far superior to the other metallic oxides as vulcanization activator.

Thus, vulcanization of mixes based on rod-polymerized SKB in presence of accelerators of different classes is activated considerably in presence of metallic oxides. Oxides of magnesium and calcium are practically equivalent to zinc oxide in their activating effects, except in mixes with thiuram.

A different situation is seen in the vulcanization of mixes based on SKB polymerized by the rodless method. In such cases vulcanization proceeds vigorously in absence of the usual activator – zinc oxide. Addition of the latter to mixes containing Captax, Altax, or sulfenamide BT retards vulcanization. Figure 4 shows that the modulus – vulcanization time curve for a mix containing zinc oxide lies considerably below the curve for the mix without activators. Other metallic oxides – calcium oxide and calcium hydroxide – have practically no influence on the vulcanization kinetics, while magnesium oxide even shows a slight tendency to increase the vulcanization effect.

* Only the kinetic aspects of the process are considered here. The effects of metallic oxides on the technical properties of vulcanizates will be described in another communication.

These results show that, in contrast to mixes based on rod-polymerized SKB, in mixes based on the rodless rubber, zinc oxide not only does not activate vulcanization, but even decreases the vulcanization effect (Fig. 5). This is also illustrated by the curves for variation of maximum swelling.

It is known that changes in the nature of swelling give an indication of structural changes in vulcanizates. The equation proposed by Flory and Rehner represents the relationship between swelling and concentration of cross links in the vulcanizate:

$$V=\left[\frac{M_a(1-k)}{2dv_1}\right]^{\frac{3}{5}},$$

where V is the degree of swelling, defined as the ratio of the volume of the system to the original volume of the rubber; M_a is the average molecular weight of chain segments between cross links; d is the density of the polymer; v_1 is the molar volume of the solvent; k is a constant which depends on the temperature and the composition of the components.

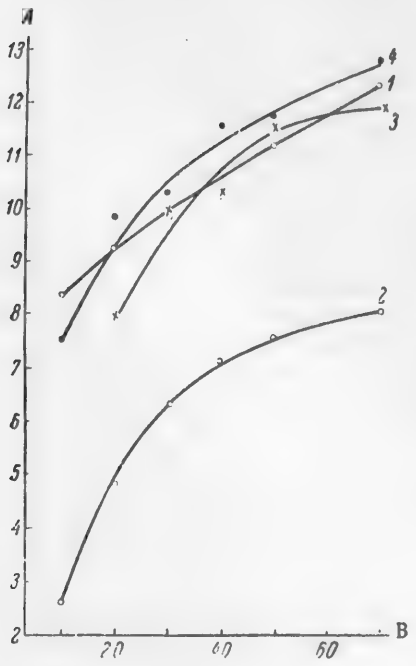

Fig. 4. Vulcanization of rodless sodium butadiene rubber in presence of Captax (0.6 part by weight). A) Modulus at 400% elongation (in kg/cm^2), B) vulcanization time (minutes). Contents of activators (in parts by weight): 1) without activator; 2) zinc oxide 5.0, 3) magnesium oxide 1.0, 4) calcium hydroxide 1.0.

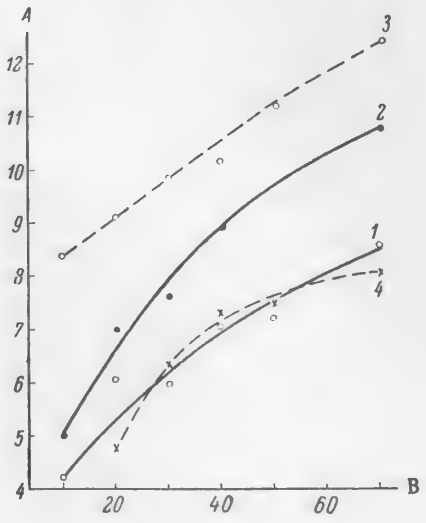

Fig. 5. Vulcanization of sodium butadiene rubbers polymerized by the rod (SKB-r) and rodless (SKB-v) methods, in presence of Captax. A) Modulus at 400% elongation (in kg/cm^2), B) vulcanization time (minutes). Contents of activators (in parts by weight): 1) SKB-r, without activator; 2) SKB-r, zinc oxide 5.0; 3) SKB-v, without activator; 4) SKB-v, zinc oxide 5.0.

Vulcanizates based on rod-polymerized rubber (Fig. 6), made without activators, have considerably higher swelling in benzene than vulcanizates with zinc oxide. The reverse is true of rodless rubber vulcanizates, which have greater swelling if zinc oxide is present. This indicates that in the latter case zinc oxide retards structure formation. What is the reason for this effect of zinc oxide? The answer to this question is provided by data on the kinetics of sulfur addition.

The amount of sulfur which reacted with rubber was found from the total sulfur content determined after prolonged extraction of the vulcanizates with acetone. The analytical data for the bound sulfur contents in vulcanizates based on sodium butadiene rubbers containing mercaptobenzothiazole as accelerator are given in Fig. 7. It follows from Fig. 7 that in mixes with rod-polymerized rubber, zinc oxide gives a higher rate of sulfur addition than any other metallic oxide activator. In mixes with rodless rubber, zinc oxide retards the addition of sulfur to rubber. In such mixes the rate of sulfur addition is highest in absence of metallic oxides.

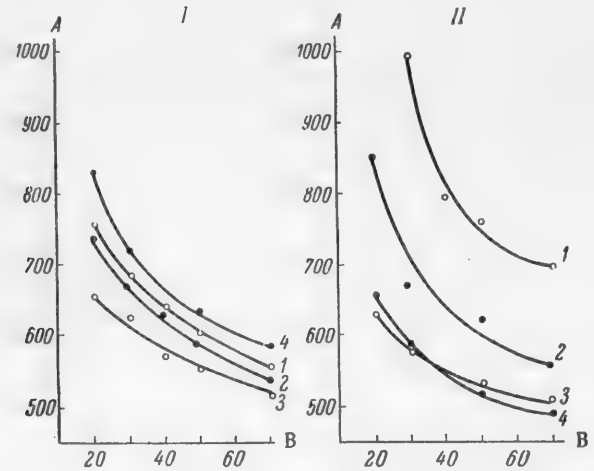

Fig. 6. Kinetics of the variation of the maximum swelling of vulcanizates after 24 hours of swelling in benzene. Captax accelerator. A) Maximum swelling (%), B) vulcanization time (minutes). I) Rod-polymerized SKB, II) rodless SKB. Contents of activators (in parts by weight): 1) zinc oxide 5.0, 2) calcium oxide 1.0, 3) magnesium oxide 1.0, 4) without activator.

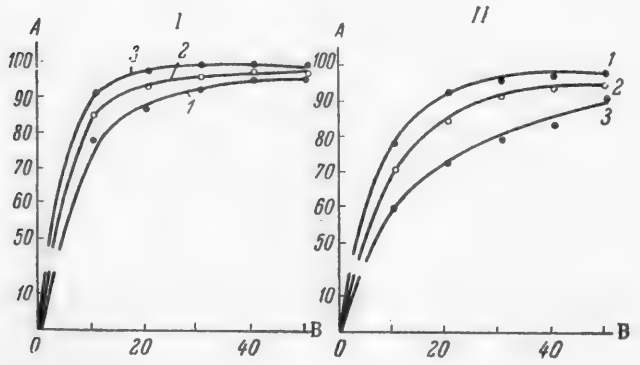

Fig. 7. Kinetics of sulfur addition. Captax accelerator. A) Amount of sulfur added (in %), B) vulcanization time (minutes). I) Rod-polymerized SKB, II) rodless SKB. Contents of activators (in parts by weight): 1) without activator, 2) magnesium oxide 1.0, 3) zinc oxide 5.0.

The presence of magnesium oxide also retards the binding of sulfur (although less so than zinc oxide). It should be noted in this connection that the somewhat higher modulus values and the practically equivalent maximum swelling values, with a correspondingly lower amount of added sulfur, found for mixes containing magnesium oxide as compared with a mix without metallic oxides, indicate that magnesium oxide has an influence not only on the kinetics of sulfur addition but also on the relative contents of sulfur and other types of bonds between the molecular chains of the vulcanizates.

We have therefore established the extremely interesting fact that zinc oxide has different effects in mixes (unloaded) of sodium butadiene rubber polymerized by the rod and rodless methods, respectively. In rodless rubber mixes, in presence of such accelerators as Captax, Altax, and sulfenamide BT, zinc oxide retards vulcanization, decreasing sharply the rate of reaction of the rubber with the vulcanizing agent – sulfur. However, with accelerators of the thiuram type no such difference between the effects of metallic oxides in rod-polymerized and rodless rubber mixes is found – both require the use of zinc oxide as activator.* All this shows that the groups of activators studied – the thiuram type, on the one hand, and the thiazole and sulfenamide type, on the other – operate by different activation mechanisms. The mechanism depends not only on the chemical nature of the accelerator used, but also on the type of rubber. In the latter case, the presence of various impurities in the technical products may be significant. It is known that alkalinity of the

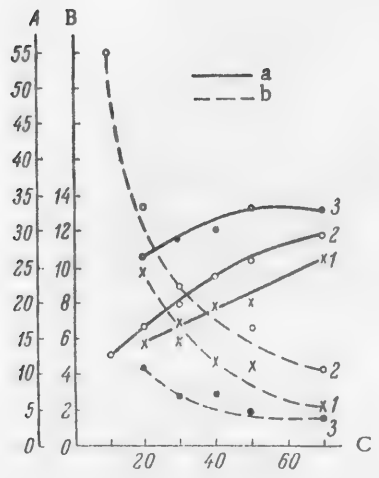

Fig. 8. Vulcanization of rodless SKB (0.22% alkali) in presence of Captax. A) Residual elongation (%), B) modulus at 400% elongation (kg/cm^2), C) vulcanization time (minutes). a) Modulus, b) residual elongation. Contents of activators (in parts by weight): 1) without activator, 2) zinc oxide 5.0, 3) magnesium oxide 3.0.

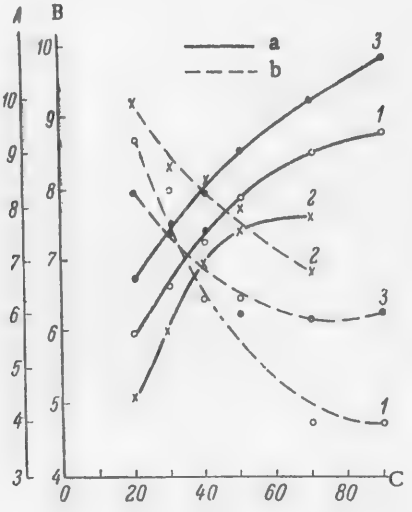

Fig. 9. Vulcanization of rodless SKB (0.22% alkali) in presence of Altax. A) Residual elongation (%), B) modulus at 200% elongation (kg/cm^2), C) vulcanization time (minutes). a) Modulus, b) residual elongation. Contents of activators (in parts by weight): 1) without activator, 2) zinc oxide 5.0, 3) magnesium oxide 3.0.

---

* Zinc oxide is not always needed in presence of thiuram. For example, we found that in butadiene – styrene rubber mixes with thiuram, calcium hydroxide is a better activator than zinc oxide. However, we are not concerned here with the role of activators in vulcanization of butadiene – styrene rubber. This question needs a separate investigation.

rubber has a considerable influence on the kinetics of vulcanization. The question arises whether the anomalous action of zinc oxide in mixes containing rodless sodium butadiene rubber is associated with the presence of definite amounts of alkali, or whether this action of zinc oxide is specific for this type of rubber irrespective of its alkalinity. To answer this question, experiments were carried out with different batches of SKB polymerized by the rodless method, differing considerably from each other in alkali contents. The first batch contained 0.22% alkali, and the second, 0.6% (calculated as sodium carbonate).

The variations of the physicomechanical properties of vulcanizates based on rodless SKB containing 0.22% alkali are plotted in Fig. 8. It follows from the data in Fig. 8 that vulcanization is most rapid in presence of magnesium oxide. The data on the action of zinc oxide are contradictory in character. Thus, vulcanizates with zinc oxide have higher modulus and greater residual elongations than vulcanizates obtained without activators. Hence, according to the values of the modulus, zinc oxide activates the process, whereas according to the residual elongations vulcanization is retarded.

In presence of Altax (Fig. 9) both the modulus data and residual elongation data clearly indicate that zinc oxide retards the interaction of the vulcanizing agent with the rubber.

Mixes containing sulfenamide BT (Fig. 10) show similar behavior to mixtures with Captax (Fig. 8). Here zinc oxide gives higher modulus values on the one hand, and greater residual elongations on the other, than are found in mixes without activators.

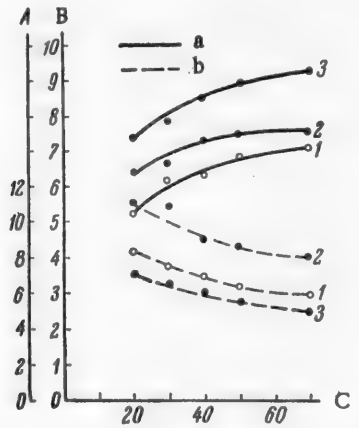

Fig. 10. Vulcanization of rodless SKB (0.22% alkali) in presence of sulfenamide BT. A) Residual elongation (%), B) modulus at 200% elongation (kg/cm^2), C) vulcanization time (minutes). a) Modulus, b) residual elongation. Contents of activators (in parts by weight): 1) without activator, 2) zinc oxide 5.0, 3) magnesium oxide 3.0.

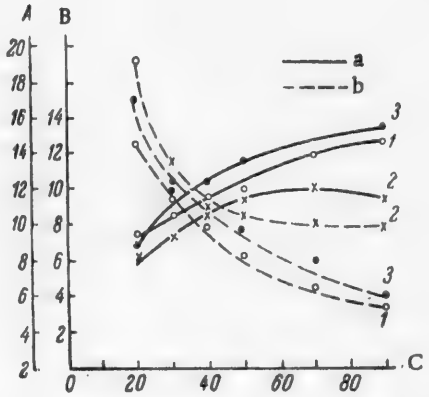

Fig. 11. Vulcanization of rodless SKB (0.6% alkali) in presence of Captax. A) Residual elongation (%), B) modulus at 400% elongation (kg/cm^2), C) vulcanization time (minutes). a) Modulus, b) residual elongation. Contents of activators (in parts by weight): 1) without activator, 2) zinc oxide 5.0, 3) magnesium oxide 3.0.

With higher alkali contents in the rodless rubber (0.6% in this instance) the retarding effect of zinc oxide on the vulcanization kinetics is fairly prominent. The data in Fig. 11 indicate that both characteristics – lower modulus and higher residual elongation – definitely show that zinc oxide has this effect. This is confirmed by data on the kinetics of sulfur addition (Fig. 12).

In connection with these results it was of interest to determine what effect on the action of zinc oxide in mixes based on rodless rubber with a relatively low alkali content further addition of alkali would have. The alkali contents of the mix were increased by additions of 1.0, 3.0, and 5.0 parts by weight of sodium carbonate. It follows from Fig. 13 that while in a rodless rubber mix of low alkali content (0.22%), zinc oxide gives higher

modulus values than those for a mix without metal oxides, after addition of sodium carbonate the vulcanizates with zinc oxides have lower moduli.. Thus, the effect produced by addition of sodium carbonate to mixes of low alkali content is analogous to the effect found in mixes based on sodium butadiene rubber with a high alkali content. The retarding effect of zinc oxide on the vulcanization kinetics is increased with increasing alkali content.

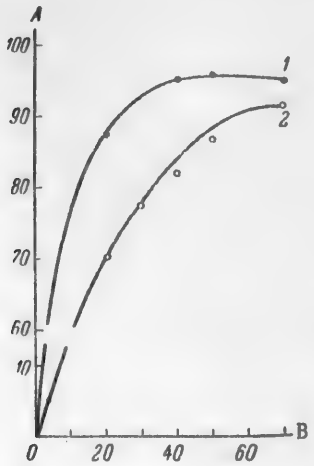

Fig. 12. Kinetics of sulfur addition in the vulcanization of rodless SKB (0.6% alkali) in presence of Captax. A) Amount of sulfur reacted (%), B) vulcanization time (minutes). Contents of activator (in parts by weight): 1) without activator, 2) zinc oxide 5.0.

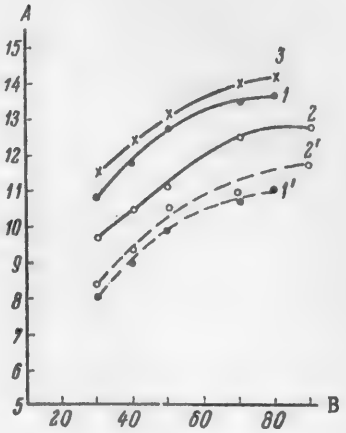

Fig. 13. Effect of sodium carbonate on vulcanization of mixes based on rodless SKB (0.22% alkali). Captax accelerator. A) Modulus at 400% elongation (kg/cm^2), B) vulcanization time (minutes). Contents of activators (in parts by weight): 1') without activator; 1) sodium carbonate 3.0, 2') zinc oxide 5.0, 2) zinc oxide 5.0, sodium carbonate 3.0, 3) magnesium oxide 5.0, sodium carbonate 3.0.

This behavior of zinc oxide may be explained as follows. In presence of considerable amounts of alkali, vulcanization is so rapid that addition of zinc oxide has no practical influence on the vulcanization kinetics. Moreover, at vulcanization temperatures, reactions of zinc salts with vulcanization accelerators and sulfur lead to formation of zinc sulfide and therefore some of the sulfur is lost. This loss results in a decrease of the number of direct interactions between sulfur and rubber, as compared with the situation in absence of zinc oxide. This ultimately leads to retardation of the vulcanization.

As a consequence of the foregoing, further investigations of the influence of metallic oxides on the kinetics of formation of organically bound sulfur compounds, and on the processes of structure formation occurring during vulcanization, are desirable.

The results described in this paper account for the contradictory information available in the literature on the activating action of zinc oxide on sodium butadiene rubber, since in different investigations polymers of different alkalinity were used.

SUMMARY

1. Differences have been found in the action of metallic oxides as vulcanization activators for sodium butadiene rubbers polymerized by the rod and rodless methods.

2. It was found that unloaded mixes based on rodless sodium butadiene rubber, containing accelerators of the thiazole and sulfenamide types, do not require the addition of metallic oxides as vulcanization activators.

3. It was shown that addition of zinc oxide to mixes based on rodless rubber with high alkali contents retards the vulcanization process.

We express our gratitude to P. F. Badenkov for initiating this investigation.

LITERATURE CITED

[1] E. Petrov, J. Rubber Ind. 12, 665 (1935); Caoutchouc and Rubber 2, 51 (1937).

[2] G. Bruni and E. Romani, India-Rubber J. 62, 89 (1921).

[3] C. Bedford et al., Ind. Eng. Chem. 12 (1920); 13 (1921); 14 (1922).

[4] B. Barton, Ind. Eng. Chem. 42, 4, 671 (1950).

[5] B. Dogadkin, M. Feldshtein, and D. Pevzner, J. Appl. Chem. 28, 5 (1955).*

[6] A. Ermolaev and G. Buiko, J. Rubber Ind. 9, 3, 216 (1933).

[7] B. Karmin, J. Rubber Ind. 8-9, 898 (1936); 11, 1144 (1936); K. Kaluzhenina, Dissertation, Lomonosov Inst. Chemical Technology, (Moscow, 1945).

[8] B. Dogadkin, M. Feldshtein, A. Dobromyslova, V. Shkurina, and M. Kaplunov, Proc. Acad. Sci. USSR 92, 1 (1953).

Received July 6, 1955.

* Original Russian pagination. See C. B. Translation.

INVESTIGATION OF THE DEHYDROGENATION OF ETHYLTOLUENE TO VINYLTOLUENE

A. V. Bondarenko, M. I. Bogdanov, and M. I. Farberov*

The Yaroslav Technological Institute

It has been reported in the literature that copolymerization of vinyltoluene with divinyl yields a rubber similar in quality to divinyl – styrene rubber.

It has also been reported that vinyltoluene has certain advantages over styrene for the production of alkyd resins and unsaturated polyesters [1, 2].

In our opinion, the only synthesis of vinyltoluene which can be of industrial significance is synthesis carried out by the following two stages:

a) alkylation of toluene with ethylene in presence of aluminum chloride**

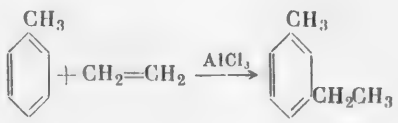

and

b) catalytic dehydrogenation of the ethyltoluene to vinyltoluene

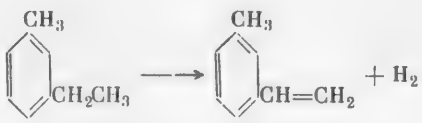

This paper gives the results of a study of the dehydrogenation of ethyltoluene to vinyltoluene, carried out in order to determine the conditions for effecting this reaction on the technical scale.

The literature contains a number of papers on dehydrogenation of ethylbenzene [3-7], isopropylbenzene [8, 9], and cymene [10, 11]. No information is available on dehydrogenation of ethyltoluene to vinyltoluene.

---

* A. Yu. Bruk took part in the experimental work.

** Our study of the alkylation of toluene with ethylene (in presence of $AlCl_3$) showed that mostly the meta isomer of ethyltoluene ($\sim 70\%$) is formed, with smaller amounts ($\sim 30\%$) of the para isomer.

Thermodynamic calculations of the reaction. We calculated the equilibrium constants for the reaction of dehydrogenation of ethyltoluene to vinyltoluene at various temperatures and with various proportions of inert diluents. The usual reaction isotherm equation was used for calculations of the equilibrium constants.

The free energies of formation of the reactants were taken from recent data [12].

The logarithms of the equilibrium constants for the dehydrogenation of ethyltoluene to vinyltoluene are plotted against the reciprocal absolute temperature in Fig. 1.

The equilibrium compositions were calculated with the aid of the reaction equilibrium equation [13] in the following form:

$$\frac{n_R^r \cdot n_S^s}{n_B^b \cdot n_C^c} = \frac{K_a}{K_\gamma}\left[\frac{n_B + n_C + \ldots + n_R + n_S + \ldots n_{in}}{P}\right]^{\Delta n} \qquad (a)$$

where K_a is the equilibrium constant in terms of activities; K_γ is a factor which represents the deviation of real gases from ideality, in this case equal to unity (as the process is carried out at atmospheric pressure); hence, here we have $K_a = K_p$; n_B, n_C, n_R, n_S, n_{in} are the numbers of moles of the starting substances (B, C), reaction products (R, S), and inert gas (in) at equilibrium; Δn is the difference of stoichiometric coefficients between the gaseous reaction products and the starting substances; P is the pressure, 1 atmosphere in this instance.

For a definite composition of the initial mixture, if the conversion of ethyltoluene into vinyltoluene is represented by α, the equilibrium composition can be expressed in the following form:

Components of reaction system	Molar composition	
	of initial mixture	at equilibrium
Ethyltoluene	1	$1-\alpha$
Vinyltoluene	–	α
Hydrogen	–	α
Inert diluent	w	w
Total	$1+w$	$1+\alpha+w$

Substitution of the molar contents of each reactant at equilibrium into Equation (a) gives:

$$\frac{\alpha^2}{1-\alpha} = K_p(1+\alpha+w) \qquad (b)$$

Solving Equation (b) for α, we have:

$$\alpha = -\frac{wK_p \pm \sqrt{(wK_p)^2 + 4K_p(w+1)(K_p+1)}}{2(K_p+1)}. \qquad (c)$$

This equation was used for calculation of the equilibrium composition of the reaction mixture in dehydrogenation of ethyltoluene to vinyltoluene at 427-727° under atmospheric pressure, both without diluent and with dilution of the ethyltoluene with an inert diluent in molar ratios of 1:8–1:16 (Fig. 2).

EXPERIMENTAL

Apparatus and method. The reaction vessel was a quartz tube 22 mm in bore and 1 m long, placed in a vertical tubular electric furnace. 40 ml of the catalyst was placed in the uniform-temperature zone of the furnace.

A thermocouple for temperature measurement was placed in the center of the catalyst tube in the middle of the layer of catalyst. The temperature during the reaction varied within ± 2°. Ethyltoluene and water were fed into the contact furnace from burets through liquid flow meters. The gas from the furnace passed through a condenser, the condensate being collected in a flask, and entered a graduated gas holder through a control flask. Before the start and after the end of each experiment 2-3 ml of water was fed through the system for 10 minutes, to displace air and the reaction gas respectively.

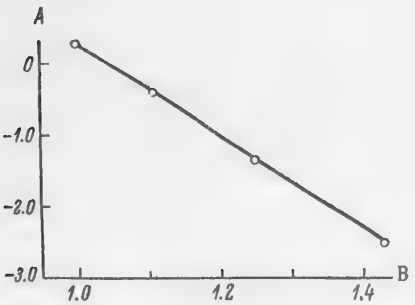

Fig. 1. Logarithm of the equilibrium constant as a function of the reciprocal absolute temperature. A) Logarithm of the equilibrium constant (log K_p), B) reciprocal of the absolute temperature $1/T \cdot 10^3$ (in °K).

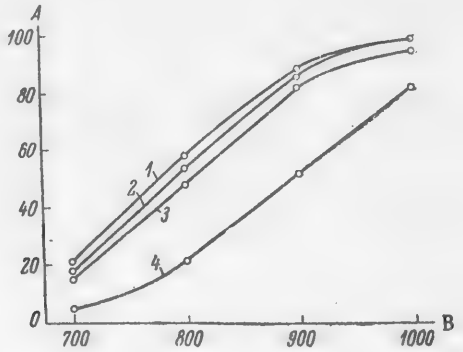

Fig. 2. Effect of inert diluent on conversion of ethyltoluene into vinyltoluene, as a function of temperature, by thermodynamic calculation. A) Conversion of ethyltoluene (%), B) temperature (in °K). Molar dilution with inert diluent: 1) 1:16, 2) 1:12, 3) 1:8, 4) no dilution.

Ethyltoluene, thoroughly purified by distillation, with b. p. 159-162° and n_D^{20} = 1.4970 was used for the experiments. The standard catalyst based on zinc oxide, as used for dehydrogenation of butylene, was used. After each experiment the activity of the catalyst was checked by determination of the refractive index of the catalyzate obtained under standard conditions. If the refractive index deviated from the accepted constant value, the catalyst was regenerated with steam – air mixture.

The volume feed rate was expressed in ml of ethyltoluene passed per liter of catalyst per hour (ml/liter • • hour). Ethyltoluene was diluted with steam in molar ratios 1:8, 1:12, and 1:16, corresponding to volume ratios 1:1, 1:1.5, and 1:2 in the liquid state. The yield of catalyzate was found from the ratio of the weight of catalyzate after separation from water (furnace oil) to the weight of ethyltoluene passed. The percentage conversion of ethyltoluene was calculated from the weight ratio of the ethyltoluene decomposed to ethyltoluene passed.

Analysis of the catalyzate. The vinyltoluene in the catalyzate was found from the contents of unsaturated hydrocarbons determined by the bromine number method. Concordant results were also obtained by refractometric determinations of vinyltoluene (in wt. %) based on additivity of the refractive indices in ethyltoluene – vinyltoluene mixtures (n_D^{20} for ethyltoluene, 1.4970, and for vinyltoluene, 1.5403). The difference between the total weight of catalyzate and the unsaturated hydrocarbons was taken to be unreacted ethyltoluene.

This simplified analytical procedure was adopted in studies of the effects of individual factors on the dehydrogenation of ethyltoluene to vinyltoluene. In more accurate experiments (for determination of material balance), the catalyzate (after addition of hydroquinone) was fractionated through a laboratory column (33 theoretical plates). The 110-115° fraction was assumed to be toluene; in the 130-150° fraction the unsaturated hydrocarbons were taken to be styrene, and the saturated hydrocarbons were counted as xylene – ethylbenzene mixture. The small amount of side products in this fraction (consisting of toluene, xylene, ethylbenzene, and

styrene, all totalling < 9% of the weight of the catalyzate) does not significantly influence the results obtained by the simplified method of analysis.

The gas after catalysis was analyzed in the Orsat apparatus for carbon dioxide, unsaturated hydrocarbons (by absorption in mercuric sulfate solution in 20% sulfuric acid), and oxygen. In some experiments the hydrogen in saturated hydrocarbons was determined by fractional combustion over copper oxide.

TABLE 1

Effects of Temperature, Volume Feed Rate, and Degree of Dilution on Dehydrogenation of Ethyltoluene

Temperature, (°C)	Volume feed rate of ethyltoluene in ml/liter·hr	Molar dilution of ethyltoluene with steam	Content of vinyltoluene in catalyzate (wt. %)	Yield of vinyltoluene (molar %)		Catalyzate yield as % ethyltoluene passed	Conversion of ethyltoluene (%)
				on ethyltoluene passed	on ethyltoluene decomp.		
540	400	1 : 12	29.4	27.2	85.8	95.5	31.7
560	400	1 : 12	38.0	34.9	82.5	93.0	42.2
580	400	1 : 12	43.3	38.6	80.3	90.5	48.5
600	400	1 : 12	47.5	35.3	58.0	74.6	60.6
560	200	1 : 12	40.0	33.1	71.5	87.0	46.5
560	400	1 : 12	38.0	34.9	82.5	93.0	42.2
560	600	1 : 12	34.5	31.5	85.0	94.5	37.0
560	800	1 : 12	30.0	29.5	87.5	95.0	33.7
560	400	1 : 8	—	31.8	82.7	—	38.3
560	400	1 : 12	—	34.9	82.5	—	42.2
560	400	1 : 16	—	35.3	89.6	—	39.4

Influence of individual factors on dehydrogenation of ethyltoluene to vinyltoluene. The experimental results are summarized in Table 1 (each result given is the average for 2-3 experiments). In all cases steam was used as the inert diluent, as it has a number of important technical advantages: a) the dehydrogenation products (catalyzate) are easy to separate from the aqueous condensate; b) the process can be carried out in an adiabatic reactor, which makes it much simpler to bring about on the technological scale; c) interaction of steam with the carbon deposits on the catalyst results in "autoregeneration" of the catalyst, with a considerable increase of contact time before regeneration is required.

TABLE 2

Material Balance Experiment on the Dehydrogenation of Ethyltoluene to Vinyltoluene. (Temperature 560°; volume feed rate 400 ml/liter·hour; molar dilution with steam 1:12; 57 g of ethyltoluene passed, duration of experiment 4 hours).

Reaction products	Yield (molar %) on ethyltoluene	
	passed	decomposed
Vinyltoluene	33.3	73.2
Styrene	1.7	3.7
Toluene	2.3	5.1
Ethylbenzene Xylene	4.2	9.3
"Returned" ethyltoluene	54.5	–
Carbon on catalyst*	3.15	6.8
Losses	0.85	1.9
Total	100.0	100.0

* "Carbon" on the catalyst was determined from the total amount of carbon dioxide in the catalysis gas and regeneration gas.

The influence of temperature on dehydrogenation of ethyltoluene was studied over the 540-600° range, at a constant feed rate of 400 ml/liter·hour, at 1:12 (molar) dilution with steam.

The influence of volume feed rate was studied at constant temperature (560°) with steam dilution in 1:12 ratio (molar), for feed rates between 200 and 800 ml/liter·hour.

The influence of dilution with steam was determined at a constant feed rate of 400 ml/liter·hour, 560°, for dilutions in the range 1:8 - 1:16 (molar).

The results show that as the temperature is raised above 580° and the volume feed rate is decreased below 400 ml/liter·hour, the yields of catalyzate and of vinyltoluene calculated on the decomposed ethyltoluene decrease considerably; this must be attributed to partial decomposition of the vinyltoluene formed.

As a result of this investigation, the optimum conditions for dehydrogenation of ethyltoluene to vinyltoluene were determined: temperature 560-580°, volume feed rate 400-800 ml/liter·hour, dilution with steam in 1:12 - 1:16 ratio (molar).

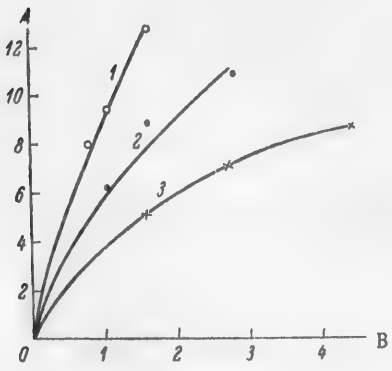

Fig. 3. Conversion of ethyltoluene as a function of contact time at different temperatures. A) Conversion of ethyltoluene (%), B) contact time (seconds). Temperature (in °C): 1) 500, 2) 480, 3) 460.

The data in Table 1 also show that our yields of vinyltoluene were far from the equilibrium values, (Fig. 2) owing to the relatively low activity of the catalyst. Dehydrogenation at lower volume feed rates and higher temperatures is not feasible, as the vinyltoluene yields decrease owing to the instability of vinyltoluene under such conditions.

Material balance experiment. Results of a typical balance experiment carried out under the optimum process conditions are given in Table 2.

For determination of the apparent activation energy, experiments were carried out at low temperatures in order to exclude the possibility of side reactions. The effect of contact time on the conversion of ethyltoluene at 460-500° is shown in Fig. 3. The contact time was calculated from the equation:

$$\tau = \frac{v_c \cdot 273}{v_g \cdot T},$$

where v_c is the bulk volume of the catalyst in ml, T is the absolute temperature of the reaction, v_g is the volume of vapors (ethyltoluene + water) entering the reaction zone in ml/second.

The curves in Fig. 3 were used to calculate, for constant conversion of ethyltoluene (6%), the apparent activation energy with the aid of the Arrhenius equation, by substitution of the inverse ratio of the contact times for the ratio of the rate constants (for equal degrees of conversion, $K_2/K_1 = \tau_1/\tau_2$):

$$E = \frac{4.575 \log \frac{\tau_1}{\tau_2} \cdot T_1 \cdot T_2}{T_2 - T_1}.$$

The average value of the apparent energy of activation was 32,700 cal/mole.

Investigation of the thermal stability of ethyltoluene in mixtures with vinyltoluene under the reaction conditions (temperature 560°, volume feed rate 400 ml/liter·hour, steam dilution ratio 1:12 molar) showed that these substances are fairly stable in absence of catalyst. For example, in pyrolysis of a mixture containing 40.5% of vinyltoluene the decomposition of the hydrocarbons (determined by the amounts of carbon dioxide in the gas) was 2%. When the same mixture was passed over the catalyst in the same conditions, the degree of

decomposition increased to 8.4%. When the vinyltoluene concentration in the mixture was increased to 78%, the decomposition of the hydrocarbons reached 25%. It follows that the catalyst accelerates decomposition of the vinyltoluene formed, probably by way of polymerization of the latter.

Identification of the reaction products. Because of the similar boiling points of ethyltoluene and vinyltoluene, laboratory distillation through a precision column with an efficiency of 60 theoretical plates (at 22 mm) only yielded a distillate containing 95% of vinyltoluene, with the following constants b. p. 74°/22 mm, d_4^{20} 0.899, n_D^{20} 1.5403. Vinyltoluene readily polymerizes on standing. Literature data are available only for 2-vinyltoluene and 4-vinyltoluene [14] (2-vinyltoluene: b. p. 169°/752 mm, 55-54°/12 mm, $d_4^{14.1}$ 0.9155, $n_D^{14.1}$ 1.5490; 4-vinyltoluene: b. p. 170-175°/760 mm, 77-79°/33 mm, 59-60°/12 mm, $d_4^{16.4}$ 0.9003, $n_D^{16.4}$ 1.5446).

On the basis of the composition of the ethyltoluene used (70% of the meta isomer and 30% of the para isomer), we assume that the isomer contents of the vinyltoluene correspond to this; this is in agreement with literature data [2].

From the 110-115° fraction of the catalyzate, additional fractionation yielded toluene boiling at 110.0-111° at 760 mm, n_D^{20} 1.4955. The 130-150° fraction (mixture of ethylbenzene, xylene, and styrene) was additionally fractionated, the 133-139° fraction being collected. Oxidation of this fraction with potassium permanganate gave benzoic acid (m. p. 122°) and phthalic acids (insoluble in chloroform) in approximately equal amounts, confirming the presence of ethylbenzene and xylene in the catalyzate.

SUMMARY

1. The equilibrium constants and equilibrium compositions for the dehydrogenation of ethyltoluene to vinyltoluene have been calculated on the basis of thermodynamic data, for the 427-727° range, both for the undiluted reactants and at 1:8 - 1:16 dilutions with an inert diluent.

2. The optimum conditions for the process have been determined by studies of the catalytic dehydrogenation of ethyltoluene to vinyltoluene at 540-600°, volume feed rates of 200-800 ml/liter·hour, with dilution with steam in 1:8 - 1:16 ratio (molar).

LITERATURE CITED

[1] F. I. Buege, Ind. Eng. Chem. 46, 1695 (1954).

[2] Chem. Week, November 19, 37 (1955).

[3] Yu. S. Zalkind and A. G. Bulavsky, Plastics 3, 9 (1935).

[4] A. A. Balandin, N. D. Zelinsky, G. M. Marukyan, and O. K. Bogdanova, J. Appl. Chem. 14, 161 (1941).

[5] A. A. Balandin and G. M. Marukyan, J. Appl. Chem. 19, 623 (1946).

[6] R. R. Wenner and E. C. Dubdal, Chem. Eng. Progress. 44, 275 (1948).

[7] N. I. Shuikin and I. I. Levitsky, Bull. Acad. Sci. USSR 4, 592 (1952);* 3, 403 (1953).*

[8] A. A. Balandin and G. M. Marukyan, Proc. Acad. Sci. USSR 48, 509 (1945).

[9] I. E. Nickels, G. A. Webb, W. Heintzelman, and B. B. Corson, Ind. Eng. Chem. 41, 563 (1949).

[10] A. A. Balandin, G. M. Marukyan, and R. S. Seimovich, Proc. Acad. Sci. USSR 41, 71 (1943).

[11] K. A. Kobe, and R. T. Romans, Ind. Eng. Chem. 43, 1755 (1951).

* Original Russian pagination. See C. B. Translation.

[12] Physicochemical Properties of Individual Hydrocarbons III (State Fuel Tech. Press, 1951).*

[13] M. Kh. Karapetyants, Chemical Thermodynamics (Goskhimizdat, 1953).*

[14] I. Heilbron and H. Bunbury, Dictionary of Organic Compounds II (1949). **

Received October 22, 1956.

---

* In Russian.

** Russian translation.

BRIEF COMMUNICATIONS

ALUMINUM MONOBROMIDE

S. A. Semenkevich

During the past decade many papers have been published on the thermodynamic properties of aluminum monofluoride and monochloride [1].

The enthalpies and isobaric potentials, both for formation from the elements and for addition of the metal to the corresponding salt of normal valence, were determined for these substances.

Until now, aluminum monobromide and monoiodide had not been studied experimentally.

This gap was filled to some extent by the calculated data in the book by Antipin et al. [2], calculated by means of the Haber–Born cycle for crystalline monohalides of aluminum.

A later paper by Irmann [3] gives calculated values for the enthalpies of monohalides in the crystalline and vapor states. It is pointed out in the paper, however, that the data for the vapor state are tentative.

In view of the great importance of aluminum monohalides in applied and theoretical chemistry, a study of aluminum monobromide was carried out and the results are presented here.

The vapor pressure of aluminum monobromide was measured by the method developed by Gross [4].

In principle, this method is a modification of the "dynamic" method for vapor pressure determination.

The substance is placed in a hermetically closed vessel with a small capillary orifice for escaping vapor.

The components are so chosen that two independent (univariant) equilibria are established, the equilibrium constant for one being known with certainty.

For investigation of the equilibrium partial pressure of monobromide vapor we used the reactions

$$NaBr_{(l)} + Al_{(l)} \rightleftarrows Na_{(v)} + AlBr_{(v)} \quad (I)$$

$$NaBr_{(l)} \rightleftarrows NaBr_{(v)} . \quad (II)$$

The vapor pressure of sodium bromide has been accurately determined [5].

When a mixture of aluminum powder is heated with sodium bromide, sodium and aluminum monobromide vapors escape through the capillary orifice in the vessel, according to Reaction (I), together with sodium bromide vapor formed by evaporation as shown by (II).

The Na and AlBr vapors interact in the condenser at a lower temperature, so that Reaction (I) proceeds to the left with formation of the original substances.

As a result, the final products in the condenser are sodium bromide and metallic aluminum only; some of the sodium bromide reaches the condenser by evaporation.

After the amounts of aluminum and of sodium bromide distilled over into the condenser have been determined by analysis, it is possible to calculate the molecular ratio of aluminum to sodium bromide carried over by direct evaporation. The product of this ratio and the vapor pressure of sodium bromide gives the partial pressure of aluminum monobromide vapor.

Correct data for the equilibrium Reaction (I) can only be obtained if the reaction

$$Al + 3NaBr \rightleftarrows AlBr_3 + 3Na \qquad (III)$$

does not occur to any appreciable extent, and if aluminum does not evaporate.

It was found experimentally that practically pure sodium bromide is deposited in the condenser, with mere traces of aluminum bromide (0.06%).

Direct evaporation of aluminum cannot influence the results, as its vapor pressure under the experimental conditions is only 10^{-7} atm.

An advantage of this method is the absence of any strongly hygroscopic substances in the main chemical reaction.

The use of reactions of the type $2Al + AlBr_3 \rightleftharpoons 3AlBr$, used previously for studies of aluminum monohalides, is inappropriate in the present instance owing to the extremely hygroscopic nature of aluminum bromide, which introduces complications into the experimental procedure and gives rise to errors.

EXPERIMENTAL

The apparatus used for the equilibrium studies is shown in the figure.

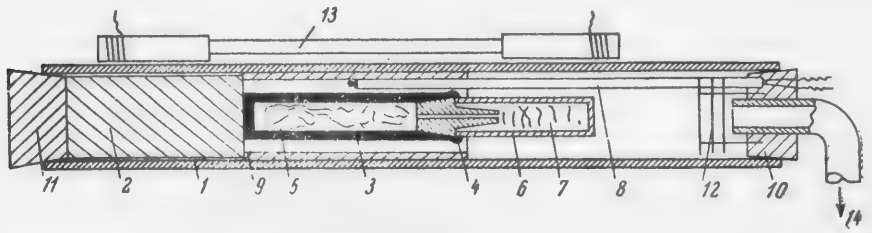

Apparatus for equilibrium studies.
Explanation in text.

The apparatus consists of an external tube 1, made from sintered alumina, which holds vacuum satisfactorily at high temperatures. A corundum beaker 3 with a ground stopper 4 of the same material was placed in the tube on the support 2. The substance under investigation 5 was placed in the beaker. Stoppers with 2.5 and 2.0 mm capillaries were tested. A corundum tube 6, which acted as the condenser, was firmly attached to the stopper. The condenser tube was packed with copper foil 7 for trapping the aluminum formed in the reaction between sodium and aluminum monobromide vapors.

The reaction temperature was measured by means of a platinum–platinum–rhodium thermocouple 8. A nickel tube 9 was inserted to equalize the temperature.

The outer tube was plugged with rubber bungs 10 and 11. To protect the bung from radiation, a shield 12 was inserted.

Very pure aluminum of AV2 grade (GOST 3549-47), containing 99.85% of aluminum (with iron and silicon as the principal impurities) was used.

Sodium bromide of analytical purity (GOST 4169-48) was recrystallized twice and used in this form for the experiments.

To prevent fusion of the metallic aluminum into beads, coarsely ground corundum powder was added to the mixture. The amount of powder added was 50% of the weight of the charge. The grain size of the powder was 0.5-0.7 mm. The weight of the charge (without corundum) was 7-10 g.

The experiments were performed as follows. The charged tube was heated by means of the heater 13 (to 300-400°) and evacuated with the aid of the vacuum pump 14 to remove absorbed gases. The evacuation was continued for 2-3 hours.

The temperature was then raised rapidly to the predetermined value of 1175° K, and the thermoregulator was connected.

After 4-5 hours at the experimental temperature, the corundum tube was pushed out of the hot zone and cooled by a blast of air from a fan. The cooling was performed under reduced pressure in the tube.

After the cooling, the cylinder containing the charge was taken out. The condenser tube was removed together with the foil and immersed in warm water to dissolve sodium bromide.

The sodium bromide in the solution was determined by analysis.

The washed foil was dissolved in nitric acid and the solution, after dilution, was electrolyzed to extract copper. The aluminum remaining in solution was precipitated with ammonia, filtered off, dried, heated, and weighed as alumina.

The experimental results are given in the table.

Results of Equilibrium Studies. Average Molar Ratio $Al/NaBr \cdot 10^2 = 1.375$.

Duration of expt. (hours)	Amt. of Al in condensate, in mg, by analysis	Total NaBr in condensate (g)	Amt. of NaBr (in g) obtained by		Weight ratio $Al/NaBr^* \cdot 10^2$
			Reaction (I)	evaporation	
4	16.0	5.234	0.633	4.601	3.482
4	17.1	5.659	0.677	4.982	3.434
4	17.0	5.693	0.673	5.020	3.391
3.5	15.6	5.059	0.618	4.441	3.512
5	19.8	6.514	0.784	5.730	3.450
5	21.8	7.004	0.862	6.142	3.551
				Mean	3.470

* Moles of sodium bromide entering the condenser by evaporation.

The vapor pressure of sodium bromide at 1175° K is $6.12 \cdot 10^{-3}$ atm. (The vapor pressure of sodium bromide was found by means of the interpolation equation $\log P = -\frac{40100}{4.57T} + 8.14$, based on Ruff's data [5].

$P_{AlBr} = 1.375 \cdot 10^{-2} \cdot 6.12 \cdot 10^{-3} = 0.8415 \cdot 10^{-4}$ atm. For Reaction (I) $P_{(Na)} = P_{(AlBr)}$ and therefore $K_p = P^2_{(AlBr)} = 0.708 \cdot 10^{-8}$ and $\log K_p = -8.15$.

The isobaric-isothermal potential for Reaction (I) was found to be 43.76 kcal. from the expression

$$\Delta\Phi^\circ = -RT \ln K_p.$$

The enthalpy change in Reaction (I) at 1175° was found from the equation

$$\Delta H = \Delta\Phi + \Delta ST.$$

The entropy changes of the substances involved in Reaction (I) were calculated from data given by Britske and Kapustinsky [6], and Brewer et al. [7].

Data on the entropy change of aluminum monobromide are not available in the above sources, and the entropy change was calculated from its average specific heat.

The specific heat of aluminum monobromide was calculated by the methods of quantum mechanics, with the use of Miescher's [8] value of 378 cm^{-1} for the wave number.

The average specific heat of aluminum monobromide in the 298-1175° range was found to be 8.80 cal/g, and the entropy change for the same range, 12.0 cal/g.

The entropy change for Reaction (I) was found to be 49.64 cal/g. The calculation of enthalpy for Reaction (I) is given below.

$$\Delta H_{(I)} = 43.76 - 49.64 \cdot 1175/1000 = 102.0 \text{ kcal.}$$

From the equation for Reaction (I), the enthalpy for the reaction

$$Al_{(l)} + {}^1/_2Br_{2(g)} \rightleftarrows AlBr_{(g)}$$

was calculated; this was the object of the present investigation.

The enthalpy change for the formation of aluminum monobromide was calculated from the equation

$$\Delta H_{(AlBr)} = \Delta H\ (I) + \Delta H_{(NaBr)}.$$

The enthalpy of formation of sodium bromide at 1175° K is − 106.1 kcal. [7]. Therefore at

$$1175^\circ K\ \Delta H_{(AlBr)} = -4.1 \text{ kcal.}$$

The enthalpy of formation of the monobromide from the elements at 298° K was calculated from the equation

$$\Delta H_{(298)} = \Delta H_{(s)} - (H_{\text{products}} - H_{\text{reactants}}).$$

The enthalpy of formation of the monobromide by the reaction

$$Al_{(s)} + {}^1/_2Br_2\ (g) \rightleftarrows AlBr\ (g)$$

at 298.1° K is 1.1 kcal.

This value for $\Delta H_{(AlBr)}$ is very close to the value published in "Selected Values" [9]. However, it differs considerably from the values found by Antipin et al. and by Irrmann [3].

This is illustrated by the following data:

	Our data	Selected values [9]	Antipin et al. [2]	Irrmann [3]
$\Delta H_{(AlBr)}$ at 298.1° K (in kcal.)	1.1	1.8	21	12

The discrepancy between our value and the calculated values is probably the consequence of the considerable proportion of nonionic bonds in the molecule of aluminum monobromide. This is in agreement with the great deformability of the electron shell of the bromine atom. We do not know to what degree of accuracy the enthalpy value given in "Selected Values" was calculated. It is therefore impossible to estimate how significant is its similarity to our value.

SUMMARY

The partial pressure of aluminum monobromide vapor in the reaction $Al_{(l)} + NaBr_{(l)} \rightleftharpoons Na_{(g)} + AlBr_{(g)}$.

The value found for the vapor pressure of aluminum monobromide, known thermodynamic data, and the specific heat of AlBr calculated from spectroscopic data, were used to calculate its enthalpy of formation in the reaction $Al_s + \frac{1}{2} Br_2\,(g) \rightleftharpoons AlBr_{(g)}$.

At 298.1° K $\Delta H_{(AlBr)}$ was found to be 1.1 kcal.

I offer my deep gratitude to Corresponding Member, AN SSSR, P. F. Antipin for scrutiny of the manuscript and valuable comments.

LITERATURE CITED

[1] J. P. McGreer, Progr. Chem. 4, 499 (1953).

[2] P. F. Antipin et al., Electrochemistry of Fused Salts 1 (1937).

[3] Irrmann, Helv. Chimica Acta, 23, 188, 1449 (1950).

[4] P. Gross, J. Research 3, 28 (1949).

[5] O. Ruff and S. Mugdan, Z. anorg. u. allg. Chem. 117, 3, 147 (1921).

[6] E. V. Britske and A. F. Kapustinsky, Thermal Constants of Inorganic Substances (1949). *

[7] L. Brewer, A. Bromley, et al., Chemistry and Metallurgy of Miscellaneous Materials IV, 19B, 76-192 (1950).

[8] I. Miescher, Helv. phys. Acta 56, 305 (1950).

[9] Selected Values of the Chemical Thermodynamic Properties, National Bureau of Standards, (Washington, 1947).

Received January 17, 1956.

* In Russian.

INVESTIGATION OF THE STRUCTURE OF POROUS CERAMICS

A. S. Berkman

In recent years porous ceramic materials have been increasingly widely used in many branches of chemical industry. They are used as filters for mechanical purification of various liquids and gases, for diaphragms in electrolytic processes and electroplating technology, for bubbling of liquids and gases, in plates for aeration and conveying of powders, for equipment used for high-temperature reactions in fluidized beds, etc.

When porous ceramics are used as filters for mechanical purification of fluids, separation of precipitates, and production of sterile filtrates, the maximum pore size of the material is of decisive importance. The pores should not be larger than the particles of the precipitates or, in bacteriological filters, the bacteria.

Therefore when filters were developed and tested only the maximum pore sizes were usually determined. For such determinations, air was forced through the specimens previously impregnated with the liquid, and the pore size was calculated from the equation

$$D = \frac{4\alpha}{gdh}, \tag{1}$$

where D is the pore diameter (in cm), α is the surface tension of the liquid (in dynes/cm), g is the acceleration due to gravity (in cm/sec^2), d is the density of the liquid (in g/cc), and h is the height of the liquid column (in cm). This equation was derived for liquids which wet the surface completely ($\cos\theta = 1$).

If the pore diameter is calculated in μ, and the air pressure is measured by means of a mercury manometer, Equation (1) becomes

$$D_\mu = \frac{4\alpha \cdot 10^4}{981 \cdot 13.6 \cdot h} \tag{2}$$

or, in simplified form

$$D_\mu = \frac{3\alpha}{h}. \tag{3}$$

The pressure is gradually increased during the experiment. The first appearance of air bubbles over the specimen covered with liquid indicates that the largest pores have been opened at the given pressure.

The cross section of a capillary in a porous body is always variable along its length. The above method gives the minimum cross sections of the capillaries or, more accurately, the diameter of the widest region among the narrowest regions of all the capillaries in the specimen.

The single maximum pore diameter in no way represents the structure of the material and, in particular, it does not determine its permeability (filtration rate), which depends on the numbers of pores of different sizes

in the material or, in other words, on the pore size distribution in the material. If the total amount of fluid or the permeability of the porous material are known, it is possible (for a given porosity) to evaluate the structure in terms of the effective pore size or of the number of such pores per unit area of the specimen.

These relationships are expressed by Equations (4) and (5):

$$\gamma = A\left(\frac{D}{124.47}\right)^2, \tag{4}$$

$$\gamma = 82.2\frac{A^2}{N}, \tag{5}$$

where γ is the air permeability coefficient, with the dimensions $\frac{m^3 \cdot cm}{m^2 \cdot hour \cdot mm\ H_2O\ column}$, A is the open porosity of the specimen (in %), D is the average effective pore diameter (in μ), N is the number of pores with the average effective diameter (per cm^2).

These equations were derived on the assumption (usually made in calculations of effective pore diameters) that the capillaries are all of circular section with uniform diameter. The second assumption is that the capillaries are parallel to each other and perpendicular to the surface of the specimen.

From Formulas (4) and (5) we obtain Formulas (6) and (7) for calculation of the average effective pore diameter and the number per 1 cm^2:

$$D_\mu = 124.47\left(\frac{\gamma}{A}\right)^{\frac{1}{2}}, \tag{6}$$

$$N = 82.2\frac{A^2}{\gamma}. \tag{7}$$

As already stated, the size of the largest pores does not determine the permeability of the material. Specimens with maximum pores of equal size may differ considerably in their permeability to air, just as the average effective pore sizes and their numbers per unit area may differ.

This can be illustrated by an example. Two specimens made from clay – grog bodies had maximum pores of the same diameter, 11 μ. The porosity of Specimen 1 was 20.3 %, and of Specimen 2, 28.7 %. The air permeability coefficients differed sharply, being 0.058 for Specimen 1 and 0.222 for Specimen 2. Both specimens were made from bodies containing 70% grog and 30% clay. Body 1 was based on Novo-Shveitsarsk clay, and Body 2, on Latnaya clay. They also differed in the grain composition of the grog used. The grog in Body 1 consisted of grains of three fractions; 16.7% was 0.175 mm grains, 66.6% was 0.135 mm grains, and 16.7% was 0.104 mm grains, while the grog in Body 2 was of uniform particle size, consisting entirely of grains of average size 0.135 mm.

As was to be expected from the air permeability coefficients, the average effective pore diameter for Specimen 2 was nearly double that of Specimen 1: the values were 10.94 μ and 6.65 μ respectively. The numbers of pores per cm^2 were $305 \cdot 10^3$ and $584 \cdot 10^3$, respectively. It seems remarkable at first sight that the average effective pore size in Specimen No. 2 reaches the value of the maximum pore size for the same specimen. This apparent inconsistency is explained if it is remembered that the maximum pore size was determined by forcing air through the specimen impregnated with liquid.

These results suggest that the specimens differ substantially in structure, namely: smaller pores predominate in Specimen No. 1, while in Specimen No. 2 most of the pores are larger.

This question can be clarified by investigations of the structure of the materials, by means of pore volume distribution curves.

The most convenient method for determination of the structure of porous ceramics is the mercury-pressure method widely used for studying structures of adsorbents and other finely divided and porous bodies [1].

As is known, only pores less than 15 μ in diameter can be determined by the mercury method with the existing porosimeters, as the dilatometer of the instrument is filled at atmospheric pressure and all the pores larger than this become filled with mercury before the start of the determination [1, 2, 3]. For this reason the existing methods do not provide a complete characterization of the structure of porous ceramic materials with larger pores, which play the decisive role in the permeability of such materials.

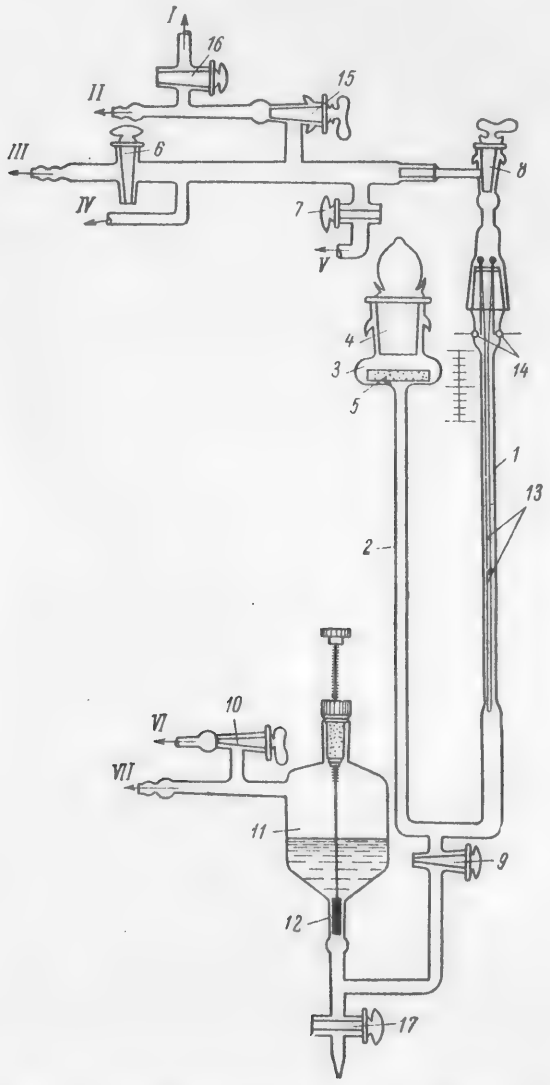

Fig. 1. Instrument for determination of pore size. Tubes: I) to air, II) to compressor, III) to vacuum pump, IV) to U-tube manometer, V) to NcLeod gage, VI) to air, VII) to vacuum pump. The remaining designations are explained in the text.

We developed and used the following method for determination of the volumes of large pores. The porosimeter is an instrument so designed that large pores can be determined, between 2-4 mm and 5-8 μ in

diameter. The main part of the instrument (Fig. 1) is a glass dilatometer operating on the communicating-vessel principle. One of the vessels is the capillary 1, and the other the tube 2, with a wide top 3, closed by means of the ground glass stopper 4.

The specimen 5, dried to constant weight, is placed in the wide top of the dilatometer, and air is then pumped out of the system with the cocks 6, 7, 8, and 9 open. When a residual pressure of 10^{-3} mm, as shown by a McLeod gage, is reached, the system is disconnected from the vacuum pump by means of the stopcock 8. The stopcock 10 is then gradually opened and mercury is admitted into the system from the glass vessel 11, provided with a metallic seal with a ground cone 12.

After the dilatometer has been filled with mercury, the cock 9 is closed and the pressure exerted on the specimen by the mercury is read off. This pressure is found from the difference of the mercury levels in the capillary and the wide part of the dilatometer and the height of the layer of mercury over the specimen.

The size of the pores filled with mercury at this pressure is calculated from Formula (8)

$$D_{\mu} = -\frac{3\alpha \cdot \cos\theta}{h}, \qquad (8)$$

where α is the surface tension of mercury (in dynes/cm), θ is the contact angle, and h is the pressure (in cm Hg).

As the dilatometer consists of communicating vessels, when it is being filled with mercury a low pressure (close to zero) of 3-5 mm Hg is exerted on the specimen; this corresponds to pores 2-4 mm in diameter.

When the minimum pressure has been determined, R_0 (initial resistance) of a platinum wire 13 in the dilatometer, connected to a direct-current bridge through the leads 14 sealed in the glass, is measured. With the vacuum pump running, air is then admitted through the cock 15 with cock 16 open, and in the part of the system which is isolated from the porosimeter proper by the stopcock 8 a predetermined pressure is set up, measured by means of a U-tube manometer. The cock 8 is then opened and the same pressure is established in the dilatometer.

The mercury level in the dilatometer capillary drops as the mercury enters the pores of the specimen. The wire in the dilatometer becomes partially exposed, and R_1 is measured. If the dilatometer constant is known, it is easy to calculate the volume of mercury which entered the pores at the given pressure.

The pressure in the porosimeter is consecutively increased up to atmospheric, with corresponding readings being taken of the increasing resistance of the wire.

This instrument can also be used for determinations at pressures above atmospheric (for pores smaller than 15 μ), up to 2-3 atmospheres, corresponding to pores 5-8 μ in diameter.

For such determinations the vacuum pump is disconnected when the atmospheric pressure is reached, and compressed air is fed into the system from a compressor. The amount of air entering the system is adjusted by means of the stopcock 16.

The procedure for feeding air into the system and taking the resistance readings is the same as before.

When the determinations have been completed the mercury is returned from the system into the evacuated vessel 11. Mercury is withdrawn from the system through the stopcock 17. The specimen is taken out and weighed.

As the initial weight of the specimen and the amount of mercury forced into it, as determined by means of the porosimeter, are known, it is easy to find by difference the volume of mercury contained in the pores of the specimen at the start of the determinations or, more precisely, when the first resistance reading was taken (pores larger than 2-4 mm in diameter).

The results can be used to plot distribution curves for pore volumes corresponding to different pore diameters, from the largest, 2-4 mm in diameter, down to 5-8 μ.

For porous ceramics, in which most of the pores are larger than the lower limit given above, the use of our instrument is sufficient in most cases.

If it is required to investigate smaller pores, this can be done by means of porosimeters of known design, intended for use at high pressures. The porosimeter designed and constructed in the Lensoviet Technological Institute, Leningrad [4], is used by us for this purpose.

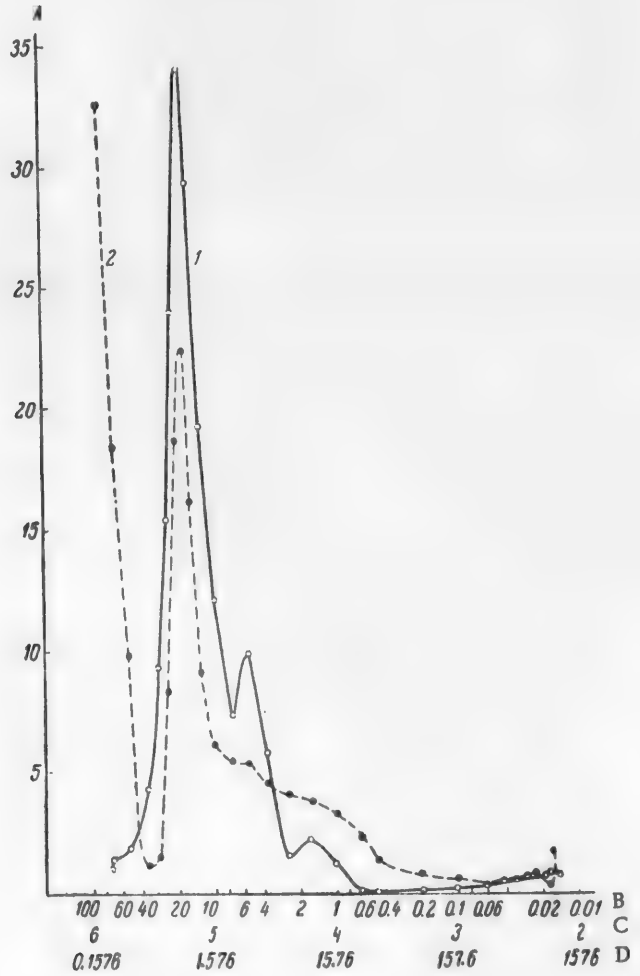

Fig. 2. Differential pore volume – log pore diameter distribution curves. A) $\frac{dV}{d \log D} \cdot 10^2$; B) D, μ; C) log D (D, Å); D) P (kg/cm^2). 1) Specimen 1; 2) Specimen 2.

With high-pressure porosimeters the first reading can be taken at a pressure of 1.2-1.3 atm., whereby pores not larger than 12-13 μ in diameter can be determined.

Figure 2 shows our combined differential curves, which represent the pore volume distributions in the two porous ceramic specimens Nos. 1 and 2 over a very wide range.

These curves clearly reveal the difference in structure between the two specimens, and it becomes clear why, with equal sizes of the so-called maximum pores, they differ considerably in their coefficients of air permeability.

SUMMARY

1. The maximum pore dimensions do not characterize the structure of porous bodies, and do not determine their properties, including permeability.

2. A porous material can be definitely assessed by calculation of the average effective pore size and the number of pores per unit area, for a given degree of porosity. However, these values are not sufficient for complete characterization of the structure and explanation of the consequent properties of porous ceramics.

3. A convenient method for characterization of the structure of porous ceramics is by means of pore volume distribution curves, determined by the mercury-pressure method.

4. For investigations of coarsely porous ceramic materials, a simple instrument and a method are described for determination of pore volume distributions by the mercury-pressure method at pressures below 1 atmosphere. Finer pores are then determined at high pressures with the aid of porosimeters of conventional design.

The distribution curves so obtained, covering a wide range of pore diameters from several millimeters down to tens of angstroms, provide a complete picture of the structure of porous ceramic materials.

LITERATURE CITED

[1] H. L. Ritter and L. C. Drake, Ind. Eng. Chem. Anal. Ed., 17, 12, 782 (1945).

[2] T. G. Plachenov, V. A. Aleksandrov, and G. M. Belotserkovsky, Coll. Methods for Studying the Structure of Highly Disperse and Porous Bodies (Izd. AN SSSR, 1953), p. 59. *

[3] N. M. Kamakin, Coll. Methods for Studying the Structure of Highly Disperse and Porous Bodies (Izd. AN SSSR, 1953), p. 47. *

[4] T. G. Plachenov, J. Appl. Chem. 28, 4, 245 (1955). **

Received April 29, 1956.

* In Russian.

** Original Russian pagination. See C. B. Translation.

METHOD FOR CALCULATION OF THE CRYSTALLIZATION REGION OF SODIUM CHLORIDE IN THE QUATERNARY SYSTEM $CaCl_2 - MgCl_2 - NaCl - H_2O$

V. Ya. Rudin and N. L. Yarym-Agaev

The N. S. Khrushchev Industrial Institute of the Donets

The quaternary system $CaCl_2-MgCl_2-NaCl-H_2O$ in the main conforms to the crystallization laws for brines in lakes of the calcium chloride type [1]. However, complete investigation of this system over a wide temperature range involves very laborious experiments, and such investigations have not been carried out fully hitherto. The main efforts in such studies should be directed toward determination of the crystallization region of sodium chloride, which is considerably greater than the crystallization regions of other salts in isothermal sections of the phase diagram.*

This paper presents a calculation method for determination of salt concentrations in the quaternary system in saturated sodium chloride solutions, based on data for the solubility of sodium chloride in the ternary systems $CaCl-NaCl-H_2O$ and $MgCl_2-NaCl-H_2O$, which have been studied in considerable detail.

The calculation method was based on the following considerations, confirmed by experimental data [2].

The solubility of sodium chloride, expressed in weight percentages, is, within the limits of experimental error, determined only by the total concentrations of calcium and magnesium chlorides and is independent of the relative proportions of these salts. Here the concentrations of the salts should be expressed in terms of moles per 100 g of solution.

Thus, we have

$$C_{CaCl_2} = C_{MgCl_2} = C_{\Sigma CaCl_2,\ MgCl_2} \qquad (1)$$

where C_{CaCl_2} is the number of moles of calcium chloride in 100 g of liquid phase in the system $CaCl_2-NaCl-H_2O$ corresponding to a definite solubility of sodium chloride (in wt. %); C_{MgCl_2} is the number of moles of magnesium chloride in 100 g of liquid phase in the system $MgCl_2-NaCl-H_2O$ for the same solubility of sodium chloride; $C_{\Sigma CaCl_2,\ MgCl_2}$ is the sum of the numbers of moles of calcium and magnesium chlorides in 100 g of liquid phase in the system $CaCl_2-MgCl_2-NaCl-H_2O$ for the same solubility of sodium chloride.

This is confirmed by experimental data obtained at 25°, contained in the table. Analogous results are obtained at other temperatures. The data in the 2nd and 3rd columns were obtained by graphical interpolation of tabular data for 25° [2]; the values in the 4th, 5th, and 6th columns were obtained by interpolation of the results of polythermal investigations to 25° [3], and graphical interpretation of the isotherms; $k:l$ is the ratio of calcium chloride to magnesium chloride by weight.

* For example, at 25° only sodium chloride crystallizes from solutions containing 35.6 wt. % of $CaCl_2$ and $MgCl_2$ and 0.6 wt. % of NaCl [2].

One unit in the third decimal place represents about 0.1 wt. % of calcium and magnesium chlorides in the solution.

The differences between the values in each horizontal line of the table lie within the limits of experimental error. Therefore in calculations of the solubility of sodium chloride, use should be made of experimental data for the two ternary systems, the most probable value of the calcium or magnesium chloride concentration being taken to be the average of these concentrations, C_{av}

$$C_{av} = \frac{C_{CaCl_2} + C_{MgCl_2}}{2}. \tag{2}$$

The foregoing may be interpreted graphically as follows: the solubility of sodium chloride (in wt. %) as a function of C_{CaCl_2}, C_{MgCl_2}, and of $C_{\Sigma CaCl_2, MgCl_2}$ is represented by the same isotherm. This isotherm completely characterizes the crystallization area of sodium chloride for solutions containing calcium chloride and magnesium chloride in any proportions. A number of such isotherms for different temperatures forms a surface in the chosen coordinate system, and this surface represents the crystallization volume of sodium chloride for other methods of expressing the composition.

The concentrations of the salts in the quaternary system for solutions saturated with respect to sodium chloride are calculated from the experimental data for the corresponding ternary systems as follows: the number of moles of calcium chloride C_{CaCl_2} or of magnesium chloride C_{MgCl_2} in 100 g of solution in the corresponding ternary system for the given solubility of sodium chloride is first calculated.

The value of C_{av} is found from experimental data for the two ternary systems.

According to the literature [1], these numbers of moles are equal to the sum of the numbers of moles of calcium and magnesium chlorides in the quaternary system for any relative proportions of these salts, for the same solubility of sodium chloride as in the ternary system. With a given weight ratio of calcium chloride to magnesium chloride $k:l$, the weight percentages of these salts can be determined as follows.

If we represent the weight percentage of $CaCl_2$ in the solution by n_{CaCl_2}, and of $MgCl_2$ by n_{MgCl_2}, we can write

$$\frac{n_{CaCl_2}}{n_{MgCl_2}} = \frac{k}{l}. \tag{3}$$

The numbers of moles of $CaCl_2$ and $MgCl_2$ in 100 g of solution are $\frac{n_{CaCl_2}}{M_{CaCl_2}}$ and $\frac{n_{MgCl_2}}{M_{MgCl_2}}$ where M_{CaCl_2} and M_{MgCl_2} are the molecular weights of calcium and magnesium chlorides. Since C is the number of moles of the two salts in 100 g of solution, we have

$$C = \frac{n_{CaCl_2}}{M_{CaCl_2}} + \frac{n_{MgCl_2}}{M_{MgCl_2}}. \tag{4}$$

Solving Equations (3) and (4) simultaneously for n_{CaCl_2}, n_{MgCl_2} and $n_{\Sigma CaCl_2, MgCl_2} = n_{CaCl_2} + n_{MgCl_2}$, we find

$$n_{CaCl_2} = \frac{M_{CaCl_2} \cdot M_{MgCl_2}}{kM_{MgCl_2} + lM_{CaCl_2}} kC = \frac{111}{k + 1.165l} kC \tag{5}$$

$$n_{MgCl_2} = \frac{M_{CaCl_2} \cdot M_{MgCl_2}}{kM_{MgCl_2} + lM_{CaCl_2}} lC = \frac{111}{k + 1.165l} lC \tag{6}$$

$$n_{\Sigma CaCl_2, MgCl_2} = \frac{M_{CaCl_2} \cdot M_{MgCl_2}}{kM_{MgCl_2} + lM_{CaCl_2}} (k + l) C = \frac{111}{k + 1.165l} (k + l) C. \tag{7}$$

Formulas (5) and (6) may also be used for calculations of the salt concentrations in ternary systems; here in Formula (5) $k = 1$ and $l = 0$, and in Formula (6) $k = 0$ and $l = 1$.

Salt Concentrations in the Ternary and Quaternary Systems

Solubility of NaCl (in wt. %)	C_{CaCl_2}	C_{MgCl_2}	$C_{\Sigma CaCl_2,\ MgCl_2}$		
			$k:l=3:1$	$k:l=1:1$	$k:l=1:3$
2	0.295	0.290	0.289	0.290	0.293
5	0.232	0.232	0.237	0.234	0.238
10	0.166	0.164	0.170	0.168	0.168
15	0.112	0.107	0.113	0.113	1.111
20	0.060	0.057	0.062	0.062	0.060
25	0.013	0.012	0.014	0.014	0.013

The figure shows the solubility isotherm for sodium chloride in the quaternary system at $k:l = 1:3$.

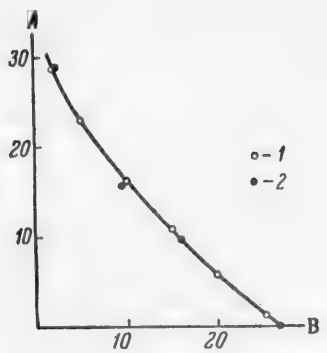

Solubility isotherm for NaCl in the ternary and quaternary systems. A) $n_{\Sigma CaCl_2, MgCl_2}$ is the sum of the weight percentages of $CaCl_2$ and $MgCl_2$, B) n_{NaCl} is the solubility of NaCl (in wt. %). 1) Calculated concentrations, 2) experimental data for the quaternary system.

The isotherm was plotted with the aid of Equation (7) after substitution of values of C_{av} found from the 2nd and 3rd columns of the table. For comparison, points corresponding to experimental data interpolated to 25° [3] are shown on the figure.* Any scattering of the points on the graph can probably be ascribed to experimental error.

It is clear from the above that concentrations in the quaternary system at any $k:l$ ratio can also be calculated from solubility data in the quaternary system at a definite $k:l$ ratio.

The basis for the proposed method can be substantiated by the following reasoning.

It is known that the activity of a component (in this instance sodium chloride) in solution, in equilibrium with a solid phase consisting of this component only, is a constant at a given temperature. The relationship between activity and concentration is represented by the expression

$$N = \frac{a}{\gamma}, \qquad (8)$$

where γ is the activity coefficient, a is the activity of the given salt in the solution, and N is its mole fraction. If the solutions were dilute, then, by the law of constancy of ionic strength, the activity coefficient could be regarded as constant at constant ionic strength of the solution. Replacement (total or partial) of

* As the solubility of sodium chloride depends little on the temperature, interpolation over a small temperature range cannot distort the experimental results.

magnesium chloride by an equivalent amount of calcium chloride in the solution should not cause any changes in the ionic strength of the solution, as the ionic strength depends only on the valence and concentration of the ions present in the solution.

The proposed rule reduces to the assumption that in the system in question the activity coefficient remains unchanged even for concentrated solutions on replacement of a given number of moles of calcium chloride by the same number of moles of magnesium chloride. In other words, the assumption is that the activity coefficient of sodium chloride in the solution depends on the sum of the numbers of moles of calcium and magnesium chlorides present, and not on their relative proportions. If, for a given total of mole fractions, the activity coefficient of sodium chloride is constant, then according to Equation (8), the solubility of sodium chloride (expressed in mole fractions) is also constant.

Calculations show that equal molar percentages of sodium chloride in the two solutions in question correspond to weight percentages of sodium chloride which are equal within the limits of experimental error.

Consequently, the sodium chloride concentration can be expressed in weight percentages in such calculations. The concentrations of calcium and magnesium chloride must then be expressed in moles per 100 g of solution.

SUMMARY

A method is described for calculation of salt concentrations in the crystallization region of sodium chloride in the quaternary system

$$CaCl_2—MgCl_2—NaCl—H_2O$$

from known values of the solubility of sodium chloride in ternary systems. The calculated values agree with experimental data within the limits of experimental error.

LITERATURE CITED

[1] N. S. Kurnakov and A. V. Nikolaev, Bull. Acad. Sci. USSR, Chem. Ser. 2, 403 (1938).

[2] N. P. Luzhnaya and I. P. Vereshchitina, J. Appl. Chem. 19, 723 (1946).

[3] A. B. Zdanovsky, E. I. Lyakhovskaya, and R. E. Shleimovich, Reference Book on Solubilities of Salt Systems, I (Leningrad-Moscow, 1953). *

Received June 18, 1955.

* In Russian.

INVESTIGATION OF ORGANIC COMPOUNDS WHICH RETARD THE OXIDATION OF SULFIDE ORES AT ELEVATED TEMPERATURES

F. N. Pavlov, V. G. Plusnin, and E. F. Iordan

We showed earlier [1] that if sulfide ores are moistened with diluted tar water (1:10) or 0.4% xylenol solution, oxidation of the ores by atmospheric oxygen is retarded approximately 14 fold as compared with the oxidation rate of ores sprayed with water only.

In this paper we give the results of a study of the effects of the same organic compounds and their condensates on the oxidation of sulfide ores at elevated temperatures (50-350°).

EXPERIMENTAL

Apparatus and method. Two similar, vertical, tubular electric furnaces of stainless steel were constructed for the investigation.

Run-of-the-mine sulfide ore from one of the Ural deposits was used. Each furnace was charged with 1.25 kg of ore, the temperature was raised to the desired level, and the ores were then sprayed by means of dropping funnels with the antioxidant in one furnace, and with town water or the same antioxidant but at a different concentration in the other. The temperature in the heated furnaces was kept constant by means of a special bimetallic thermoregulator. The ore in each furnace was sprayed with 100 ml of liquid in each experiment. The sprayed ore was kept at the test temperature for 5 hours. At the furnace exits receivers were installed, in which condensates of the test solutions were collected after passing through condensers. At the end of an experiment the reaction spaces were hermetically closed, the heat was switched off, and the furnaces were cooled to room temperature. Condensates were tested in the same way as the fresh antioxidant solutions in order to determine whether they retain their protective properties.

TABLE 1

Oxygen Absorption As A Function of Time for Ore Previously Heated to 300° and Freshly Crushed Ore

Time from start of experiment (days)	Oxygen absorbed (in cc/kg ore)		
	ore previously heated and moistened with antioxidant solution	freshly crushed ore moistened with	
		antioxidant condensate	town water
3	–	–	22.49
4	14.53	9.15	–
8	20.26	15.10	88.24
12	28.46	23.81	136.64
16	32.56	28.45	186.92
20	36.35	30.94	225.42
23	38.00	33.14	252.76
27	40.42	35.37	304.82
30	46.07	39.82	350.57

The cooled ores were discharged from the furnaces into separate glass vessels; in one vessel the ore was again sprayed with the same antioxidant solution as in the furnace, and in the other, with town water. In addition, ore which had not been heated was put into another similar vessel, and moistened with condensate from the same antioxidant solution. In every case 20 ml of liquid per 1 kg of ore was used for moistening. The vessels were then placed in a thermostat, and the subsequent observations and calculations of the results were carried out by the procedure described previously [1]. Daily readings were tabulated, and the data were plotted graphically. The antioxidants tested were tar water from the peat gas producer station of the Ural Heavy Machine Building Works, and aqueous solutions of technical xylenols from the Nizhne-Tagilsky Works.

TABLE 2

Average Rates of Absorption of Oxygen by Ore Treated With Tar Water (at 1:10 dilution)

Pretreatment temperature (in °C)	Average rates of oxygen absorption (in cc/kg per day) over 25 days	
	ore treated with	
	fresh solution	solution condensate
300	1.57	1.37
250	1.86	2.14
150	2.21	2.38
100	1.80	0.85
50	1.45	1.20
Average for 50-300° range	1.78	1.59

TABLE 3

Oxygen Absorption as a Function of Time for Ore Previously Heated to 350° and Freshly Crushed Ore

Time from start of experiment (days)	Oxygen absorbed (in cc/kg ore)			
	ore from furnace		freshly crushed ore moistened with	
	dry	moistened with anti-oxidant	antioxidant condensate	town water
3	21.32	19.85	13.91	22.49
6	31.80	27.54	19.16	58.19
9	42.46	35.73	24.56	103.79
13	48.71	43.90	31.13	150.82
15	50.55	47.01	33.69	180.16
18	57.80	54.97	39.04	205.74
21	67.02	58.83	46.25	240.03
24	70.80	59.97	47.73	256.77
27	74.35	65.90	52.80	304.82
30	79.20	68.39	54.33	350.57
34	93.21	77.19	57.22	422.32
37	98.32	81.63	60.64	442.89
41	110.74	89.12	66.03	489.31

Effect of moistening with tar water (1:10 dilution) on oxidation of ore heated to 300°. The results obtained with ores previously heated to 300° are given in Table 1.

Similar experiments were carried out at other temperatures (50, 100, 150, and 250°). The results were used to calculate the average rates of absorption of oxygen by ores previously heated to these temperatures; the values are given in Table 2.

Over the same period freshly crushed ore sprayed with water only absorbs, on the average, 10.78 cc of oxygen per kg per day. Comparison of the average rates of oxygen absorption by the treated ore and by freshly crushed ore shows that tar water retains its protective properties for ores previously heated to 300°. This protection retards oxidation 6-fold in comparison with untreated ore over the same period. Tar-water condensates collected after passing through heated ore retard the oxidation of freshly crushed ore to the same extent as fresh solutions.

Effect of moistening with xylenol solution on the oxidation of ore previously heated to 350°. Investigations with the use of xylenol solutions showed that the most suitable concentration, which produces appreciable retardation of oxidation at normal temperatures, is 0.4%; the same optimum concentration of xylenols in water was therefore used for tests of the protective properties of xylenols at higher temperatures.

The results of tests on ore previously heated to 350° are given in Table 3.

Similar experiments were performed with ore previously heated to 90, 150, 250, and 300°. The results are given in Table 4 in the form of calculated average rates of oxygen absorption by the ore at these temperatures.

TABLE 4

Rates of Oxygen Absorption by Ore Treated With 0.4% Aqueous Xylenol Solution (Average Values for Different Temperatures)

Ore pretreatment temperature (°C)	Average rate of oxygen absorption (in cc/kg ore per day) over 41 days			
	ore from furnace		freshly crushed ore moistened with	
	dry	moistened with anti-oxidant	anti-oxidant condensate	town water
350	2.70	2.17	1.61	
300	2.25	1.50	1.58	—
250	2.18	1.67	2.52	—
150	1.21	1.41	1.77	—
90	1.63	0.58	1.29	
20	—	—	—	11.93
Average for temperatures up to 350°	1.99	1.47	1.75	11.93

Comparison of the average rates of oxygen absorption by the treated ore, and by freshly crushed ore sprayed with water only, shows that at higher temperatures, from 90 to 350°, xylenol solution produces a 6-fold retardation of the rate of oxygen absorption by the ore.

Condensates of these solutions, collected after passing through the heated ore, also retard the oxidation of freshly crushed ore to about the same extent as the fresh solutions.

SUMMARY

1. Tar water from peat gas producer stations and technical xylenols from peat tar, used at low concentrations, protect sulfide ores against oxidation by atmospheric oxygen both at low and at elevated temperatures (50-350°).

2. Condensates of solutions passed through the hot zone (300-350°) retain their protective properties for freshly crushed ore at normal temperatures.

3. The optimum concentrations of the aqueous solutions for ore treatment at elevated and low temperatures are 0.4% for xylenols, and 10-fold dilution for tar water.

LITERATURE CITED

[1] F. N. Pavlov, V. G. Plyusnin, and E. F. Iordan, J. Appl. Chem. 29, 2, 166 (1956). *

Received January 2, 1956.

* Original Russian pagination. See C. B. Translation.

THE SYSTEM $Na_2SO_4 - NaHCO_3 - H_2O$ (CARLSBAD SALT) AT 25 AND 38° *

G. V. Sukmanskaya and P. S. Bogoyavlensky

The Lvov Zooveterinary Institute. Chair of Inorganic Chemistry

Study of equilibria in the system $Na_2SO_4 - NaHCO_3 - H_2O$ apart from the general problems with which our studies of Carlsbad salt [1] are concerned, is of independent importance, as ternary aqueous solutions containing Na_2SO_4 and $NaHCO_3$ are also used for medicinal and prophylactic purposes.

Makarov and Vaksberg [2] studied the system $Na_2SO_4 - NaHCO_3 - H_2O$ at 25°. According to their results, the solubility isotherm has only two crystallization branches – for $NaHCO_3$ and $Na_2SO_4 \cdot 10H_2O$ – sodium sulfate is not dehydrated by the action of sodium bicarbonate. From these results it may be assumed that liquid phases in the ternary system $Na_2SO_4 - NaHCO_3 - H_2O$ at 25° should contain stably hydrated sodium ions over the entire range of possible salt concentrations. Since the ionic composition of aqueous salt solutions is important in pharmacological investigations, it was decided to verify the results obtained by Makarov and Vaksberg, especially as it appears that no other data on the subject are available.

As far as we could establish from the literature, the system $Na_2SO_4 - NaHCO_3 - H_2O$ has not been studied at 38°.

EXPERIMENTAL

The usual isothermal method was used for studying equilibria in the system $Na_2SO_4 - NaHCO_3 - H_2O$ at 25 and 38°. The composition of the liquid phase was found by quantitative determinations of HCO_3^- and SO_4^{--}. The HCO_3^- determinations were carried out by the acidimetric method with methyl orange indicator; SO_4^{--} was determined gravimetrically. Samples of liquid phase for quantitative determinations of these ions were taken only after equilibrium had been shown to be established; in most cases this was after 24 hours or more. As a rule, the determinations of the solution composition were duplicated.

The composition of the solid phases was determined from the results of microscopical observation of the external form of the crystals taken from the reaction vessel after equilibrium had been established. Crystals of Glauber salt, anhydrous sodium sulfate, and sodium bicarbonate differ appreciably in appearance under the microscope, so that it was possible to determine the solid phase compositions in the system $Na_2SO_4 - NaHCO_3 - H_2O$ fairly accurately. The solid phases for the univariant lines of the isotherm at 25° are $NaHCO_3$ and $Na_2SO_4 \cdot 10H_2O$, for the isotherm at 38°, $NaHCO_3$ and Na_2SO_4 and for the eutonic points, mixtures of the salts. Thus, our investigations confirmed Makarov and Vaksberg's data on the composition of the solid phases in the system $Na_2SO_4 - NaHCO_3 - H_2O$ at 25°.

The formation of sodium carbonate in the system $Na_2SO_4 - NaHCO_3 - H_2O$ was prevented by the methods described in detail in one of our papers [3].

---

* Communication IV in the series on the physicochemical analysis of aqueous salt systems of pharmacological significance.

The results of our investigations of the system $Na_2SO_4-NaHCO_3-H_2O$ are given in Table 1 and in Figs. 1 and 2.

TABLE 1

Solubility in the System $Na_2SO_4-NaHCO_3-H_2O$ at 25 and 38°.

Composition of liquid phase					Solid phase
in weight percent			in moles per 1000 g H_2O		
Na_2SO_4	$NaHCO_3$	H_2O	Na_2SO_4	$NaHCO_3$	
Isotherm for 25°					
21.90	—	78.10	1.974	—	$Na_2SO_4 \cdot 10H_2O$
21.21	2.53	76.26	1.958	0.395	
20.77	3.76	75.47	1.989	0.594	
20.73	4.19	75.08	1.944	0.664	$Na_2SO_4 \cdot 10H_2O + NaHCO_3$
19.55	4.36	76.09	1.809	0.682	$NaHCO_3$
15.81	5.03	79.16	1.406	0.756	
13.28	5.48	81.24	1.151	0.803	
10.36	6.27	83.37	0.875	0.895	
6.60	7.28	86.12	0.540	1.006	
3.19	8.30	88.51	0.254	1.116	
—	9.31	90.69	—	1.222	
Isotherm for 38°					
33.06	—	66.94	3.48	—	Na_2SO_4
32.60	0.76	66.64	3.44	0.14	
32.22	1.34	66.44	3.41	0.24	
30.79	2.95	66.26	3.26	0.53	$Na_2SO_4 + NaHCO_3$
28.80	3.64	67.56	3.00	0.64	$NaHCO_3$
27.54	3.75	68.71	2.82	0.65	
25.13	4.12	70.75	2.50	0.69	
21.37	4.82	73.81	2.04	0.78	
17.50	5.67	76.83	1.60	0.88	
14.60	6.42	78.98	1.30	0.97	
11.34	7.35	81.31	0.98	1.08	
8.68	8.00	83.32	0.73	1.17	
5.81	9.10	85.09	0.48	1.27	
4.12	9.70	85.99	0.34	1.37	
2.00	10.45	87.55	0.16	1.42	
—	11.16	88.84	—	1.50	

Joint solubility in the system $Na_2SO_4-NaHCO_3-H_2O$ at 25 and 38° is characterized by a fairly pronounced salting-out effect of Na_2SO_4 on $NaHCO_3$. Thus, at 25° the molalities of Na_2SO_4 and $NaHCO_3$ in the eutonic solution are in a ratio of 2.94 : 1. The ratio of the molality of a saturated solution of Na_2SO_4 to the molality of Na_2SO_4 in the eutonic solution is 1.02. The corresponding ratio for $NaHCO_3$ is 1.89. The corresponding data for 38° show a further increase in the salting out of $NaHCO_3$ from the ternary system.

It follows from the foregoing that the appreciable decrease of the individual solubility of $NaHCO_3$ in the ternary system at 25° is probably the principal factor which determines the absence of the transition $Na_2SO_4 \cdot 10H_2O \rightarrow Na_2SO_4$ in the system $Na_2SO_4-NaHCO_3-H_2O$. It is evident that this transition is possible with considerable salting out of Na_2SO_4 from the ternary system of the crystallization branch of $Na_2SO_4 \cdot 10H_2O$, and at fairly high concentrations of the nonsaturating salt in the solution at the transition point. Comparison of the solubility isotherms at 25° for the systems $Na_2SO_4-NaHCO_3-H_2O$ and $Na_2SO_4-NaCl-H_2O$ may be informative in this respect. The molality of the solution at the transition point in the system

$Na_2SO_4-NaCl-H_2O$ is 1.51 with respect to Na_2SO_4 and 3.39 with respect to NaCl, i.e., the molality of the nonsaturating salt is more than double that of the saturating salt [1]. No such or any similar ratio of salt concentrations is found in the system $Na_2SO_4-NaHCO_3-H_2O$, and therefore sodium sulfate is not found dehydrated in the solid phase.

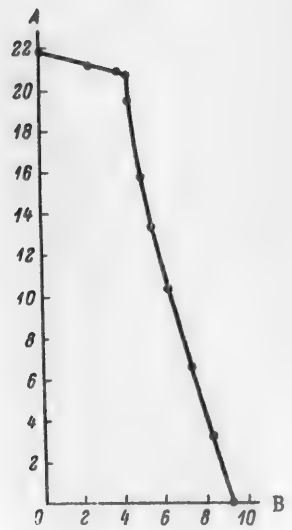

Fig. 1. Solubility in the system $Na_2SO_4-NaHCO_3-H_2O$ at 25°. A) Na_2SO_4 content (in wt. %), B) $NaHCO_3$ content (in wt. %).

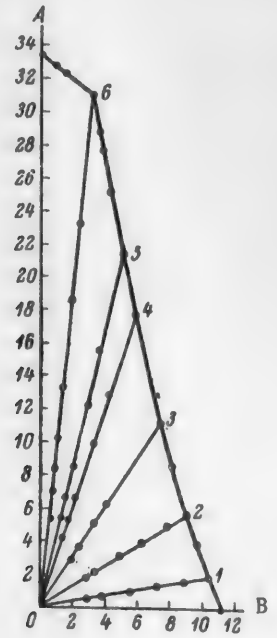

Fig. 2. Solubility in the system $Na_2SO_4-NaHCO_3-H_2O$ at 38°. A) Na_2SO_4 content (in wt. %), B) $NaHCO_3$ content (in wt. %). The remaining designations are given in the text.

The above characteristics of mutual solubility in the system

$$Na_2SO_4-NaHCO_3-H_2O$$

must be taken into account in pharmacological investigations of the ternary solution systems, since the ionic composition of these solutions is not the same at 25 and 38°.

It was reported by one of us [4] that a useful characteristic of liquid aqueous salt phases of pharmacological significance is the ionic strength, especially in the case of dilute solutions, which are used widely in medical and veterinary practice. In this paper we use solubility isotherm data for the system $Na_2SO_4-NaHCO_3-H_2O$ at 38° to consider certain methods for using isothermal diagrams for selection of solutions of equal ionic strengths.

For this it is first necessary to study the region of unsaturated solutions in the diagram, by means of a series of rectilinear paths connecting the water corner of the diagram to definite points on the univariant curves of salt crystallization. The solutions corresponding to all points of a given path will all have equal ratios of salt concentrations and equal ratios of the partial ionic strengths of the salts. Moreover, over a

definite range of ionic strengths all the paths will contain figurative points for solutions of equal ionic strength, although the concentrations and the ratios of the salt concentrations in these solutions will be different. As shown in Fig. 2, we studied the region of unsaturated solutions, bounded in the diagram by the univariant curve for $NaHCO_3$ crystallization, by this path method.

TABLE 2

Compositions and Ionic Strengths of Two-Salt Solutions in the System $Na_2SO_4-NaHCO_3-H_2O$ at 38°.

Path No.	Composition (wt. %)		Ionic strength			Ionic strength ratio for $NaHCO_3 : Na_2SO_4$	Composition (in moles per 1000 g H_2O)	
	Na_2SO_4	$NaHCO_3$	Na_2SO_4	$NaHCO_3$	$Na_2SO_4 + NaHCO_3$		Na_2SO_4	$NaHCO_3$
1	2.00	10.45	0.482	1.421	1.903	2.945	0.161	1.421
	1.70	8.89	0.402	1.184	1.586		0.134	1.184
	1.40	7.26	0.322	0.947	1.269		0.107	0.947
	1.07	5.57	0.241	0.710	0.951		0.080	0.710
	0.73	3.80	0.161	0.474	0.635		0.054	0.474
	0.55	2.88	0.121	0.355	0.476		0.040	0.355
2	5.81	9.10	1.442	1.273	2.715	0.883	0.481	1.273
	4.97	7.78	1.203	1.061	2.264		0.401	1.061
	4.07	6.38	0.961	0.849	1.810		0.320	0.849
	3.14	4.92	0.721	0.637	1.358		0.240	0.637
	2.15	3.37	0.481	0.424	0.905		0.160	0.424
	1.86	2.91	0.412	0.364	0.776		0.137	0.364
3	11.34	7.35	2.945	1.076	4.021	0.365	0.982	1.076
	8.06	5.23	1.964	0.717	2.681		0.655	0.717
	6.25	4.05	1.473	0.538	2.011		0.491	0.538
	5.11	3.31	1.178	0.430	1.608		0.393	0.430
	3.74	2.42	0.842	0.307	1.149		0.281	0.307
	2.95	1.91	0.655	0.239	0.894		0.215	0.239
4	17.50	5.67	4.811	0.878	5.689	0.183	1.604	0.878
	12.71	4.12	3.207	0.586	3.793		1.069	0.586
	9.90	3.21	2.405	0.439	2.844		0.802	0.439
	6.90	2.24	1.604	0.293	1.897		0.535	0.293
	5.30	1.72	1.203	0.220	1.423		0.401	0.220
	4.30	1.39	0.962	0.176	1.138		0.321	0.176
5	21.37	4.82	6.114	0.777	6.891	0.127	2.038	0.777
	15.60	3.52	4.076	0.518	4.594		1.359	0.518
	12.30	2.77	3.057	0.389	3.446		1.019	0.389
	8.63	1.95	2.038	0.259	2.297		0.679	0.259
	6.65	1.50	1.529	0.194	1.723		0.510	0.194
	5.41	1.22	1.223	0.155	1.378		0.408	0.155
6	30.79	2.95	9.792	0.530	10.322	0.054	3.264	0.530
	23.09	2.22	6.528	0.353	6.881		2.176	0.353
	18.49	1.78	4.896	0.265	5.161		1.632	0.265
	13.21	1.27	3.264	0.177	3.441		1.088	0.177
	10.29	0.99	2.448	0.132	2.580		0.816	0.132
	8.42	0.81	1.958	0.106	2.064		0.653	0.106
	7.12	0.68	1.632	0.088	1.720		0.544	0.088
	5.45	0.52	1.224	0.066	1.290		0.408	0.066

To find the concentrations of solutions with the same ionic strength, several points corresponding to known compositions are chosen on each path. The concentrations of the solutions corresponding to the individual points were either predetermined from the composition of the solution corresponding to the point in the path lying on the univariant curve for $NaHCO_3$ crystallization, or the compositions of the solutions corresponding to the points in the paths were determined graphically. The accuracy of the graphical determination is easily checked from the ratio of salt concentrations, known for the given path. The known concentration of each solution was used to calculate its ionic strength. Composition and ionic strength data for two-salt solutions in the six-paths chosen are given in Table 2.

TABLE 3

Two-Salt Solutions of Equal Ionic Strengths in the System Na_2SO_4–$NaHCO_3$–H_2O.

Ionic strength	Path No.	Composition (wt. %)		Ionic strength	Path No.	Composition (wt. %)	
		Na_2SO_4	$NaHCO_3$			Na_2SO_4	$NaHCO_3$
2.0	1	—	—	0.5	1	0.54	2.80
	2	4.40	6.90		2	1.15	1.80
	3	5.86	3.80		3	1.54	1.00
	4	6.79	2.20		4	1.85	0.60
	5	6.65	1.50		5	1.77	0.40
	6	7.29	0.70		6	2.08	0.20
1.8	1	1.91	10.0	0.2	1	0.23	1.20
	2	3.96	6.20		2	0.51	0.80
	3	5.24	3.40		3	0.77	0.50
	4	6.02	1.95		4	0.93	0.30
	5	6.21	1.40		5	1.10	0.25
	6	6.25	0.60		6	1.04	0.10
1.5	1	1.57	8.20				
	2	3.32	5.20				
	3	4.47	2.90				
	4	4.94	1.60				
	5	5.32	1.20				
	6	6.04	0.58				

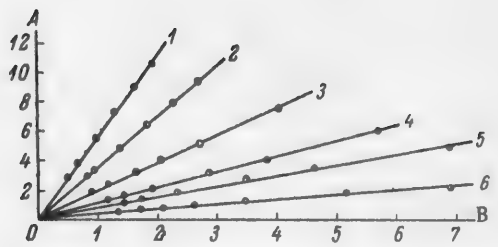

Fig. 3. Variations of ionic strength of two-salt solutions with the concentration of one of the salts. A) Concentration of $NaHCO_3$ (in wt. %), B) ionic strength. The remaining designations are given in the text.

The data for the composition and ionic strength of solutions corresponding to definite points on the paths in the isothermal diagram are then used for the construction of the same number of auxiliary curves as there were paths, showing the variations of the ionic strengths of the two-salt solutions with the concentration of one of the salts. It follows from Fig. 3 that the plots of ionic strength against $NaHCO_3$ concentration, in percent by weight, are linear for all the salt concentrations used in the two-salt solutions of the system in question. The straight lines in Fig. 3 are numbered to correspond with the paths in Fig. 2. We also found that there are slight deviations from linearity at relatively high Na_2SO_4 concentrations in the relationship between the ionic strength and the concentration of the second salt, Na_2SO_4, expressed in percent by weight, but it is precisely linear if the Na_2SO_4 concentration is expressed in moles per 1000 g H_2O. These results evidently suggest that the ionic strength of a solution containing two salts is a linear function of the molality of each of the salts. The two diagrams – the isothermal and the auxiliary – may be used to determine with great accuracy the compositions of two-salt solutions of given ionic strength. The results of our determinations of the concentrations of solutions of the same ionic strengths are given in Table 3.

SUMMARY

1. It was found in a study of the joint solubility of Na_2SO_4 and $NaHCO_3$ in water at 25 and 38° that the liquid phases at 25°, in contrast to the liquid phases at 38°, contain stably hydrated sodium ions, and possibly stably hydrated sulfate ions also.

2. An account is given of methods for using the isothermal diagram for a ternary water – salt system to select concentrations of solutions of equal ionic strengths.

LITERATURE CITED

[1] P. S. Bogoyavlensky and G. V. Sukmanskaya, J. Appl. Chem. 28, 208 (1955).*

[2] S. Z. Makarov and N. M. Vaksberg, J. Russ. Phys. Chem. Soc., Chem. Section, 62, 8-9, 1863 (1930).

[3] P. S. Bogoyavlensky and A. S. Manannikova, J. Appl. Chem. 28, 325 (1955).*

[4] P. S. Bogoyavlensky, J. Appl. Chem. 28, 104 (1955).*

Received November 12, 1955.

* Original Russian pagination. See C. B. Translation.

THE SELECTIVE CORROSION OF ZINC*

I. I. Zabolotnyi

The I. Fedorov Polygraphic Institute of the Ukraine

As has already been reported [1], there have been several investigations of the selective corrosion of metals, but the details of this highly complex corrosion process are not yet quite clear. The selective corrosion of zinc in nonoxidizing and oxidizing acids only partially explains the complexity of the selective corrosion of zinc [1]. In the course of this investigation a number of questions arose with regard to the dependence of the selective corrosion of zinc on the acid content of the solution, the temperature, and the presence of various oxidants in solutions of nonoxidizing acids. The present paper deals with these questions.

EXPERIMENTAL METHODS

The same method as before [1] was used for preparation of the specimens from sheet zinc, but the zinc plates were smaller (20 × 20 mm), and asphalt, being more stable, was used for acid insulation. Drops of a solution of asphalt in benzene were placed at the center and at the corners of the zinc plate surface in order to determine differences in the selective corrosion of zinc at these regions of the plate.

Two hundred ml of the acid solution was used in each experiment, so that the height of the layer of liquid over the attacked surface was the same in every case. The acid solutions were left unstirred for different times, which depended on the degree of attack of the zinc plate necessary to give a selective corrosion profile.

After removal of the corrosion products from the attacked surface, and of the asphalt layer from the rest of the plate, the instrument of our design [2] was used to determine the thickness of the plate from the continuously etched surface to the places which were under the layer of asphalt and which were therefore not attacked. It should be noted that in measurements between the minimum and the maximum plate thickness the varying pressure on the point of the needle caused by tension in the indicating mechanism did not, according to our observations, produce any traces, visible under a lens, on the plate surfaces. The results of measurements along the distance from the region of continuous etching to the insulating layer represented the selective corrosion profile.

Effect of acid concentration on the selective corrosion of zinc. Hydrochloric, sulfuric, and nitric acids of various normalities were used to determine the effects of acid concentration on the selective corrosion of zinc. The results of repeated determinations of selective corrosion at the edges of the acid-insulating layers in the center and at the corners of the plate showed that such corrosion is more pronounced at the plate corners. This is probably the consequence of greater changes of acid concentration in these regions of the plate during corrosion.

It follows from the selective corrosion curves (Fig. 1) which represent the selective corrosion profiles for zinc in sulfuric acid solutions, that as the sulfuric acid concentration increases, the region between the start of

---

* Communication II.

selective corrosion to continuous relatively uniform etching of the zinc surface decreases. There is no doubt that the difference in the size of the regions is primarily the consequence of the difference in the size of the bubbles which can be retained at the edge of the asphalt layer. In our opinion, when the corrosion rate of zinc is low, which is the case in dilute nonoxidizing acid media, the conditions are favorable for prolonged growth of hydrogen bubbles and therefore for formation of large bubbles at the boundary between the metal and the nonmetallic material – asphalt. However, as the acid concentration increases, the corrosion of zinc

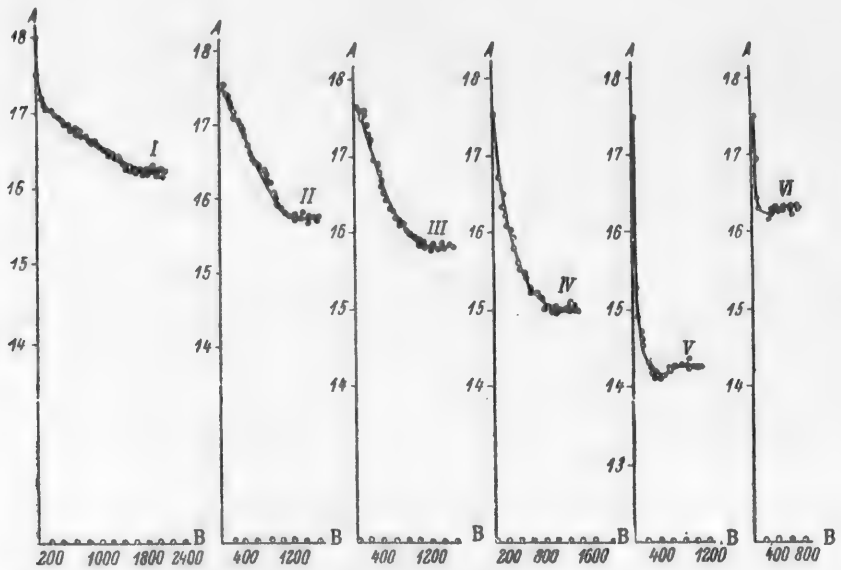

Fig. 1. Variation of the thickness of a zinc plate with distance from the acid-insulating layer. A) Thickness of the zinc plate (in $1 \cdot 10^2$ μ), B) distance from the acid-insulating layer (in μ).
Corrosion in sulfuric acid solutions of the following strengths: I) 0.25 N, II) 0.5 N, III) 1.0 N, IV) 3.0 N, V) 5.0 N, VI) 7.0 N.

is accelerated, and so is the rate of formation of hydrogen bubbles; the attacked zinc plate becomes considerably heated [3], and this, together with the agitation of the solution near the attacked zinc surface by the detaching hydrogen bubbles, prevents the growth and retention of bubbles at any of the regions on this surface. The development of these effects corresponds to the decrease of the selective corrosion region with increasing concentration of hydrochloric acid in the solution. Thus, selective corrosion becomes more pronounced with increasing content of nonoxidizing acid in the solution and, at the same time, the corrosive attack on the etched zinc surface becomes more uniform. This provides additional confirmation of the relationship, found by us earlier [4], between the size of the hydrogen bubbles evolved during acid corrosion and the uniformity of etching of the zinc surface; the smaller the bubbles evolved during corrosion in conditions of predominant hydrogen depolarization, the more regular is the etching of the zinc surface.

While the profile for the selective corrosion of zinc in hydrochloric acid of different concentrations is similar to Curves I - IV (Fig. 1), when zinc is corroded in sulfuric acid solutions of higher concentrations grooves appear in the profile, as is seen in Curves V and VI (Fig. 1), which are more pronounced at higher sulfuric acid concentrations. This fact, and also the curves for the selective corrosion of zinc in nitric acid (Fig. 2), provide further confirmation of our finding [1] that the occurrence of a groove in the selective corrosion profile is the consequence of oxidative depolarization in the electrochemical corrosion process. The nature of the curves in Fig. 2 indicates that, as in the selective corrosion of zinc in hydrochloric and sulfuric acid solutions, an increase of the nitric acid concentration in the solution diminishes the region of selective corrosion of zinc.

It should be pointed out that this decrease of the region of selective corrosion of zinc with increasing acid concentration is undoubtedly significant in relation to faulty etching of zinc stereotype plates. In particular, attempts to accelerate the production of zinc plates by increases of the acid concentration in the etching bath result in increased faults in the plates.

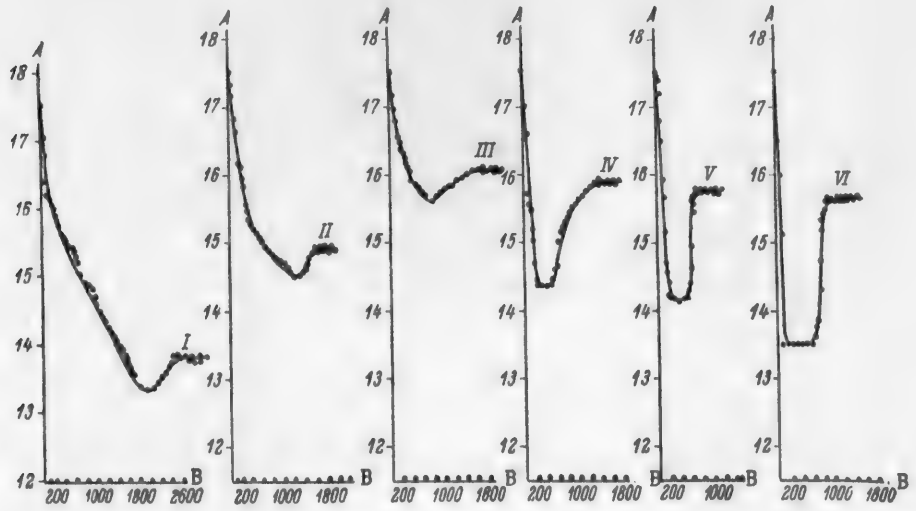

Fig. 2. Variation of the thickness of a zinc plate with the distance from the acid-insulating layer. A) Thickness of the zinc plate (in $1 \cdot 10^2$ μ), B) distance from the acid-insulating layer (in μ).
Corrosion in nitric acid solutions of the following strengths: I) 0.26 N, II) 0.52 N, III) 1.04 N, IV) 2.08 N, V) 3.12 N, VI) 4.16 N.

It is possible that the variations in the curves in Fig. 1 and Fig. 2 are caused not only by the specific characteristics of the elementary electrochemical process, but also by a number of phenomena which accompany this process. Support for this suggestion is provided by certain differences in the formation and state of the gaseous corrosion products, and also in the thermal processes which occur at the etched zinc plate in corrosion of zinc in hydrochloric and sulfuric acid, which form nonoxidizing media in solution, and in nitric acid, where zinc corrodes in conditions of oxidative depolarization. The groove in the selective corrosion profile for solutions containing nitric acid is the consequence, not only of the low degree of gas formation in the corrosive process, but also of the flow of fresh solution of nitric acid from the surface of the acid-insulating layer to the directly etched zinc surface, which may occur under such conditions. The probability of the latter becomes more evident if it is taken into account that considerable heat is evolved in the course of acid corrosion in conditions of oxidative depolarization [3], so that the metal and the adjacent acid layer become heated and therefore flow of cooler nitric acid solution onto the etched surface from the surface of the acid-insulating layer is quite natural. This temperature-gradient effect is undoubtedly less likely to occur in hydrochloric or sulfuric acid solutions, owing to their vigorous agitation by the hydrogen bubbles evolved during corrosion of zinc; according to our observations, the bubbles are liberated in the shape of a fan near the regions of their preferential accumulation, usually in the form of a necklace, at the edges of the acid-insulating layer.

Effect of temperature on the selective corrosion of zinc in acids. For studies of the effect of temperature on the selective corrosion of zinc, the experimental zinc plates were immersed in acid solutions previously heated to 20, 40, and 60° and kept at these temperatures until the end of the experiments. It follows from the curves in Fig. 3 that the nature of the selective corrosion of zinc at the temperatures studied does not vary in hydrochloric acid solutions, but variations occur in sulfuric and nitric acid solutions. As the temperature of the sulfuric acid solutions increases, the groove in the selective corrosion profile becomes larger, while in nitric acid

solutions under the same conditions the groove becomes both deeper and wider. Therefore, increase of the solution temperature increases both the influence of oxidative depolarization in the selective corrosion of zinc, and the processes of convection and diffusion in the corrosive solution.

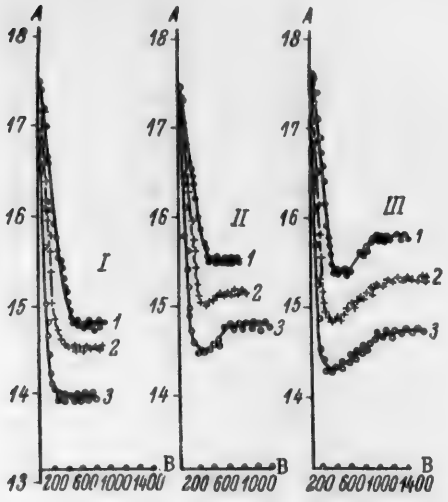

Fig. 3. Variation of the thickness of a zinc plate with the distance from the acid-insulating layer. A) Thickness of the zinc plate (in $1 \cdot 10^2$ μ), B) distance from the acid-insulating layer (in μ). Corrosion in 10% solutions of: I) HCl, II) H_2SO_4, III) HNO_3. Temperature (in °C): 1) 20, 2) 40, 3) 60.

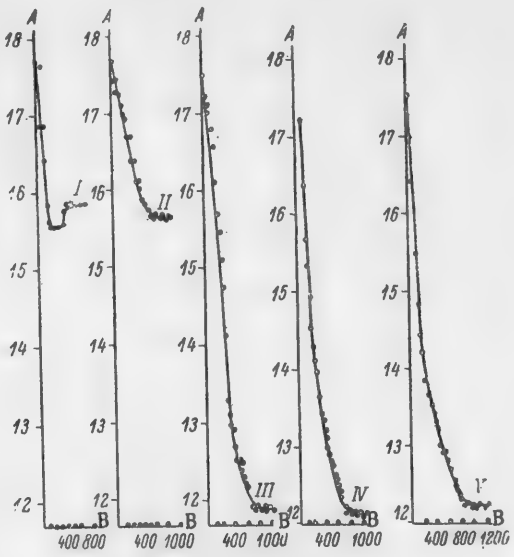

Fig. 4. Variation of the thickness of a zinc plate with the distance from the acid-insulating layer. A) Thickness of zinc plate (in $1 \cdot 10^2$ μ), B) distance from the acid-insulating layer (in μ). Corrosion in 18.4% sulfuric acid solution containing: I) 6% HNO_3, II) 2% $NaNO_2$, III) 2% $K_2Cr_2O_7$, IV) 2% $KMnO_4$, V) 2% H_2O_2.

Effects of oxidizing agents on the selective corrosion of zinc in 18.4% sulfuric acid. The oxidizing agents used were $NaNO_2$, $K_2Cr_2O_7$, $KMnO_4$, H_2O_2 as 2% additions to 18.4% sulfuric acid. As the corrosion tests in these solutions were all carried out at the same temperature, the curves in Fig. 4 represent the influence of each of these agents on the selective corrosion of zinc. An interesting fact is that the selective corrosion profile of zinc in 18.4% sulfuric acid did not change in presence of these oxidizing agents. The explanation is that corrosion in these solutions, as in the same acid without oxidizing agents, was accompanied by copious liberation of hydrogen bubbles, and corrosion products were formed on the etched zinc surface, indicating the predominant influence of hydrogen depolarization. However, with a gradual increase of the nitric acid contents in hydrochloric or sulfuric acid solutions, it was found [4] that gas liberation diminished and there was a decrease in the formation of corrosion products on the etched surface. This change in the state of the corrosion products of zinc in sulfuric acid solution containing nitric acid is represented by the selective corrosion profile I in Fig. 4. From this we may conclude that these changes in the state of the corrosion products are the consequence of a transition from hydrogen depolarization to oxidative depolarization in the elementary electrochemical process of zinc corrosion. One of the objects of our future investigations will be the determination of a more detailed relationship between these effects and the consequences of the selective corrosion of zinc.

SUMMARY

1. Increase of the acid concentration in solution decreases the region of selective corrosion of zinc, represented by the distance over which the etching of the zinc surface gradually increases, from the acid-insulating layer to the region of complete etching.

2. Increase of the temperature of an oxidizing acid medium increases the influence of oxidative depolarization by increasing the groove in the selective corrosion profile of zinc.

3. The form of the selective corrosion profile of zinc in acid media containing oxidizing agents depends not only on the depolarization processes of electrochemical corrosion, but also on a number of accompanying effects.

4. These findings concerning the profile and region of selective corrosion of zinc in acids provide an explanation of the faulty etching effects which occur in the production of zinc stereotype plates.

LITERATURE CITED

[1] I. I. Zabolotnyi, V. P. Kovtun, and B. M. Krimerman, J. Appl. Chem. 28, 655 (1955).*

[2] I. I. Zabolotnyi, Factory Labs. 21, 248 (1955).

[3] I. I. Zabolotnyi, E. D. Lazebnik, and L. G. Shelepenko, Printing Trade 10, 21 (1949).

[4] I. I. Zabolotnyi, Printing Trade 10, 16 (1948); Reports of the Scientific Session of the Ivan Fedorov Polygraphic Institute of the Ukraine 10, 67 (1952).

Received October 7, 1955.

* Original Russian pagination. See C. B. Translation.

INVESTIGATION OF A THIOCYANATE ELECTROLYTE FOR COPPER PLATING

B. S. Krasikov and A. M. Gvozd

For replacement of the relatively unstable and poisonous cyanide electrolytes for copper plating of steel, numerous electrolyte compositions have been proposed, based on lactic acid, oxalic acid [1, 2], ammonia [3], and pyrophosphoric acid [4, 5]. One suitable electrolyte is the pyrophosphate electrolyte, but in order to avoid contact deposition of copper the articles to be plated should be suspended in the electrolyte while the current is flowing, which is not always convenient. Moreover, for better adherence of the coating to the basis metal the latter should first be treated in sodium pyrophosphate solution [5], which also complicates the procedure.

We have carried out tests on the use of thiocyanate electrolytes for the production of dense copper coatings with good adherence to the steel surface.

An installation consisting of an electrolytic and a potentiometric circuit was used for studying the electrode position conditions. A coulometer was connected in the electrolytic circuit. The anodes were made from copper of M-O grade, and steel articles of various shapes were used as the cathodes. The electrolyte was made by solution of Chevreul's salt ($CuSO_3 \cdot Cu_2SO_3 \cdot 2H_2O$), in potassium thiocyanate; this method was used to prepare electrolytes of the following compositions (in moles/liter): 0.05 CuCNS + 1.7 KCNS, 0.1 CuCNS + + 2.5 KCNS, 0.2 CuCNS + 5 KCNS.

To determine the copper concentration in the electrolyte, the $KCu(CNS)_2$ complex was decomposed by boiling with sulfuric acid; the solution was evaporated to dryness, diluted with water, and titrated with thiosulfate.

The free thiocyanate content was determined by titration of a standard solution of $AgNO_3$ with the original electrolyte, in presence of ferric iron.

The electrode potentials were determined to an accuracy of ± 2 mv, the current density was determined to the nearest ± 0.5 % , and the current efficiency also to the nearest ± 0.5%.

EXPERIMENTAL

Cathodic and anodic polarization curves for thiocyanate electrolytes of different compositions are shown in Fig. 1.

It is seen that the cathodic polarization curves are shifted in the direction of more negative potentials with increasing thiocyanate concentration; this can be explained on the assumption that the stage of discharge of the complex ion $Cu(CNS)_2^-$ according to the scheme: $Cu(CNS)_2^- + e \rightarrow Cu + 2CNS^-$, is retarded; this scheme does not differ in principle from that suggested by Vagramyan [6] for the discharge of complex copper cyanide anions $[Cu(CN)_2^-]$.

In this case the presence of specifically adsorbed CNS^- anions on the cathode surface will prevent the discharge of $Cu(CNS)_2^-$ anions, in complete harmony with the theory of delayed discharge [7]. It is known from the literature [8] that the CNS^- anion shows well-defined specific adsorption.

The anodic polarization curves are also shifted in the direction of more negative potentials with increasing thiocyanate concentration in the electrolyte, owing to increased solubility of the dense film of Cu(CNS) formed on the anode. It also follows from the figure that limiting currents are reached at fairly high current densities.

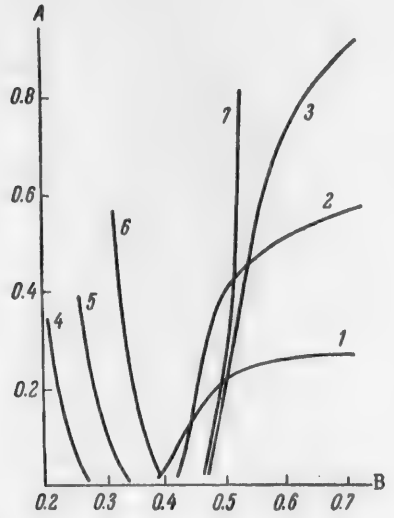

Fig. 1. Anodic and cathodic polarization curves for a copper electrode in $KCu(CNS)_2$ + KCNS solutions. A) Current density D_c (in amp/dm^2), B) potential φ (in v). Curves: 1, 2, 3, 7) cathode; 4, 5, 6) anode. Concentrations of $KCu(CNS)_2$ and KCNS, respectively (in normalities): 1,4) 0.05 and 1.7; 2, 5) 0.1 and 2.5; 3,6, 7) 0.2 and 5.0 (7—with stirring of the electrolyte).

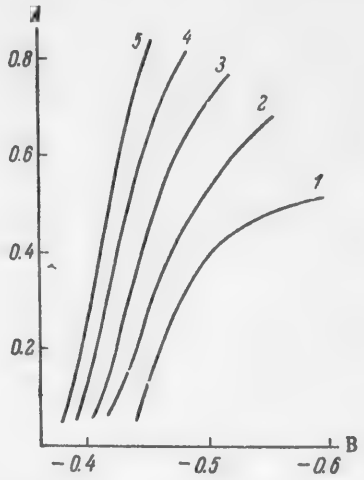

Fig. 2. Effect of temperature on cathodic polarization of a copper electrode in a solution of 0.1 N $KCu(CNS)_2$ + 2.5 N KCNS. A) Current density D_c (in amp/dm^2), B) potential φ_c (in v). Temperature (in °C): 1) 5, 2) 20, 3) 30, 4) 40, 5) 50.

Thus, it follows from a consideration of the dependence of φ_c on the adsorption potentials of the CNS^- ion and the limiting currents that the course of the polarization curve is determined by the combined influence of the retardation of the discharge stage, and of concentration polarization. The value of i_{lim} is directly proportional to the concentration of $Cu(CNS)_2^-$ in the electrolyte. Stirring of the solution (Fig. 1) and increase of temperature (Fig. 2) diminish the influence of concentration polarization, but do not eliminate it completely.

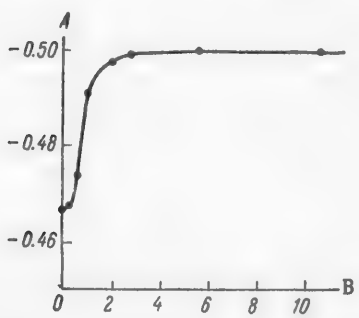

Fig. 3. Variation of cathode potential in a solution of 0.1 N $Cu(CNS)_2$ + 2.5 N KCNS with concentration of thiourea (D_c = 0.3 amp/dm^2). A) Cathode potential φ_c (in v); B) concentration of thiourea (in g/liter).

The combined influence of the retarded discharge and of concentration polarization is also seen in i / φ curves for different temperatures. It is known that the temperature coefficient of the rates of reactions in which concentration effects form the rate-determining step is close to 1.2 [9]. If the electrochemical stage is retarded, the temperature coefficient is close to 2 [10]. Therefore: $K_{\text{electrochem.}} = \frac{i_{t+10}}{i_t} \simeq 2$, $K_{\text{conc.}} = \frac{i_{t+10}}{i_t} \simeq 1.2$.

In the case under consideration, the lower the current density and the more positive the cathode potential, the greater must be the role of the retardation of the discharge stage. This is well illustrated by the data in Table 1.

TABLE 1

Values of $K = \frac{i_t + 10}{i_t}$ at Different Cathode Potentials.

Temperature (°C)	$\varphi_c = -0.42$ V		$\varphi_c = -0.44$ V		$\varphi_c = -0.46$ V		$\varphi_c = -0.48$ V		$\varphi_c = -0.50$ V		$\varphi_c = -0.52$ V	
	i	K	i	K	i	K	i	K	i	K	i	K
5	—	—	—	—	0.2	—	0.31	—	0.39	—	0.46	—
15	—	—	0.16	—	0.3	1.5	0.40	1.29	0.48	1.23	0.54	1.17
20	—	—	0.22	—	0.36	—	0.46	—	0.54	—	0.60	—
25	—	—	0.28	1.75	0.44	1.47	0.55	1.37	0.64	1.33	0.72	1.33
30	0.17	—	0.36	1.63	0.51	1.42	0.63	1.36	0.74	1.37	0.83	1.37
35	0.25	—	0.44	1.57	0.60	1.37	0.73	1.33	0.82	1.28	—	—
40	0.33	1.94	0.54	1.50	0.69	1.35	0.80	1.27	—	—	—	—
45	0.44	1.80	0.63	1.43	0.76	1.28	0.86	1.18	—	—	—	—
50	0.53	1.60	0.72	1.34	0.84	1.22	—	—	—	—	—	—

Moreover, specific adsorption of CNS^- ions decreases with rise of temperature, and this partially accounts for the shift of the cathodic polarization curves in the positive direction under these conditions.

We also studied the discharge of the complex thiocyanate anion $Cu(CNS)_2^-$ in presence of thiourea, which is recommended by a number of authors [11] as a brightening additive for copper electrolytes.

The results of the experiments are plotted in Fig. 3; it is seen that the presence of thiourea in the electrolyte results in some displacement of the polarization curves in the direction of more negative potentials. At high enough concentrations of thiourea, further additions of it to the electrolyte do not cause any additional shift of potential. It is likely that adsorption of molecules of thiourea on the cathode surface produces further retardation of the discharge of $Cu(CNS)_2^-$ anions. In the presence of 0.8 to 1.6 g of urea per liter in the electrolyte bright copper deposits are obtained at $D_c = 0.2$-0.4 amp/dm^2.

TABLE 2

Effect of Current Density on Current Efficiency (Cathode and Anode)

Current density D_c (in amp/dm^2)	0.12	0.20	0.40	0.60	0.80
Current efficiency (η_c) (%)	80.0	86.3	98.2	72.1	56.0
Current density D_a (in amp/dm^2)	0.03	0.05	0.10	0.15	0.20
Current efficiency η_a (%)	83.0	92.0	94.1	99.8	99.6

The anode and cathode current efficiencies are given in Table 2. It is seen that both the cathode and the anode current efficiencies increase with increasing current density. However, at $i > i_{lim\,Cu}$, at the given

concentration of copper in the electrolyte, the current efficiency drops sharply owing to simultaneous discharge of hydrogen. The anode current efficiency increases with increasing thiocyanate concentration in the electrolyte, whereas the cathode current efficiency remains almost unchanged. Moreover, it must be pointed out that at high anode current densities the anode current efficiency exceeds 100% owing to partial chemical dissolution of copper in the thiocyanate; the passivating film on the anode disappears in the process. Similarly, the current efficiency exceeds 100% with the use of newly cleaned anodes, and then decreases to values corresponding to the given current densities. After prolonged operation under the appropriate conditions (high D_a, frequent cleaning of the anodes), copper builds up in the electrolyte, with eventual precipitation of CuCNS on the floor of the cell. To avoid frequent adjustment of the electrolyte composition, the ratio of the cathode area (S_c) to the anode area (S_a) should be in the range $0.2 \leq S_c/S_a \leq 0.5$; under these conditions the electrolyte composition is maintained and no adjustment is needed for considerable periods (6-8 months).

The most suitable electrolyte for the production of finely crystalline copper deposits, for a number of reasons (less passivation of the anodes, better throwing power, etc.) proved to have the following composition: 0.1 mole of Cu^+ + 2.5 moles of KCNS per liter, under the following process conditions: temperature not higher than 25°, D_c = 0.15-0.25 amp/dm^2.

Under these conditions good deposits, with firm adherence, are obtained only on copper, copper-based alloys, and iron of low carbon content (not more than 0.1%C). Coatings on steel often had poor adherence to the basis metal. This defect can be avoided by a brief increase of current density at the start of electrolysis; prolonged electrolysis at high current densities yields spongy deposits. Therefore, the best procedure for production of deposits with good adherence to steel consists of an initial current "shock" at D_c = 1.0-1.6 amp/dm^2 followed by deposition of copper at D_c = 0.15-0.25 amp/dm^2. This procedure was tested on a large number of specimens.

Copper coatings deposited from thiocyanate electrolytes under the above conditions, and also thickened to 25-30 μ by subsequent deposition of copper from an acid copper electrolyte, did not peel off during repeated bending of the specimens according to the GOST test procedure.

The porosity of the deposits was investigated by means of the ferroxyl test [12]. It was found that a nonporous coating is obtained when the deposit is 1.0-1.25 μ thick.

SUMMARY

1. A thiocyanate electrolyte for copper plating, with the composition (in moles/liter): 0.1 CuCNS, 2.5 KCNS has been studied and tested. This electrolyte is recommended for use instead of cyanide electrolytes.

The process conditions are: temperature not over 25°, $0.2 \leq \frac{S_c}{S_a} \leq 0.5$, $D_{c\ init.}$ = 1.2-1.6 amp/dm^2, $\tau_{init.}$ = 2-3 seconds, D_c = 0.15-0.25 amp/dm^2, τ = 10-15 minutes, l = 1.0-1.8 μ.

2. Addition of 0.8-1.6 g of thiourea per liter to the electrolytegives bright copper deposits.

3. The throwing power of the electrolyte and the uniformity of the coating over articles of complex configuration are similar to those of cyanide baths.

In conclusion, the authors express their deep gratitude to Head of the Laboratory of Physical Chemistry of the State Institute for the Planning of the Nickel Industry, V. L. Kheifets, for valuable advice on the development of a thiocyanate electrolyte for copper plating.

LITERATURE CITED

[1] V. I. Lainer and N. T. Kudryavtsev, Fundamentals of Electroplating, I (State Sci.-Tech. Press, Moscow, 1953).*

[2] S. V. Gorbachev and A. V. Izmailov, J. Phys. Chem. 2 (1952).

[3] Yu. V. Baimakov and R. B. Popov, Coll. Trans. Sci. Res. Inst. Aluminum (1934); O. Kudra and Kleibs, Mem. Inst. Chem. Acad. Sci. USSR 6 (1940).

* In Russian.

[4] A. N. Gershevich and L. V. Gamburg, Corrosion and its Prevention 6 (1940).

[5] L. I. Kadaner, Latest Progress in Electroplating (Kharkov Univ. Press, Kharkov, 1951).*

[6] A. T. Vagramyan and N. N. Balashova, Trans. Conf. on Electrochemistry (Izd. AN SSSR, Moscow, 1953), p. 237. *

[7] A. N. Frumkin, Z. Electrochem. A 164, 121 (1933).

[8] O. A. Esin and V. N. Shikhov, J. Phys. Chem. 14, 3 (1940).

[9] Ya. V. Durdin and Z. U. Dukhnyakova, Collected Papers on General Chemistry I, 157 (Leningrad State Univ. Press, 1953).*

[10] Ya. V. Durdin and S. A. Nikolaev, J. Leningrad Univ. 5, 163 (1955).

[11] Metal Finishing 48, 1, 73 (1950).

[12] G. T. Bakhvalov, L. N. Birkgan, and B. P. Labutin, Electroplater's Manual (Metallurgy Press, Moscow, 1953). *

Received December 15, 1955.

* In Russian.

OXIDATION OF CYCLOPENTANONE WITH NITRIC ACID

E. N. Zilberman and A. I. Kirillov

Oxidation of cyclopentanone with nitric acid yields glutaric acid with succinic acid as a side product [1-3]. The use of 50% nitric acid is recommended for oxidation of cyclopentanone [2]. It is reported in the patent literature [3] that cyclopentanone is oxidized with 8-18% nitric acid to obtain glutaric acid. It has been shown [4] that in the oxidation of cyclohexanol with nitric acid the principal reaction product may be either adipic or glutaric acid, depending on the concentration of nitric acid. This suggests that the formation of glutaric acid in the oxidation of cyclopentanone also depends on the nitric acid concentration. No information on this is available in the literature. Neither is there any information in the published papers on the composition of the gas phase of the oxidation products of cyclopentanone (or other ketones or alcohols) with nitric acid.

We studied the oxidation of cyclopentanone with nitric acid in the range of 5 to 85% concentration. The yields of glutaric and succinic acid were determined by partition chromatography [4, 5]. The principal gaseous reaction products were: nitrogen dioxide, nitric oxide, nitrous oxide, nitrogen, and carbon dioxide. The gaseous mixture also contained dimerized NO_2. The concentration of N_2O_4 depended on the temperature of the gas and the partial pressure of NO_2. A method for quantitative analysis of this mixture was developed. To determine NO_2 and N_2O_4, the gas was treated with NaOH solution. The following reaction took place:

$$2NaOH + NO_2 + NO \rightarrow 2NaNO_2 + H_2O. \quad (1)$$

Since more NO than NO_2 was formed in all the experiments, the reaction

$$2NaOH + 2NO_2 \rightarrow NaNO_2 + NaNO_3 + H_2O \quad (2)$$

did not occur [6]. The separate contents of NO_2 and N_2O_4 were determined from the equilibrium constants for the dimerization reaction of nitrogen dioxide [7]. Another sample of the gas was oxidized with hydrogen peroxide. The contents of NO, NO_2, and N_2O_4 in the gas were calculated from the amount of nitric acid formed. The gas which did not dissolve in the peroxide solution was passed consecutively through alkaline pyrogallol solution, alkali, methanol (to absorb nitrous oxide), and water. The residue was nitrogen. A third sample of the gas was used for determination of carbon dioxide (by precipitation with barium hydroxide). The concentration of water vapor was calculated from the vapor pressure of H_2O over aqueous nitric acid solutions at 20° [8]. The nitrous oxide content was found by difference.

The experimental results are summarized in the table. The data were used to calculate the yields of glutaric and succinic acids (Fig. 1). From the known amount of HNO_3 reduced to nitrogen oxides (found by difference from the HNO_3 contents in the original nitric acid and in the liquid reaction products) and the percentage contents of N_2, N_2O, NO, NO_2, and N_2O_4 in the exit gases at the end of each experiment it was easy to calculate the absolute amounts of each of these gases formed in the oxidation of cyclopentanone under various conditions (Fig. 2). The absolute amount of carbon dioxide formed in the oxidation of cyclopentanone was found from the absolute amounts of nitrogen oxides and the percentage of CO_2 in the gaseous products (Fig. 1, Curve 3).

Oxidation of Cyclopentanone With Nitric Acid

Experiment No.	Oxidation temperature (°C)	Cyclohexanone (in g)	Nitric acid before oxidation: in g	Nitric acid before oxidation: as % HNO_3	Nitric acid after oxidation: in g	Nitric acid after oxidation: as % HNO_3	Acid yields, % of theoretical: succinic	Acid yields, % of theoretical: glutaric	Gas phase composition (in vol. %) at 20°: N_2	N_2O	NO	NO_2	N_2O_4	CO_2
1	75	15.5	367.0	85.0	340.0	73.4	68.5	17.8	5.6	7.8	49.1	7.4	5.7	24.0
2	75	15.5	354.5	76.0	331.0	63.7	66.8	22.8	6.2	9.7	47.4	7.0	5.4	23.7
3	75	15.7	347.5	65.3	330.5	54.1	58.3	34.2	7.1	11.9	46.5	6.5	4.5	22.6
4	75	14.7	378.0	55.8	369.0	46.3	44.5	48.8	10.0	26.5	31.5	5.1	2.7	23.0
5	75	14.5	323.0	46.0	321.0	37.1	35.2	57.0	8.0	43.3	14.1	3.9	1.7	27.5
6	75	14.6	312.5	39.9	312.5	31.9	37.0	58.7	8.5	59.0	5.3	2.5	0.6	22.4
7	75	10.8	302.5	34.6	302.5	28.2	35.8	63.5	6.7	72.6	2.7	1.4	0.2	14.6
8	75	10.8	296.5	30.7	298.5	24.6	28.6	69.5	6.3	73.6	2.3	0.5	0.05	15.3
9	75	10.9	286.0	25.0	292.0	19.8	18.7	81.2	6.2	77.0	2.0	0.3	0.0	12.5
10	90	13.6	334.0	20.0	340.5	14.5	14.4	85.4	5.8	70.5	5.7	0.5	0.05	15.3
11	90	14.0	325.0	15.0	332.0	9.4	10.1	87.5	5.4	74.4	5.4	1.0	0.1	11.5
12	100	14.0	316.0	10.0	320.0	4.5	12.9	80.0	6.1	62.9	3.6	1.6	0.3	23.3

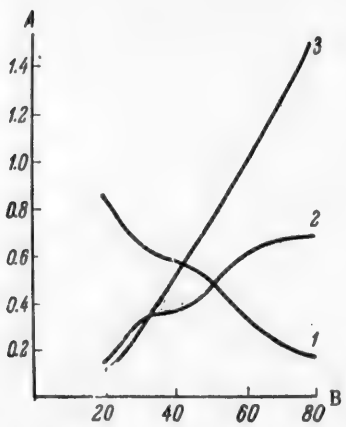

Fig. 1. Variation of the composition of the oxidation products of cyclopentanone with the nitric acid concentration.
A) Amounts of glutaric acid (1), succinic acid (2), and carbon dioxide (3) (in moles) obtained from one mole of cyclopentanone; B) HNO_3 concentration (in %).

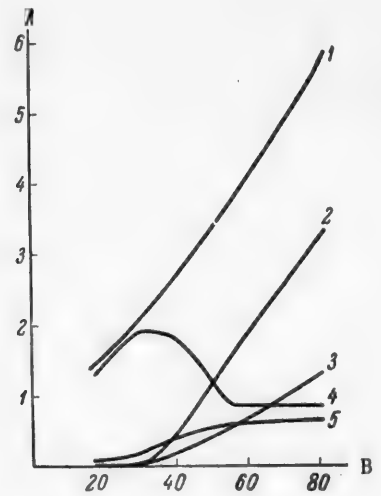

Fig. 2. Variation of the composition of the reduction products of nitric acid with its concentration.
A) Composition of HNO_3 reduction products (molar); B) HNO_3 concentration (%).
1) HNO_3, 2) NO, 3) NO_2, 4) N_2O_4, 5) N_2.

Cyclohexanone is oxidized mainly by the three over-all reactions:

$$C_5H_8O \xrightarrow{+3\,O} \underset{\text{glutaric acid}}{HOOC(CH_2)_3COOH} \qquad (3)$$

$$C_5H_8O \xrightarrow{+6\,O} \underset{\text{succinic acid}}{HOOC(CH_2)_2COOH} + CO_2 + H_2O \quad (4)$$

$$C_5H_8O \xrightarrow{+13\,O} 5CO_2 + 4H_2O. \quad (5)$$

It follows from Fig. 1 that Reaction (4) predominates at high HNO_3 concentrations in the reaction mixture, while Reaction (3) predominates at low HNO_3 concentrations. Increase of the HNO_3 concentration favors complete oxidation of cyclopentanone to CO_2. At nitric acid contents below 35-40% the effect of Reaction (5) is negligible and CO_2 is formed only by Reaction (4). With decreasing concentration of HNO_3 its reduction to NO, NO_2, and N_2 diminishes. When the HNO_3 content is below 30% only very small amounts of NO and NO_2 are formed. It is clear from Fig. 2 that the curve for the reduction of nitric acid to N_2O follows a different course. There are some deviations from the above-named relationships with increase of the oxidation temperature (Experiments Nos. 10-12). No direct relationship could be established from the results of these experiments between Reactions (3), (4), or (5) and the reduction of HNO_3 to any given substances.

The highest yield of glutaric acid (85-87% of theoretical) was obtained by oxidation of cyclopentanone under the following conditions: nitric acid concentration in the reaction mixture 10-20%, temperature 90° (oxidation was slow at lower temperatures). In these experiments 0.1 g of ammonium vanadate was added to 300-350 g of nitric acid and the oxidation was continued for 15-20 minutes.

EXPERIMENTAL

Cyclopentanone (b. p. 130°, d_4^{20} 0.948) was obtained by pyrolysis of adipic acid in presence of barium hydroxide.

The apparatus used for oxidation of cyclopentanone was the same as that described previously for the oxidation of cyclohexanol to adipic acid [4]. Cyclopentanone was added for 15-20 minutes to nitric acid containing 0.1 g of ammonium vanadate. The other conditions of the reaction are given in the table. The temperature showed fluctuations of ± 1.5°. A liquid reaction product and exit gases were obtained in the oxidation. Nitric acid in the liquid was determined by the Devarda method, and glutaric and succinic acids were determined chromatographically [4]. In Experiments Nos. 1-3, a small solid residue was also formed; this was mainly succinic acid. To simplify the chromatographic analysis, water was added to the reaction products in Experiments Nos. 1-3 until the solid phase dissolved, and only the liquid reaction product was analyzed. (In Column 7 of the table, the nominal HNO_3 concentrations, which would be present if the products were homogeneous, are given for Experiments Nos. 1-3).

SUMMARY

When cyclopentanone is oxidized with 10-20% nitric acid, the main reaction products are glutaric acid and nitrous oxide. As the nitric acid concentration is increased, larger amounts of succinic acid, nitric oxide, nitrogen dioxide, and nitrogen are formed.

LITERATURE CITED

[1] W. Hentzschel and W. Wislicenus, Ann. 275, 315 (1893).

[2] C. F. H. Allen, Organic Syntheses, I IL, (Moscow, 1949), p. 138.*

[3] S. H. Mc Allister, U. S. Patent 2,286,559; Chem. Abstr. 36, 7031 (1942).

[4] E. N. Zilberman, S. N. Suvorova, and Z. S. Smolyan, J. Appl. Chem. 29, 4, 621 (1956).**

[5] V. Zbinovsky and R. H. Burris, Anal. Chem. 26, 208 (1954).

* Russian translation.

** Original Russian pagination. See C. B. Translation.

[6] D. A. Epshtein, Chemistry and Technology of Bound Nitrogen (ONTI, 1935), p. 435.*

[7] Yu. P. Bernatsky, J. Chem. Ind. 6, 21 (1944); I. N. Kuzminykh, Control of Nitrose Gases (Goskhimizdat, Moscow, 1945), p. 73.*

[8] Chemist's Reference Book, III (Goskhimizdat, Moscow-Leningrad, 1952), p. 248.*

Received November 23, 1955.

* In Russian.

THERMOCATALYTIC CONVERSIONS OF ALKYLNAPHTHALENES (ISOAMYLNAPHTHALENE)

B. G. Gavrilov and N. Kim

Ipatyev and Klyukvin [1] heated naphthalene at 450-480° in presence of nickel oxide and aluminum oxide catalyst under hydrogen at a pressure of 100 atm. and obtained 30% of hydrocarbons of the benzene series and 50% of tetrahydronaphthalene.

Dobryansky and Katsman [2] obtained naphthalene and dinaphthyl by the cracking of tertiary butylnaphthalene.

In later studies of the reactions of ethyl- and butylnaphthalenes in presence of active clay (at temperatures not greater than 300°) migration of the alkyl radicals was observed, with formation of di- and trisubstituted naphthalenes, and also formation of methanic and naphtheno-aromatic hydrocarbons by reactions involving redistribution of hydrogen [3, 4].

To establish the laws governing these reactions it was necessary to carry out further studies of the reactions of alkylnaphthalenes, on members of the series having both more complex and branched radicals. β-sec-amylnaphthalene was investigated for this purpose.

Conditions	Experiment No. 1	Experiment No. 2	Experiment No. 3	Experiment No. 4
Apparatus	Autoclave	Flask under reflux	Autoclave	Autoclave
Temperature (in °C)	250 ± 5°	260 ± 2	275 ± 5	275 ± 5
Pressure (mm)	11	1	12	5
Heating time (hours)	10	5	15	11
Conversion (%)	67.5	60.4	72.4	69.3
Starting material	Monoamylnaphthalene	Monoamylnaphthalene	Monoamylnaphthalene	Diamylnaphthalene
Substances formed in the experiments (in %)				
Pentane	0.86	1.1	1.15	1.06
Naphthalene	34.31	35.2	39.8	16.51
Monoamylnaphthalene	32.46	39.6	27.6	20.3
Diamylnaphthalene	9.62	10.4	10.85	30.75
Dinaphthyl	–	–	4.72	–
Tar	8.83	3.1	5.65	16.56
Carbon on catalyst	2.67	1.6	2.0	2.87
Losses	11.23	9	8.25	11.85
Total	100.0	100.0	100.0	100.0

The starting material had the following properties: b. p. (at 5 mm Hg) 128-131°, n_D^{20} 1.5796, d_4^{20} 0.9709.

The position of the amyl radical was determined by oxidation of the original hydrocarbon with 5% nitric acid in sealed tubes at 170-175°. The resultant β-naphthoic acid melted at 183.5-185°.

The catalyst used in the experiments was activated with dilute hydrochloric acid and washed free of chloride ions.

The experiments were carried out in an autoclave and in a flask fitted with a reflux condenser with a ground-glass joint. Diamylnaphthalene prepared and collected in the earlier experiments was used for Experiment No. 4. In the autoclave experiments, the reaction was assumed to be ended when the pressure became constant; in the flask experiments, when the temperature of the hydrocarbon layer over the catalyst, which gradually fell during the reaction, became constant.

In all the experiments the catalyst – hydrocarbon ratio was 1:0.5.

The melting point (301-302°) of the dinaphthoic acids obtained from the resultant diamylnaphthalenes indicated that the structure of the latter was 2,7-diamyl or 2,6-diamyl, or a mixture of the two was present.

The results of the experiments are given in the Table.

The principal reaction in all the experiments with monoamylnaphthalene yields naphthalene, diamylnaphthalene, and pentane.

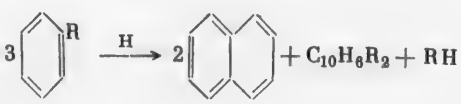

Formation of naphthalene and pentane is possible only by internal hydrogenation.

In the experiment under normal pressure the formation of amylene can be ascribed to pyrolysis of the starting material accompanying the above reaction.

Because of the absence of high pressure in this experiment, the olefin was preserved

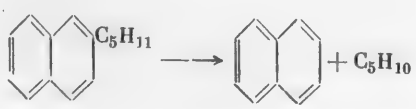

Increase of the temperature to 275° in the experiments with monoamylnaphthalene resulted in formation of dinaphthyl

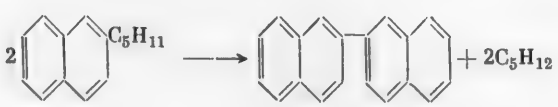

In the experimental conditions used, the principal reaction of diamylnaphthalene conversion was:

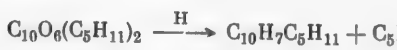

This reaction, too, is possible only if internal hydrogenation occurs.

The formation of a trisubstituted derivative of naphthalene, by analogy with the alkylbenzenes [5],

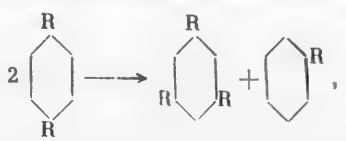

is evidently impossible in this case owing to the low thermal stability of the corresponding naphthalene derivatives in these conditions.

Comparison of the results of experiments on thermocatalytic conversions of amylnaphthalenes over active clays with the conversion of alkylbenzenes under analogous conditions showed that, in addition to the migration of unchanged alkyl radicals, characteristic for the alkylbenzenes, specific reactions also took place, with formation of naphthalene, dinaphthyl, pentane, and pentene.

SUMMARY

1. It was shown in a study of the thermocatalytic conversions of β-sec-amylnaphthalene and diamylnaphthalene over active natural clay that characteristic reactions of the original hydrocarbons result in the formation of pentane, naphthalene, diamylnaphthalene, and dinaphthyl. Reactions of pentane and naphthalene formation are impossible without internal hydrogenation. The hydrogen sources can be either the carboids deposited on the catalyst, or complex aromatic hydrocarbon structures with condensed nuclei of depleted hydrogen content, present in the tar.

2. The β-monoamylnaphthalene and 2,6- or 2,7-diamylnaphthalene formed in the experiments are the most stable isomers under the given conditions.

3. Increased pressure favors the formation of saturated hydrocarbons, primarily paraffins.

LITERATURE CITED

[1] V. I. Ipatyev and N. A. Klyukvin, J. Russ. Phys.-Chem. Soc. 11, 5, 245 (1925).

[2] A. F. Dobryansky and S. V. Katsman, J. Gen. Chem. 7, 1355 (1937).

[3] B. G. Gavrilov and S. K. Pushnoi, Sci. Mem. Leningrad State Univ. 169, 13 (1953).

[4] B. G. Gavrilov and E. N. Nikitina, J. Gen. Chem. 24, 303 (1954). *

[5] B. G. Gavrilov and O. I. Zhgun, Sci. Mem. Leningrad State Univ. 163, 177 (1953).

Received June 26, 1956.

* Original Russian pagination. See C. B. Translation.

USE OF ETHYL ETHERS OF AMYLENE CHLOROHYDRINS IN MIXTURES WITH DICHLORIDES FOR DEPARAFFINIZATION (DEWAXING) OF AVIATION OIL

A. K. Seleznev

Organic Chemistry Laboratory, the Grozny Petroleum Institute

Seleznev [1, 2] has described the synthesis of β-chloro ethers from cracking propylene and butylenes, and their use as solvents for dewaxing of aviation oil.

The aim of the present investigation was to prepare ethyl ethers of amylene chlorohydrins mixed with dichlorides, from the pentane – amylene cracking fraction, and to test the product as solvent for dewaxing of aviation oil.

EXPERIMENTAL

The refinery pentane – amylene cracking fraction was distilled through a column and the 30-40° fraction was collected. This fraction was treated [3] with concentrated hydrochloric acid in the cold to yield a fraction containing normal-chain amylenes. As is known, strong hydrochloric acid has no action on normal-chain amylenes under these conditions. The fraction had iodine number 88, corresponding to 23.9% of amylenes. This product was used for synthesis of chloro ethers mixed with dichlorides.

258 g of caustic potash in the form of a fine powder, 218 ml of ethyl alcohol, and 1760 ml of the pentane – amylene fraction (30-40°) was put into a flask. This mixture was cooled to – 10°, and chlorine was passed into the mixture, with mechanical stirring, from a cylinder at 5 liters per hour (controlled by a flow meter). At the end of the reaction the product was diluted with water to dissolve calcium chloride, the upper layer was washed to remove alcohol, dried over calcium chloride, and distilled.

Distillation yielded 265 g of a fraction boiling in the 126-156° range; this consisted of ethyl ethers of normal-chain amylene chlorohydrins mixed with dichlorides (d_4^{20} 1.0294, n_D^{15} 1.444).

Analysis of the 126-156° fraction, by Carius: 0.142 g substance: 0.21 g AgCl, 0.07275 g (51.3%) chloro ethers. 0.136 g substance: 0.20 g AgCl, 0.0708 g (52.0%) chloro ethers.

The contents of chloro ethers and dichlorides were calculated from the weight of the 126-156° fraction taken for the Carius analysis and the weight of silver chloride formed.

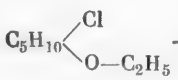

$C_5H_{10}Cl_2$—2AgCl

$(0.142 - y) - x$ $\qquad$ $y - (0.21 - x)$

These results show that the 126-156° fraction contains 51.6% chloro ethers and 48.4% dichlorides.

The yield of chloro ethers was 137 g, 51.6% of the theoretically calculated for amylenes in the 30-40° fraction.

Petrov [4] used the alkali method for synthesis of the ethyl ether of pentene-2 chlorohydrin (b. p. 153-156°, d_4^{15} 0.9612, n_D^{15} 1.4312).

Test of the 126-156° fraction for deparaffinization of aviation oil. A raffinate obtained from Karachukhur – Surakhany heavy oil, with the following characteristics, was used in the tests of dewaxing of aviation oil: d_4^{20} 0.881, Saybolt viscosity at 98.9° 96, viscosity-weight constant 0.803, coke 0.215%, Pensky – Marten flash point 218, NPA color 7.

A mixture of the raffinate and the 126-156° fraction solvent was warmed to 60° to dissolve the raffinate, cooled to – 25° in the freezer, and filtered.

The raffinate – solvent ratio was 1:4 in all the experiments. The filtrate was distilled under vacuum to remove the solvent, and the pour point and oil yields were determined. The results are given below.

Results of dewaxing of aviation oil with the 126-156° fraction:

Experiment No.	Solvent	Oil yield (%)	Pour point of dewaxed oil (°C)
1	126-156° fraction	76.6	–15.5
2	126-156° fraction	75.8	–16.0
3	Dichloroethane – benzene (refinery solvent)	73.6	–18.5

These results show that the 126-156° fraction, consisting of 51.6% chloro ethers and 48.4% dichlorides, extracts more oil than the refinery solvent (dichloroethane – benzene) from the raw material, but the pour point of this oil is somewhat higher than that of the oil obtained by means of the refinery solvent.

The dewaxed oils obtained in Experiments 1 and 2, with the use of the 126-156° fraction, were mixed; the mixture had the following constants: d_4^{20} 0.8965, kinematic viscosity (centistokes) 23.71 at 100°, 174.68 at 50°, ratio of kinematic viscosity at 50° to kinematic viscosity at 100°, 7.37 (standard for MS 20, not over 7.85). Viscosity index 95.

According to GOST 1013-49, the kinematic viscosity of refinery aviation oil (in centistokes) is not less than 20. The ratio of the kinematic viscosities at 50° and 100° is not greater than 7.85.

SUMMARY

A mixture of β-chloroethers and dichlorides, obtained from the pentane – amylene cracking fraction, can be used as solvent for dewaxing of aviation oil.

LITERATURE CITED

[1] A. K. Seleznev, J. Appl. Chem. 27, 3 (1954).*

[2] A. K. Seleznev, J. Appl. Chem. 27, 6 (1954). *

[3] E. D. Gimpelevich, Bull. Acad. Sci. Azerbaidjan SSR 6 (1947).

[4] A. A. Petrov, Trans. Voronezh. Univ. 9, III (1937).

Received January 16, 1956.

* Original Russian pagination. See C. B. Translation.

USE OF THE GUSTAVSON – FRIEDEL – CRAFTS REACTION FOR THE PRODUCTION OF LUBRICATING OILS FROM EXTRACTS

I. F. Radzevenchuk

The production of high-grade motor fuels and lubricating oils is the main task of the petroleum industry. The interests of the national economy demand that this problem should be solved by the most complete utilization of the petroleum possible [1, 2]. However, in the modern processes about a half of the petroleum remains in the form of low-grade residues [3]. It therefore becomes necessary to find ways of converting these residues into useful products. Such conversion may be effected by synthesis, by chemical conversion of hydrocarbons in extracts into lubricating-oil and motor-fuel hydrocarbons.

Our earlier investigation of alkylation of avtol-6 *distillate with chlorinated paraffin wax in presence of aluminum chloride showed that an oil with a high viscosity index can be obtained from low-grade oil by this reaction [4]. In the present study, the Gustavson – Friedel – Crafts alkylation reaction was extended to extracts obtained in the selective purification of oil, for production of lubricating oils. Extracts from selective purification of oil are usually burned. This utilization of the extracts is quite uneconomic, as they consist of mixtures of high-boiling hydrocarbons, mainly naphthenic–aromatic, aromatic, and naphthenic hydrocarbons with short aliphatic chains [5].

The chemical composition of extracts obtained in selective purification of oils has been studied by a number of authors [6-8]. Mair and Willingham, who studied the extract from selective purification of a mid-continent petroleum, concluded that the hydrocarbons in the extract consist of: 1) 60% of naphthenes with 1 to 3 rings in the molecule; 2) 15% of hydrocarbons with 1 aromatic and 1-3 naphthenic rings in the molecule; 3) 14% of hydrocarbons with 2 aromatic and 2 naphthenic rings in the molecule; 4) 14% of hydrocarbons with more than 2 aromatic and 1-2 naphthenic rings in the molecule. Fractions 2, 3, and 4 contained small amounts of sulfur, nitrogen, and oxygen.

Because of the different aniline points of the oil hydrocarbons, separation by means of selective solvents is not sharp enough [7, 8] and valuable oil hydrocarbons are partially extracted. Neyman-Pilat [8] divided oil hydrocarbons into two groups, which pass into the raffinate and extract respectively. The following pass into the extract:

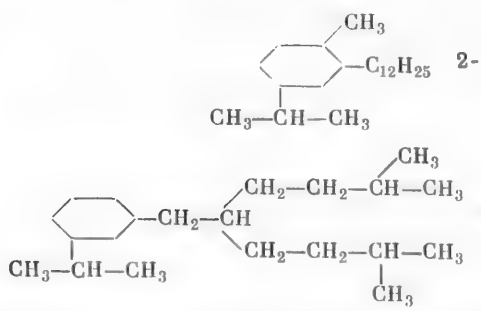

2-n-dodecyl-p-menthane

α-perhydrocarvacryl-β-diisoamylethane

* Avtol is an automobile lubrication oil available in various grades: avtol-6, avtol-18, etc. Publisher's note.

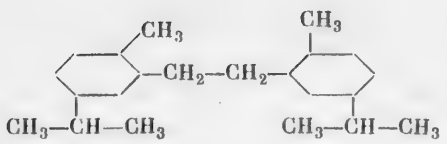

α,β-diperhydrocarvacrylethane, etc.

If the extracts are not processed for oils, these hydrocarbons and a number of others (it must be remembered that extracts from selective purification of oils also contain part of the good oil) are lost to oil production.

If long aliphatic chains are attached to the aromatic, naphtheno–aromatic, and naphthenic hydrocarbons of the extract, hydrocarbons are formed similar in structure to the hydrocarbons of high-grade oil [9, 10] and oil of a high viscosity index can be obtained from the extract.

In the present investigation an attempt was made to convert the hydrocarbons in the extracts by means of the alkylation reaction.

The extracts or their fractions were used as aromatic components in the alkylation reaction. The other reaction component was chlorinated paraffin wax. The catalyst was aluminum chloride.

EXPERIMENTAL

Two extracts were used in the alkylation experiments: 1) an extract obtained from avtol-6 distillate of Lok-Batan oil after purification with furfural; 2) an extract obtained at the Baku refinery after furfural purification of avtol-18 distillate from a mixture of light Bibi-Eibat and Lok-Batan oils (furfural consumption 100%).

Alkylation experiments with avtol-6 extract. The furfural extract of avtol-6 distillate was prepared by a laboratory method. 1.5 part of technical furfural per 1 part of oil by weight was taken. The oil and furfural were heated to 95° without stirring. They were then stirred for 15 minutes at the same temperature. The settling lasted for 4-5 hours at 90°. The solvent was removed from the extract and raffinate by steam distillation to a negative reaction for furfural. The yield of extract was 14% calculated on the raffinate. The constants of the extract are given in Table 1.

TABLE 1

Constants of the Original Extract and of Oils Obtained From It.

Experiment No.	% $AlCl_3$	Amt. of chlorinated wax (%)	Kinematic viscosity (in centistokes) at temp. (°C)		Viscosity index	$d_{15.6}^{15.6}$	$n_D^{24.5}$	Solidification pt. (°C)	Yield (% on extract)
			37.8	98.9					
Original extract	—	—	235.5	11.025	—48.9	0.9838	—	—20	—
Treated extract	3	—	176.87	9.72	negative	0.9626	1.540	—	—
1	3	13	123.5	9.03	21.18	—	—	—4°	40
2	3	23	87.48	7.93	44.6	0.9534	1.5288	0°	65
3	3	28	69.60	7.403	64.9	0.9507	—	0°	60
4	3	37	34.71	5.47	101.7	0.9423	1.5120	0°	65
5	1.5	13	125.36	9.93	29.56	0.9644	—	—	60

The chlorinated wax was made from white Grozny wax with m. p. 52°. Chlorine was passed through it at 60-70° to give 12-13% weight increase. The product was dissolved in ligroine, the solution was cooled, and unchanged wax was filtered off. The ligroine was not removed from the chlorinated wax, and acted as the solvent in alkylation.

TABLE 2

Constants of Fractions Obtained by Vacuum Distillation of Avtol-18 Extract

Fraction No.	Temperature range (°C)	Yield (wt. %)	Color	$d_{15.6}^{15.6}$	d_{20}^{20}	Viscosity-weight constant	Kinematic viscosity (in centistokes) at temp. (°C)		Viscosity index	Solidification point (°C)	n_D
							98.9	50			
1	80—192	7.9	Transparent yellow-orange	0.9725	—	0.9499	4.667	43.053	—100	—21.5	1.540
2	192—195	9.5	Yellow-orange	—	0.9918	0.9594	8.948	78.47	negative	— 3	1.5602
3	195—214	10.6	Yellow-orange with green fluorescence	—	1.0007	0.9681	13.75	237.2	negative	— 3	1.566
4	214—230	12.9	Greenish	1.0141	—	0.9732	19.52	421	negative	— 2	1.571
5	230—234	13.3	Green	1.085	—	—	28.35	—	—	0—5	1.575
6	234—293	31.6	Dark green	1.032	—	—	viscous, low mobility		—	+ 3	—
7	residue in steam 330°	14.2	black	—	—	—	solid		—	—	—

After removal of the ligroine the chlorinated wax had $d_{15.6}^{15.6} = 0.9067$ and contained 15% of chlorine.

The technical aluminum chloride catalyst had the following composition: 1) water-soluble portion – Fe 1.89%, Al 20.18%, Cl 76.63%; 2) insoluble portion – Fe_2O_3 0.72%, Al_2O_3 – absent, SiO_2 0.22% (total).

The reaction conditions were the same as are used for synthesis of Paraflow [11]. A mixture of chlorinated wax solution in ligroine and of the extract of avtol-6 distillate was heated to 60°. Aluminum chloride was then added by small portions with vigorous stirring. The mixture was stirred and heated for 2 hours and then settled. The top oily layer was decanted from the tarry deposit, washed with water, and heated with 10% of activated gumbrin at 240°. The ligroine solvent was distilled off in the process; the oil was neutralized and freed from suspended tarry particles. The product was filtered. At first the amount of aluminum chloride used was constant, 3%, while the amounts of chlorinated wax were varied. Constants of oils obtained by alkylation of the extract with different amounts of chlorinated wax are given in Table 1. Constants of the original extract and of the extract after treatment with 3% aluminum chloride are given for comparison.

It follows from the data in Table 1 that the viscosity index of the oil produced from the extract reaches 101. Its viscosity and density are considerably lower than those of the original extract. A decrease of the amount of aluminum chloride from 3% to 1.5% improved the quality and yields of the alkylation products. As has been reported [12], a small amount of $AlCl_3$ is sufficient for the alkylation reaction. If excess $AlCl_3$ is present, polymerization and condensation reactions take place, especially if the product is viscous (see experiments with extract of Soz avtol-18).

Thus, it is seen that the alkylation reaction can be used for reforming of hydrocarbons in avtol-6 extract in the desired direction, with production of good oils from the extract.

Experiments on alkylation of extract of Soz avtol-18 extract. The Soz avtol-18 extract (obtained at the refinery after purification of avtol-18 distillate with furfural) had the following constants: d_{20}^{4} = = 1.0317, Engler viscosity at 100°, 8.06. The viscosity index was strongly negative. The softening point by the "ring-ball" method was 0-5°.

Group composition of avtol-18 extract. (Marcusson method): asphaltenes 1.21, oil 80.90, tars: 1) benzene 7.89, 2) alcohol-benzene 10.05.

For a more detailed chemical characterization, the avtol-18 extract was fractionated under vacuum (0.3 mm). The constants of the fractions collected are given in Table 2. It follows from these data that avtol-18 extract has a high content of hydrocarbons, and rational utilization of these hydrocarbons is very desirable.

A series of experiments was carried out to determine the amount of aluminum chloride necessary for stabilization and purification of the extract. As a result of these experiments it was decided to use 5% of aluminum chloride for the alkylation reaction, as a high percentage did not have any significant effect on the quality of the extract. Alkylation of avtol-18 was carried out under the same conditions as for avtol-6. Table 3 contains the constants of the products formed by alkylation of the extract with different amounts of chlorinated wax.

It follows from the data in Table 3 that the viscosity index of the products increases considerably with increasing amounts of chlorinated wax used for alkylation. There was a particularly large increase of viscosity index as the result of the reaction with 28% of chlorinated wax. The value rose from − 10 to + 29. The viscosity and density of the oils formed decrease considerably. However, the change of the viscosity index is less for this raw material (avtol-18 extract) than for avtol-6 extract, while the viscosity decrease is greater. The alkylation product lowered the solidification points of other oils. Addition of 1% of the oil from Experiment 5 to standard avtol decreased the solidification point by 10°.

TABLE 3

Constants of Oils Obtained by Alkylation of Avtol-18 Extract with Different Amounts of Chlorinated Wax.

Expt. No.	%, $AlCl_3$	Amt. of chlorinated wax	Kinematic viscosity (in centistokes) at temp.		Viscosity index	$d_{15.6}^{15.6}$	Viscosity-weight constant	Solidification point (°C)	Yield, %
			37.8	98.9					
1	5	—	5043	42.01	negative	1.016	0.9673	+10	50
2	5	12	2117.5	35.24	negative	0.9984	0.9431	0	54
3	5	23	860.15	26.41	−10	0.9890	0.9343	0	77
4	5	28	430.9	19.21	29.14	0.9765	0.9263	+ 4° flows	70
5	3	33	292.9	16.03	39.92	0.9735	0.9214	0° sets 0°	91

The alkylation product from Experiment 4 was analyzed chromatographically. A solution of the oil in ligroine was passed through activated gumbrin. Two pale fractions were eluted by means of ligroine. A third fraction was extracted with alcoholic benzene. The yield of the first, colorless fraction was 1%, of the second, pale orange, 52%, and of the alcohol–benzene fraction, 40%. The alcohol–benzene fraction was dark brown and became covered with a hard film on exposure to air. The newly synthesized hydrocarbons were probably in the second fraction, as in the alkylation of avtol-6 distillate [4]. The constants of the second fraction were: viscosity index 47.63, kinematic viscosity at 37.8° = 149.3, at 98.9° = 11.002.

As the avtol-18 extract was very viscous and had a high content of tars and asphaltenes, it was decided to distill it before alkylation, and to alkylate the distillate. Steam distillation of avtol-18 extract yielded 50%

of a broad pale fraction with the following constants: $d_{15.6}^{15.6} = 0.9942$; kinematic viscosity at 37.8° = 400.7, at 98.9° = 10.48; viscosity index 27; solidification point + 1°. This distillate was alkylated under the same conditions as before in presence of 3% of aluminum chloride and 33% of chlorinated wax.

The product was treated as follows: 30 minutes before the end of the reaction 10% of activated gumbrin was added. The mixture was settled at 60° for two hours. 1.8% of tar was formed. The alkylation product was washed with water, and the solvent (ligroine) was distilled off in steam (up to 200°). The constants of the original distillate and of the oil obtained from it by alkylation are compared in Table 4.

TABLE 4

Constants of the Original Distillate and of the Oil Obtained From It

Material	% $AlCl_3$	Amount of chlorinated wax, %	Kinematic viscosity (in centistokes) at temp.(° C)		Viscosity index
			37.8	98.9	
Distillate of extract	–	–	400.9	10.48	– 27
After alkylation	3	33	87.79	7.93	44.72

It follows from this experiment that not the whole extract but its distillate should be alkylated. Alkylation of the distillate gives an oil similar to avtol-6 in viscosity and viscosity index. The residue from steam distillation of the extract may be converted into gilsonite.

Rational and total utilization of the hydrocarbons even in such viscous extracts as the extract of Soz avtol-18 is possible in this way.

In some experiments the distillate of avtol-18 extract was alkylated at a higher temperature and in presence of a larger amount of aluminum chloride. The products had very high viscosities and low viscosity indices. Evidently, increases of the amount of aluminum chloride and of the reaction temperature are inadvisable.

SUMMARY

1. The alkylation of extracts of avtol-6, Soz avtol-18, and of a distillate of the latter with chlorinated wax in presence of aluminum chloride was studied, and it was found that the extracts can be converted into lubricating oils by alkylation.

2. It was found that the viscosity indices of the oils formed increase with increasing percentage of the chlorinated wax used for alkylation. For example, the reaction of avtol-6 extract with 23% of chlorinated wax yielded 65% of an oil of viscosity index 44.6. When the amount of chlorinated wax was increased to 37%, the viscosity index of the oil rose to 101.

3. It was found that in the case of highly viscous extracts such as Soz avtol-18 extract it is preferable to alkylate the steam distillates of the extracts rather than the extracts themselves. The steam distillate of avtol-18 extract yielded an oil with viscosity close to that of avtol-6 and viscosity index 44.7.

LITERATURE CITED

[1] S. R. Sergienko, Petroleum Economy 2 (1953).

[2] V. I. Karzhev, D. I. Orochko, et al., Petroleum Economy 9 (1953).

[3] S. R. Sergienko, Petroleum Economy 2 (1955).

[4] I. F. Radzevenchuk, J. Appl. Chem. 29, 11, 1697 (1956).*

[5] N. I. Chernozhukov, S. E. Krein, and B. V. Losikov, Chemistry of Mineral Oils (1951), p. 156.**

[6] B. Mair and C. Willingham, Ind. Eng. Chem. 30, 11, 1256 (1938).

[7] B. Mair and C. Willingham, Ind. Eng. Chem. 28, 12, 1452 (1936).

[8] Neyman-Pilat and S. Pilat, Ind. Eng. Chem. 33, 11, 1328 (1941).

[9] L. G. Zherdeva, Grozny Petroleum Producer 6-7 (1937).

[10] K. van Nes and H. van Westen, Aspects of the Constitution of Mineral Oils (1954), pp. 390, 391, 392.

[11] G. H. B. Davis, U. S. Patent 1, 815,022 (1931).

[12] Z. N. Nazarova, Bull. Univ. Central Asia 26, 59 (1949).

Received October 31, 1955.

* Original Russian pagination. See. C. B. Translation.

** In Russian.

SYNTHESIS OF SOME NEW DIALLYL ESTERS OF DIBASIC ACIDS

M. F. Shostakovsky, A. M. Shur, and B. F. Filimonov

Because of the relative simplicity of their synthesis and their ability to form space polymers, diallyl esters of dibasic acids are of considerable practical interest.

The diallyl esters of the following acids were synthesized in the present investigation: diglycolic acid, di(carboxyethyl) ether, di(carboxyethyl) ether of ethylene glycol, glutaric acid, and pimelic acid.

EXPERIMENTAL

The original acids. Glutaric acid was prepared by oxidation of cyclopentanone [1], which was itself prepared from adipic acid [2]. Diglycolic acid was prepared by Eichloff's method [3], based on the reaction of monochloroacetic acid with barium hydroxide. Pimelic acid was prepared by reduction of salicylic acid [4].

Di(carboxyethyl) ether and ethylene glycol di(carboxyethyl) ether were synthesized by saponification of the cyanoethylation products of water and ethylene glycol respectively.

Water was cyanoethylated by a method based on an American patent specification [5] at 45° in dioxane in presence of 10% aqueous NaOH; a mixture of 53 g of acrylonitrile, 50 g of dioxane, and 10 g of aqueous NaOH was stirred in a flask fitted with a stirrer and thermometer. After 6 hours the mixture was cooled to room temperature, neutralized with hydrochloric acid until neutral to Congo red, and heated to remove dioxane. Fractionation of the residue yielded 28 g of substance (45% of the theoretically calculated yield of a product, boiling at 155-157° at 2.5 mm Hg). The boiling point and refractive index (n_D^{20} = 1.4380) of this di(cyanoethyl) ether practically coincided with literature data [5]. It was found during the experiment that the dioxane distilled off can be used repeatedly without any decrease of the yield of ether; moreover, our experiments showed that if the time of heating is increased from 6 to 10 hours the yield can be raised to 55%. Glycol was cyanoethylated [6] in presence of 40% NaOH, followed by neutralization, filtration, and vacuum distillation. The yield of β, β'-dicyanodiethyl ether of ethylene glycol was 62%. The boiling point (160-169° at 2 mm Hg) and the refractive index (n_D^{20} = 1.4490) agreed closely with literature data [6].

The dinitriles were saponified by boiling with concentrated hydrochloric acid [6]. The filtrate obtained after separation of the precipitated ammonium chloride was evaporated on the water bath under vacuum until a semiliquid mass was formed; this solidified to a crystalline mass after standing for three days over sulfuric acid in a vacuum desiccator. Residual ammonium chloride was extracted with acetone; removal of the acetone and drying over phosphoric anhydride in a vacuum desiccator yielded the solid acid. The yield of ethylene glycol di(carboxyethyl) ether after recrystallization from alcohol was 73%; di(carboxyethyl) ether was not recrystallized; alkali titration showed that it was 91.2% pure.

Synthesis of diallyl esters. Allyl alcohol (b. p. 94-97°, n_D^{20} = 1.412) was synthesized from glycerol and formic acid [7]. In some cases the 70% alcohol was used, prepared by the same method, but not dried by treatment with calcined potash.

The esterification was performed by the azeotropic method in apparatus similar to the Dean and Stark apparatus for determination of water in oil distillates, in presence of sulfuric acid.

The organic acid, allyl alcohol, benzene,* and sulfuric acid were put into the flask of the apparatus and the mixture was heated on a boiling water bath until the lower layer in the water-separation tube ceased to increase. The reaction mass was then washed twice with water, once with sodium carbonate, and again with water. The product was dried over anhydrous sodium sulfate, heated to remove benzene, and fractionated under vacuum. Table 1 gives the synthesis conditions, yields, and boiling points of the esters, and Table 2 gives their constants and analytical data.

TABLE 1

Synthesis Conditions and Properties of Diallyl Esters

Diallyl ester of	M. p. of original acid (°C)	Amounts taken				Reaction time, (hrs)	Yield of ester		B. p. °C	Pressure, (mm Hg)
		organic acid (g)	allyl alcohol (ml)	C_6H_6 (ml)	H_2SO_4 (ml)		in g	in %		
Glutaric acid	97	8.6	35	10	1	8	9.4	68	119	20
Diglycolic acid	146—148	8.6	35	10	1	4.2	11	80.3	139—140	5—6
Pimelic acid	101—103	9.5	50**	30	0.8	15	10.5	92	145—147	
Di(carboxyethyl) ether	—***	16.5	41	15	1	6	11	50	131—133	2
		27	100**	55	1.7	25	21	58	131—133	2
Ethylene glycol di(carboxyethyl) ether	62.3	20.6	27**	15	1	5	10	55	163—165	2.5

** Esterification with 70% allyl alcohol.

*** Unrecrystallized acid, 91.2% pure (by titration).

As the experiments with di(carboxyethyl) ether showed that the yield of ester is not decreased if 70% allyl alcohol is used, the latter was used for esterification of pimelic acid, sebacic acid, and ethylene glycol di(carboxyethyl) ether.

The esters are colorless liquids (the diglycolic acid ester turns yellow on standing). They are all heavier than water, insoluble in water, but soluble in organic solvents. They are easily absorbed by the skin, causing strong irritation.

Most of the esters have a fairly faint odor similar to that of allyl alcohol; the esters of diglycolic acid and di(carboxyethyl) ether have an odor similar to the odor of herring brine. All the esters polymerize on heating with benzoyl peroxide.

Polymerization. If the diallyl esters are heated with benzoyl peroxide for 30-35 hours in sealed tubes, soft gelatinous or loose polymers are formed. Copolymerization of these esters with divinyl adipate, pimelate,

* In the experiments with glutaric and diglycolic acid 0.2 g of hydroquinone was also added; later experiments showed that this addition is unnecessary, as the diallyl esters do not polymerize to any great extent during synthesis.

or sebacate yields, after 15 hours, transparent, colorless products the hardness of which depends on the monomer ratio in the original mixture. All the polymers and copolymers are insoluble in benzene and in acetone.

TABLE 2

Constants and Analytical Data of Diallyl Esters

Diallyl ester of	d_4^{20}	n_D^{20}	$MR_{theoret.}$	$MR_{exptl.}$	Elementary analysis						
					weight taken (g)	CO_2 (g)	H_2O (g)	C (%) found	C (%) calc.	H (%) found	H (%) calc.
Glutaric acid	1.0483	1.4520	55.37	54.60	0.2104	0.4805	0.1378	62.28	62.26	7.33	7.55
					0.2008	0.4585	0.1352	62.40		7.53	
Diglycolic acid	1.1046	1.4580	52.39	52.85	0.2016	0.4136	0.1171	55.95	56.07	6.45	6.54
					0.2012	0.4133	0.1175	56.02		6.49	
Pimelic acid	1.0119	1.4562	64.60	64.20	0.1358	0.3224	0.1021	65.02	64.97	8.43	8.39
					0.1502	0.3589	0.1129	65.30		8.40	
Di(carboxyethyl) ether	1.0679	1.4542	61.63	61.50	0.1779	0.3872	0.1191	59.40	59.49	7.48	7.49
					0.1404	0.3063	0.0941	59.58		7.51	
Ethylene glycol di(carboxyethyl) ether	1.0869	1.4613	72.44	72.51	0.1101	0.2354	0.0768	58.40	58.70	7.81	7.74
					0.1347	0.2873	0.0938	58.22		7.79	

SUMMARY

Diallyl esters of glutaric, diglycolic, and pimelic acids, of di(carboxyethyl) ether, and of ethylene glycol di(carboxyethyl) ether not previously described in the literature, have been synthesized (in yields of 36-92% of theoretical); when these esters are heated on the water bath in presence of benzoyl peroxide they yield transparent but soft polymers of low strength. Copolymerization with divinyl esters of dibasic acids yields colorless, glassy, strong products; both the polymers and the copolymers are insoluble in benzene and in acetone.

LITERATURE CITED

[1] Organic Syntheses 1 (IL, 1949), p. 174.*

[2] Organic Syntheses 1 (IL, 1949), p. 518.*

[3] R. Eichloff, Ann. 342, 105 (1905).

* Russian translation.

[4] Organic Syntheses 2 (IL, 1949), p. 414.*

[5] U. S. Patent 2,382,031; Chem. Abstr. 40, 347 (1946).

[6] I. N. Nazarov, G. A. Shvekhgeimer, and V. A. Rudenko, J. Gen. Chem. 24, 333 (1954).**

[7] Organic Syntheses 1 (IL, 1949), p. 25.*

Received August 23, 1956.

---

* Russian translation.

** Original Russian pagination. See C. B. translation.

WATER-REPELLENT TREATMENT OF LEATHER WITH ORGANOSILICON COMPOUNDS*

E. K. Maminov and M. G. Voronkov

In recent years organosilicon compounds have been widely used for conferring hydrophobic properties on (increasing the water resistance of) various materials [1-3].

In particular, it is reported in the foreign periodical [4-7] and patent [8-11] literature that polyalkyl siloxanes and polyalkyl silazanes can be used for making leather water-repellent. However, these data refer to proprietary organosilicon water-repellent preparations, the exact composition of which is not known. Therefore, it is not always possible to reproduce the results obtained by foreign investigators and firms.

The purpose of the present investigation was to develop a method of water-repellent treatment for leather and leather articles with the use of organosilicon compounds developed mainly in the Institute of Silicate Chemistry, Academy of Sciences, USSR.

As is known, repeated soaking and drying of leather in use results in deterioration of a number of its useful properties. The leather shrinks, becomes hard, and wears out more rapidly. The tensile strength and the heat-insulating properties of the leather decrease, and it becomes considerably more permeable to water.

Water-repellent treatment of leather with organosilicon compounds confers very high and stable water resistance on leather, owing to chemical bonding of the water-repellent film by the collagen of the leather. The leather does not lose its other favorable properties in the process. It is especially important that the volume of the pores in the leather remains practically unchanged, so that its permeability to vapors and air does not diminish.

Water-repellent leather dries much more rapidly than ordinary leather after being wetted, and does not harden after drying but retains its softness and elasticity. Leather treated with organosilicon compounds soils much less readily, has a higher resistance to the usual destructive factors (perspiration, moisture, light, weather, etc.) and to mechanical influences (repeated flexing), while fat-liquored leather (Russian cowhide boot leather) is less defatted by the action of water, dust, and dirt.

In a search for organosilicon compounds which would confer the best and most stable water-repellent properties on leather, the following compounds were tested.

Compound	Formula	Code
Polymethylsiloxane	$(CH_3SiHO)_n$	MN-1
Polyethylsiloxane	$(C_2H_5SiHO)_n$	EN-1
Dimethyldiacetoxysilane + methyltriacetoxysilane (1:1 molar)	$(CH_3)_2Si(OCOCH_3)_2$ + + $CH_3Si(OCOCH_3)_3$	A-3

* Communication IV.

Compound	Formula	Code
Methyldiacetoxystearoxysilane	$CH_3Si(OCOCH_3)_2OCOC_{17}H_{35}$	A-4
Diethyldiacetoxysilane + tetra-acetoxysilane (1:1 molar)	$(C_2H_5)_2Si(OCOCH_3)_2$ + + $Si(OCOCH_3)_4$	A-11
Poly(trimethylsiloxy)acetoxysiloxane	$[(CH_3)_3SiOSi(OCOCH_3)O]_n$	A-12
Sodium methylsiliconate	$CH_3Si(OH)_2ONa$	MSN
Sodium ethylsiliconate	$C_2H_5Si(OH)_2ONa$	ESN
Sodium phenylsiliconate	$C_6H_5Si(OH)_2ONa$	FSN
Methyldimethoxysilane	$CH_3SiH(OCH_3)_2$	MDS-9
Methylbis(2-ethoxyethoxy)silane	$CH_3SiH(OCH_2CH_2OC_2H_5)_2$	GMS-9

Specimens of chrome–vegetable tanned cowhide shoe leather and chrome–tanned calf leather, 8 × 36 mm, were treated. The specimens were coated either on the outer or on the flesh side with a solution of a given compound in toluene or (for MSN, ESN, FSN, MDS-9, and GMS-9) in water, by means of a brush or by spraying until the leather was impregnated right through.

In addition, treatment with the water-soluble organosilicon preparations was carried out by immersion of the leather specimens in aqueous solutions of definite concentrations. The impregnated specimens were dried in air at room temperature for different times, according to the solvent and compound (from 1 to 3 hours) and then heated for 5-6 hours at 60-70° (this was found to be the optimum temperature in preliminary experiments). The treated leather specimens were tested for permeability to water, vapor, and air as specified in GOST 938-45. Of the 11 organosilicon preparations tested as water-repellent treatments for leather uppers, A-4 and ESN gave the best results. The data on their effects are summarized in Table 1.

The most effective treatment is with 5% toluene solution of A-4 preparation, containing 0.01% of ethyl orthotitanate as catalyst. Aqueous 0.5-1% solutions of ESN produce a smaller reduction of water permeability and require the addition of 1.25% of sulfonated train oil to preserve softness of the leather. However, they have the advantage that the solvent is water.

The results were then applied in the treatment of a small experimental batch of army leather boots with fabric tops, in order to test the retention of the water-repellent properties of the leather during wear.

For comparison of the water-repellent properties of army boots in wear, each left boot was treated with 5% solution of A-4 in toluene with 0.01% ethyl orthotitanate as catalyst, and with 1% aqueous solution of ESN containing 1.25% of sulfonated train oil as plasticizer. The right boots were untreated and served as controls.

The boots were worn by soldiers of an operational unit under the most severe weather and seasonal conditions (February to June); no complaints were made by the soldiers of leaks through the leather uppers of the left experimental boots, while the control right boots nearly all leaked through the uppers, confirming the effective water-repellent properties of A-4 and ESN preparations.

After 4 months of wear several pairs of boots were withdrawn from service, and their water permeability was tested in the laboratory, water being poured inside to a height of 200 mm. The results of the leakage tests are given in Table 2.

It is seen that despite the fact that the experimental left boots, like the control right boots, had been subjected to the effects of snow, water, mud, dust, mechanical impacts, and repeated flexing during 4 months of wear, their water resistance was retained.

The data in this brief communication show that water-repellent treatment of leather and leather articles with organosilicon compounds is very promising.

TABLE 1
Effects of Organosilicon Preparations ESN and A-4

Type of leather specimens	Chrome-vegetable tanned cowhide						Chrome-tanned calf					
	1% ESN solution, 1.25% of sulfonated train oil as plasticizer			5% solution of A-4 catalyst 0.01% Ti (OC_2H_5)$_4$			0.5% ESN solution, 1.25% of sulfonated train oil as plasticizer			5% solution of A-4 catalyst 0.01% Ti (OC_2H_5)$_4$		
	water permeability (in ml/cm^2 · hour)	relative vapor permeability (%)	air permeability (in cc/cm^2 · hour)	water permeability (in ml/cm^2 · hour)	relative vapor permeability (%)	air permeability (in cc/cm^2 · hour)	water permeability (in ml/cm^2 · hour)	relative vapor permeability (%)	air permeability (in cc/cm^2 · hour)	water permeability (in ml/cm^2 · hour)	relative vapor permeability (%)	air permeability (in cc/cm^2 · hour)
Untreated controls	1.04	49.2	9.3	1.76	48.0	75.6	0.85	73.7	21.0	1.09	84.0	21.5
Treated	0.047	54.5	21.0	0.075	58.3	133.0	0.05	90.2	26.7	0.025	89.0	28.5
Relative decrease of water permeability	22	—	—	23	—	—	17	—	—	43	—	—

TABLE 2
Leakage Tests on Boots

Leakage conditions	Leather army boots		
	right boots, controls	left boots, treated with	
		A-4	ESN
Start of leakage (minutes)	18-20	120	158
Complete soaking (minutes)	70-108	500	556

LITERATURE CITED

[1] M. G. Voronkov and B. N. Dolgov, Nature 5, 22 (1952).

[2] B. N. Dolgov and M. G. Voronkov, J. Leningrad Univ. 5, 185 (1954).

[3] R. R. McGregor, Silicones and Their Uses (New York, 1954).

[4] N. D. Cheronis et al., J. Amer. Leather Chem. Assn. 44, 282 (1949); see also Shoe and Leather Reporter 278, 9, 13; 12, 15; 279, 3, 13; 8, 15 (1950).

[5] R. L. Sykes, Tanner 8, 12, 11 (1954).

[6] W. T. Rossiter, Leather and Shoes 128, 19, 44 (1954); Leather and Shoes 129, 12, 14 (1955); Shoe and Leather Reporter 277 (7) 32, 63 (1955).

[7] A. Jonescu, Rev. Chim. 6, 591 (1955).

[8] T. A. Kauppi, U. S. Patent 2,678,893 (1954).

[9] Dow Corning Ltd. British Patent 706,719 (1954).

[10] C. C. Currie, U. S. Patent 2,672,455 (1954).

[11] N. D. Cheronis, U. S. Patents 2,635,059 (1953); 2,635,060 (1953).

Received December 12, 1956.

JOURNAL OF APPLIED CHEMISTRY OF THE U.S.S.R. IN ENGLISH TRANSLATION

June, 1957

TABLE OF CONTENTS

	Page	Russ. Page
1. Study of the Reactions of Sulfur Dioxide with Metal Oxides in Presence of Carbon. V. V. Pechkovsky	873	825
2. Determination of the Solubility of Carbon Dioxide in Aqueous Solutions of Sulfuric Acid by the Isotopic Dilution Method. M. K. Shchennikova, G. G. Devyatykh, and I. A. Korshunov	881	833
3. Secondary Processes on Amphoteric Ion-Exchange Resins and the Possibility of Their Practical Utilization. A. B. Davankov, V. M. Laufer, and L. A. Shits.	887	839
4. Chemical Selectivity of Phosphate and Calcite in Ores with Recovery of the Reagents. A. S. Chernyak	892	844
5. Thermodynamic Analysis of the System Ca–C–O. F. S. Maron	899	851
6. Calculation of Batch Rectification Columns. Fu Tszyui-fu	911	862
7. Hard Gold Plating. A. G. Atanasyants, N. T. Kudryavtsev, and V. M. Karataev	926	876
8. Electrochemical Methods for Decorative Surface Treatment of Aluminum Articles. P. V. Shchigolev	931	882
9. Investigation by an Ultrasonic Method of the Formation of a Solid Phase in a Paraffinic Distillate. A. P. Grishin	936	887
10. Production of Ethyl Alcohol on the Basis of Electrocracking of Methane Gases. M. G. Terekhova, E. N. Eremin, and N. I. Kobozev	942	893
11. Resin in Spruce Wood. S. S. Malevskaya	951	903
12. Aromatization of Tree-Stump Turpentine. V. G. Plyusnin, S. I. Chertkova, E. P. Babin and M. A. Mikhailova	959	911
13. Action of Metal Oxides as Vulcanization Activators of Sodium Butadiene Rubber. M. Feldshtein P. Orlovsky, and B. Dogadkin	966	917
14. Investigation of the Dehydrogenation of Ethyltoluene to Vinyltoluene. A. V. Bondarenko, M. I. Bogdanov, and M. I. Farberov.	975	927
Brief Communications		
15. Aluminum Monobromide. S. A. Semenkevich.	982	933
16. Investigation of the Structure of Porous Ceramics. A. S. Berkman.	987	937
17. Method for Calculation of the Crystallization Region of Sodium Chloride in the Quaternary System $CaCl_2$–$MgCl_2$–NaCl–H_2O. V. Ya Rudin and N. R. Yarym-Agaev		
18. Investigation of Organic Compounds Which Retard the Oxidation of Sulfide Ores at Elevated Temperatures. F. N. Pavlov V. G. Plusnin, and E. F. Iordan	997	944
19. The System Na_2SO_4–$NaHCO_3$–H_2O (Carlsbad Salt) at 25 and 28°. G. V. Sukmanskaya and P. S. Bogoyavlensky	1001	947

20. The Selective Corrosion of Zinc. I. I. Zabolotnyi. 1007 952

21. Investigation of a Thiocyanate Electrolyte for Copper Plating. B. S. Krasikov and A. M. Gvozd. 1012 956

22. Oxidation of Cyclopentanone with Nitric Acid. E. N. Zilberman and A. I. Kirillov 1017 960

23. Thermocatalytic Conversions of Alkylnaphthalenes (Isoamylnaphthalene) B. G. Gavrilov and N. Kim 1021 963

24. Use of Ethyl Ethers of Amylene Chlorohydrins in Mixtures with Dichlorides for Deparaffinization (Dewaxing) of Aviation Oil. A. K. Seleznev 1024 965

25. Use of the Gustavson – Friedel – Crafts Reaction for the Production of Lubricating Oils From Extracts. I. F. Radzevenchuk 1026 966

26. Synthesis of Some New Diallyl Esters of Dibasic Acids. M. F. Shostakovsky, A. M. Shur, and B. F. Filimonov. 1032 971

27. Water-Repellent Treatment of Leather with Organosilicon Compounds. E. K. Mamlnov and M. G. Voronkov 1036 974